MEASUREMENT AND SIMULATION OF TRANSIENT MOISTURE AND HEAT DIFFUSION IN A POTASH LAYER

A Thesis
Submitted to the College of Graduate Studies and Research
in Partial Fulfillment
of the Requirement for the
Degree of

Master of Science

In the Department of Mechanical Engineering
University of Saskatchewan

By
Qiang Zhou
Saskatoon, Saskatchewan
May 2000

COPYRIGHT

This thesis is dedicated to my parents, Yu-Ru Bao and Yu-Lin Zhou who have encouraged me when I faced frustration in 1996.

I would also like to thank my wife, Jiang Wei, for her love and care when I worked hard on my thesis to midnight everyday. This thesis is also part yours.

ABSTRACT

Potash fertilizer is granular bulk product and is comprised almost entirely of potassium chloride. It is used widely, often with other fertilizers, for agricultural soils low in potassium, an essential nutrient for plant growth. It readily accumulates moisture when subjected to humid air for extended time periods during handling and storage.

In this thesis, the moisture accumulation near the surface of granular potash fertilizer products is studied. The coupled heat and moisture transfer during handling processes and warehouse storage is modeled as a coupled one-dimensional transient heat and moisture diffusion problem at the air-potash interface.

A one-dimensional transient numerical model of heat and moisture transfer, including adsorption/dissolution and condensation, is developed. Temperature and moisture accumulation profiles within potash bed are simulated and compared to measured data under a wide range of operating conditions for two types of potash. The numerical model is validated using experimental data from potash layer in a test facility subject to a wide range of test conditions.

For humid airflow over the top of a potash layer with three different supply air humidities (i.e.45%, 65% and 80% RH), moisture accumulation and temperature distribution have been investigated under the constant room temperature (i.e.22°C) with and without a cold temperature at the bottom boundary. When the local relative

humidities are less than 52% RH, water vapor accumulates on the particle surface by adsorption which causes a very small moisture accumulation. When local relative humidities exceed 53% RH, water vapor accumulates on potash by dissolution which creates a thin layer of electrolytic solution on particle surfaces and causes significant moisture accumulation. A 20°C temperature difference across the potash layer results in moisture contents 10 time larger than the case with no temperature difference, implying that the moisture transfer in potash is strongly coupled with temperature distribution in the heat and moisture diffusion processes.

To illustrate the application of the simulation model, simulations were done for the problems of moisture redistribution within potash after mixing and the rapid moisture gains for cold potash placed on a conveyor belts exposed to humid air. It is found that the process of moisture redistribution in potash will continue as long as temperature and moisture content differences persist anywhere within potash bed. The rapid moisture accumulation is only significant for a narrow surface layer which is about 10% of potash mass placed on a conveyor belts. Heating the potash on a conveyor belt near the surface layer to that of ambient air temperature could reduce the moisture accumulation by 4 to 8 times.

It is concluded from this research that the complex physical and chemical processes for water vapor accumulation in exposed granular potash can be modeled and simulated.

ACKNOWLEDGMENT

I would like to express my sincere thanks and appreciation to my supervisor, Professor R.W.Besant, who has helped me with both my academic research work and personal life. Thanks for your support, guidance and expertise throughout this work.

I would also like to extend my sincere thanks to Dr. Shi-Wen Peng for his assistance and input during this research work. Also thanks to Mr. Dave Deutscher for his help with the experimental studies.

A special thanks goes to Hong Chen, who works with me in the same research group and is expecting to achieve his Ph.D. degree in May, 2000. I really appreciate Hong's helpful guidance and friendly encouragement whenever I needed help.

Financial assistance from the NSERC and P.C.S. during my graduate program is also acknowledged and appreciated.

TABLE OF CONTENTS

LIST OF FIGURES

LIST OF TABLES

NOMENCLATURE

A	surface area, m^2
A_{sf}	solid-fluid interface area, m^2
a'	empirical constant in the adsorption/dissolution model
b'	empirical constant in the adsorption/dissolution model
$\vec{b}$	second order tensor
c'	empirical constant in the adsorption/dissolution model
c_p	specific heat at constant pressure, J/(kg•k)
C	empirical constant in the adsorption/dissolution model
d	average pore size diameter, m
d_p	average particle size, m
d'	empirical constant in the adsorption/dissolution model
D	vapor diffusivity, m^2/s
e'	empirical constant in the adsorption/dissolution model
f'	empirical constant in the adsorption/dissolution model
g'	empirical constant in the adsorption/dissolution model
h_{fg}	heat of vaporization, J/kg
h_h	heat transfer coefficient, $W/(m^2 \bullet K)$
h_m	mass transfer coefficient, m/s
k	thermal conductivity, W/(m•K)
K	permeability, m^2

l	diameter of the elementary volume, m
L	thickness of potash bed in the test section, m
m	mass, kg
$\dot{m}$	rate of phase change per unit volume, kg/(m^3•s)
$\dot{m}''$	rate of phase change per unit area, kg/(m^2•s)
Δm	mass of water adsorbed, kg
M	molecular weight, g/mol
$\vec{n}$	unit vector normal to surface
Pa	atmosphere pressure, Pa
P	pressure, Pa
ΔP	pressure difference, Pa
Q	average enthalpy change, J/kg
R	gas constant, T/(kg•K)
R_{ct}''	thermal contact resistance, (m^2•K)/W
Re	Reynolds number
Re_{dp}	Reynolds number based on particle size
S_g	specific surface area per unit mass, m^2/kg
S_v	specific surface area per unit volume, m^2/m^3
t	time, s
T	temperature, K
ΔT	temperature difference, K
U	velocity, m/s

U_D Darcy Velocity, m/s

V volume, m^3

W humidity ratio of air

$\Delta\bar{W}$ mean value of the difference in humidity ratio

X moisture content

$\bar{X}$ average moisture content

X_{ad} equilibrium moisture content for ϕ=0.48

$X_{cr,d}$ dissolution equilibrium moisture content corresponding to ϕ=0.53

X_m empirical constant in the adsorption/dissolution model

x coordinate axis, m

Δx grid space in x direction for numerical model, m

y coordinate axis, m

y* dimensionless vertical distance, y*=y/L

GREEK SYMBOLS

α thermal diffusivity of dry potash, m^2/s

ε volumetric fraction

δ_s thickness of surface lumped system, m

δ penetration depth, m

δ* displacement thickness, m

φ a general transport variable

ϕ relative humidity

μ viscosity of air, kg/(m•s)

ν specific volume of dry potash particles, m^3/kg

Ω_β volume change of aqueous solution layer per unit mass of moisture, m^3/kg

Ω_σ volume change of solid potash per unit mass of moisture, m^3/kg

ρ density, kg/m^3

τ tortuosity

∇ gradient

SUBSCRIPTS

a dry air

c cold bottom plate

eff effective property

g gas

i interface between water vapor and solid potash

m moisture

s solid phase

t thermal

w water vapor

∞ ambient air

$^\circ$ reference or initial value

β liquid phase

σ solid phase

γ gaseous phase

CHAPTER 1

INTRODUCTION

1.1 INTRODUCTION

Potash is an important fertilizer product that is essential for plant growth in soils low in potassium. The granular potassium fertilizer is made from potash ore mined from ore deposits in Saskatchewan. Commercial potash fertilizer producers in Saskatchewan are the Potash Corporation of Saskatchewan (PCS), Saskatoon, SK, IMC Kalium Canada Ltd., Belle-Plain SK and Agrium Inc, Vanscoy, SK. Typically more than 13 million tons of potash are produced each year in Saskatchewan and this represents more than 1/3 of the world production. Almost all this fertilizer is handled as a bulk granular product.

Potash fertilizer is mainly composed of sylvite (i.e. potassium chloride (KCl)). After mining and during processing (i.e. floatation or recrystallation process, followed by a subsequent drying process) the surface of each potash particle is coated by a thin layer of mixed salts composed of sylvite or potassium chloride (KCl), halite or sodium chloride (NaCl), and carnallite ($KMgCl_2 \bullet 6H_2O$) crystals. Carnallite is the most soluble in water while potassium chloride is the least soluble. The existence of these surface impurities causes the potash-moisture interactions to deviate significantly from that of pure potassium chloride.

When exposed in humid air, potash particles will adsorb moisture from the surrounding air. Subsequently, when the relative humidity drops, moisture will be removed from the granular particles by a drying process. If this occurs at moisture contents greater than about 0.2%, the small particles may cake to form larger particles or clumps (i.e. caking) and break to form dust sized particles. The risk of caking and dust formation increases with moisture content but it will be influenced by cyclic variations in moisture content and mechanical pressure. Clumps or dust in potash impedes the handling and flow of this granular material and is especially unfavorable for uniform distribution by most agriculture machines. The photographs in Figure 1.1 show a sample of potash after moisture addition and removal with and without caking.

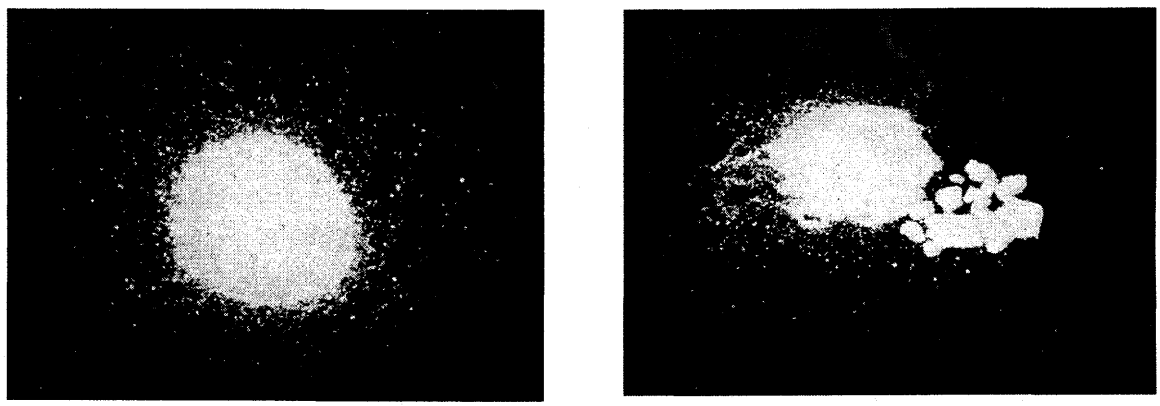

(a) Dry granular Potash Particles without Caking

(b) Caked Granular Potash with Some Caking

Figure 1.1 Comparisons of Granular Potash with and without Caking

In this study there is no direct measurement of caking or dust content; rather, the moisture content is measured because it can be accurately quantified whereas caking and dust formulation can not be easily characterized. Typical values of moisture content

within granular potash fertilizer during the warehouse storage and transportation processes range from 0.1% to 1.0% so this is the primary range of investigation.

1.2 HEAT TRANSFER DURING HANDLING AND STORAGE OF BULK POTASH

Millions of tons of potash fertilizer products are exported every year to the United States, Australia, China, Japan and other countries. During these shipments, potash is moved from one location to another and stored in large warehouses or storage sheds for extended periods. Moisture accumulation in the bulk potash occurs at the air-potash interface during each step after processing at the mine until it is finally put in the soil along with other fertilizers and seeds. Over time this moisture accumulation may be redistributed within the bulk mass of potash but it rarely leaves the bulk mass unless it is heated to well above normal room temperature. In this sense it behaves much like a desiccant.

Three methods are used to transport bulk potash: conveyors, rail cars and ships. Conveyor belts are used to move potash from storage sheds into rail cars or ships or to move the same potash back to other bulk storage sheds after it has been transported. When potash is transported from a storage pile to a conveyor belt into a rail car or ship or vice versa the potash is mixed such that the particles or volume elements near the surface in the bulk storage pile are folded into mostly interior volume elements in each rail car or

ship. At the same time, interior volume elements from the storage pile dominate the new surface elements in the rail car or ship and similarly when the process is reversed.

Mixing potash dominates the physical phenomena each time the potash is transferred from one storage vessel to another and diffusion processes dominate the physical process while the potash is within a vessel such as a storage shed, rail car, ship or conveyor belt. Two types of diffusion processes are important: heat transfer and mass transfer of water vapor. Heat transfer is important when it causes the temperature of the bulk potash to decrease below the adjacent ambient air temperature. When the potash surface temperature is significantly lower than the adjacent ambient air temperature the rate of diffusion of water vapor into the potash is greatly increased even for typical ambient air relative humidity of 40-50%. Consequently, when mixing causes large volume fractions of colder potash to be exposed on or near new air-potash interfaces water vapor diffusion and deposition near the new surface will be greatly enhanced.

The data from this research will show that there is often an order of magnitude difference between the rate of moisture accumulation when the potash is at or higher than the ambient air temperature and when it is significantly colder than the ambient air temperature. Thus it is very important to consider both the heat transfer and the mass transfer processes. The heat transfer process with no mass transfer can be easily estimated when the surface temperatures are nearly constant. The mass transfer process is always coupled to heat transfer which is very complex and it is the main purpose of this research.

The heat transfer process without mass transfer is briefly explained below for the case of potash at a uniform internal temperature suddenly exposed to a cold external surface.

The thermal penetration depth (δ_t) and thermal displacement thickness (δ_t*) are used to represent the thermal response of a bulk mass of potash during storage or transportation which is initially at a uniform temperature and subject to a step change in the surface temperature. They are defined as [Apaci and Larsen (1984)]:

$$\delta_t = (12\alpha t)^{1/2} = 0.0022\sqrt{t} \text{ (m)} \tag{1.1}$$

for the maximum practical penetration depth of the heat diffusion process in dry potash and

$$\delta_t^* = \frac{1}{3}\delta_t \tag{1.2}$$

for the displacement thickness which represents the thickness of layer at the surface temperature with the same sensible energy content as δ_t.

where

t = storage or thermal exposure time (s)

$$\alpha = \frac{k}{\rho \cdot C_p} = \frac{0.60}{1987x750} = 0.40x10^{-6} \text{ m}^2/\text{s}$$

is the thermal diffusivity of dry potash

Table 1.1 shows the typical values of δ_t and δ_t^* in each handling process at different times. These transient, step-change results show that thermal diffusion may penetrate large distances relative to the size of the storage vessel. For example, this distance is about 6.5 m into stored potash piles when potash is placed on cold warehouse floors for 100 days, about 3.5 m from the hull of a ship when potash is placed in a hold of a single hulled bulk carrier ship for 30 days, about 1.5 m from the surfaces of rail cars when potash is placed in a cold rail car for 5 days, or conversely, for a thermal reheating process of 1 day after a cold rail car arrives in Vancouver from Saskatchewan, the penetration depth will be about 2/3 m while most of the potash will be colder as a result of travelling through the mountains. The corresponding thermal displacement thickness shown in Table 1.1 can be used to estimate the fraction of total volume of potash influenced by cold temperatures. The heat transfer process is explained in more detail below for each step during the potash storage, handling and transportation process.

Table 1.1 Typical Values of Thermal Penetration Depth(δ_t) and Displacement Thickness (δ^*_t) for Different Time Periods

Time (Day)	δt (m)	δt* (m)	Time (min)	δt (mm)	δt* (mm)
1.00	0.67	0.22	5.00	38.00	13.00
5.00	1.50	0.50	15.00	66.00	22.00
30.00	3.68	1.23	30.00	94.00	31.00
100.00	6.72	2.24	60.00	132.00	44.00

When potash is stored on the cold floor of a storage building as in Figure 1.2, about 40-50% of the potash pile volume will be cooled over 100 days because the

thermal displacement thickness will be δ_t*=2.25 m. In this case, the floor temperature may be about 10°C for about 7 to 8 months from December to July and slightly warmer from August to November so when T_∞ = 15°C dissolution of potash will commence on potash at 10°C at an ambient air humidity of only 35% R.H and condensation will occur at 75% R.H. Dissolution and condensation will cause the potash temperature to rise at the interface with moist air and may only add about 0.1% moisture content to stored potash on average. However, since moisture accumulation tends to be irreversible, each 0.1% added during each process step is important because it can cause caking or dust formation before the potash is used as an agricultural fertilizer. Dissolution and condensation will occur at much lower relative humidities when the ambient air temperature is warmer (e.g. 23% R.H and 40% R.H at T_∞=25°C). In summary, dissolution will almost always occur when potash at 10°C is exposed to ambient air and condensation may sometimes occur. For very low ambient air relative humidity in the storage shed or for potash at ambient or high temperature adsorption of water vapor will always occur. These sheds are usually leaky buildings regarding air infiltration from outside air (e.g. 0.2<volume air changes per hour<2), especially if the doors are left open for extended durations.

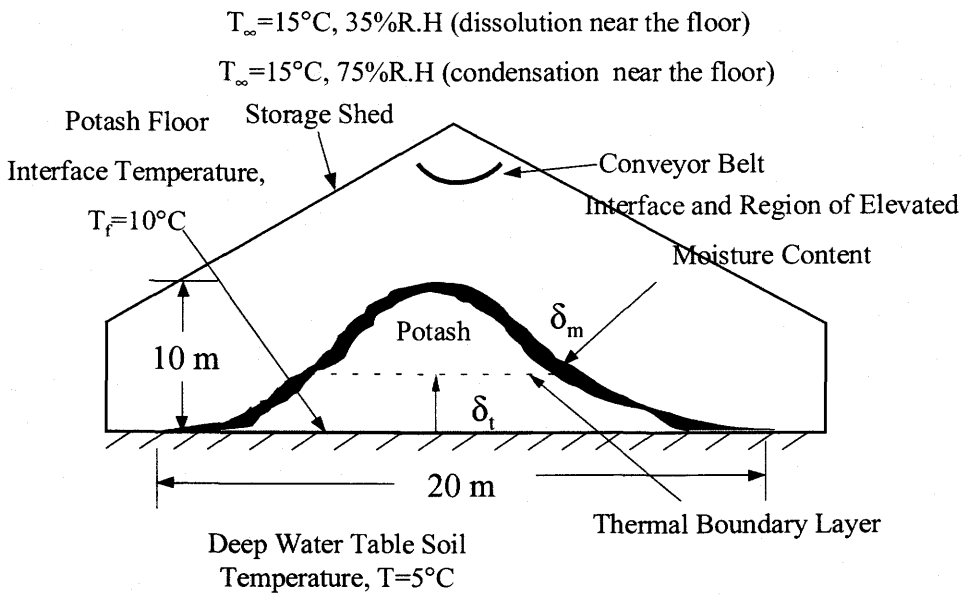

Figure 1.2. Potash Pile Storage on a Cool Warehouse Floor

Shipping by rail car is a unique problem because often potash is taken from a cool pile in a Saskatchewan shed and shipped over several days (e.g.5) to various locations in North America where it is transferred by conveyors to storage sheds. Cool potash at 10 to 15°C in summer warms up due to the ambient air and solar exposures or in winter cools down even more as a consequence of thermal heat transfer penetrating from the railcar surface as shown in Figure1.3. Diurnal temperature changes and solar exposures in rail cars cause significant time variation of the rail car surface temperature, Ts (e.g. 10 <Ts<30°C in summer and 0>Ts>-30°C in winter). The diffusion process causes some moisture adsorption and perhaps dissolution each day. Moisture uptake in winter will be negligible unless the potash is delivered to a warm humid environment (e.g. southern US regions). At the same time, vibrations of rail car on a moving train cause consolidation of the bed of potash in each rail car so that the porosity goes to a minimum and caking is

enhanced if the moisture content exceeds 0.2% when it is loaded. At the end of a five-day rail trip from loading to unloading of a rail car, about 50% of the potash will remain at a temperature close to the warehouse storage temperature (i.e. 10 to 15°C) and the thermal boundary layers effects near the rail car surface will reflect the entire five-day diurnal cyclic history of surface temperatures. These cycles enhance caking and dust formulation. For a typical well-sealed rail car, air infiltration into and out of the rail car space will be mostly a consequence of daily variations in the average internal air temperature in each car because internal-to-external air pressure differences will always be small.

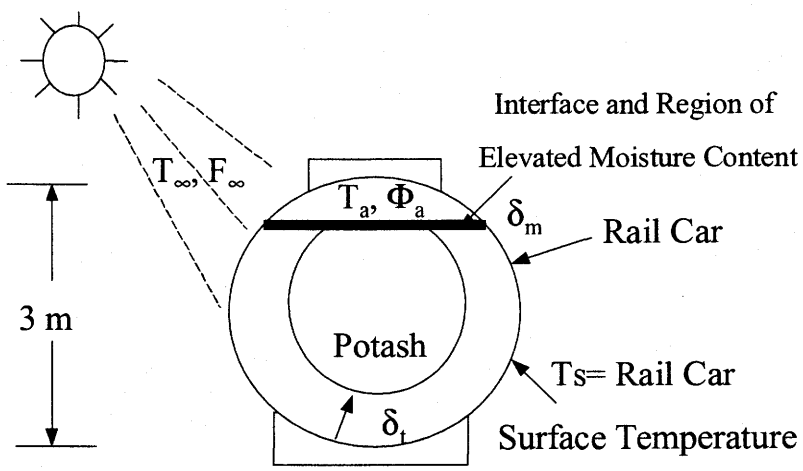

Figure 1.3. Cross-Section of a Rail Car with Potash

In the hold of a single hulled ship shown in Figure 1.4 where the ocean water temperature is about 5°C while the air is 15°C, the displacement thickness (δ_t*) may result in about 10% of the product cooled to a temperature near 5°C over a period of 30

days from the time of loading to unloading of a ship. In this case, an air temperature of 15°C and 52% R.H will result in condensation on the product with 100% R.H at the air-potash interface near the hull and 25% R.H will cause dissolution. Air infiltration into the hold of the ship is expected to be small and it will be mostly due to the diurnal temperature changes in the ship's hull when the hatch covers are tightly closed. Rain directly into the hold of a ship with open hatches will rapidly increase the moisture accumulation. For a double-hulled ship these temperature differences will be smaller as will the potential for moisture uptake.

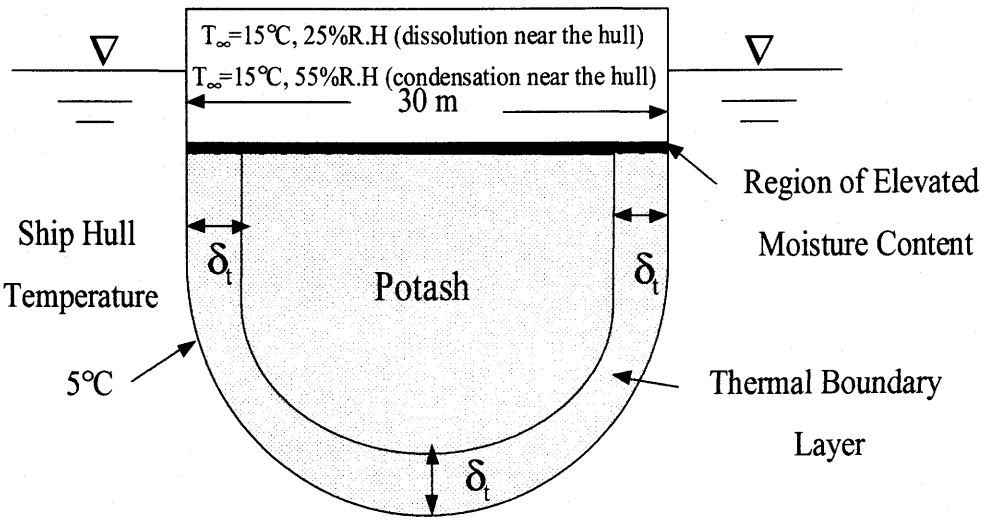

Figure 1.4 Cross Section of a Single Hulled Ship with Potash in the Hold

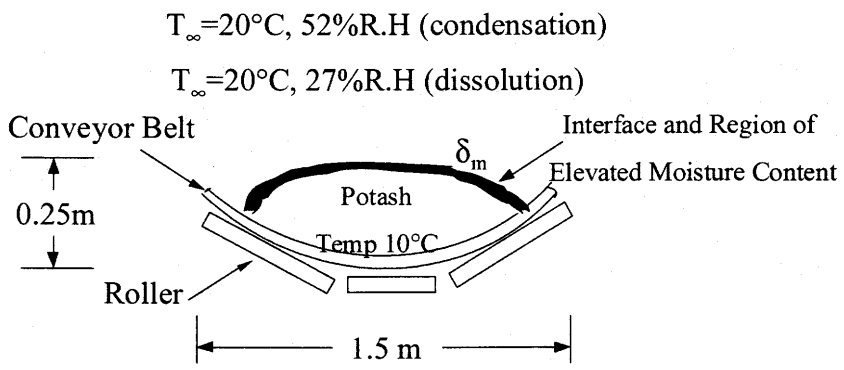

Figure 1.5 Cross Section of a Conveyor Belt

In all three examples above, adsorption of water vapor will occur for local humidity less than 52% R.H and dissolution of potash will occur for local humidity more than 52% R.H.

Placing cool potash on a long conveyor belt as in Figure 1.5 and conveying the product over long distance (e.g. 100 to 500 m) through warm humid air (e.g. 20°C and RH>27% or 52%) may cause significant moisture uptake on the potash due to dissolution or even condensation in spite of the short duration of exposure (e.g. 5 to 20 minutes). During these conveyor belt exposures, the convective mass transfer coefficient due to forced convection will be much higher than during storage or transport vessel exposures where there is mostly natural convection. These convective mass transfer coefficients are expected to be approximately ten times larger on a conveyor belt than elsewhere so the fraction of the potash volume exposed to moisture will be significant (e.g. 2 to 10%). Of

course, if the conveyor transport is exposed and used during rainy or foggy weather the moisture content of the exposed potash surface layer could be very high. Stopping the conveyor belt with potash loaded over the length will add considerably to the moisture content for that length.

The penetration depth of the added moisture layer on a conveyor belt will be much less than the thermal boundary layer penetration depths implied in Figure 1.1. Heat transfer during the conveying process is expected to be small because the main resistance to heat transfer will be a consequence of resistance in the surrounding air. So the average potash temperature may increase only 0.25°C to 1.0°C for a total temperature difference of 10°C due to heat transfer through the bottom. On the other hand, energy gains due to the phase change (dissolution and condensation) of water on the top exposed surface may be five times as large. As a result the top exposed surface will quickly rise to the ambient temperature or slightly higher while the interior remains slightly cooler. This type of interface heat and mass transfer is complex. It is the main focus of the research in this thesis.

1.3 MOISTURE TRANSFER FROM AIR TO POTASH

Generally the moisture accumulating in potash takes place through the air-potash interface. This mass transfer process at the interface is complex and it is the purpose of this thesis. Even though it is difficult to estimate the typical risk of moisture transfer through the interface during each step in the various handling, shipment and storage

process some estimate of the relative importance of each step in the handling and storage processes can be used to guide this research.

In this very simplified analysis, the risk of moisture gain is assumed to be due to humid air convection over the interface (i.e. no rain or moisture gain from floors is considered). The rate of moisture transfer into potash from humid ambient air can be written using the mass transfer equation:

$$\dot{m} = \rho_{air} h_m A(W_\infty - W_i) \tag{1.3}$$

where ρ_{air}= density of air(kg/m^3)

h_m= mass transfer coefficient (m/s)

A = surface area (m^2)

W = humidity ratio of air

and subscript ∞ and i refer to the ambient air and interface respectively.

Integrating equation (1.3) over the duration of exposure, Δt, gives:

$$m = \rho_{air} h_m A \bar{\Delta W} \Delta t \tag{1.4}$$

where $\bar{\Delta W}$ is the mean value of the difference in humidity ratio.

In general, $\bar{\Delta W}$ depends strongly on the ambient air temperature and relative humidity as well as the temperature and moisture content of the potash at the interface ($\bar{\Delta W}$ is a parameter that is difficult to estimate for practical applications and requires

further research). The other terms in equation (1.4) are, perhaps, more readily estimated. Table 1.2 presents the relative values, $[\rho_{air} h_m A \Delta t / M]$ per unit mass of potash in a vessel or piled on the floor of storage shed or $\bar{X} / \Delta \bar{W}$, for each of the modes of potash handling, shipment and storage discussed previously. In this table, this dimensionless ratio, $\bar{X} / \Delta \bar{W}$ (i.e. average moisture mass content of the potash in the vessel or pile divided by the average driving potential), is taken to be 1 for the least accumulation risk during rail transportation.

Table 1.2. Relative Risk of Moisture Gain in Potash from Humid Air

Relative Risk Factor for Moisture Accumulation	Shed Storage	Rail Car	Ship	Conveyor Belt
$\bar{X} / \Delta \bar{W}$	40 to 80	1	1 to 2	10 to 40

In this table, it is assumed that there will be two 100-day potash shed storage periods, one 5-day rail car shipment, one 30-day ship transport period, and 3 to 6 conveyor belt exposure durations of about 10 minutes each.

Table 1.2 implies the relative risk of moisture gain in potash from humid air during each exposure process. It does not imply the coupling of risk from one process to the next as a consequence of potash temperature or heat transfer and mixing between processes. Table 1.2 implies the research directions that will provide data and models to permit better predictions of moisture accumulation in potash. It is evident from these relative risk factors that surface area for air-potash interface per unit mass of potash, time

duration of exposure and forced convective mass transfer coefficients are all very important. Conveyor belt exposures are especially complex because they may be subject to loading much cooler potash from sheds, rail cars and ships onto conveyor belts in warm humid air. Table 1.2 also implies the need for research to characterize the moisture content of potash at the air-potash interface.

It is not evident from Table 1.2 that the distribution of moisture in potash is much more important than the average values of moisture content, $\bar{X}$. Moisture content, X, may be one or two orders of magnitude higher near a moist surface layer than in an interior dry region. Like caking and dust formulation problems the moisture content will not be uniformly distributed. To answer the question, "how does moisture move or diffuse in potash", the accumulation and distribution of moisture in potash will have to be measured and modeled as a transient physical and chemical phenomenon.

Other areas of research on potash that are not considered in this thesis are: (1) the effect of static loads on potash caking and dust formulation and (2) modeling of mixing during potash handling. These important areas are left to future research.

1.4 PREVIOUS RESEARCH

Research work on moisture interaction between water and granular fertilizers like potash goes back many decades. This research has been published in a variety of journals

and monographs. In the last decade, the intensity of this research appears to have increased as export sales of bulk granular fertilizer product to places around the world have increased over the past 20 years and problems with quality control resulting from the formulation of dust and caking have become more frequent for all types of fertilizers. Most of the past research was entirely experimental and aimed at measuring certain physical properties and sometimes developing empirical correlations. Until recently, there has been no research to develop theoretical models of the adsorption and dissolution processes in potash from first principles.

Chemical adsorption and dissolution research on salts has been confined to pure substances like NaCl crystals subject to various water vapor partial pressures or relative humidities under isothermal conditions (e.g. 25°C). Peters and Ewing (1997) present results to show that adsorption of water molecules on NaCl crystals occurs for water P_v/P_{vd} [vapor pressure/vapor pressure at the deliquescence point (75% RH)] less than 0.25 as a nonuniform monolayer and continues until about 0.8 where the multilayers of water molecule start some irreversible dissolution of the smooth crystal surface. At $P_v=P_{vd}$ water droplets are clearly visible and extensive dissolution of the NaCl surface is evident. The literature shows that the distribution of water molecules on the cleaved NaCl crystal surface is not entirely uniform at any humidity below the deliquescence point. Water molecules form islands with some hydrogen bonding such that there may be more than one layer of water molecule in an island and vacant adjacent spaces. Furthermore, the water molecules on the surface appear to be ice-like for monolayers but multilayers soon

appear to be more like a liquid with respect to reflected infrared radiation spectroscopic signals.

Using the X-Ray deffraction method Chikazawa et al. (1972) investigated hydroscopic effects on KCl powders. They found an abrupt change in the X-Ray intensity at 55% RH when the relative humidity was increased from 25% to 75% suggesting, perhaps, a change from monolayer adsorption below 55% RH to multilayer adsorption. The X-Ray result on KCl appears to be consistent with the infrared study of NaCl by Peters and Ewing (1997) but the critical P_v/P_{vd} ratios differ slightly.

The research findings for pure crystal and water adsorption/dissolution raise some interesting speculation for multicomponent crystalline surfaces such as potash that have a small but significant concentration of carnallite ($KMgCl_3 \bullet 6H_2O$) and halite (NaCl) along with the main content sylvite (KCl). Peng et al. (1999) found the deliquescence point for crystalline potash surfaces to be 52% RH and this is primarily because carnallite is present in a sufficient concentration to dominate the low humidity water vapor adsorption and dissolution of the surface. At increasing relative humidities the dissolution process continues where some NaCl and KCl dissolution may occur but carnallite is first depleted from the surface (e.g. 52% RH and X=0.3%) and at still higher humidities (e.g. 75% RH and X=2.5%) halite is depleted. Depending on the temperature and at about 85%RH, the sylvite deliquescence point is reached so the surface humidity can not increase while thermodynamic equilibrium exists. That is, higher humidities will lead to the dissolution all the KCl. Berner (1978, 1980, 1981) has known that rate of such a dissolution process is diffusion limited.

If the same pressure ratios (P_v/P_{vd}) apply to potash particles as to pure NaCl crystals, then we might expect water vapor adsorption to start below 13%RH and dissolution of the surface to start at about 40% to 45% RH and continue to increase for increasing relative humidities. Since the distribution of water molecules is non-uniform over the surface of NaCl crystals. many questions can be raised for potash with its three types of surface species. How will water be distributed on multicomponent potash particle surfaces? At what moisture concentration will dissolution cause dust formulation and caking to occur after drying? At what moisture content will this surface layer be continuous enough to allow the flow of liquid water due to gravity? Will the top layers of potash be somewhat depleted of carnallite when some of the liquid drains by gravity through a potash bed to lower regions? If so, how will this redistribution of carnallite alter the dissolution process and redrying if that occurs? How do small concentrations of anti-caking agents on the particle surfaces inhibit the formation of dust and caking after redrying of surfaces that have undergone some dissolution? This thesis does not deal with any of these important questions directly. However, it will be shown that the question of the moisture concentration when capillary drainage appears to start in potash and when it is significant can be inferred from the results. It is speculated that when this occurs, the problems with dust formulation and caking, which likely starts at humidites slightly higher than the onset of dissolution, will be amplified and made worse as the moisture content is increased and the initial distribution of surface constituents will be substantially altered as a result of any flow of the surface liquid.

Pyne et al. (1996) studied the interaction between water vapor and granular potash fertilizers. He used an isothermal heat conduction calorimeter to measure the rate of water vapor uptake by potash as a function of water vapor pressure over very small potash samples. Their results show that there are two transition reactions for moisture uptake with increasing relative humidity, one occurring at about 60% R.H where significant moisture accumulation begins and the other at about 85% R.H. In a recent research work, Hansen et al. (1998) use the same method to investigate the effect of anticaking agents on the thermodynamics and kinetics of water sorption by potash fertilizers. Caking research is reported by Walker et al. (1998) for mixed granular nitrogen, phosphorus and potassium (NPK) fertilizers. Their research indicates that the caking process is dominated by free water accumulation and movement through capillary adhesion and a crystal bridging process after drying.

Recently, Peng et al. (1999) modeled the thermodynamic state of potash particle surface aqueous solution to describe the interaction between the aqueous ions. Using the thermodynamics of electrolyte solutions, Peng solved the problem of the equilibrium dissolution reaction of potash with moisture as a function of the adjacent air relative humidity. In the initial stage of dissolution at a low moisture content with the surface aqueous solution saturated with three solids (sylvite, halite and carnallite), the equilibrium relative humidity of the surface aqueous solution is about 52%, with a slight temperature dependence. This relative humidity is defined as critical relative humidity for the onset of dissolution as a consequence of multi-layers of water molecules on the surface. It has this critical humidity because carnallite is on the surface. When a dry

potash sample is exposed to humid air with a humidity less than the critical relative humidity, potash will adsorb some water vapor by Van der Waals forces. When the relative humidity exceeds 52% R.H, the chemical potential (partial Gibbs free energy) of water vapor in humid air is higher than that of water in surface aqueous solution, then the water vapor will condense continuously and dissolve part of the potash near the interface until a new equilibrium is reached. This dissolution equilibrium calculation establishes the relationship between the relative humidity and equilibrium moisture content.

Heat and moisture transfer in granular potash beds is a coupled process. The heat released by adsorption, condensation, and dissolution will change the temperature of both the potash particles and the air within the pores of a particle bed. The enthalpy change of potash-moisture interaction was measured by Pyne and Hansen. For all the different types of potash, they reported a combined enthalpy change around 2090±165 kJ/kg regardless of moisture content, which is equal to the latent heat of condensation of water vapor (44 kJ/mole) minus the heat of solution (6±3 kJ/mole).

A somewhat different result was presented in recent research work submitted for review by Peng et al.(2000a). They measured the thermal energy released during a potash-moisture interaction using the method developed by Tao et al. (1992) for two typical types with slightly different surface chemical composition of potash fertilizer. The combined enthalpy change (including heat of adsorption, heat of dissolution and heat of solution) is found to be a function of moisture content and trace chemical impurities of potash fertilizer produced using the flotation method and the recrystallization method. At

low moisture content, the enthalpy change is much larger than the latent heat of condensation which declines with the increasing moisture content to about 85% of the latent heat of condensation.

Heat and mass transfer due to air flow through a granular potash bed is also studied by Peng et al.(2000b) where experimental measurements are compared to simulation results from a numerical model. A one-dimensional experimental set-up was used to measure the temperature and air humidity response and mass gain of a potash bed subject to a step change in air flow. A porous media mathematical model was developed to predict the transient temperature and moisture content distributions. The transport processes were modeled as non-equilibrium heat and mass transfer process between the porous solid and air flow gaseous phases. The state of the surface electrolyte solution is modeled by the thermodynamics of an electrolytic solution (Peng et al. 1999). Agreement between the experimental data and numerical model is found to be within the experimental uncertainty for most tests indicating that the temperature of the air flow through the potash bed differs from that of the adjacent potash particles while the transient process continues.

Research on caking in fertilizer products has been ongoing since the early 1930s. Thompson et al. (1972) presented a comprehensive review and experimental study of the caking process in typical granular fertilizer products. His results showed that moisture content, pressure, temperature and time are all necessary to create any significant caking measured in exposed plastic bags subject to a drop test at the end of the test duration. He

concluded that crystal bridging is not a major cause of caking. Rather, stress is essential because it alters the solubility of salts and the pore pressure of thin aqueous films. Anticaking agents restrict crystal dislocations, by inhibiting crystal dissolution and growth, and by reducing the tensile strength of the caking bond by surfactant action. Walker et al.(1998) continued the research work on caking for mixed granular nitrogen, phosphorus and potassium fertilizers. He indicated that the caking process is dominated by free water through capillary adhesion and crystal bridging processes.

1.5 OBJECTIVES

It appears that no research has been published in which experimental data are compared with numerical model simulations for humid air flowing over potash by free or forced convection. This problem is fundamental to most potash handling and storage situations so it is of the most practical significance. The moisture accumulation thickness, or boundary layer is usually small with respect to other dimensions. It was shown that moisture accumulation of the bulk volume of potash is most important during storage and conveying of potash. Moisture accumulation may also occur during potash mixing processes but these are of such a short duration that they are likely insignificant regarding moisture accumulation. Nonetheless, the mixing processes are very important regarding the redistribution of potash from one storage container or building to another. The surface exposure of low temperature potash and the folding into internal potash regions of layers of moist potash are the most important consequences of these mixing processes.

In this research it is proposed to treat the potash handling process and warehouse storage diffusion processes as a coupled one-dimensional transient heat and moisture diffusion problem at the air-potash interface. The previous discussions imply that the main objectives of this research should be:

(1) to develop a numerical model to simulate the one-dimensional transient heat and moisture transfer process during a typical handling and storage period.
(2) to validate the model using measured data of temperature and moisture distributions and specify the uncertainty in these data.
(3) to investigate a wide range of property variations with this model.
(4) to investigate with this model some typical alternative physical processes with typical bulk potash configurations.

In order to achieve the above objectives, a number of steps are required to measure potash properties and prepare the test section and test facility for the experiments. These are:

1. Measure the properties of granular potash fertilizer in a bed that are essential for modeling, namely: permeability and porosity, average particle size, specific surface area of particle and apparent thermal conductivity.

2. Develop and instrument a one-dimensional potash bed test facility and implement a data acquisition system to record the necessary parameters related to each test. Calibrate the sensors required to perform the experiments.

3. Select a wide range of typical quasi-steady test conditions and measure the temperature profiles and moisture accumulation profiles throughout the potash test bed during and after one-dimensional transient diffusion tests. Investigate the influence of changing key parameters such as: temperature gradient through the potash bed, particle size and test duration on temperature profiles and moisture accumulation profiles.

4. Compare the measured data and numerical simulations for each test and discuss any discrepancies that are outside the uncertainty limits of the data. For various parameters used in the model, investigate the sensitivity of the important properties.

1.6 OVERVIEW OF THE THESIS

The description and formulation of the theoretical / numerical model is in Chapter 2. The method of solution is outlined.

The test apparatus is presented in Chapter 3 along with the instrumentation and the uncertainty expected for measurement of temperature, humidity and moisture content.

Four specially designed trays are used to allow moisture transfer through a potash bed in the test section of the test loop.

Chapter 4 shows the comparisons between experimental data and numerical simulations. This includes a sensitivity study of the key parameters used in the model.

Chapter 5 presents simulation studies of the case of moisture diffusion from a thin layer of moist potash that has been folded into the interior of a large potash bed and for moisture diffusion into cold potash that has been placed on a typical conveyor belt.

The summary and conclusions are presented in Chapter 6.

The Appendices include: (1) experimentally measured data for potash properties with their uncertainties, (2) experimental data and simulation comparisons for other tests, and (3) computer program written in Fortran.

CHAPTER 2

THEORETICAL / NUMERICAL MODEL

In this chapter, a theoretical/numerical model is developed. The purpose of this model is to simulate the transient heat and moisture transfer within granular potash fertilizer during shipping and warehouse storage. After the model has been developed and validated by experimental data, it can be employed as a convenient tool to predict moisture accumulation under a wider range of operating conditions which differ somewhat from the test conditions.

This chapter gives a detailed description of the coupled heat and moisture transfer problem. The analytical formulation of the problem is reduced to a transient one-dimensional problem because two or three-dimensional effects are rarely significant. The governing equations and appropriate boundary conditions are discussed. Modeling the adsorption of water vapor and dissolution of granular potash is presented as a transient one-dimensional problem which is at a thermodynamic equilibrium condition at each point in space and time. Finally, the numerical formulation and simulation method is outlined.

2.1 PROBLEM STATEMENT

A one-dimensional heat and moisture transfer problem in porous media is illustrated in Figure 2.1. In this problem a dry bed of potash at room temperature, T_r, is suddenly subjected to a step change in the airflow speed, V_∞, temperature, T_∞, and

relative humidity, ϕ_∞, over the top of the potash test bed while the cold surface temperature at the bottom is changed to T_c. The impermeable adiabatic side walls cause the problem to be one-dimensional.

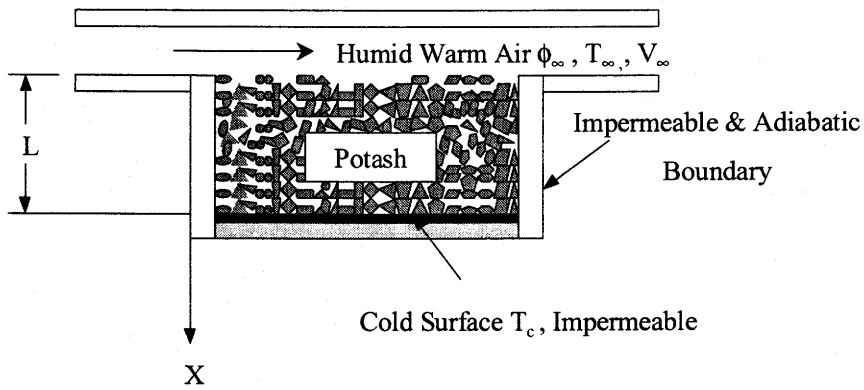

Figure 2.1 Schematic Diagram of the Test Section

The system test section is a rectangular porous media of granular potash particles which are initially dry and at temperature T_∞. All the side walls are impermeable and insulated. At time zero, humid air flows steadily across the top of the test section at $x = 0$ at room temperature (T_∞) with humidity ratio (ϕ_∞). At $x = L$ a uniform temperature (T_c) is implied on an impermeable cold bottom surface at time zero.

2.2 LOCAL VOLUME AVERAGING

The governing equations for the heat and mass transport in a porous medium are derived by employing the local volume averaging technique on the basic equations of mass, and energy transport. A representative elementary volume (**V**) is selected to represent the local average properties at each point in the domain of granular potash particles. The elementary volume **V** is composed of three phases: the solid phase V_σ, the liquid phase V_β, and the gaseous phase V_γ. Figure 2.2 shows the schematic of such an elementary volume within a bed of potash of thickness L.

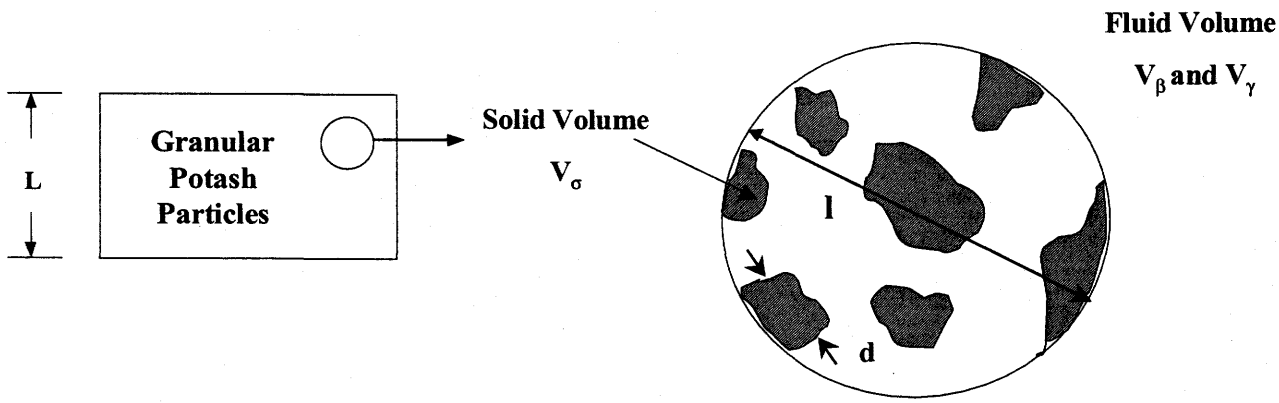

Figure 2.2 Elementary Average Volume

The elementary volume is chosen as the smallest differential volume that gives statistically meaningful local averaged properties. The addition of extra pores and surrounding solid to this elementary volume will not change the average value of local properties. This porous media model requires that $d \ll l \ll L$, where; L is the characteristic length of the potash section ($L \approx 40$ mm), l is the diameter of the elementary volume, and d is the average particle diameter, d which ranges from 0.8 to 2.6 mm depending on the type of potash.

The local volume average of a dependent variable or property, Ψ (tensor of any order), is defined as,

$$\langle \Psi \rangle = \frac{1}{V} \int_V \Psi \, dV \tag{2.1}$$

Where $\langle \ \rangle$ represents the local volume average and V is the volume of the representative elementary volume. The average values of any variable are assigned to the centroid of the elementary volume. When dealing with a quantity that has non-zero values in each phase (solid, liquid or gaseous) the volume average in equation (2.1) is not the preferred notation so we define the intrinsic phase average for phase i as,

$$\langle \Psi_i \rangle = \frac{1}{V} \int_{V_i} \Psi_i \, dV \tag{2.2}$$

Therefore, the total volume average is related to the intrinsic phase average by the volume fraction of the phase i. That is,

$$\langle \Psi \rangle = \varepsilon_i \langle \Psi_i \rangle \tag{2.3}$$

Where ε_i is the volume fraction of phase i .

The equations governing the transport phenomenon within the granular particles also deal with the gradient terms. Therefore, in order to average the properties locally for the porous medium in the transport equations, the average of a spatial gradient has to be replaced with the gradient of an average. This transformation was presented by Slattery (1969; and 1981 p.196-199), and a detailed version was given by Whitaker (1969). The resulting theorem for the volume average of a gradient is given by

$$\langle \nabla \Psi \rangle = \nabla \langle \Psi \rangle + \frac{1}{V} \int_{A_{sf}} \Psi \cdot \vec{n} dA \tag{2.4}$$

where A_{sf} is the interface area between solid and fluid inside V.

The theorem for the volume average of a divergence (for a vector or a second order tensor, $\vec{b}$) is given in equation 2.5.

$$\left\langle \nabla \cdot \vec{b} \right\rangle = \nabla \cdot \left\langle \vec{b} \right\rangle + \frac{1}{V} \int_{A_{sf}} \vec{b} \cdot \vec{n} dA \tag{2.5}$$

Another important fact that follows from the length scale constraints is that the volume average of a volume averaged quantity is equal to the volume average of that quantity. That is,

$$\langle \langle \Psi \rangle \rangle = \langle \Psi \rangle \tag{2.6}$$

Using these definitions and equations, the general transport equations can be locally volume averaged. The closure problem is to find a good representation for the surface interface area terms in (2.2), (2.4) and (2.5). A detailed discussion of this problem can be found in Carbonell and Whitaker (1984).

2.3 ASSUMPTIONS AND GOVERNING EQUATIONS

There are many assumptions used in obtaining the local volume averaged governing equations. Those assumptions are not discussed here but may be found in

detailed derivations such as Carbonell and Whitaker (1984), and Kaviany (1991). The formulation presented here is to give a flavor of the approach used, not the details. As a result, only the most important assumptions and restrictions to the equations will be discussed.

These are:

(1) The airflow over the top of granular particle test bed is one-dimensional and steady.

(2) The transport processes within the potash bed are strictly molecular diffusion for moisture transfer and conduction for heat transfer. There is no bulk fluid flow by forced convection or natural convection. Experimentally this will be verified by measuring the pressure drop across the top of the test section. In addition, the radiation between and through the potash particles is assumed to be either negligible or small enough so that it could be included as part of the thermal conductivity.

(3) The configuration used in the model is cooling from below with warm air above. This configuration supresses natural convection and permits the assumption of no significant convection in the gaseous phase.

(4) The heat and mass transfer problem is assumed to be independent of any bulk motion of surface liquids that accumulate on the particles during the dissolution process.

(5) The porous system, which consists of the solid, liquid and gaseous phase, is assumed to be in a local thermodynamic equilibrium state. Peng et al.(2000b) showed that this is not the case when air flows through the potash at a significant speed(e.g. 0.1 m/s). The gas phase is treated as an ideal gas mixture and all phases have the same temperature and pressure at any point implying that surface tension effects are negligible with respect to heat and mass transfer.

(6) It is further assumed that the porous medium properties are homogeneous and isotropic except for effective thermal conductivity and latent heat term which depend on moisture content.

(7) When granular potash uptakes moisture, a thin layer of electrolyte with ions of K^+, Na^+, Mg^{++}, and Cl^-.will form on the particle surface. The state of this surface electrolytic solution is modeled by the thermodynamics of the electrolytic solution proposed by Peng et al.(1999). It is assumed that the chemical reaction at the particle surface only changes the solid phase volume fraction. It doesn't change other physical properties of the system.When local relative humidity is less than 52% within potash, the moisture accumulation is determined by adsorption / desorption isotherm; when local relative humidity exceeds 52%, the moisture accumulation is determined by dissolution. When the local relative humidity reaches 85%, all the solid phase granular potash will be dissolved to liquid state electrolyte.

(8) Liquid electrolyte solution motion due to capillarity and gravity is assumed to follow Richards equations for the drainage of liquids in a partly saturated porous media. This is coupled to the other equations only through the mass transfer rate.

The resulting governing equations are presented below. The local volume averaging symbols, $\langle\ \rangle$, are eliminated here and throughout the rest of the thesis because all the dependent variables are volume averaged. The set of governing equations required to solve for each dependent variable is:

1. Gas diffusion of water vapor:

$$\frac{\partial\left(\varepsilon_\gamma \rho_\gamma\right)}{\partial t} - \dot{m} = \frac{\partial}{\partial x}\left(D_{eff} \frac{\partial \rho_\gamma}{\partial x} \right) \tag{2.7}$$

where:

$$D_{eff} = \frac{\varepsilon_\gamma \cdot D}{\tau} \tag{2.8}$$

2. Energy transfer through temperature gradients:

$$\frac{\partial\left(\rho C_p T\right)}{\partial t} = \frac{\partial}{\partial x}\left(K_{eff} \frac{\partial T}{\partial x} \right) - \dot{m} Q \tag{2.9}$$

where the phase-averaged properties are defined as:

$$\rho = \rho_\sigma \varepsilon_\sigma + \rho_\beta \varepsilon_\beta + \rho_\gamma \varepsilon_\gamma \tag{2.10}$$

$$C_p = \frac{\varepsilon_\sigma (\rho_\sigma C_{p\sigma}) + \varepsilon_\beta (\rho_\beta C_{p\beta}) + \varepsilon_\gamma ((\rho C_p)_a + (\rho C_p)_v)}{\rho} \tag{2.11}$$

$$K_{eff} = K_{eff(X=0)} + 0.45X \tag{2.12}$$

3. Continuity Equations:

3-a. Continuity equation for the solid phase

$$\frac{\partial \varepsilon_\sigma}{\partial t} - m\Omega_\sigma = 0 \tag{2.13}$$

where:

(1) When all three solid component exist in the early stage, i.e. carnallite, halite and sylvite

$$\Omega_\sigma = \frac{m_{KCl} \cdot M_{KCl}}{1000 \cdot \rho_{KCl}} + \frac{m_{NaCl} \cdot M_{NaCl}}{1000 \cdot \rho_{NaCl}} + \frac{m_{KMg} \cdot M_{KMg}}{1000 \cdot \rho_{KMg}} \tag{2.14}$$

(2) When moisture increases, all carnallite will become exhausted with only halite and sylvite left

$$\Omega_\sigma = \frac{m_{KCl} \cdot M_{KCl}}{1000 \cdot \rho_{KCl}} + \frac{m_{NaCl} \cdot M_{NaCl}}{1000 \cdot \rho_{NaCl}} \tag{2.15}$$

(3) In the last stage, only sylvite remains on the surface

$$\Omega_{\sigma} = \frac{m_{KCl} \cdot M_{KCl}}{1000 \cdot \rho_{KCl}} \tag{2.16}$$

3-b. Continuity equation for the aqueous phase

$$\frac{\partial \varepsilon_{\beta}}{\partial t} + \dot{m} \cdot \Omega_{\beta} = 0 \tag{2.17}$$

where:

(1) When all three solid component exist in the early stage, i.e. carnallite, halite and sylvite

$$\Omega_{\beta} = \frac{1}{\rho_{w}} + \frac{m_{KCl} \cdot M_{KCl}}{1000 \cdot \rho_{KCl}} + \frac{m_{NaCl} \cdot M_{NaCl}}{1000 \cdot \rho_{NaCl}} + \frac{m_{KMg} \cdot M_{KMg}}{1000 \cdot \rho_{KMg}} \tag{2.18}$$

(2) When moisture increase, all carnallite is exhausted with only halite and sylvite left

$$\Omega_{\beta} = \frac{1}{\rho_{w}} + \frac{m_{KCl} \cdot M_{KCl}}{1000 \cdot \rho_{KCl}} + \frac{m_{NaCl} \cdot M_{NaCl}}{1000 \cdot \rho_{NaCl}} \tag{2.19}$$

(3) In the last stage, only sylvite remains on the surface

$$\Omega_\beta = \frac{1}{\rho_w} + \frac{m_{KCl} \cdot M_{KCl}}{1000 \cdot \rho_{KCl}} \tag{2.20}$$

4. Volume Constraint:

$$\varepsilon_\sigma + \varepsilon_\beta + \varepsilon_\gamma = 1 \tag{2.21}$$

5. Thermodynamic Relations:

$$P_\gamma = \rho_\gamma R_\gamma T \tag{2.22}$$

$$P_a = \rho_a R_a T \tag{2.23}$$

$$P_g = P_a + P_\gamma \tag{2.24}$$

$$\rho_g = \rho_a + \rho_\gamma \tag{2.25}$$

6. The Clapeyron equation for the saturation condition:

$$P_{cg} = P_{cg}^0 \exp\left[-\left[\frac{\Delta i}{R_{cg}}\left(\frac{1}{T} - \frac{1}{T_0}\right)\right]\right] \tag{2.26}$$

7. Moisture Content:

$$\frac{\partial X}{\partial t} = \frac{m \cdot \nu}{\left(1 - \varepsilon_\gamma^0\right)} \tag{2.27}$$

The above set of equations constitute the basic equations required to solve the heat and water vapor transfer problem at any point in the porous media. Aside from the chemical mass equations they are the same equations. To complete this formulation the appropriate boundary and initial conditions must be specified as used by Tao et al.(1992), Simonson et al.(1993), Mitchell at el. (1993) and Hong and Besant (1996) when they modeled heat and mass transfer in fiberglass insulation.

This formulation does not account for any liquid drainage through the potash bed due to gravity forces. Liquid drainage must be accounted for using the Richards equation for liquid drainage in a porous media. This is left for future research.

2.4 BOUNDARY AND INITIAL CONDITIONS

For the airflow over the test section, the temperature and water vapor density are known values or calculated from the known properties. The bottom plate is impermeable and the temperature is known from experiment data. For the insulated side walls, the heat flux and mass flux are set to zero. Since the granular potash is put into the test section without any mechanical vibration and shaking the test bed properties are taken for unshaken case. Figure 2.3 shows the appropriate boundary conditions for the governing equations.

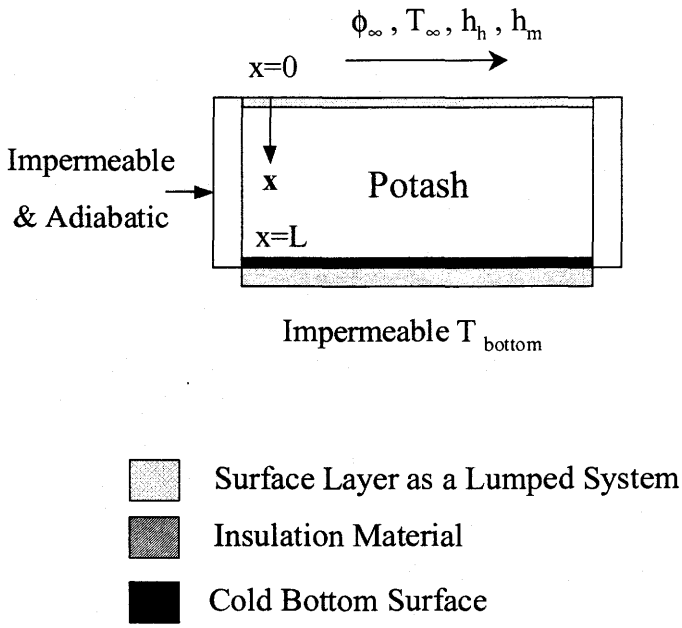

Figure 2.3 Boundary condition for simultaneous heat and mass transfer

The boundary condition at x=0 is taken to be a lumped system (i.e. this layer has no temperature or humidity gradient) and includes a convective boundary condition. The exact rate of this moisture pick up at the top surface node will be confirmed from experimental findings. Mathematically, these boundary conditions for a thin layer of thickness δ_s are:

$$\delta_s \frac{\partial(\rho C_p T)}{\partial t} + \dot{m}''|_{x=0} Q = K_{eff} \frac{\partial T}{\partial x}|_{x=0} - h_h(T|_{x=0} - T_\infty) \tag{2.28}$$

for energy and

$$\delta_s \frac{\partial(\rho')}{\partial t} + \dot{m}''|_{x=0} = D_{eff} \frac{\partial \rho_\gamma}{\partial x}|_{x=0} \tag{2.29}$$

for moisture transfer

where:

$$\rho' = \varepsilon_\beta \rho_\beta + \varepsilon_\sigma \rho_\sigma X + \varepsilon_\gamma \rho_\gamma \tag{2.30}$$

These equations apply to the small region, δs, at the surface of the potash bed where it is assumed there is a small but significant air velocity through the porous media. Below this region in the potash bed there is assumed to be no air movement – so the moisture in the air is transferred by molecular diffusion only.

The subscript ∞ refers to the ambient airflow over the potash test section. δs is the thickness of the first or top layer which is estimated to be about the size of the average particle diameter and $\dot{m}''$ is the water vapor phase change rate per unit surface area of particles in the top layer and is expressed as:

$$\dot{m}''\big|_{x=0} = h_m S_v \delta_s \rho_\gamma \left(W\big|_{x=0} - W_\infty\right) \tag{2.31}$$

where :

S_V is specific surface area of the granular potash (m^2/m^3)

$W|_{x=0}$ & W_∞ are moisture content of the interface of the first layer and ambient air respectively.

The heat and mass transfer coefficients are related by analogy using Lewis relation. That is, for air and water vapor mixtures:

$$h_m = \frac{h_h \cdot U_{dp}}{\rho_g \cdot C_p \cdot U_\infty} \tag{2.32}$$

where:

U_{dp} is the selected Darcy velocity within the top surface region δ_s. This velocity is estimated using experimental data and much less than the average ambient air velocity over the top, U_∞

The heat transfer coefficient h_h is found from the Gnielinski correlation for turbulent flow at low Reynolds number [Incropera and Dewitt (1996)].

The bottom boundary condition at x=L is slightly more complicated than an impermeable plate at a specified temperature. In the experiment, a contact resistance inevitably exists between granular particles and aluminum plate. This is accounted for in the numerical model using the method by Tao et al. (1992). A similar approach is taken for any internal discontinuity in the potash test bed such as between two test bed trays where a screen separates one tray from the next.

The energy balance for the granular particles and contact resistance allows the determination of the temperature boundary condition for granular particles at x=L. Assuming a quasi-steady state at the cold plate boundary, the mathematical expression of the energy balance is:

$$-K_{eff}\left.\frac{\partial T}{\partial x}\right|_{x=L} - \dot{m}''|_{x=L} Q = \frac{T|_{x=L} - T_{bottom}}{R''_{ct}} \qquad (2.33)$$

where R''_{ct} is the contact resistance which is estimated using the experiment data and $\dot{m}''|_{x=L}$ is the rate of phase change at x=L.

When the local relative humidity at x=L is below saturation, the local water vapor density at x=L is solved by applying the condition of an impermeable plate. Mathematically, it is:

$$\frac{\partial \rho_\gamma}{\partial x}\Big|_{x=L} = 0 \tag{2.34}$$

When the air at x=L reaches saturation, the local relative humidity is set to 100% and Clapeyron equation (2.24) is used to calculate the vapor density boundary condition at x=L.

With phase change taking place at the surface of the cold plate at x=L, the physical character of this phase change surface area changes abruptly from the solid cold plate to granular potash particles. Moisture is unable to penetrate the cold plate at x=L. If the local humidity is less than 100%, the liquid solution is assumed to have the same state as in the adjacent potash in the test cell. However, when saturation exists at x=L the boundary phase change flux is determined from :

$$\dot{m}'' = D_{eff} \frac{\partial \rho_\gamma}{\partial x}\Big|_{x=L} \tag{2.35}$$

Initially, the granular potash test bed is assumed to be at room temperature and equal to the air inlet airflow temperature and has a very small moisture content. Mathematically, the initial conditions are:

$$T(t=0,x)=T_\infty, \text{ and } \phi(t=0,x)=10^{-3}\,\% \tag{2.36}$$

2.5 ADSORPTION /DISSOLUTION MODELING

In the previous section, the governing equations for the problem are given for the case that does not fully specify the hygroscopic effects (adsorption/dissolution). In the region throughout the potash bed where the local relative humidity is less than 100%, the granular potash will undergo an adsorption or dissolution process. During these processes, the Clapeyron equation cannot be used to describe the relation between the vapor pressure and temperature. Therefore, when hygroscopic effects are included, additional equations are required to formulate the problem correctly. These supplementary equations describe the equilibrium adsorption and dissolution masses and heats of adsorption, desorption, and dissolution.

Potash is mainly composed of potassium chloride (KCl). The existence of the surface impurities (i.e.$KMgCl_3 \bullet 6H_2O$, NaCl), which are deposited on the surface of each particles during processing potash (i.e. flotation or recrystallation process, with a subsequent drying process), causes the potash-moisture interactions to significantly deviate from that of pure KCl. In a humid environment, potash will adsorb moisture from the surrounding air to form a monolayer. Then, as more water molecules are adsorbed multilayers are formed. Finally, a part of the potash is dissolved in a aqueous electrolytic solution on the surface of each particle. As soon as the aqueous layer is formed, the chemical potential differences of every component in the system become important in determining the final equilibrium moisture content for a given relative humidity in the air.

2.5.1 ADSORPTION ISOTHERM DATA AND DISSOLUTION DATA

In the research work by Peng et al. (1999), the interaction between potash and moisture at equilibrium has been experimentally and theoretically investigated and modeled. According to Peng's findings, there is a critical relative humidity around 52% for the onset of condensation. When totally dry potash is exposed to air with a relative humidity lower than this critical humidity, potash can adsorb some moisture, but water vapor condensation will not occur. However, when the relative humidity is higher than this critical one, the chemical potential (partial Gibbs free energy) difference between the water vapor in the air and the water in the surface aqueous solution will provide a diffusion driving force, and the water vapor will condense continuously on the surface until a chemical equilibrium is reached. During this condensation process, the surface carnallite ($KMgCl_3 \bullet 6H_2O$) will disappear first, and then, with increasing humidity, the sodium chloride (NaCl). If potash is exposed to a relative humidity higher than 85% or the deliquescent point for KCl, the water vapor condensation will continue until all the potash dissolves creating only an electrolytic solution.

Since this surface aqueous solution layer is usually very thin for tests of short duration (e.g., less than 10 μm) on each particle, diffusion within this thin liquid layer does not cause significant variations in composition within the aqueous solution. This

allows us to assume that the surface solution is uniform in concentration and it is in a thermodynamic equilibrium state with the potash solid in each particle.

Moisture content (X) has been employed to characterize the mass of water picked up by granular potash by adsorption and condensation. It is defined as:

$$X = \frac{\Delta m}{m_{dry}} \tag{2.37}$$

where Δm represents the mass of water that changes phase per unit volume and m_{dry} is the mass of dry potash per unit volume.

The moisture content of potash is described by analytical expressions for three regions of moisture uptake: adsorption, transition and dissolution [Peng et al. (1999)]. For a relative humidity less than 52%, the potash will adsorb moisture by adsorption. For adsorption, the experimental data for moisture content is best fitted by the Brunauer-Emmett-Teller (BET) equation,

$$\frac{X}{X_m} = \frac{C \cdot \phi}{(1-\phi)[1+(C-1)\phi]} \tag{2.38}$$

where X is the moisture content, ϕ is the relative humidity and X_m and C are the empirical constants. The experimental constants were found to be, C=1.54, and X_m=0.098%. The typical adsorption isotherm for one type of granular potash with an average particle diameter of 0.8-mm is shown in Figure 2.4. This adsorption isotherm at 22°C is based on the equilibrium data of Peng et al. (1999) and is in good agreement for

$0<\phi<0.48$. The moisture content of potash at 22°C does not exceed 0.09% for this adsorption region.

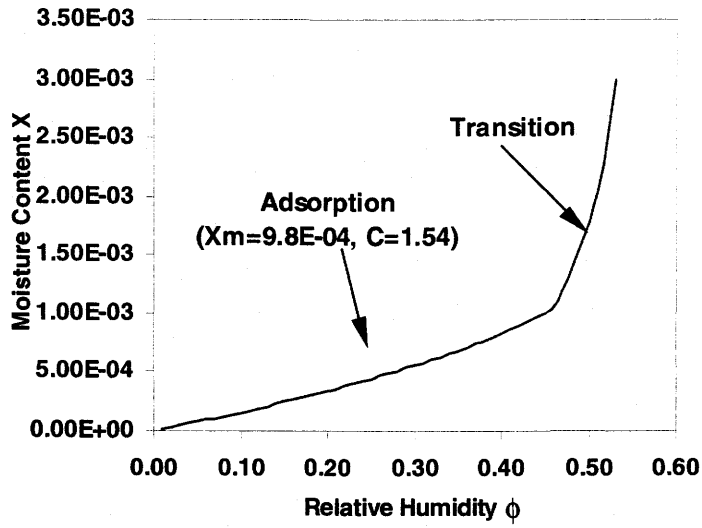

Figure 2.4. Adsorption Isotherm (22°C) for Rocanville Standard Potash ($0<\phi< 0.53$) (d_p=0.8 mm) [Peng et al. (1999)]

In the transition region of relative humidity ($0.48<\phi<0.53$), the equilibrium adsorption moisture will increase with ϕ to the dissolution equilibrium moisture content at ϕ=0.53. The transition region is approximated by a quadratic equation (2.39) by fitting measured data at three points $[0.48,X_{ad}]$,$[0.51,0.5(X_{ad}+X_{cr,d})]$, and $[0.53,X_{cr,d}]$, where X_{ad} is calculated by equation (2.38) at ϕ=0.48 and $X_{cr,d}$ is determined at the point where all the solid state carnallite disappears from potash particles and exists as Mg^{++}, Na^{+}, Cl^{-} and K^{+} ions in the electrolytic surface solution.

$$X = a'\phi^2 + b'\phi + c' \quad (0.45<\phi<0.53) \tag{2.39}$$

where a', b' and c' are experimental constants that depend on the potash surface layer compositions and temperature. These are a'=0.4228, b'=-0.3957, c'=0.0923.

When the local relative humidity is higher than 85% all the solid state potash will dissolve. In the model, we treat the water vapor as reaching its saturation state on a liquid coated surface layer when local relative humidity is higher than 53% and less than 85% as shown by Peng et al. (1999). The dissolution equilibrium moisture content isotherm is expressed using the polynomial empirical fit equation:

$$X = \frac{1}{d'+e'\phi + f'\phi^2 + g'\phi^3} \quad (0.53 \le \phi<0.85) \tag{2.40}$$

where d', e', f' and g' are constants that depend on the chemical composition and the temperature of the surface layer of the potash.

Equation (2.40) captures the main features of the moisture content isotherms modeled by Peng. It differs slightly in shape near the moisture content when halite (NaCl) is expected to run out on the surface layer of the potash particles. Peng shows a small slope discontinuity when NaCl runs out at a specified surface mass concentration whereas equation (2.40) does not. The smooth curve given by (2.40) is expected to better represent the situation where there are slight variations in the chemical composition of the surface layer of potash on various adjacent particles. Such variations in composition on potash particle surfaces are expected to occur as a result of the large variation in

particle sizes that occur during the potash product production dewatering centrifuge and drying processes and the subsequent mixing of particles.

Figure 2.5 shows two typical equilibrium dissolution moisture content isotherms with the increasing of relative humidity. In Figure 2.5 the factor of 70 change in the moisture content scale from Figure 2.4 implies a near zero moisture content for relative humidities less than 45% where adsorption of water vapor occurs without dissolution. Only the transition region and the high moisture content dissolution region are shown in Figure 2.5. This figure clearly shows the central problem of modeling moisture content in potash at high relative humidities (e.g. 80% or higher) the moisture content is nearly independent of humidity and very slight changes in temperature can cause very large changes in moisture content.

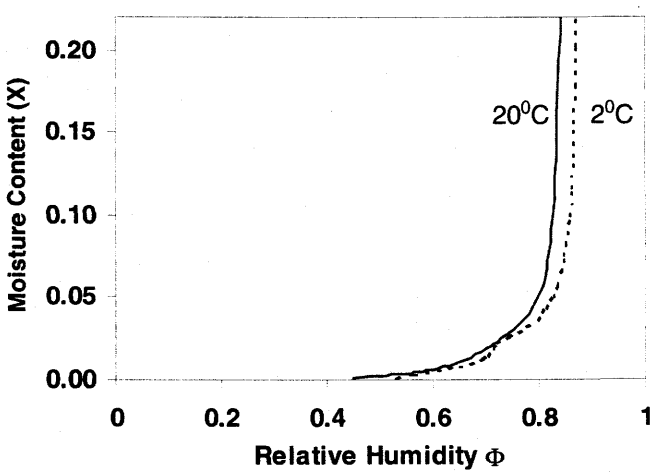

Figure 2.5 Moisture Content Isotherm for Dissolution at 22°C and 2°C for Rocanville Standard Potash ($0<\phi< 0.85$) (d_p=0.8 mm) [Peng et al. (1999)]

The rate of moisture accumulation or rate of phase change $\dot{m}$ is calculated as a residual term in the complete set of equations describing the heat and water vapor transfer. The moisture content, X, is calculated using the equation:

$$\frac{\dot{m}}{m_{dry}} = -\frac{d\left(\frac{\Delta m}{m_{dry}}\right)}{dt} = -\frac{dX}{dt} = -\frac{dX}{d\phi}\cdot\frac{d\phi}{dt} \tag{2.41}$$

Consequently, $\dot{m}$ is negative for adsorption or condensation and is positive for desorption or evaporation.

2.5.2 ENTHALPY CHANGE DURING POTASH-MOISTURE INTERCATIONS

Heat and moisture transfer in a granular potash bed is a coupled process. The heat released by adsorption, condensation and dissolution will change the temperature of both the potash particles and the pore air. When this occurs, the local relative humidity decreases, which causes the equilibrium adsorption moisture content of the particles and rate of condensation to be altered as heat is released. To simulate the heat and mass transfer process, it is necessary to characterize the enthalpy change during the potash-moisture interactions.

The enthalpy change of potash-moisture interactions was measured by Pyne et al. (1996) and Hansen et al. (1998). For all the different types of potash they tested, they reported a combined enthalpy change regardless of moisture content (X), which is equal

to the latent heat of condensation of water vapor (44kJ/mole) minus the heat of solution (6±3 kJ/mole). In a recent study, Peng et al. (2000a) measured the combined enthalpy change (including heat of adsorption, heat of condensation and heat of solution) employing the method developed by Tao et al. (1992). This measured combined enthalpy change shows a strong dependency on moisture content for small moisture content values. Peng's results agree with Pyne and Hanson when X is larger than about 1.0%.

Depending on the moisture content and local relative humidity, the potash-moisture interactions may be a monolayer adsorption, a transition multilayer adsorption with some dissolution of potash, or a water vapor condensation with dissolution of potash. Monolayer adsorption is a physical adsorption process. Moisture accumulation by this monolayer is icelike in that the water vapor has little or no transitional mobility. As the adsorption process continues, a multilayer adsorption is formed. Water molecules in thick multilayer adsorption films behave more like a large pool of free water, which will dissolve the solid potash to form a layer of electrolytic solution on the surface of each particle. When the layer is thick enough, this multilayer adsorption changes to a chemical dissolution of potash solid in a coupled physical and chemical process. Figure 2.6 illustrates these states at the surface of one solid particle where the source of water molecules deposited is from the surrounding humid air.

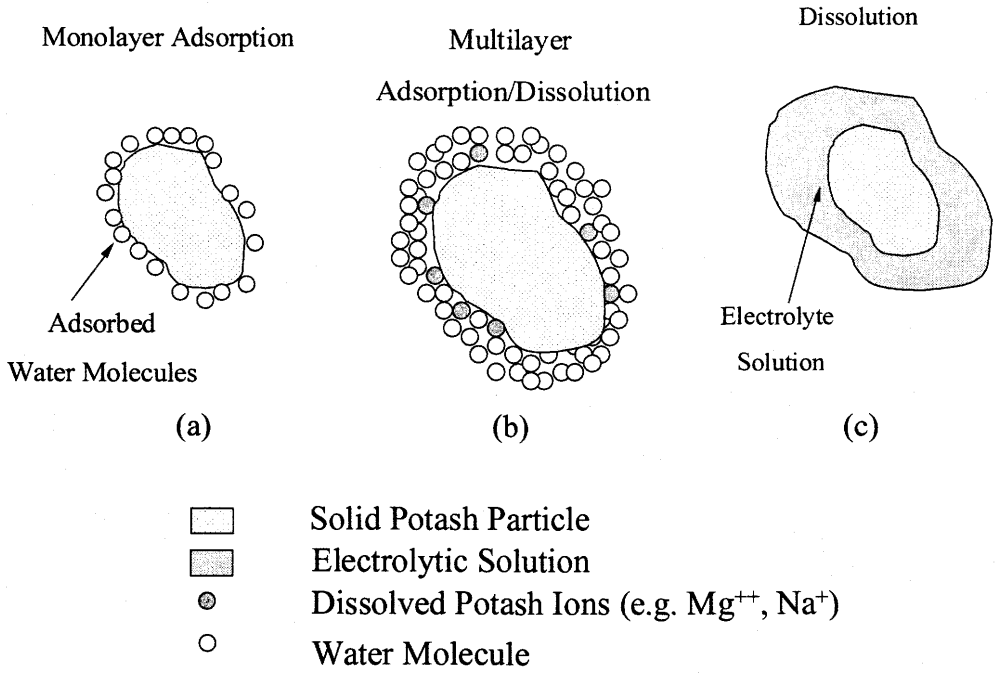

Figure 2.6 Schematic of Adsorption and Dissolution on the Surface of a Potash Particle

According to Peng's research findings, at a low moisture content the chemical dissolution is controlled by a diffusive transport process and the interface between aqueous solution and solid potash is in a saturated state. Since the aqueous solution film is usually very thin (i.e. less than 10μm), the diffusion in this thin aqueous solution film requires only a negligible concentration difference. Then the surface aqueous solution film is essentially homogeneous, and is in thermodynamic equilibrium with the solid phase. This analysis suggests that the enthalpy change in the potash-moisture interaction is a function of the particle bed moisture content, temperature, the reacting gas which is water vapor, and the composition and specific surface area of the potash bed. That is, a relationship exists such that

$$\Delta H = f(X, T, \phi, \text{potash (composition and Sv)}) \quad (2.42)$$

If the absolute temperature change is small, the dependency on temperature can be ignored.

The calculation of time average enthalpy change, Q, for a typical granular potash (Rocanville standard (dp=0.8 mm)) was empirically fit to the data using the least-squares method giving the equations:

$$\frac{Q}{h_{fg}} = -0.48X^3 + 1.77X^2 - 2.11X + 1.71 \quad (X<1\%) \quad (2.43)$$

$$\frac{Q}{h_{fg}} = 0.89 \quad (X \geq 1\%) \quad (2.44)$$

Peng et al. (2000a) did experiments where Q was measured by passing moist air at constant temperature and at various constant humidities through dry potash samples while the temperature response of the air leaving each sample was measured. The uncertainty in the calculated Q was found to be slightly sensitive to the moisture content, and is estimated to be about ±15% for most practical applications. The experimental data agree with Hansen (1998) within experimental uncertainty only for X≥1%, suggesting that Hansen's tests were done for test samples with a high moisture content.

2.6 NUMERICAL SOLUTION METHOD

The energy and vapor transfer equations are nonlinear, coupled, partial differential equations. Practically, these equations can only be solved numerically based on their discretized forms. The Control Volume Method (Patankar, 1980) is used for the discretization of the spatial terms and the fully implicit scheme is used for the transient terms (see Appendix-B for more details). A uniform one-dimensional grid mesh is built in the calculation domain with a grid point at each boundary. The TDMA is used to solve both the temperature and water vapor density profile in the space. Property spatial averaging and source term linearization techniques are used in both the energy and vapor transfer equations. The under relaxation iteration scheme is used to provide a stable solution and the solution is considered converged for any time step when the maximum difference between the current values and those of previous iteration for all of the dependent variables (T, ρ_v, $\dot{m}$, X, ε_β and ε_γ) is less than $1x10^{-4}$.

The numerical procedure starts from the property calculations based on the initial temperatures, relative humidity and moisture content distribution. The total pressure of the gas phase (P_g) is known as the atmosphere pressure. Then the density of the mixture of air(ρ_a) and water vapor (ρ_v) is obtained using the ideal gas law and the total atmosphere pressure.

The solution sequence used depends on whether the phase change is due to adsorption/dissolution (i.e. ϕ<85% at 20°C) or condensation (i.e. ϕ>85% at 20°C). In the

case of adsorption and dissolution, the rate of phase change ($\dot{m}$) is determined from adsorption isotherm curve if ϕ<48% (i.e. equation 2.38), or determined by the principle of equilibrium transition (i.e. equation 2.39) or dissolution (i.e. equation, 2.40). The volume fraction of solid state (ε_σ) and liquid state (ε_β) are calculated from the continuity equations (2.13 & 2.17). A subroutine program is used to calculate the mole number of each ion (K^+,Na^+, Mg^{++},Cl^-) in the electrolytic solution and those of the solid phase (carnallite, halite and sylvite). The volume fraction of gaseous phase is determined by the volume constraint (equation 2.21). The water vapor density (ρ_v) is calculated by gas diffusion equation (2.7). The temperature (T) is determined from energy equation (2.9) using the appropriate enthalpy change (2.43 or 2.44). Moisture content (X) is calculated from the time integral of equation (2.27).

For the case of relative humidity exceeding 85%, the particle will uptake all water vapor available until all the solid state has been dissolved or the relative humidity drops. This process can take a long time and may not be in practical except for unusual operating conditions. The solution method used treats the moisture content in saturation state when relative humidity reaches 85%. Water vapor density (ρ_v) is calculated from the Clapeyron equation and the rate of phase change ($\dot{m}$) is calculated from the gas diffusion equation. Others properties are calculated in the same way as before. More details on the numerical solution and program are included in Appendix B and J.

The problem was solved with 24 spatial nodes and 50-second time step. These number of nodes and time steps gave a stable solution. Increasing the number of spatial

nodes or decreasing the time step to 72 spatial nodes and a10-second time step had little effect on the results. The comparisons between experimental and numerical results are shown in Chapter 4.

CHAPTER 3

EXPERIMENTAL APPARATUS AND TEST PROCEDURE

The experimental apparatus and test procedure are described in this Chapter. The purpose of the experiments is to verify the theoretical/numerical model of heat and water vapor transfer and accumulation of liquid water within the potash bed. Key parameters measured in the experiments were the temperature distribution within the potash bed and moisture accumulation distribution at the end of each test. Heat flux through the bottom of the potash bed was measured but it possessed a relatively large uncertainty due to bias (± 80 W/m^2) and precision (± 30 W/m^2) for a heat flux of about 15 W/m^2. These three parameters are determined under a series of typical supply air relative humidities for constant supply and plate temperatures.

3.1 EXPERIMENT DESCRIPTION

A schematic drawing of the experimental apparatus is shown in Figure 3.1. This apparatus is designed to cause a one-dimensional transient heat and mass transfer for the selected boundary conditions at the top and bottom of the test sample of potash. Figure 3.2 shows the test section containing the test sample.

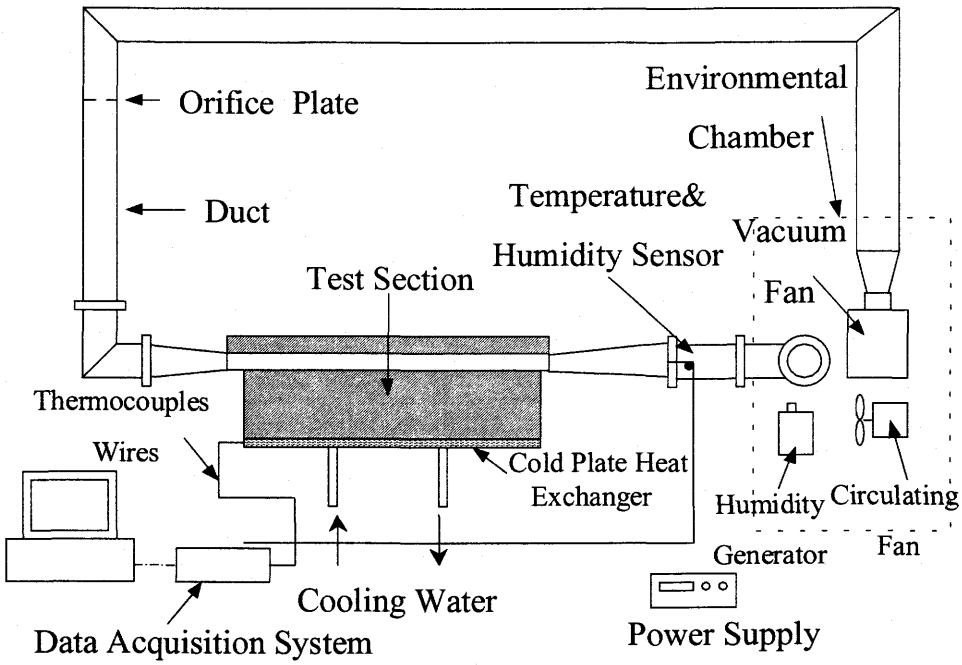

Figure 3.1 Schematic of the Experimental Apparatus Test Loop

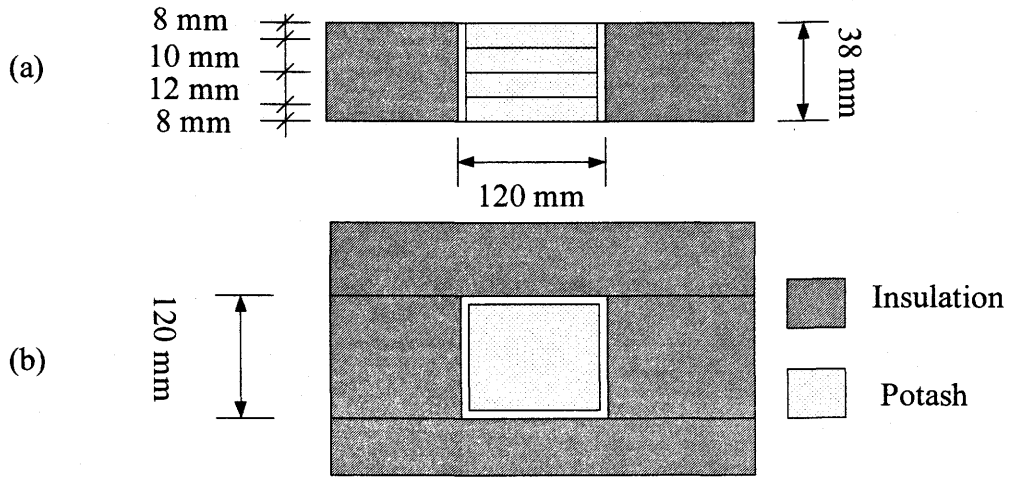

Figure 3.2 Schematic of Test Section Showing the Potash Trays Surrounded by Insulation (a) Elevation (b) Plan View

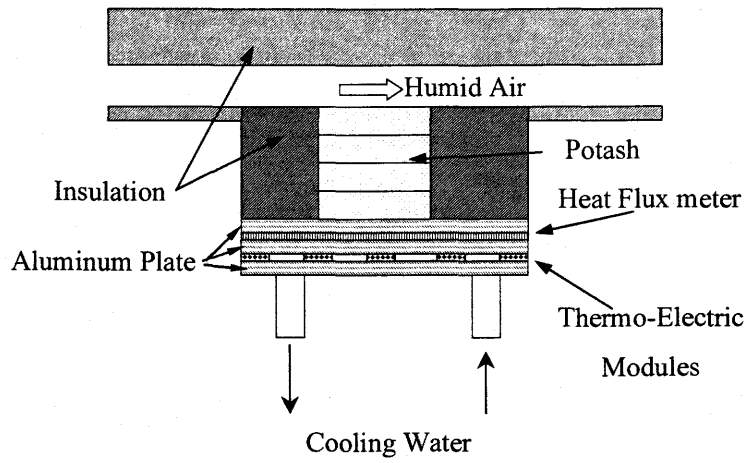

Figure 3.3 Schematic of the Test Section with Bottom Plate Cooling

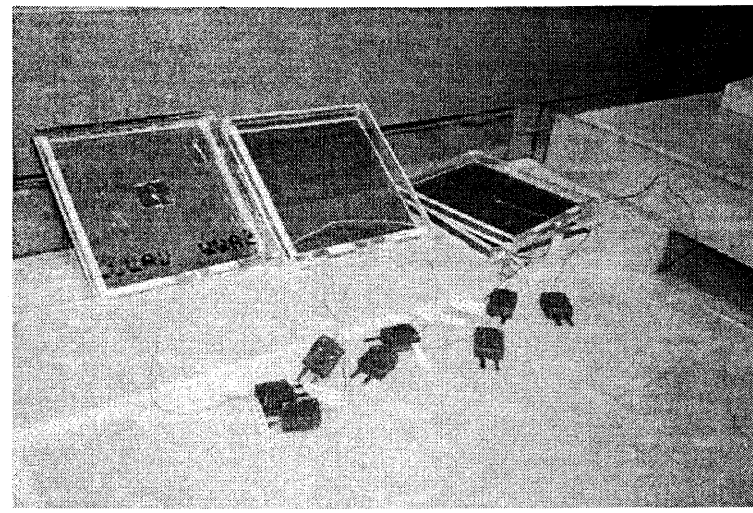

Figure 3.4 Photograph of the Trays used in the Experiments

Showing the Thermocouple Connectors for each Tray

A vacuum fan and vaporizer were placed inside the environmental chamber shown in Figure 3.1 to create the required supply air relative humidity and temperature at the test section. The water vapor generated by the vaporizer was mixed well within the environmental chamber air by another circulating fan in the chamber. The fully developed air flow was supplied to the test section through the duct covered with insulation. The temperature of the chamber was set to room temperature and was controlled using a temperature sensor. The relative humidity in the chamber was controlled by altering the electrical input to the vaporizer heater. A chilled mirror was placed inside chamber to measure the relative humidity. Sensors were mounted in the test section inlet duct as shown in Figure 3.1 to make sure the supply air temperature and relative humidity stayed within ±1°C and ±2% R.H. during each test.

The temperature distribution and mass accumulation of water vapor were measured for each tray in the test section shown in Figures 3.2 and 3.3. The test section was constructed with four layers or trays, each with a permeable fine mesh screen bottom to permit the unobstructed diffusion of heat and water vapor except for the bottom tray which had an aluminum bottom. The sides of each tray were 6mm thick Plexiglas. At the start of each test, granular potash samples are placed in each of the four stacked trays. Two or three calibrated thermocouples (uncertainty ±0.3 °C) were mounted on the bottom of each tray to measure the temperature distribution. Thermal paste (0.735 W/K•m) was used between the bottom tray and cold bottom plate for improved thermal contact. Figure 3.2 shows the dimensions of the four trays with surrounded insulation. A photograph of the four trays is presented in Figure 3.4.

The side walls of the test section were constructed by polystyrene insulation sheets (15-cm) surrounded by thin, air-tight Plexiglas walls, thereby reducing the heat loss to the surroundings and protecting against moisture transfer or air leakage. A clear space of 30mm by 120 mm between the test section lid and top of potash sample was used for the air flow. The sides and bottom edges of the test section were sealed with silicon caulking to create an air-tight box. A heat-flux meter was mounted within the bottom cold plate assembly for the measurement of heat flux. The heat-flux meter is made up of a 3.25-mm polyethylene layer sandwiched between two aluminum plates with calibrated thermocouples arranged in pairs imbedded in aluminum plates. The heat flux meter was calibrated by Mao et al. (1999) at a bottom plate temperature from -40°C to -50°C. The lower boundary condition temperature is controlled by the Melcor thermo-electric devices. Below the heat-flux meter, 15 equally spaced thermo-electric cooling devices created temperatures as low as 1°C during these tests while the heat generated by thermo-electric devices was removed by the heat exchanged using water cooling. Figure 3.3 shows the test section structure.

A standard orifice plate (uncertainty ±0.58L/s) and inclined manometer (uncertainty ±0.3 Pa) were used to measure the flow rate of air. The air flow was circulated and mixed within the environmental chamber. The air flow was steady for each test.

All the thermocouples and relative humidity sensors were connected to the channels of the data acquisition system (Model 641). This system was used to read all 63

channels of data every 50 seconds and store the data into a computer hard drive for later analysis.

3.2 KEY PARAMETERS IN THE EXPERIMENTS

Since potash has a critical relative humidity of 52% [Peng et al. (1999)], three different relative humidity values for supplied air (i.e. 45%, 65% and 80%) were chosen to represent the adsorption, humid dissolution and very humid dissolution test conditions. The supplied air temperature was room temperature at 22 °C (±1°C) and the temperature at the test section bottom was either 2°C (±1°C) or 21°C (±1°C). Although the temperature difference across a potash bed rarely exceeds 10°C in practical applications, a large difference temperature can create a significant temperature gradient and moisture accumulation in short duration tests. This test condition also helps to reduce the experimental uncertainty in the moisture measurement, which is the key parameter to be measured. Two different sizes of potash particles (0.8 and 2.2 mm) were tested for three relative humidities with and without a temperature gradient across the potash in the test section.

The channel for airflow over the top of the potash was 120mm x 30 mm and the potash in the test section had dimensions of 108 x 108 x 38 mm. The mass flow rate of air was 1.12×10^{-2} kg/s for each test. The assumption of one-dimensional molecular diffusion process in the model was checked to ensure that the any convective velocity in the potash bed would be negligible. The pressure drop across the test section was measured to

estimate the convective air velocity inside the potash test samples. Two different test conditions were tested to measure the pressure drop across the test section: polystyrene in all the four sides and potash particles at the bottom and polystyrene in the other three sides. The first condition was used to measure the pressure drop with only polystyrene sides on the channel and the second gave the pressure drop with potash on the bottom in the exact experimental condition. A very small pressure drop (i.e. 0.09 ± 0.3 Pa) across the test sample length was measured using only polystyrene sides and slightly larger (i.e. 0.12±0.3 Pa) for the case of granular potash on the bottom surface.

The Darcy velocity, U_D, was calculated from the momentum equation with an assumed air flow path length of 0.12m parallel to the top surface and experimentally measured pressure drop across the test section (0.12 Pa) and permeability ($7x10^{-9}$ m^2) for Rocanville Standard Potash (i.e. $U_D = \frac{K}{\mu} \cdot \frac{\Delta P}{L} = \frac{7x10^{-9}}{18x10^{-6}} \cdot \frac{0.12}{0.12} = 0.39 mm/s$ parallel to the open surface). Since most the airflow path lengths would be larger than 0.12m, this Darcy velocity is likely a maximum. The Reynolds number based on the average particle diameter dp=0.8 mm is calculated to be 0.02. (i.e., $\mathrm{Re}_{dp} = \frac{\rho \cdot U_d \cdot d_p}{\mu} = \frac{1.2x0.0004x0.0008}{18x10^{-6}} = 0.02$). This test condition gives justification to the assumption of molecular diffusion as the primary method of diffusion (Nield and Bejan [1992])

3.3 DATA ACQUISITION

The data acquisition system consisted of a Datatrain 386 computer and a Scientific Instruments 641 Electronic Measurement system analog to digital (A/D) board connected to sensors. The data acquisition board included 63 analog to digital (A/D) channels. These channels were used to measure analog voltage signals from the many thermocouples throughout the test apparatus and a humidity sensor in the air supply.

Sixty A/D channels were used to monitor the data. One channel was used to read the air humidity from a General Eastern Model 850 humidity sensor transducer. The rest of the channels (59) read temperatures from the type-T thermocouple sensors.

The acquisition sequence was to first read the time then read all the temperatures and air relative humidity. All these data were then stored on the hard drive every 50 seconds.

3.4 TEMPERATURE MEASUREMENT

Type-T thermocouples with accuracy of ±0.15°C were used to measure temperature. The measurements were: the upstream air temperature, the temperature distribution within the potash, the cold plate temperature and cooling water temperature. Each of these temperature measurements possessed small additional uncertainties due to positioning in the test cell.

The upstream air temperature was measured using the average of three thermocouples at the inlet of the duct. The maximum difference between these three measured temperatures was 0.4 °C for all tests and typical differences were 0.2°C during any test. This supply air temperature changed less than 1°C during an eight-hour test while the temperature difference across the depth of the potash was 20°C. Figure 3.5 shows the measured air temperature every 50 seconds for a typical test. This graph shows that the supply air temperature is nearly constant over the test duration and that all the data is well within ±0.5 °C for the entire test and ±0.15°C after the first hour of testing.

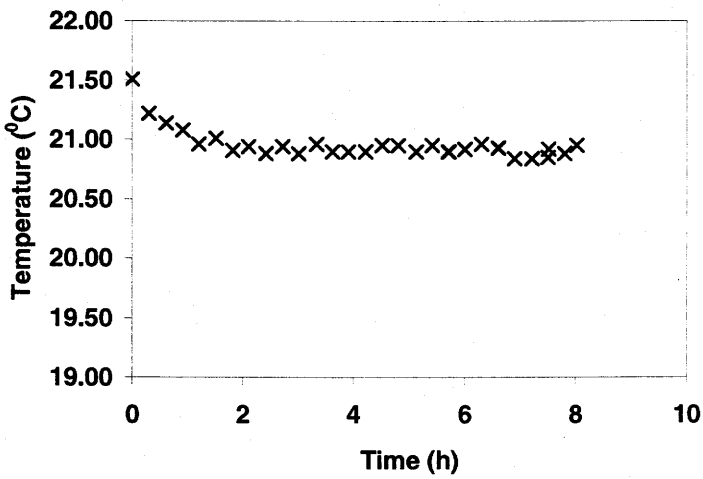

Figure 3.5 Air Supply Temperature for a Typical Test

The cold plate temperature was found by averaging readings from 20 thermocouples located on the top side of the heat flux meter which was sandwiched within a pair of aluminum plates below the potash in the test section. One thermocouple

was used to measure the temperature of water used to cool the 15 thermo-electric devices at the bottom of the test section.

Nine thermocouples were used to measure the temperature distribution within the potash bed in the test section. Figure 3.6 shows their positions in two planes. For tray #2 and #3, two thermocouples were placed in the screen on the bottom of each tray with one at the center and the other near the corner. The averaged reading was used to represent the temperature for each tray bottom. On the top tray, three thermocouples were used.

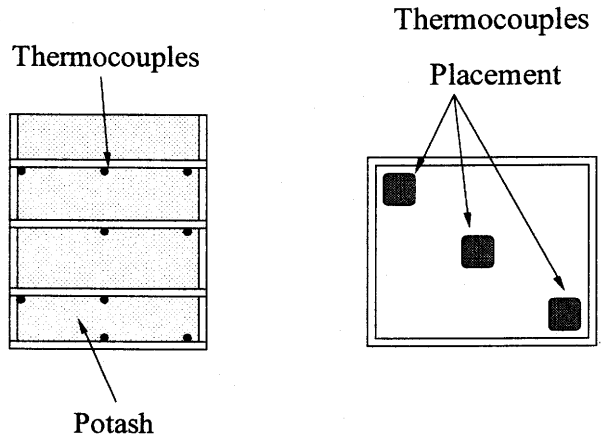

(a) Side view (b) Top View

Figure 3.6 Thermocouple arrangement for measurement of the temperature distribution within potash bed

The temperature difference measured on the bottom of each tray measured by the thermocouples was typically ±0.2 °C which is within the uncertainty limits for these temperatures.

3.5 AIR FLOW MEASUREMENT

The air flow rate was provided by a commercial wet/dry vacuum. The flow rate was measured with a 20-mm diameter orifice plate designed according to ISO standards. The orifice plate Reynolds number was around 10000 and the orifice discharge coefficient was 0.63. The pressure drop across the orifice was measured with an inclined manometer with the smallest scale of 1mm. The flow rate was constant with a fluctuation less than ±2% for each 8-hour test. The Reynolds number for the air flow above the potash test section was 8000.

3.6 HUMIDITY MEASUREMENT AND CONTROL

Humidity was measured inside the environmental chamber and in the inlet duct and upstream of the test section. A Dwyer chilled mirror (Model MB-41) was used to display the transient relative humidity inside the chamber. In the duct, a portable VAISALA relative humidity sensor was used to measure the relative humidity. This relative humidity sensor (VAISALA Model HMP 233)) was mounted inside the duct upstream of the test section. The uncertainty of the relative humidity was ±2%. Humidity control was provided by manually adjusting the power input to the humidity generator. This controller provided humidity control within ±2% R.H. Figure 3.7 shows the measured air relative humidity for the same test shown in Figure 3.6 where the average humidity is 45.3%.

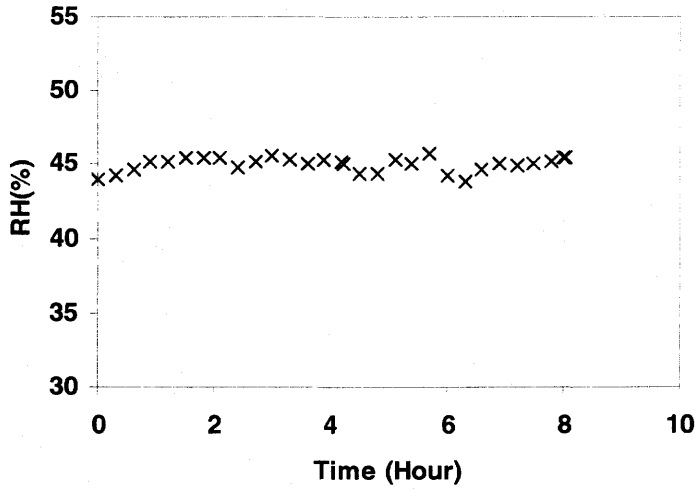

Figure 3.7 Air Supply Relative Humidity for a Typical Test

3.7 MASS OF WATER ACCUMULATION MEASUREMENT

The mass of water accumulation in the potash test bed was measured using two electronic mass scales: (a) Mettler PL200, with a resolution of 0.001g and maximum measurable mass of 200g; (b) Mettler PM6100, with a resolution of 0.01g and maximum measurable mass of 6000g. The mass in each of the four trays differed from each other. The third tray had the largest volume with a mass of potash higher than 200g and so it was measured by the type (b) scale; the other three were measured with the type (a) scale.

Because the accumulation of water in each tray is very small (i.e. often less than 0.01g), the corresponding uncertainty in the measurement is significant. Missing potash particles from trays, air movement around the scales and uncertainty within the scale

reading could all result in errors in the mass of accumulated water. Uncertainty in this mass measurement is discussed along with the data in the next Chapter.

3.8 EXPERIMENTAL TEST PROCEDURE

The test procedure used for each experiment was as follows:

1. Instruments used for measuring temperature, relative humidity, airflow rate and mass of water accumulation were selected and calibrated. Thermocouple wires were placed in the test section and quick connection thermocouples plugs were mounted on each tray.
2. Before each test, the granular potash was put in an oven to dry all the test samples at 100°C for more than 24 hours. After drying, the granular potash was removed from oven and put into a sealed plastic bucket and cooled to room temperature for another 24 hours. At this time, the granular potash was considered to be dry with a moisture content less than 10^{-4}.
3. Two hours before each test, the environmental chamber (Conviron Control System) was started with a steady state temperature set to 22°C; the water vapor generator was turned on with the electrical power to the water heater set to desired relative humidity (i.e. 45%, 65% or 85%). Two and one half hours before each each test, the cooling water valve at the heat exchanger was turned to the full-open position, the thermo-electric devices at the bottom of test section were turned on with the input power set to a selected setting. One hour before each test, the vacuum fan was turned on with

the flow rate of air determined by the reading from inclined manometer (always set to angle of 1:10) after the cover lid was placed onto the test section.

4. The mass of four empty trays with thermocouples and quick plugs attached were measured. The four clean empty plastic bags used to hold the potash test trays were labeled.
5. The computer and Scientific Instruments Electronic Measurement System were turned on. The humidity sensor was plugged in. The computer program named "Level1" was checked to read and plot such temperature profiles as: bottom plate temperatures at different positions, supply air temperature; the supply air relative humidity. The data for the operating conditions before the start of each test was read to ensure the test conditions had reached a steady state (difference of temperature less than $\pm 0.1°C$, the relative humidity less than $\pm 0.2\%$).
6. The potash samples were placed into each tray and leveled without shaking the tray. Any excess potash particles were removed by tweezers. The potash filled trays were covered with a plastic film to avoid exposing the open surface to surrounding air. Thermal paste was placed uniformly on the bottom of aluminum plate of the bottom surface of bottom tray to reduce the contact resistance between the bottom tray and bottom aluminum block plate.
7. When the system test conditions reached steady state, the "level1" program was stopped and the following steps were taken : stop the vacuum; open the cover lid; put the potash trays into test section carefully without dropping any potash particles from one tray to the lower one; plug in all of the quick connector thermocouple wires on the four trays with wires in the test section; position the insulation material

surrounding the trays with a negligible space between the surfaces; replace the section lid and seal all the joining edges with an impermeable sticky tape; place two heavy masses (around 40 kg in total) on the top of cover lid; start the vacuum again with the same flow rate; start a new program named "Test" to record all the data in the 63 analog channels; record the experimental started time. All of these steps were completed in less than 10 minutes.

8. During each test, the relative humidity in the environmental chamber was controlled by adjusting the power input. The reading of inclined manometer was recorded periodically during each test. The time elapsed during each test was recorded on computer.
9. When an experimental test was completed, the experiment was stopped using the following steps: stop the "Test" program; turn off the vacuum power; remove sealing tape and cover lid with heavy load together; cover the top tray with impermeable plate immediately; unplug all the quick connector thermocouples plugs in each tray; carefully remove surrounding insulation material around the test trays; remove the cover plate and carefully take out each potash tray; bag and seal the top three potash trays with in the pre-labeled plastic bags; carefully wipe off thermal paste at the bottom tray and pour the potash particles into labeled bag without contaminating the bag; turn off the power of thermo-electric device, environmental chamber, vapor generator, computer and Scientific Instruments Electronic Measurement System; close the cooling water valve.
10. The mass of each bagged and sealed potash tray was weighted and recorded.

11. All moist potash particles from each of the trays were placed into four labeled aluminum foil plates. Any dropped potash particles were handled by tweezers. Each empty tray was placed into its labeled bag.
12. The aluminum foil plates with the potash samples and aluminum foil tape were dried in an oven drying at 100°C. After drying these potash samples for more than 20 hours, these plates were removed from oven and cooled to room temperature for another 8 hours without opening the seals.
13. When the plates were cool, the seal was removed and the plate cover was opened. All particles in each plate were poured to the labeled bags as step (11). The mass of particles, empty tray and plastic bag were measured again and recorded.
14. The moisture content gain for each tray was calculated using equations (2.37)
15. The bag and tray were emptied and the same process from steps (2) to (14) was repeated with another potash sample for a new test.

CHAPTER 4

EXPERIMENTAL DATA AND COMPARISONS WITH NUMERICAL SIMULATIONS

In this chapter, experimental and simulation results of heat and moisture accumulation in the potash test section are compared. A parameter sensitivity study is used to show the temperature and moisture content response when several selected properties are varied separately for a specified test condition.

Validation of the numerical model consists of several steps. First, comparisons will be made between the experimental data and the corresponding simulation results for each measured dependent variable. For each dependent variable, the uncertainty of the measurement will be stated knowing the sensor characteristics and other system errors inherent in the experimental procedure. Experimental uncertainties in the boundary and initial conditions will be discussed. The numerical model is said to model the physical phenomena for a range of test conditions when the simulated results always lie within the uncertainty bounds of the data. Thus, the validity and accuracy of model is dependent on the accuracy of the sensors and the instrumentation system as well as the control of the experimental process. The numerical model contains several parameters such as apparent thermal conductivity or diffusion coefficient measured or estimated from empirical relationships. These empirically determined coefficients carry specific uncertainty limits. The validity of the model implies that the selected values for these coefficients also lie within the accepted bounds of uncertainty. Simulation of the model should show that

small variations of the model coefficients keep the simulation results within the measured data uncertainty limits. Finally, small variations of the boundary or initial condition conditions should also result in simulation results that lie within the measurement uncertainties. Discrepancies between measured data and simulation results can always be accounted for through sensors, systematic measurement errors, process control errors and modeling coefficients error for a valid numerical model. A lack of agreement between the model and measured data including the corresponding uncertainty limits implies an error or deficiency in the model.

The numerical model for heat and moisture transfer within granular potash bed is a transient one-dimensional problem. There are two independent variables, i.e. time (t) and distance (y), for each of the several dependent variables, e.g. temperature (T), water vapor density (ρ_γ), and mass accumulation rate ($\dot{m}$). The only dependent variables measured directly are temperature and total mass accumulation at the end of each test. In the presentation of results, it is important to focus primarily on the most important results for which the most accurate data are available. The distribution of temperature is available at all times, whereas the distribution of moisture content is only available for the four trays at the end of each test. Each comparison is for different operating conditions of inlet air humidity or base plate bottom temperature or different types of granular potash.

Characterization of the important properties of commercial potash types were investigated by Peng et al. (1999) and Zhou et al. (1999). These potash properties

include: permeability (K) and porosity (ε) under consolidated or unconsolidated conditions; potash particle size distribution; specific surface area per unit mass of granular potash particle (S_g) under consolidated or unconsolidated conditions; apparent thermal conductivity of granular potash bed (K_{eff}) at different moisture contents. These potash properties are presented for two types of potash and states of consolidation in Table 4.1. This table of properties includes the 95% experimental uncertainties limits (Urss(95%)) for each [ANSI/ASME PTC 19.1 (1985].

Table 4.1 Measured Properties of Two Types of Potash

Properties	Symbol	Units	Lanigan Granular Potash			
			Consolidated		Unconsolidated	
			Avg. Property	Uncertainty	Avg. Property	Uncertainty
Permeability	K	m^2	3.85×10^{-8}	1.4×10^{-9}	5.35×10^{-8}	1.9×10^{-9}
Porosity	ε		0.432	0.001	0.456	0.001
Averaged Particle Size	D_p	mm	2.200	0.055	2.200	0.055
Specific Surface Area	S_g	m^2/kg	0.570	0.025	0.560	0.025
Apparent Thermal Conductivity (Dry)	K_{eff}	W/(m.K)	0.685	0.032	0.478	0.022
Properties	Symbol	Units	RocanVille Standard Potash			
			Consolidated		Unconsolidated	
			Avg. Property	Uncertainty	Avg. Property	Uncertainty
Permeability	K	m^2	4.65×10^{-9}	9.3×10^{-11}	6.80×10^{-9}	1.36×10^{-10}
Porosity	ε		0.412	0.001	0.448	0.001
Averaged Particle Size	D_p	mm	0.800	0.002	0.800	0.002
Specific Surface Area	S_g	m^2/kg	1.490	0.064	1.490	0.064
Apparent Thermal Conductivity (Dry)	K_{eff}	W/(m.K)	0.650	0.031	0.590	0.027

In this table, the unconsolidated state refers to potash poured into a test cell without any added vibrating or shaking and the consolidated state refers to the same sample after it has been vibrated to achieve its highest density.

Experimental conditions for each test are listed in the Table 4.2 where the initial conditions of the potash are room temperature (22°C or 21°C) and dry. These test conditions cause a transient change in temperature and moisture content of the potash during each test. After about 1-1/2 hours, the temperature profiles throughout the potash bed reach a quasi-steady state. It is called quasi-steady state because the temperatures are almost steady or constant with time even though there may be slight changes over the long test period due to the moisture accumulation and continuous dissolution process in each potash test sample. Thus, the dissolution process is never exactly steady. The numerical model is validated from the start of a test until the end for the temperature profiles. Moisture accumulation profiles throughout the potash bed are only compared at the end of each test. Heat flux results are compared but not used to validate the model due their large uncertainty.

Table 4.2 Test Conditions

Test No	Averaged Granular Particle Size Dp (mm)	Air Flow Rate Q (L/s)	Air Flow Relative Humidity ϕ (%)	Test Duration t (h)
1	0.8	9.33	45	1, 2, 3, 8
2	0.8	9.33	65	1, 2, 3, 8
3	0.8	9.17	80	1, 2, 3, 8
4	2.2	9.50	45	1, 2, 3, 8
5	2.2	9.33	65	1, 2, 3, 8
6	2.2	9.33	85	1, 2, 3, 8
Cold Plate Temperature: Tc=2 ^{0}C				
Airflow Temperature: Ttop=22 ^{0}C				
Test No	Averaged Granular Particle Size Dp (mm)	Air Flow Rate Q (L/S)	Air Flow Relative Humidity ϕ (%)	Test Duration t (h)
1	0.8	9.33	45	8
2	0.8	9.33	65	8
3	0.8	9.17	80	8
4	2.2	9.50	45	8
5	2.2	9.33	65	8
6	2.2	9.33	85	8
Cold Plate Temperature: Tc=21 ^{0}C				
Airflow Temperature: Ttop=21 ^{0}C				

4.1 TEMPORAL AND SPATIAL TEMPERATURE PROFILES

The measured temperatures at the bottom of each potash tray are compared with the corresponding numerical simulation results for all the test conditions. Typical results of Rocanville Standard potash, are presented in Figure 4.1 to Figure 4.3. In these figures, a dimensionless symbol, y*, is used to represent the vertical position which is defined as the ratio of vertical height (y) to the thickness of potash bed (L). All tests in these figures have a 20°C temperature difference across the potash bed. No temperature data exists for y* =0.0 on the top surface of potash. Nonetheless, the simulated top surface temperature is shown.

It is shown in these graphs that the numerical results agree with the experimental data quite well after the 1-1/2 hours transient starting time. Typical discrepancies between data and simulations are less than the temperature measurement uncertainty (±0.5 °C). During the start up transient, the maximum temperature discrepancy is less than 2°C and this occurs at y*=0.21 and t=0.5 hour in Figure 4.1. This transient discrepancy appears to be a consequence of the model not including all the thermal capacitance effects of the potash holding trays. After 1-1/2 hours these transient discrepancies become less than the measurement uncertainty.

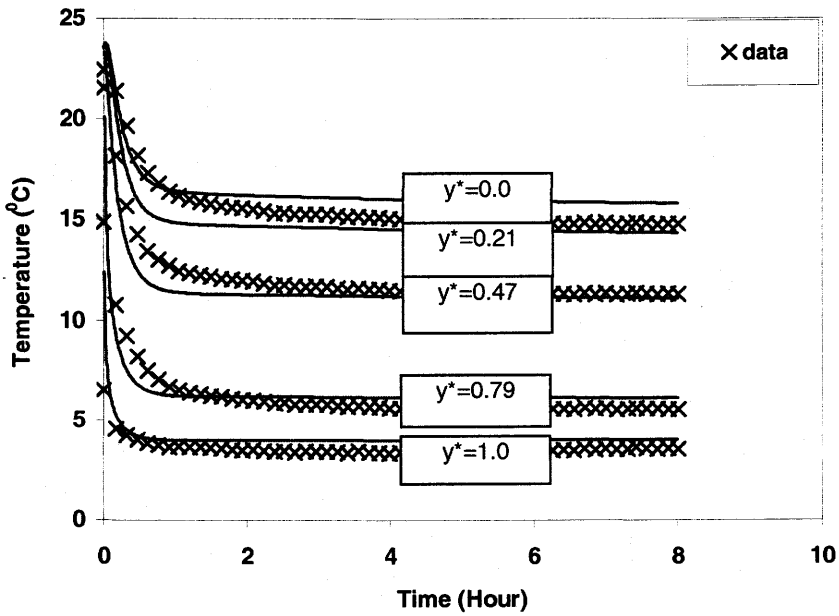

Figure 4.1 Measured and Simulated Potash Temperatures
for Q=9.33 L/s, RH=45%, T_c=2°C

It is noted in Figure 4.1 that although the bottom temperature is 2°C the bottom temperature of potash is slightly warmer. This temperature difference is due to the contact thermal resistance at the bottom.

In Figure 4.2 the transient discrepancy between the data and simulation appears to be a consequence of a small disturbance in the bottom temperature as a result of a variation in the heat removal rate at t=1/2h.

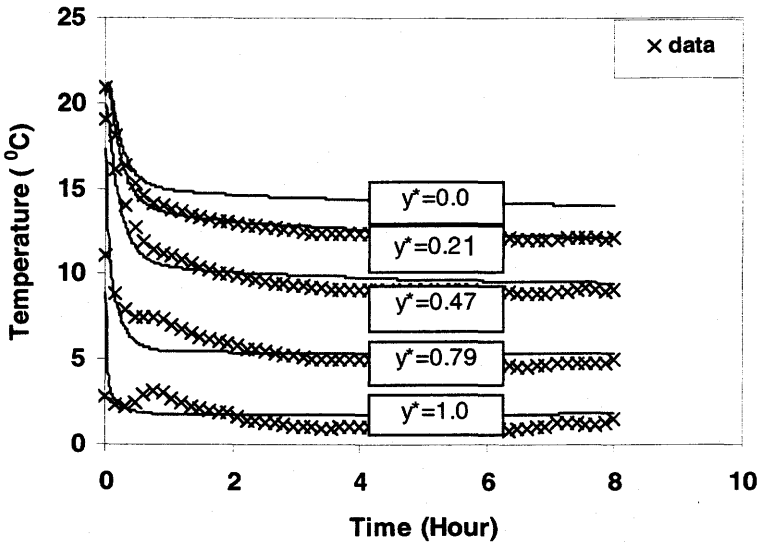

Figure 4.2 Measured and Simulated Temperatures

for Q=9.33 L/s, RH=65%, Tc=2°C

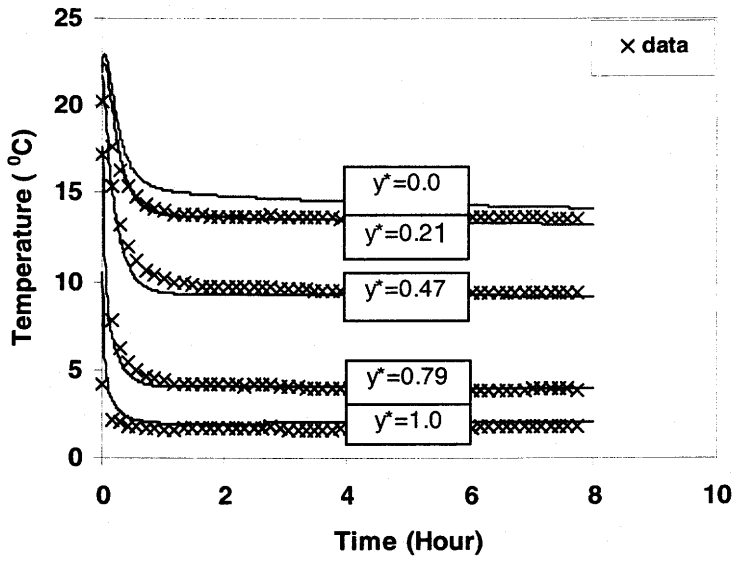

Figure 4.3 Measured and Simulated Temperature

for Q=9.17 L/s , RH=80%, Tc=2°C

At the initial condition, the temperature is 22°C (±1°C) throughout the potash sample. As soon as the experiment is started, the bottom temperature (y*=1) drops dramatically from room temperature toward the cold bottom plate temperature and pulls down all the upper trays temperatures. This heat transfer process takes about 1 hour to reach its quasi-steady state at the bottom position (y*=1) and 1-1/2 hour near the top. In all these experiments for airflow over top of potash, there is no significant temperature rise on the bottom of any potash tray due to the heating effect caused by water vapor adsorption/dissolution process as observed by Peng et al. (2000a) for humid airflow through a potash bed. On the other hand, the simulation temperature response of potash on the top surface (y*=0) clearly shows a temperature rise effect that is most significant near $t=0^+$ as implied by Peng's research.

It is found that the bottom temperature is not constant during these experiments due to small variations of city water temperature used to cool the bottom heat exchanger (e.g. 12°C initially and decreasing to 9°C at 8h). Numerically, the bottom temperature is assumed to be constant. This shift in the temperature of the cooling water causes small discrepancies between the simulation results and experimental data at $y^*=1$.

Uncertainties in the value of potash properties cause uncertainties in the simulation results. In the numerical model, the properties of potash were either experimentally measured or found in literature. These are: specific heat (C_p), density (ρ_σ), porosity (ε), apparent thermal conductivity (K_{eff}), specific surface area (S_v), adsorption isotherm and equilibrium dissolution of potash by water vapor and the heat effect of this phase change. Most of the property uncertainties are small (e.g. ±3%), but some, such as the exact chemical composition of the surface elements on the potash particle surface have a larger uncertainty and this causes the uncertainty in the adsorption / dissolution isotherms and the heat of adsorption / dissolution to be higher.

Another significant uncertainty in the simulation model is the magnitude of thermal contact resistance between each tray. Potash placed in each tray (e.g. tray#1 and #3) is supported by a fine mesh screen. The contact between this screen and the potash in the next tray below is uncertain. In the simulation model, the magnitude of this contact resistance is inferred from the measured temperature data. The magnitude of these contact resistances are inferred from a comparison between the measured data and

simulation spatial temperature profiles shown in Figures 4.4 to 4.6 corresponding to the test conditions shown in Figures 4.1 to 4.3.

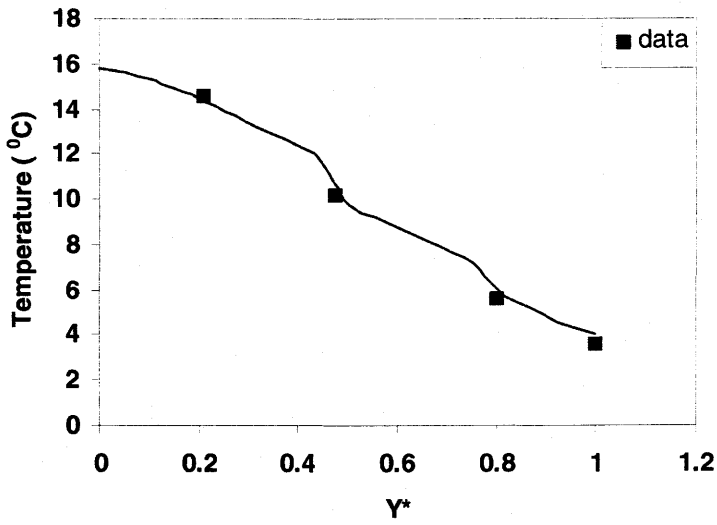

Figure 4.4 Measured and Simulated Temperatures 8h for Q=9.33 L/s, R.H=45%, Tc=2°C

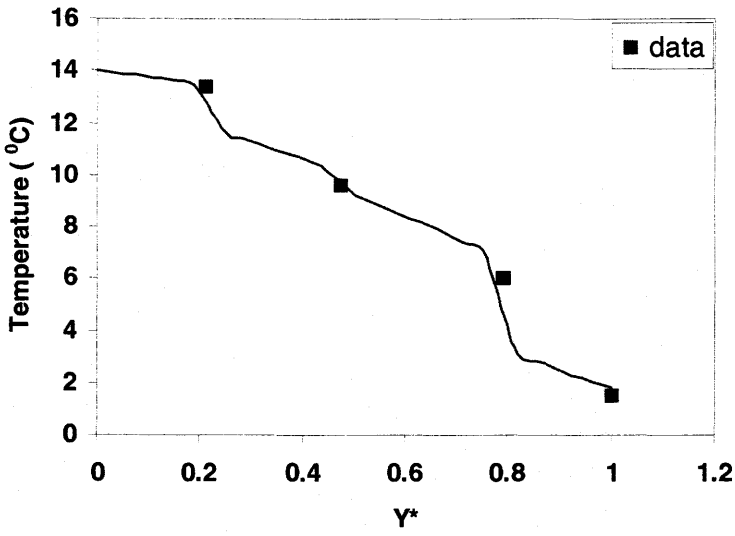

Figure 4.5 Measured and Simulated Temperatures at 8h for Q=9.33 L/s, R.H=65%, Tc=2°C

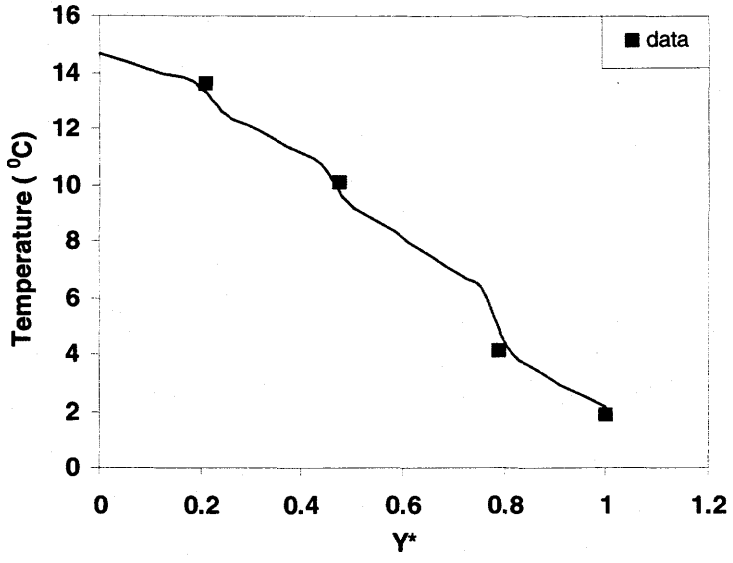

Figure 4.6 Measured and Simulated Temperatures at 8h for Q=9.17 L/s, R.H=80%, Tc=2°C

In Figures 4.7 to 4.9 similar comparisons are made except without the large temperature difference across the potash bed. The experimental data with a very small temperature difference across the bed (e.g. 1°C) are compared to the numerical results and show agreement within the measurement uncertainty (e.g. ±0.5°C). These small temperature gradient experiments may be typical of many operating conditions during the potash storage.

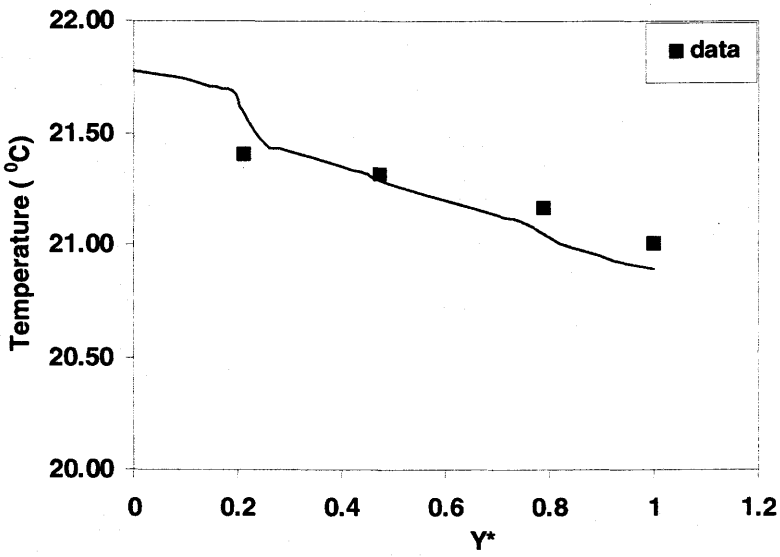

Figure 4.7 Measured and Simulated Temperatures at 8h for Q=9.33 L/s, RH=45%, Tc=21.0°C

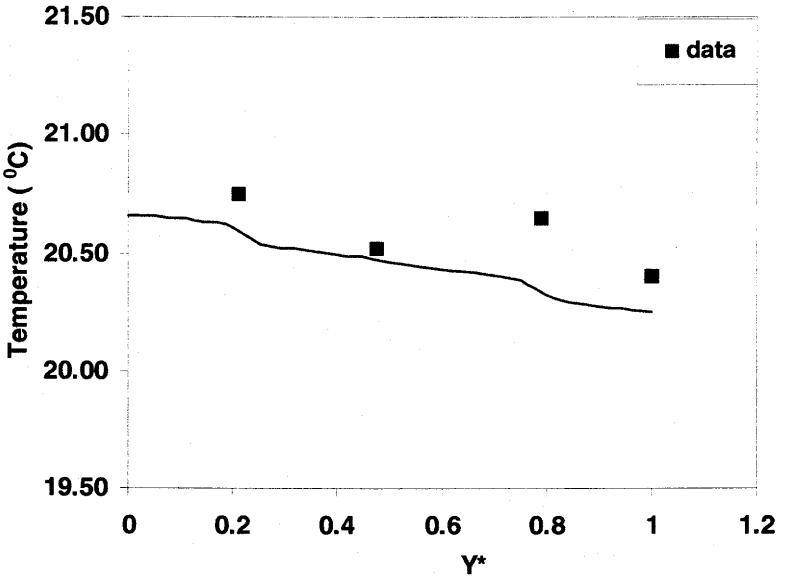

Figure 4.8 Measured and Simulated Temperatures at 8h for Q=9.33 L/s, RH=65%, Tc=20.5°C

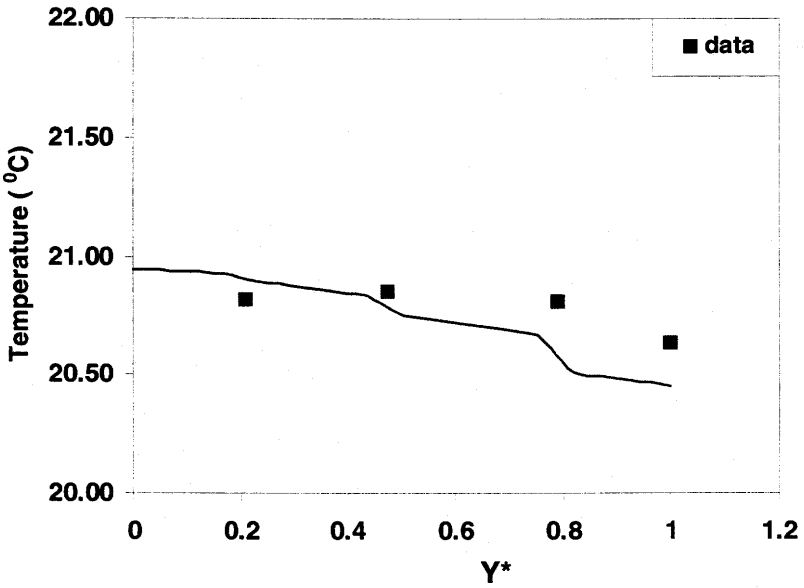

Figure 4.9 Measured and Simulated Temperatures at 8h for Q=9.17 L/s, RH=80%, Tc=20.7°C

Comparisons of spatial temperatures data with simulations for another type of potash, Lanigan Granular, (Dp=2.2-mm) give similar results as those shown above. These comparisons with data are presented in Appendix-H and I.

4.2 MOISTURE CONTENT PROFILES

The moisture content of potash is a most important property because moisture content greater than 0.20% may cause caking and the formation of dust. Moisture contents greater than 1% cause severe quality degradation problems in potash and must be avoided in applications. The test data obtained in this research are mostly less than 1% but some are well above 1%.

4.2.1 OVERVIEW OF TYPICAL MOISTURE ACCUMULATION PROFILES

For each test condition, several replication experiments were repeated, each with a different time duration (i.e. 1, 2, 3 and 8 hours). During these replication tests, there were slight variations in each test condition and the potash samples in each tray. Consequently the uncertainty due to replication differences must be considered along with other uncertainties. As a consequence of the size and importance of all uncertainties for moisture accumulation, the data are presented and discussed first and later these data are compared with the simulations.

Dry potash was placed in four different trays and the moisture content was calculated for each tray by calculating the ratio of accumulated moisture mass within each tray to the dry mass of sample in that tray. Figure 4.10 to 4.12 show typical experimental moisture accumulation results for Rocanville Standard potash (Dp=0.8 mm). The test conditions are for 20°C temperature difference across the potash bed with 9.33 L/s airflow rate over the top. The supply airflow relative humidities are 45%, 65% and 80%.

As illustrated in Figures 4.10 to 4.12, the initially dry potash accumulates moisture from surrounding air in different trays with no indication of saturation as time increases. Moisture content increases significantly with increasing supply air relative humidity and accumulation in the top tray (tray#1) increases the most dramatically with relative humidity. For a supply air humidity of 45% R.H, the highest moisture content after 8 hours diffusion reaches 0.55%. There was no dissolution phenomena observed after the experiments with a supply air relative humidity of 45% because the potash in the sample trays all appeared to be dry. Dissolution of potash was observed in the top tray in both the tests with supply air humidity of 65% R.H and 80% R.H because the potash appeared to be wet for moisture content larger than 1%.

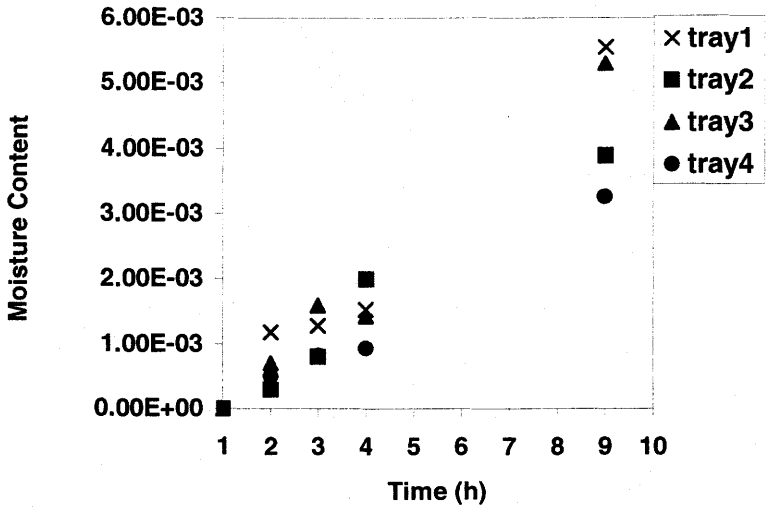

Figure 4.10 Moisture Accumulations Averaged for Each Tray

for Q=9.33 L/s, RH=45% , T_∞=22°C and Tc=2°C

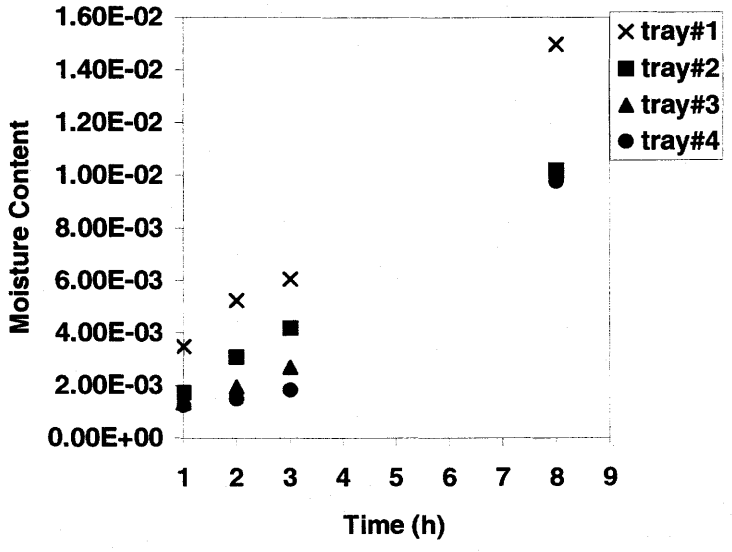

Figure 4.11 Moisture Accumulation Averaged for Each Tray

for Q=9.33 L/s, RH=65%, T_∞=22°C and Tc=2°C

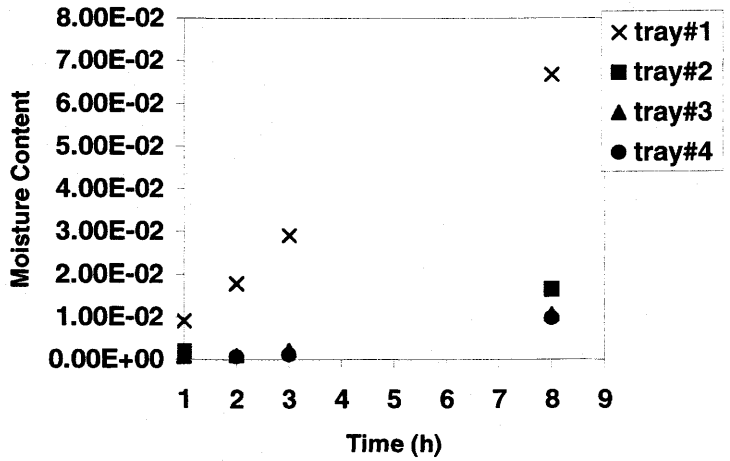

Figure 4.12 Moisture Accumulations Average for Each Tray

for Q=9.17 L/s, RH=80%, T_∞=22°C and Tc=2°C

The moisture accumulation results in Figure 4.10 to 4.12 can be explained in part by comparing these data with the corresponding adsorption/dissolution isotherm curve for the same type of potash. At thermodynamic equilibrium the moisture content is related only to the local relative humidity and temperature [Peng et al. (1999)]. For a constant average temperature in a tray, the measured moisture content corresponds to a particular relative humidity at thermodynamic equilibrium. The corresponding moisture content isotherms are presented for each average tray temperature in Figure 4.13 to 4.15 for Rocanville Standard potash.

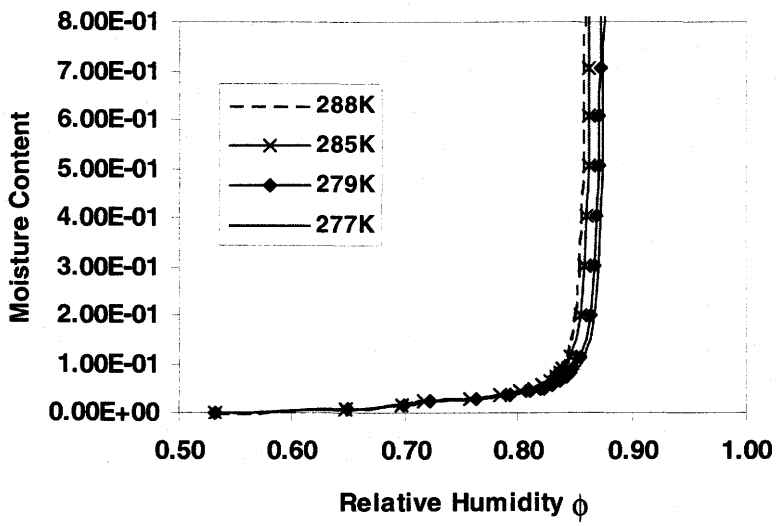

Figure 4.13 Moisture Isotherms for Dry Rocanville Standard Potash in Figure 4.10

(Chemical Composition: 98.682% KCl, 0.509% NaCl,0.809% $KMgCl_3 \bullet 6H_2O$)

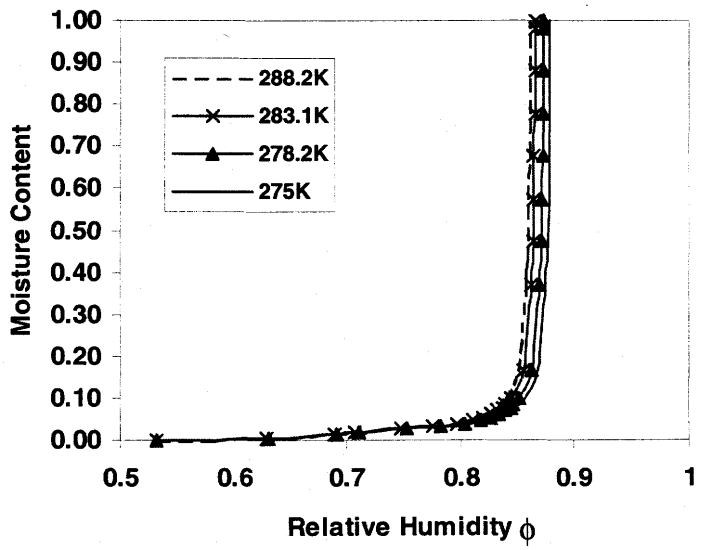

Figure 4.14 Moisture Isotherms for Dry Rocanville Standard Potash in Figure 4.11

(Chemical Composition: 98.682% KCl, 0.509% NaCl,0.809% $KMgCl_3 \bullet 6H_2O$)

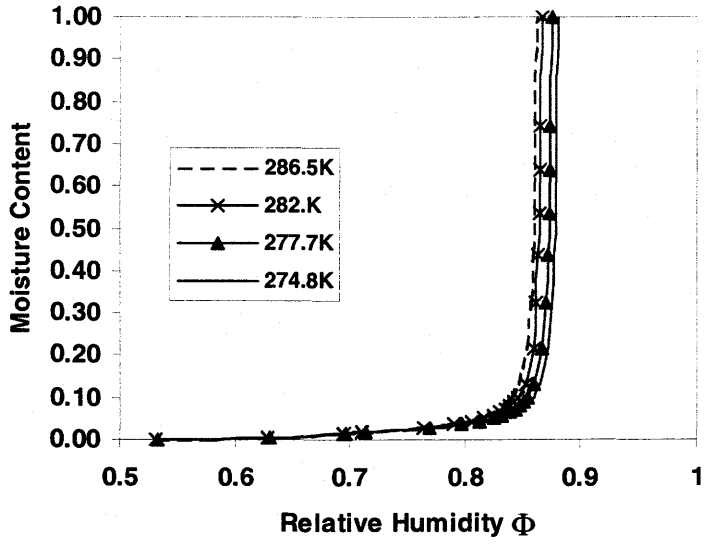

Figure 4.15 Moisture Isotherms for Dry Rocanville Standard Potash in Figure 4.12

(Chemical Composition: 98.682% KCl, 0.509% NaCl,0.809% $KMgCl_3 \bullet 6H_2O$)

These isotherms depend on the chemical composition of the surface layer on the potash particles. Unfortunately, the exact chemical composition of the potash samples tested is not known and, as discussed previously, there may be variations among the particles. Comparing these isotherms with the selected chemical composition with the measured moisture content in each tray with Figures 4.13 to 4.15 gives the average expected local relative humidity in each tray at each time. These values are presented in Table 4.1. It is evident from these results and Figures 4.13 to 4.15 that the moisture content at any location is very sensitive to temperature and humidity for high humidities. Very small changes in temperature correspond to very large changes in moisture content at local relative humidities larger than 80% R.H. Conversely, uncertainty in the expected

moisture content will always be very large when the moisture content exceeds 1% or 2%, or when air temperature and relative humidities specified are used to calculate the moisture content. Small changes in the temperature and/or humidity are expected to cause large changes in moisture content in this region of temperature and humidity.

The accurate measurement of moisture content in these experiments also poses difficulties because each data point for each tray represents a slightly different replication experiment due to variation in the sample and operating conditions of the experiment. In addition, the moisture content is often less than 0.20% implying that mass measurement accuracy of at least one part in 10000 is desirable. The uncertainty in the mass measurement can be calculated directly using calibration and precision data. The uncertainty caused by slight variations in the operating conditions requires a very large number of replication tests and/or the use of an accurate theoretical/numerical model. Both of these are used in this study. The uncertainty in the mass measurement is discussed in more detail below but the uncertainty due to replication of experiments is discussed with the simulation results and the sensitivity studies.

Due to the small mass of moisture uptake by each test tray, it is important to characterize the experimental uncertainty for each step in the measurement process. Experimental uncertainty in moisture content measurement may be caused by such factors as: dropped or misplaced potash particles before or during the mass measurement, moisture changes in the potash samples due to exposure to the ambient air, calibration of the electronic scale, contamination of the plastic cover-bag used to hold each sample and

airflow near the mass balance. Among these factors, misplaced particles, moisture exchange with the surrounding air during handling and airflow near the mass balance are the most important. During the experimental mass measurement process, one or more particles could be dropped inadvertently during inserting or taking out potash trays from test section, placing the trays in oven for drying, covering or uncovering potash to measure the mass, etc. For example, misplacing ten average-sized particles can cause a 0.05g mass decrease in a tray with a total mass of 115g to 170g. During testing, every effort was taken to avoid exposures of the test tray potash samples to the surrounding air. Since elimination of such exposures is impossible, estimates of these moisture gain or loss are important. This is done using the numerical model developed in this thesis. The total time duration of such exposures that could result in errors is estimated to be less than 60s. For a surface area of 108 mm x 108 mm for each tray the estimated moisture exchange is expected to be less than ±0.01g. Slight air movement around the mass balance can result in a fluctuation of up to ± 0.04g on the scale reading so the mass balance was shrouded from excess air currents. Typical weights of the potash trays with a average porosity of 0.35 were 115g, 136g, 170g and 131g. Considering all the effects mentioned above, an uncertainty between 0.01 and 0.1% has been estimated for all the moisture content data. In subsequent graphical presentation of these data a 0.1% uncertainty error bar is used.

The experimental data using Lanigan Granular Potash are similar and presented in Appendix-H.

4.2.2 COMPARISONS OF DATA AND SIMULATION RESULTS FOR MOISTURE ACCUMULATION PROFILES

Comparisons between numerical simulation results and experimental data are shown in Figures 4.16 to 4.21 for test conditions with 9.33 L/s airflow rate and 20°C temperature decrease across the height of potash test cell for supply air relative humidities of 45%, 65% and 80%. In these graphs, the temporal moisture content changes over 8 hours are compared for each tray and then with the space-averaged moisture content of the four trays. The uncertainty of the measurement data is shown to be $\pm 0.1\%$ and is represented by a bar. In most cases, the simulation results are within the uncertainty bounds of the measurement. Discrepancies between the simulations and the data are most pronounced when the airflow has 65% R.H and 80% R.H at the end of the 8-hour tests. It is observed that, compared to experimental data, the numerical model nearly always predicts higher moisture content values for the top two trays and lower values on the bottom two trays. Furthermore, these differences are most prominent at 8 hours. The averaged moisture content for all four trays are in better agreement with the simulations. These same observations could also be made for Lanigan Granular Potash which has a much larger particle size. These discrepancies may be explained in at least two ways: displacement of liquid water from the top two trays to the bottom trays due to capillary forces and gravity and the need for some modification to the moisture content isotherms in the theoretical model.

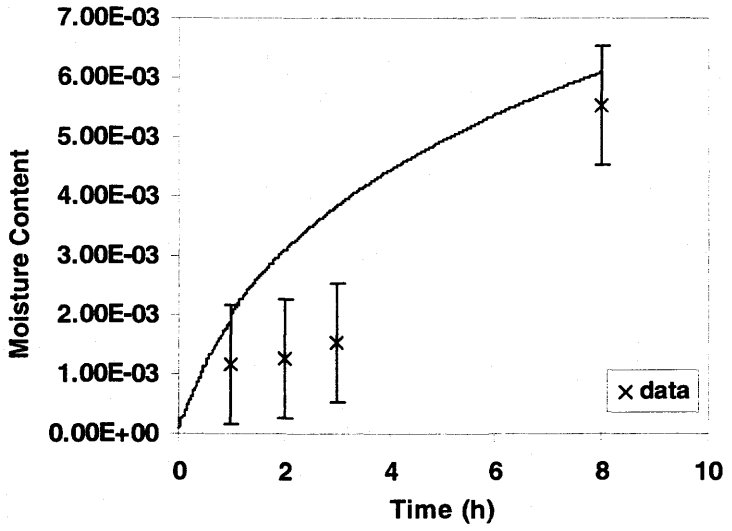

Figure 4.16 (a) Measured and Simulated Moisture Content Tray#1

(Y*=0 to 0.19) for Q=9.33 L/s, RH=45%,T_∞=22°C, T_c=2°C

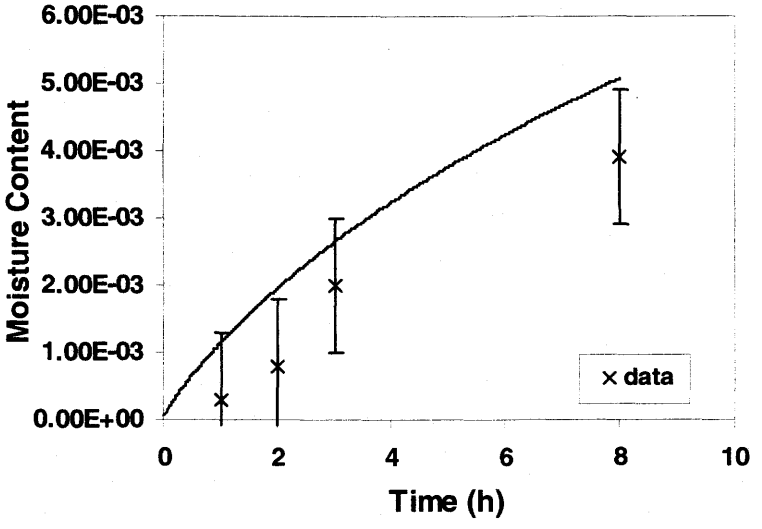

Figure 4.16 (b) Measured and Simulated Moisture Content Tray#2

(Y*=0.19 to 0.44) for Q=0.56 m^3/min, RH=45%, T_∞=22°C, T_c=2°C

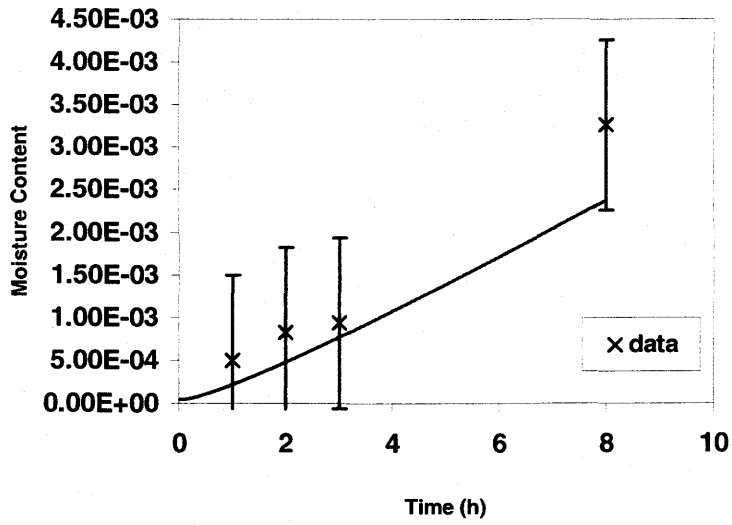

Figure 4.16 (c) Measured and Simulated Moisture Content Tray#3

(Y*=0.44 to 0.75) for Q=9.33 L/s , RH=45%, T_∞=22°C, T_c=2°C

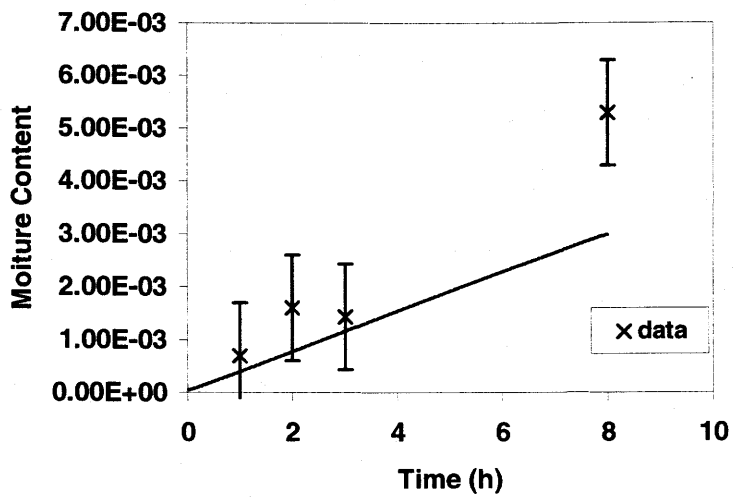

Figure 4.16 (d) Measured and Simulated Moisture Content Tray#4

(Y*=0.75 to1.0) for Q=9.33 L/s, RH=45%, T_∞=22°C, T_c=2°C

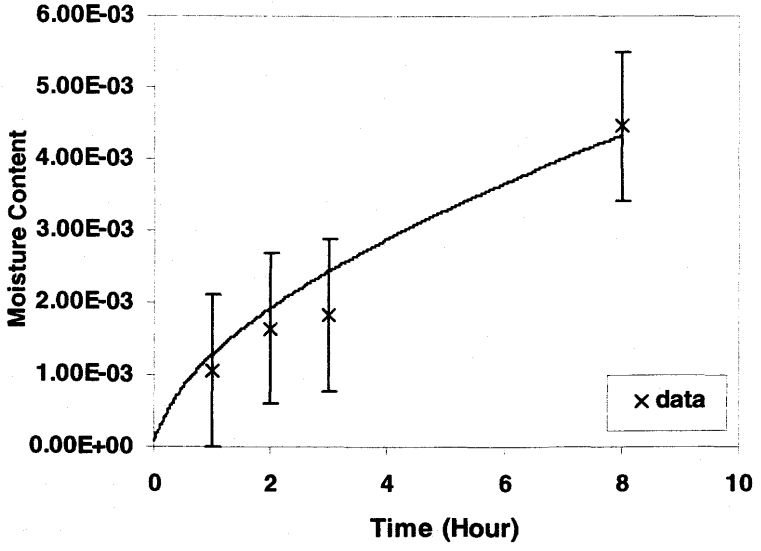

Figure 4.17 Measured and Simulated Total Averaged Moisture Content Trays #1 to #4 for Q=9.33 L/s RH=45%, T_∞=22°C, T_c=2°C

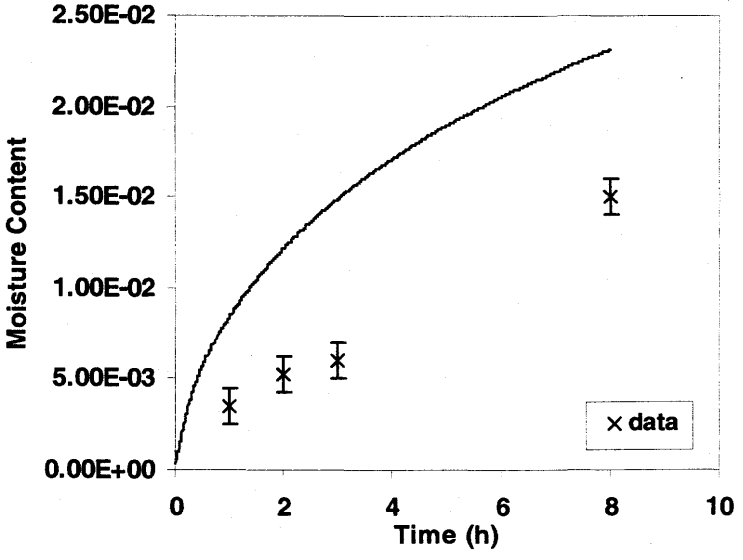

Figure 4.18 (a) Measured and Simulated Moisture Content Tray#1 (Y*=0 to0.19) for Q=9.33 L/s, RH=65%, T_∞=22°C, T_c=2°C

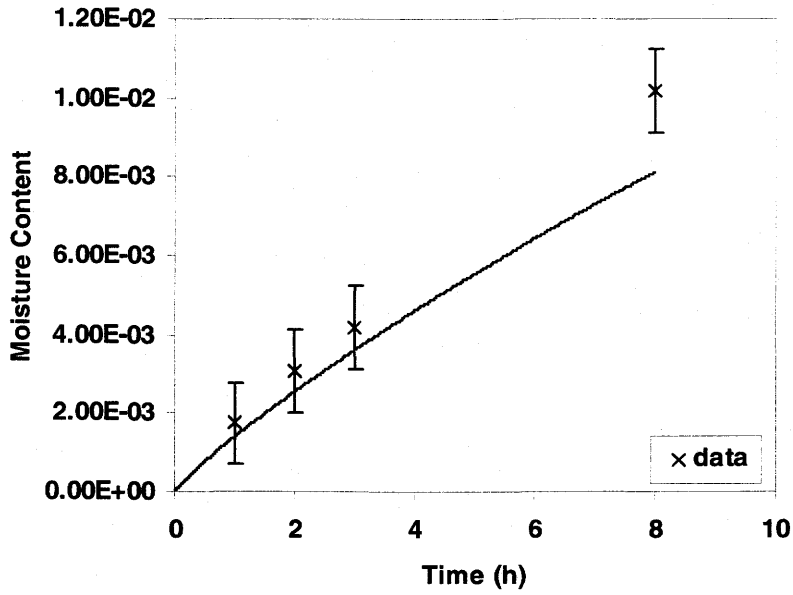

Figure 4.18(b) Measured and Simulated Moisture Content Tray#2

(Y*=0.19 to0.44) for Q=9.33 L/s, RH=65%, T_∞=22°C, T_c=2°C

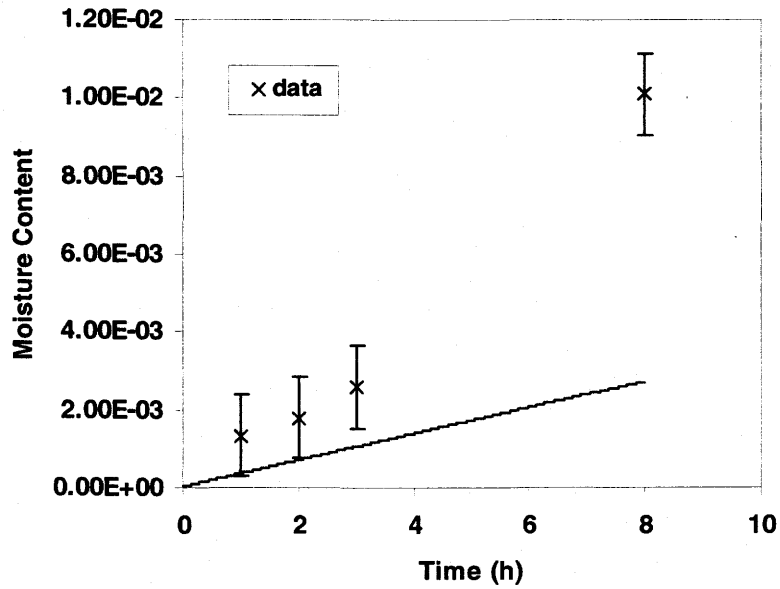

Figure 4.18 (c) Measured and Simulated Moisture Content Tray#3

(Y*=0.44 to0.75) for Q=9.33 L/s, RH=65%, T_∞=22°C, T_c=2°C

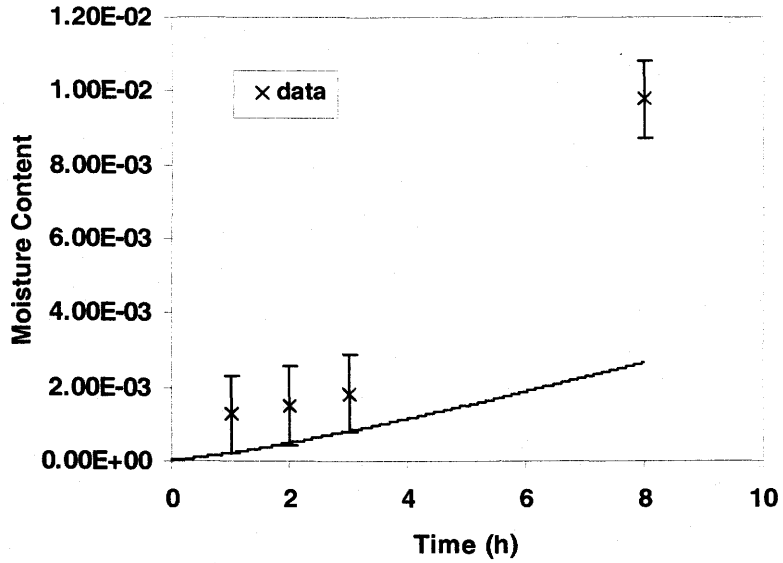

Figure 4.18 (d) Measured and Simulated Moisture Content Tray#4

(Y*=0.75 to1) for Q=9.33 L/s, RH=65%, T_∞=22°C, T_c=2°C

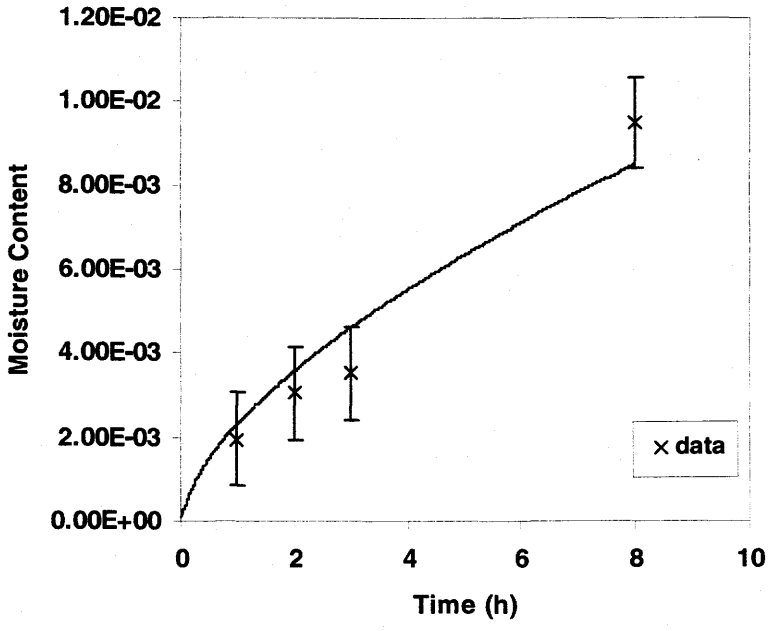

Figure 4.19 Measured and Simulated Total Averaged Moisture Content Trays#1 to#4

for Q=9.33 L/s, RH=65%, T_∞=22°C, T_c=2°C

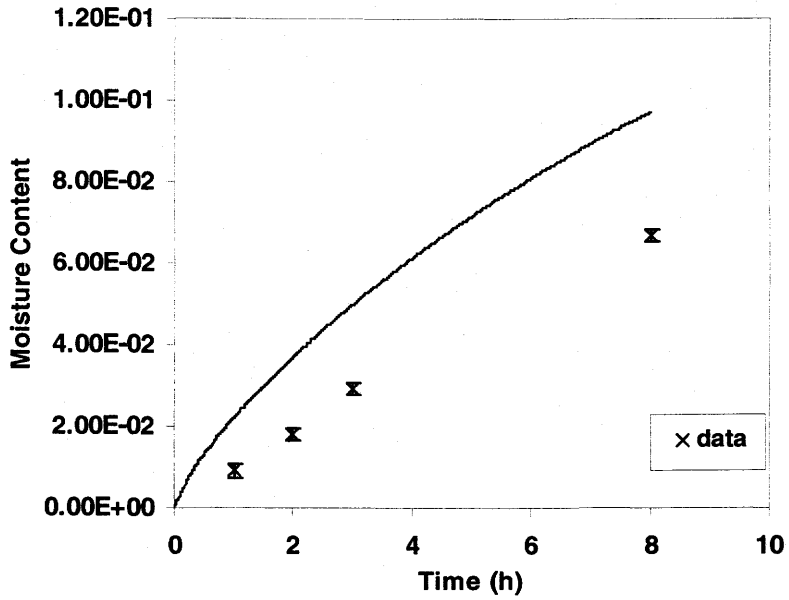

Figure 4.20 (a) Measured and Simulated Moisture Content Tray#1 (Y*=0 to0.19) for Q=9.17 L/s, RH=80%, T_∞=22°C, T_c=2°C

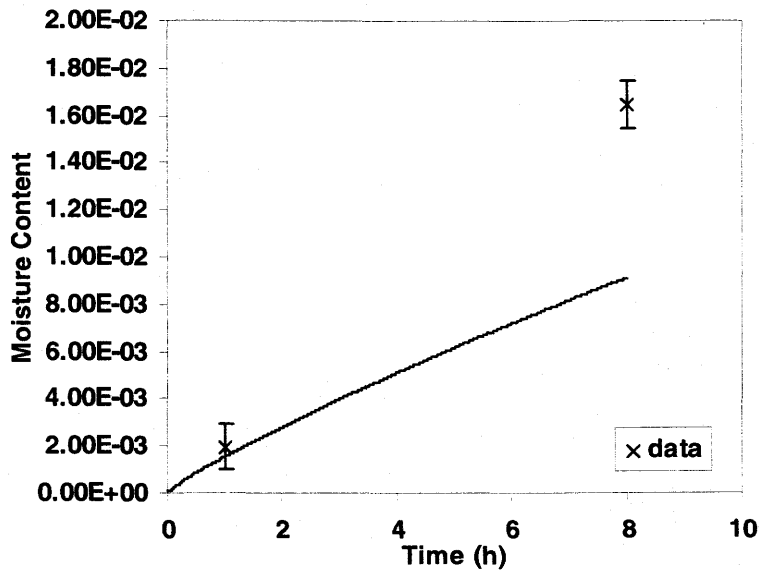

Figure 4.20 (b) Measured and Simulated Moisture Content Tray#2 (Y*=0.19 to0.44) for Q=9.17 L/s, RH=80%, T_∞=22°C, T_c=2°C

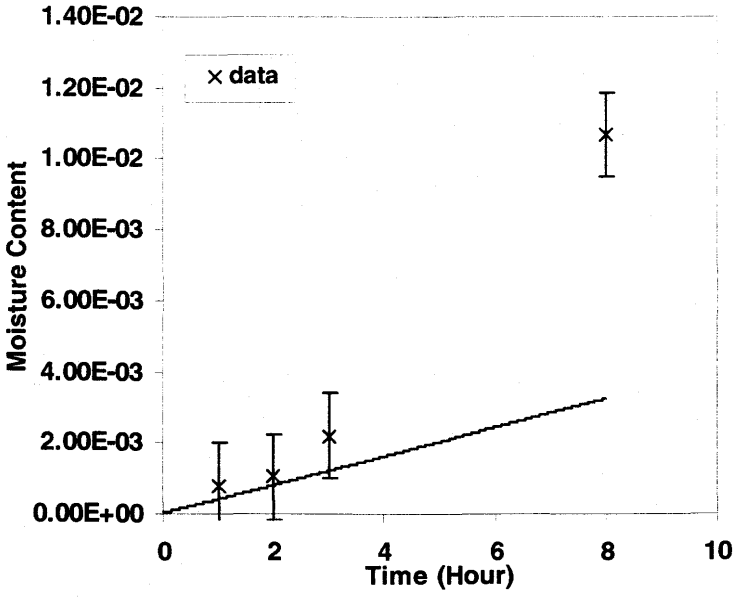

Figure 4.20 (c) Measured and Simulated Moisture Content Tray#3

(Y*=0.44 to0.75) for Q=9.17 L/s, RH=80%, T_∞=22°C, T_c=2°C

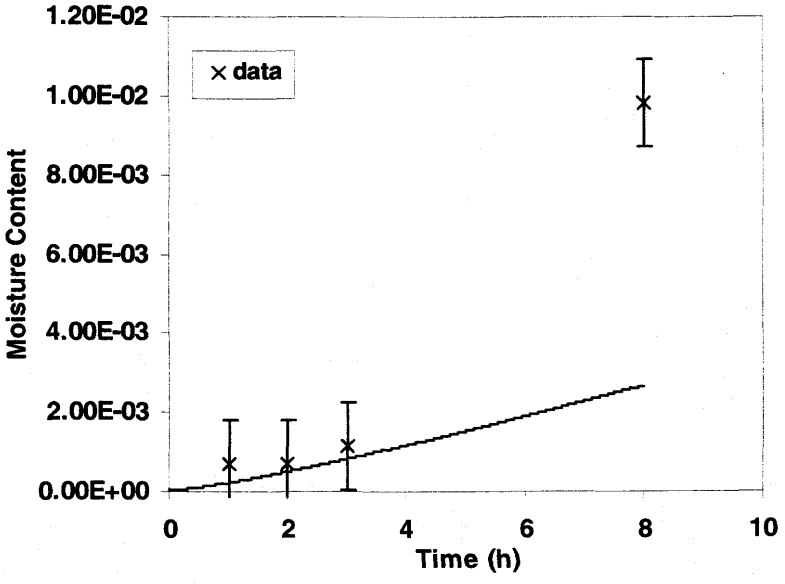

Figure 4.20 (d) Measured and Simulated Moisture Content Tray#4

(Y*=0.75 to 1) for Q=9.17 L/s, RH=80%, T_∞=22°C, T_c=2°C

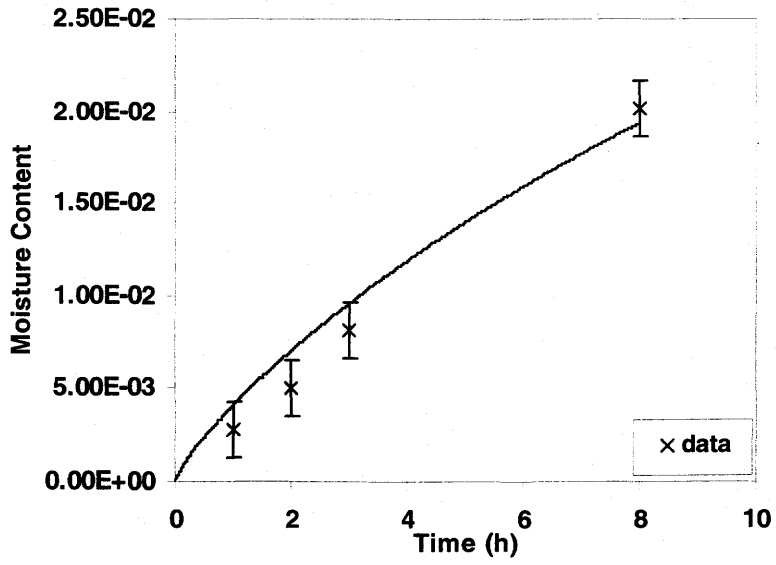

Figure 4.21 Measured and Simulated Total Averaged Moisture Content Tray#1 to #4 for Q=9.17 L/s, RH=80%, T_∞=22°C, T_c=2°C

When the local relative humidity exceeds 53% relative humidity, dissolution occurs where moisture accumulates on the particles as a liquid film. When local moisture content exceeds some unknown value, e.g. 0.5% by volume of the solid-liquid components, the electrolyte liquid state will form a continuous interconnected film throughout most of the potash bed where both the gravity and capillary effects may cause the electrolyte aqueous film to move down. Gravity forces are expected to dominate even though surface tension forces will act in the same direction because surface tension increases with decreasing temperatures (e.g. the surface tension of water in air is 4% higher at 2°C than it is at 22°C). At end of the high humidity experiments a significant number of small liquid droplet were observed on the aluminum plate in the bottom tray, implying some downward drainage of liquid. Changes to the color due to wetting the

surface particles in the third and fourth trays of potash also appeared after some tests. Rocanville potash has many bright white particles when dry and these become much darker when a surface water film exists on these particles. The above discussion on capillarity and gravity on interconnected liquid films in potash layers is plausible for high moisture contents and increasing times, but it cannot explain the measured distribution of moisture at low moisture contents when liquid moisture is expected to exist only in a pendent state without continuous interconnecting interstitial linkage of liquid films. The formulation of continuous liquid film requires both an elevated moisture content and time. At low moisture content, drainage or capillarity will not occur. The critical conditions when there may be primarily non-migratory pendent liquid films or migratory capillarity can only be inferred from the measured data because no simple means were available to observe this phenomena. The data for Rocanville Standard Potash (Dp=0.8 mm) seems to suggest that capillarity may occur when the moisture content exceeds about 0.4% and after several hours of exposure. Below this critical moisture content of about X_{crit}=0.4%, the moisture is expected to only be transferred by molecular diffusion in the form of water vapor. The data for Lanigan Granular Potash (Dp=2.2 mm) is similar to the Rocanville Standard but the critical moisture content (X_{crit}) maybe slightly higher at about 0.6%. (See Appendix-H for these data).

The numerical model for heat and mass transfer does not include drainage or capillarity so the comparisons between the model and the data for spatial distributions among the trays are only meaningful for moisture contents less than 0.4%. On the other hand, comparisons of moisture content for all the trays averaged together are meaningful

over the full range of moisture content because capillarity effects for liquid film draingae flows out of the test cell do not occur. A few discrepancies between the data and simulation are evident at moisture less than X_{crit}, especially for the top tray. Without considering the errors due to replication of the test conditions, but considering the other measurement uncertainties shown on the data points, these discrepancies may be explained as property uncertainties or deficiencies in the theoretical / numerical model and simulations.

The properties expected to be most closely related to moisture content are the moisture content isotherm, the specific surface area and the effective diffusion coefficient for water vapor. The moisture content isotherm has a good theoretical basis (Peng et al. 1999) and is expected to be very accurate when chemical composition of the particle surface are well known. Additional surface contamination is not included in Peng's model. Surface contamination could decrease the available surface area of the particles for adsorption and dissolution especially if this contamination is organic. Uncertainty in the measurement of specific surface is listed in Table 4.1 as 4.50%, an insignificant source of error unless surface contamination exists. If it does, it should be distributed uniformly in all four trays but its effect could decrease with increasing moisture content. The effective water vapor in air diffusion coefficient could, due to a small amount of bulk air movement in the top tray, be larger than the molecular diffusion coefficient. On the other hand, diffusion onto the particle surfaces may be somewhat restricted by very tiny interstitial spaces between the particles. This would decrease the effective diffusion

coefficient somewhat equally on all the trays. The sensitivity of the simulation results to these properties variations and other parameters is presented in the next section.

Figures 4.22 to 4.24 present comparisons between measured data and simulations for less than 1°C temperature difference across the potash bed but under the same flow rate and test conditions for supply air temperature and relative humidity. These results are only presented in the form of averaged values of four trays for the air supply at 45% RH. The test results typically showed about half of the mass gain due to moisture accumulation in the top tray (tray#1) and the other half distributed with decreasing mass concentration below the top tray in tray #2 and #3 with very little in tray #4. It is found that moisture accumulation on potash under these three humidity conditions is 8 to 10 times smaller than the cases of 20°C temperature difference across the potash bed. In the 8 hours test, 85% R.H caused an averaged moisture content value of 0.13%, 0.115% for 65% R.H., and 0.07% for 45%. The numerical simulations agree with the experimental data within the experimental uncertainty but the numerical simulations are all above the measured moisture content. Better agreement would occur if the initial moisture content was close to zero in the model or if the exposed specific surface area was slightly smaller. Figures 4.25 and 4.26 show the comparisons between measured data and simulation for each tray for the case of supply air humidity as 65% and 80%.

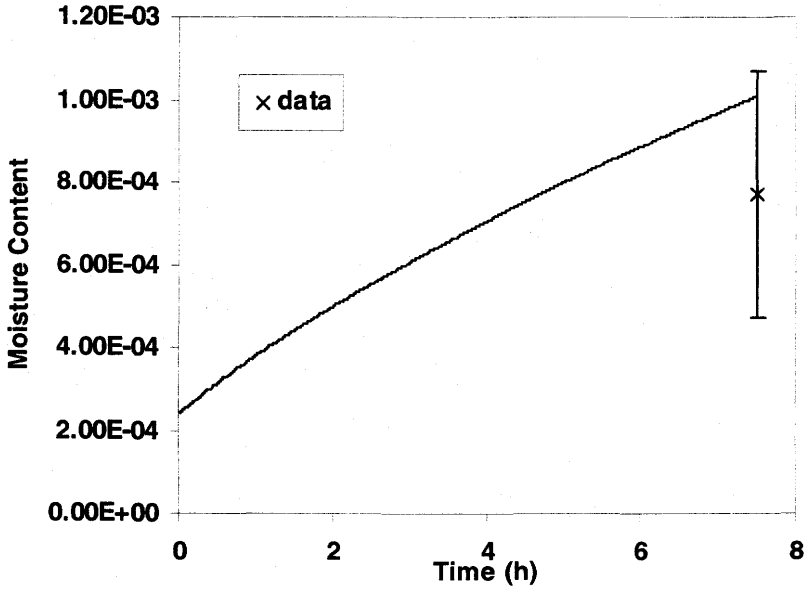

Figure 4.22 Measured and Simulated Total Averaged Moisture Content Tray#1 to #4 for Q=9.33 L/s, RH=45%, t=8 hours, T_∞=22°C, T_c=21°C

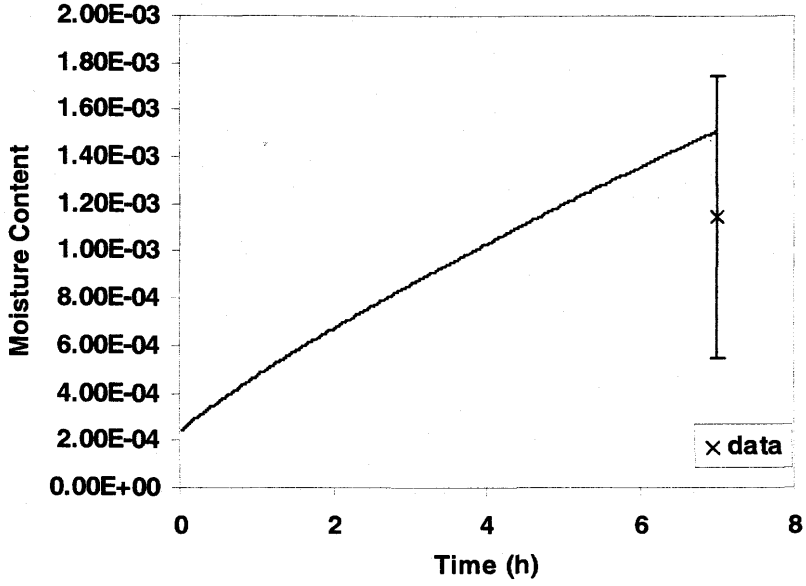

Figure 4.23 Measured and Simulated Total Averaged Moisture Content Tray#1 to #4 for Q=9.33 L/s, RH=65%, T_∞=22°C, T_c=21°C

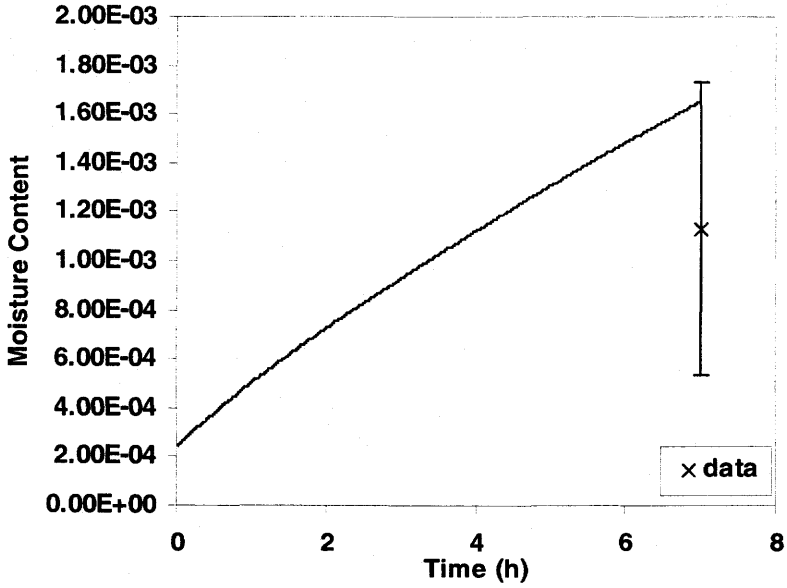

Figure 4.24 Measured and Simulated Total Averaged Moisture Content Tray #1 to #4 for Q=9.17 L/s, RH=80%, T_∞=22°C, T_c=21°C

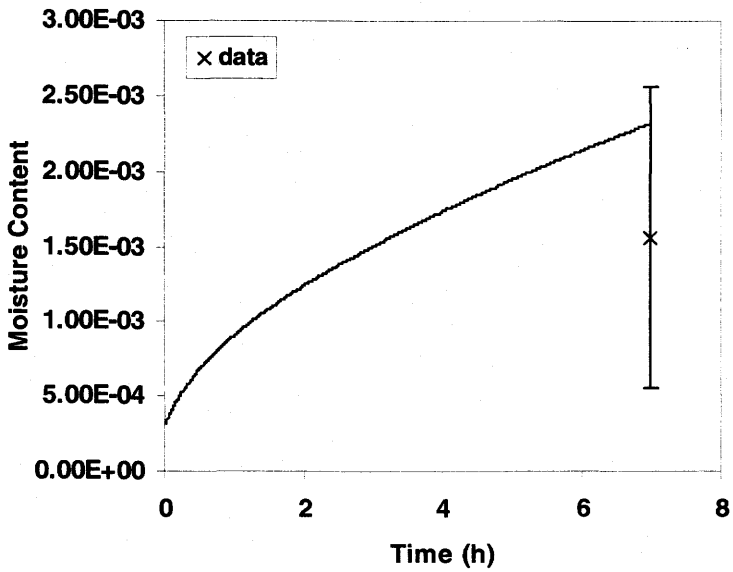

Figure 4.25 (a) Measured and Simulated Moisture Content Tray#1 (Y*=0.0 to 0.19) for Q=9.33 L/s, RH=65%, T_∞=22°C, T_c=21°C

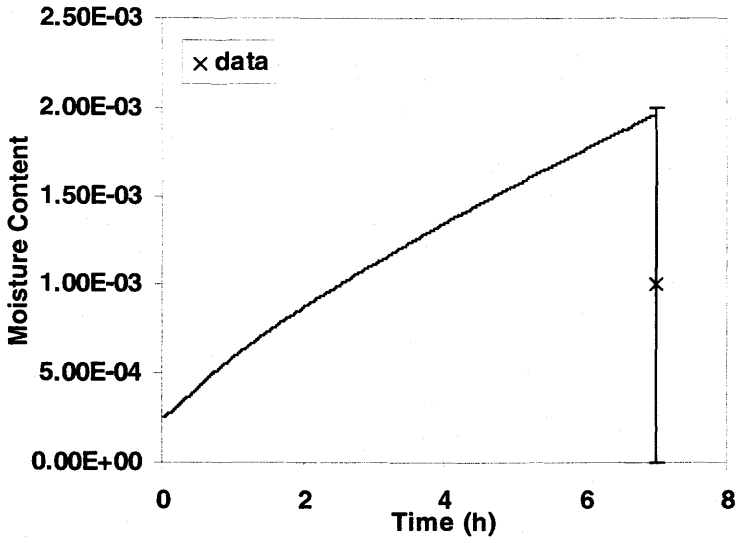

Figure 4.25 (b) Measured and Simulated Moisture Content Tray#2 (Y*=0.19 to0.44) for Q=9.33 L/s, RH=65%, T_∞=22°C, T_c=21°C

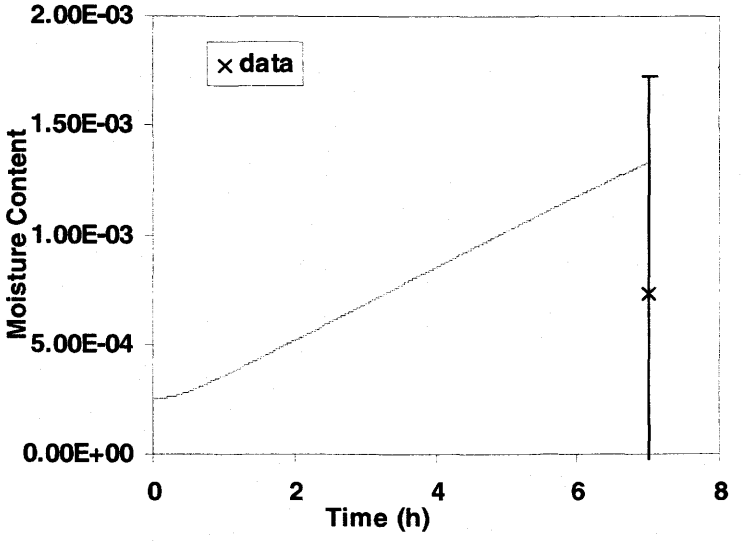

Figure 4.25 (c) Measured and Simulated Moisture Content Tray#3 (Y*=0.44 to0.75) for Q=9.33 L/s, RH=65%, T_∞=22°C, T_c=21°C

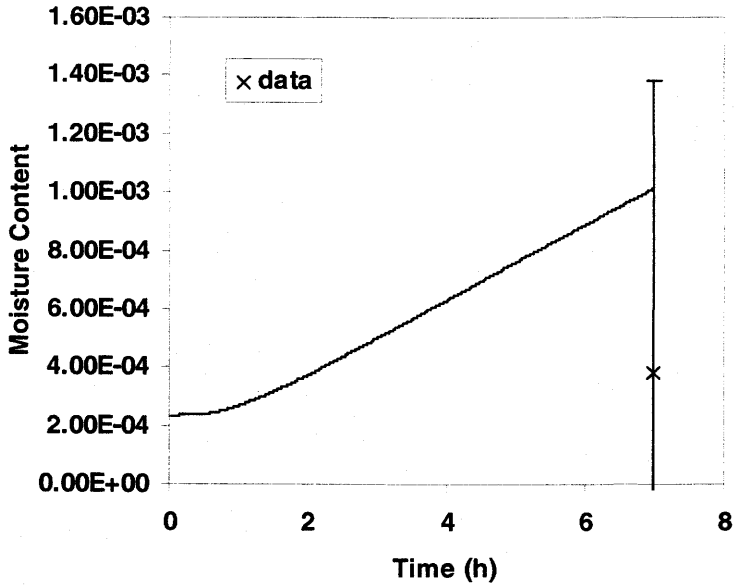

Figure 4.25 (d) Measured and Simulated Moisture Content Tray#4

(Y*=0.75 to 1) for Q=9.33 L/s, RH=65%, T_∞=22°C, T_c=21°C

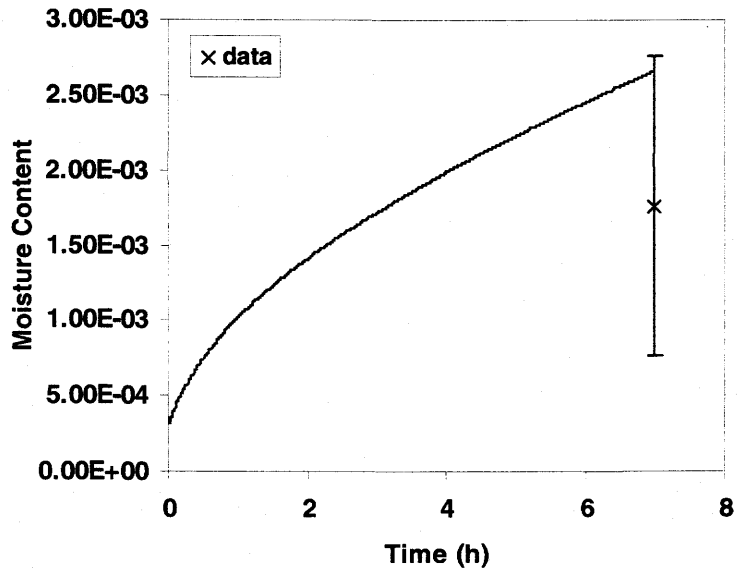

Figure 4.26 (a) Measured and Simulated Moisture Content Tray#1

(Y*=0.0 to 0.19) for Q=9.17 L/s, RH=80%, T_∞=22°C, T_c=21°C

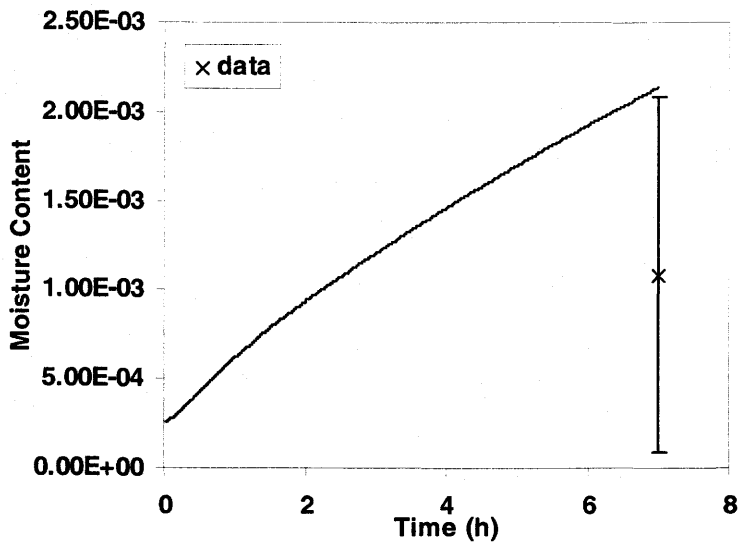

Figure 4.26 (b) Measured and Simulated Moisture Content Tray#2 (Y*=0.19 to0.44) for Q=9.17 L/s, RH=80%, T_∞=22°C, T_c=21°C

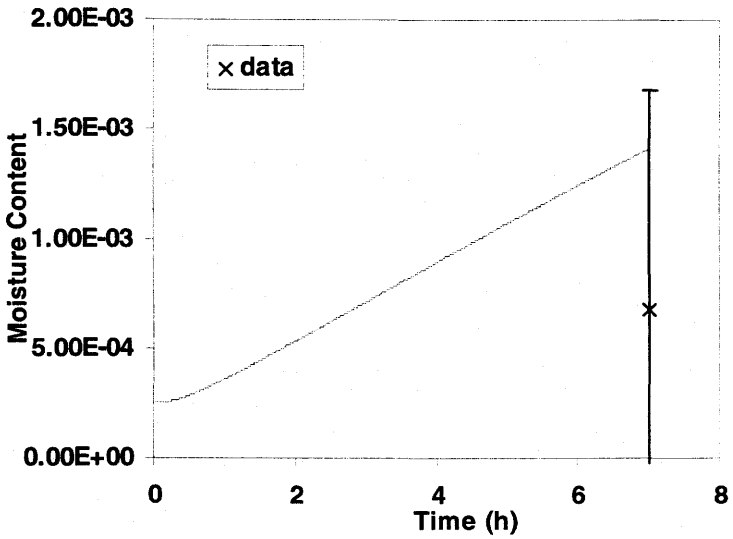

Figure 4.26 (c) Measured and Simulated Moisture Content Tray#3 (Y*=0.44 to0.75) for Q=9.17 L/s, RH=80%, T_∞=22°C, T_c=21°C

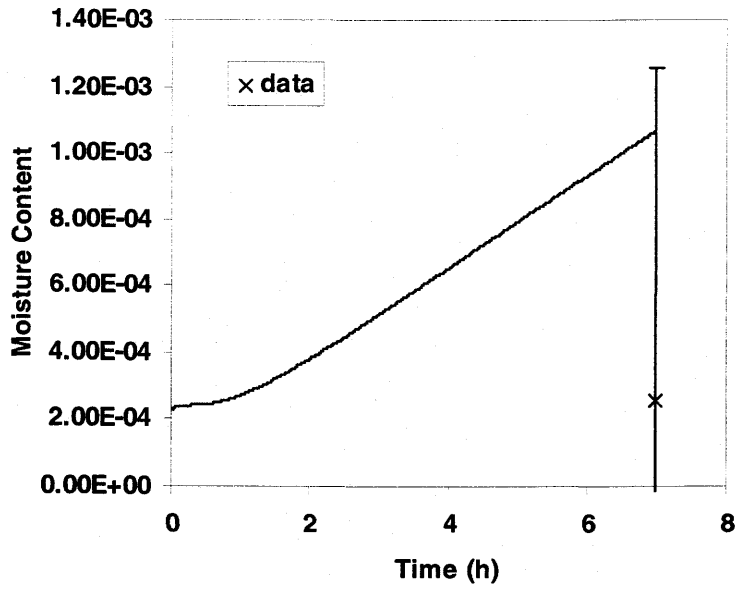

Figure 4.26 (d) Measured and Simulated Moisture Content Tray#4

(Y*=0.75 to 1) for Q=9.17 L/s, RH=80%, T_∞=22°C, T_c=21°C

4.3 SENSITIVITY STUDY OF THE NUMERICAL MODEL

A sensitivity study of the numerical model is presented in this section to illustrate the effects of changing some key parameters where there is significant uncertainty in the properties or operating conditions. Simulation sensitivity results are compared to a selected base case operating condition which is defined to be: flow rate 9.33 L/s, 20°C temperature difference step change across the potash bed, and 45% relative humidity for the supply air and using Rocanville Standard Potash with mass fraction of carnallite ($KMgCl_3 \bullet 6H_2O$) 0.81%, halite (NaCl) 0.51%, and sylvite (KCL) 98.68%. Five parameters are investigated in this sensitivity study where results for temperature and moisture content will be presented seperately. For moisture content, they are the effective diffusion coefficient (D), specific surface area (S_v), temperature difference across the potash bed (ΔT), the average temperature of the bed, and thickness of potash bed (L). For the temperature difference case, the properties investigated are the apparent thermal conductivity (K_{eff}), the effective diffusion coefficient (D), and the specific surface area (S_v).

Only one of these sensitivity study properties is altered for each simulation while the others are held as specified for the base case. Temporal moisture content and spatial temperature distribution are illustrated. The value used for each parameter investigated is increased by a factor of two and decreased by a factor of 0.3 or 0.5. These large changes in parameters are unlikely in practical applications but they clearly show the variation in the simulation results. The operating temperature difference is reduced to 5°C in one

study because it is a more practical situation in transportation and storage processes. Two test cell bottom temperatures are analyzed: warm temperature at 15°C to be representative of summer conditions and cold temperature at 2°C to be representative of winter conditions.

Figures 4.27 to Figure 4.30 compare the profiles of moisture content for each parameter against the base case for each tray. Figure 4.31 presents these comparisons averaged for all four trays. Figure 4.32 compares the spatial temperature profiles across the potash bed at 8 hours.

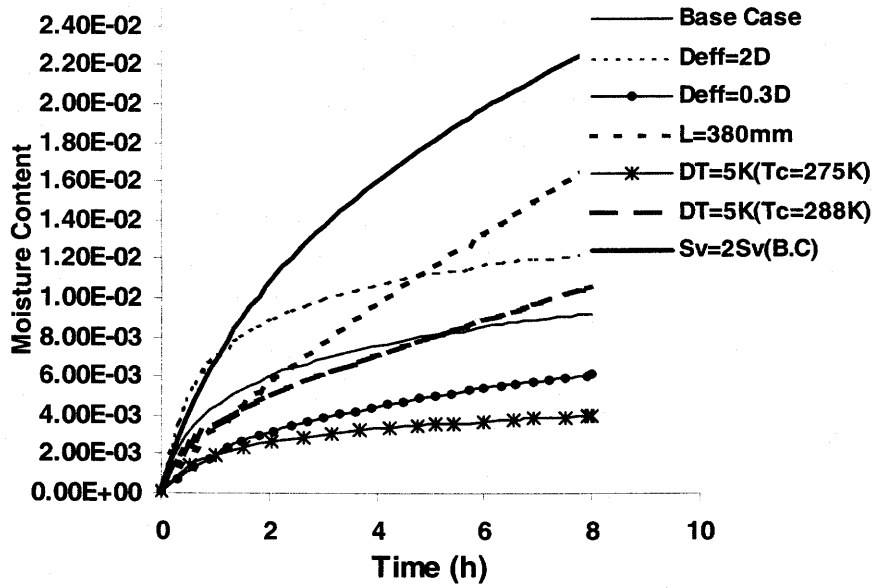

Figure 4.27. Moisture Content Profiles Tray#1 (Y*=0-0.19)

(Q=9.33 L/s, RH=45%)

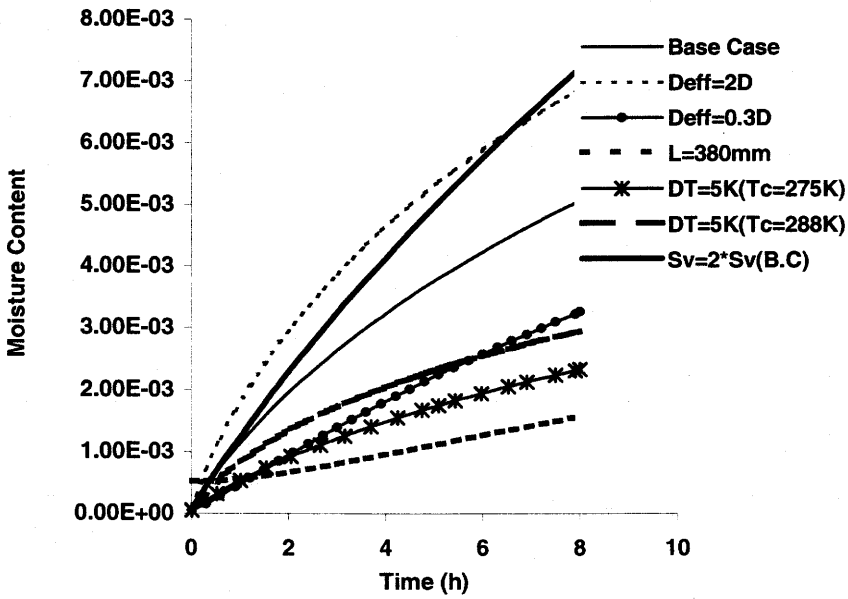

Figure 4.28. Moisture Content Profiles in Tray#2 (Y*=0.19-0.44)

(Q=9.33 L/s, RH=45%)

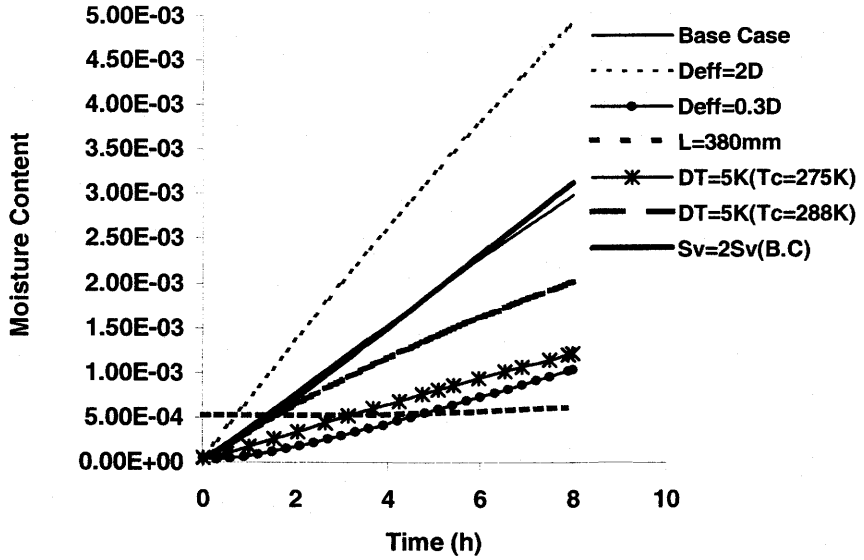

Figure 4.29. Moisture Content Profiles in Tray#3 (Y*=0.44-0.75)

(Q=9.33 L/s, RH=45%)

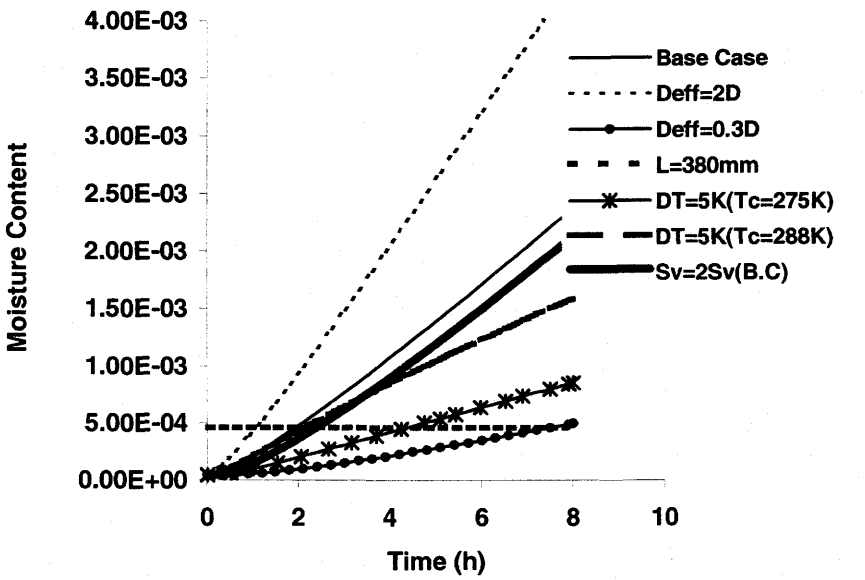

Figure 4.30 Moisture Content Profiles in Tray#4 (Y*=0.75-1.0)

(Q=9.33 L/s, R.H=45%)

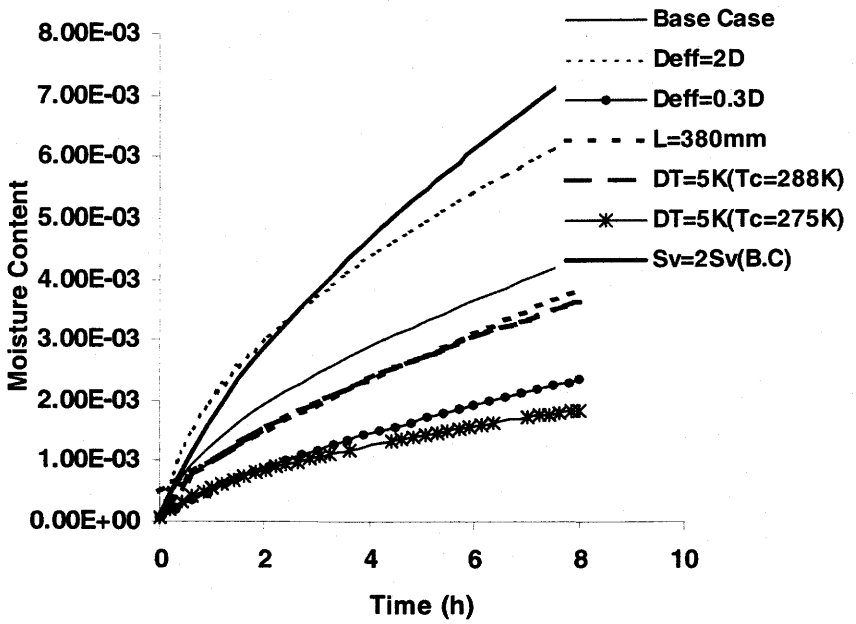

Figure 4.31 Average Moisture Content Profiles Tray#1 to #4

(Q=9.33 L/s, RH=45%)

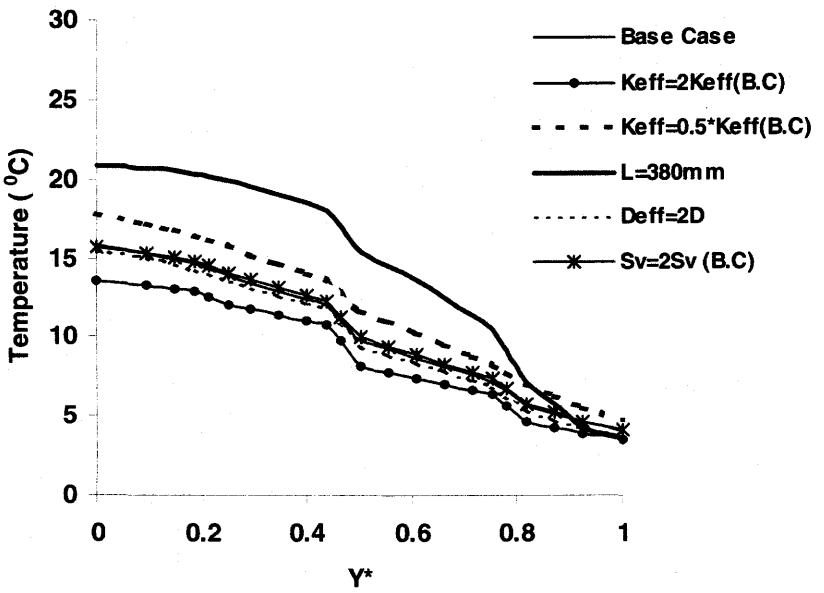

Figure 4.32 Spatial Temperature Distribution at 8 hours

(Q=9.33 L/s, RH=45%)

In application, moisture accumulation is most important because it is associated with dust formation and caking. Both the experimental data and this sensitivity study shown that the top layer accumulates the largest fraction of moisture. Increasing the vapor diffusion coefficient results in the more moisture transfer from the upper region to the lower region by molecular diffusion and decreasing the diffusion coefficient causes a significant drop in moisture content everywhere within the potash bed. Increasing the specific surface area causes more granular potash particle surface to be exposed to humid air and significantly increases the moisture accumulation in the top layers. Reducing the temperature gradient across the potash bed results in a smaller moisture accumulation in potash especially in the top surface layers. At a cold boundary temperature (i.e. 2°C) and a supply air temperature of 7°C, moisture accumulation is far less than the base case due to the smaller moisture content of air at 7°C (W=0.0027). At a cold boundary temperature of 15°C and a supply air temperature of 20°C (W=0.0065) for a supply air relative humidity 45% the moisture content is slightly higher than for the cold boundary case but still lower than the original for ΔT=20°C. Increasing the thickness of the test bed by ten times also changes the moisture accumulation in each layer. For a bed thickness of 38 mm, the maximum difference of 4°C was found at y^*=0 for a change in K_{eff} by a factor of 4 in Figure 4.32. That is, the thermal conductivity is the only factor that strongly changes the temperature distribution.

Increasing or decreasing the apparent thermal conductivity by a factor of two does not change the moisture accumulation very much (less than 10%). But the temperature profiles have a maximum change of more than 2°C in each of two cases. This is caused

by the moisture accumulation within potash. With moisture transfer, the value of apparent thermal conductivity of granular potash has been changed. Figure 4.33 presents the typical apparent thermal conductivity of granular potash in the space distribution at different times. These results show that at the end of 8 hours the value of apparent thermal conductivity is expected to be double that of the dry condition. Increasing or decreasing the vapor diffusion coefficient does not influence the temperature profiles significantly. Increasing the specific surface area does not change the temperature profile either.

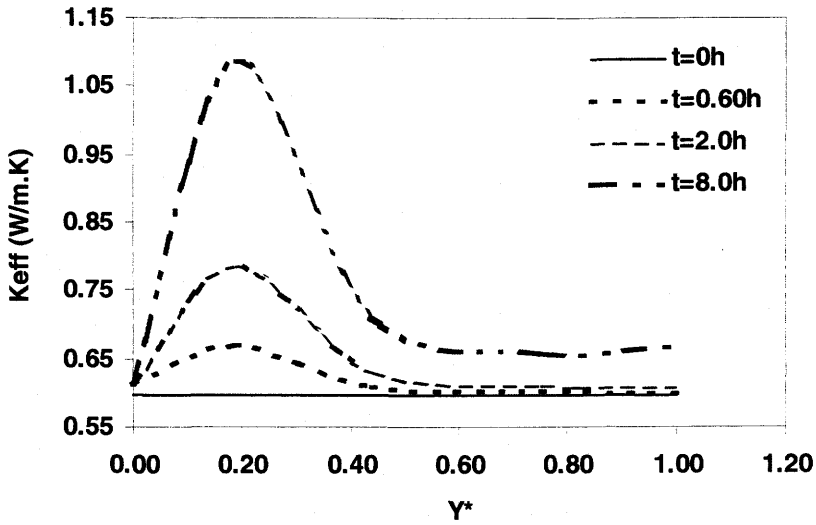

Figure 4.33 Spatial Distribution of Apparent Thermal Conductivities

(Q=9.33 L/s, RH=45% T_∞=22°C, Tc=2°C)

Another important parameter investigated here is the water vapor adsorption/dissolution isotherm by potash particles. As described before, the

thermodynamic equilibrium adsorption / dissolution isotherms of water vapor by potash particles are sensitive to temperature and local relative humidity, especially when moisture content is more than 0.5%. The question is, " if the simulation temperature error is large how will this temperature error alter the moisture adsorbed or formed as a liquid film." This sensitivity of the isotherm is investigated by fitting three different adsorption / dissolution isotherms corresponding to those of 28°C, 22°C and 5°C for the case of a supply air of 22°C and relative humidity of 65%. By altering the isotherm in this manner and fixing them regardless of the internal temperature we are investigating the sensitivity to slight differences in the isotherms or conversely errors in the internal temperatures. The results in Figure 4.34 show that moisture content increases with increasing the isotherm temperature in the potash especially at 301K. There is no significant difference in moisture content in the lower trays (tray#2 to #4) by increasing or decreasing the isotherm temperatures.

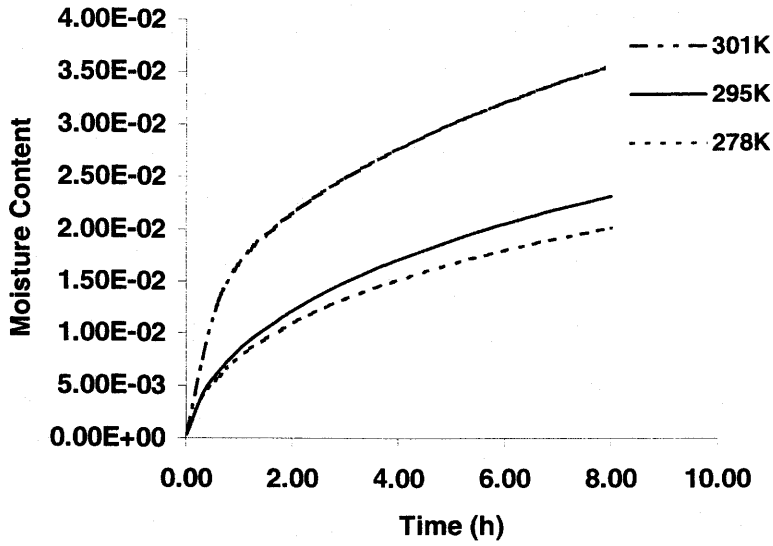

Figure 4.34 Moisture Contents By Different Isotherms in Tray#1

(Q=9.33 L/s, RH=65%, Tc=2°C)

CHAPTER 5

NUMERICAL PREDICTION OF POTASH MOISTURE REDISTRIBUTION AFTER MIXING AND WATER VAPOR ADSORPTION/DISSOLUTION WHILE ON A CONVEYOR BELT

5.1 INTRODUCTION

A valid numerical model can be used for a wide range of studies that may be difficult to experimentally measure in the field. In this chapter two such applications are considered namely, mixing to create non-uniform moisture distribution and exposing cold potash on a conveyor belt.

In practical applications, mixing always occurs when potash is handled (e.g. mixing while potash is loaded onto conveyor belts, or mixing when potash is first placed into a storage warehouse, etc). During mixing, some moist particles on the surface layers which previously have been exposed to humid atmospheric air or rains will be folded into interior dry regions of potash causing this newly deposited moist potash to undergo a redistribution process. In this redistribution process moist regions of potash will tend to become dryer while adjacent dry regions will become moist.

In the conveying process, cold dry potash at lower temperature from either shed warehouses or ships is conveyed from one point to another on the conveyor belt where

the potash is exposed to warm humid atmospheric air for 5 to 15 minutes. When the potash on the conveyor belt is much cooler than the adjacent humid air significant moisture accumulation on the potash surface layers will occur by both adsorption/dissolution and condensation.

The validated numerical model presented in Chapter 2 is used in this Chapter to predict the moisture and temperature characteristics during these two typical potash handling and storage processes. These are: short-term moisture redistribution after mixing and moisture adsorption / dissolution due to cool potash on a conveyor belt. The long-term simulation of potash moisture adsorption/ dissolution in a storage pile while the ambient air temperature and humidity cycle diurnally is left to future studies.

5.2 MOISTURE REDISTRIBUTION WITHIN POTASH AFTER MIXING

During handling, potash is mixed before and after each stage of transportation or storage. For example, the typical process sequence from warehouse storage at a Saskatchewan mine warehouse to the ship at Vancouver includes such steps as: 1) from the storage pile mixing prior to conveying to load on railcars; 2) transport by rail car to Vancouver; 3) from the rail car mixing prior to conveying to the Vancouver storage shed; 4) conveying to storage; 5) mixing while placing the potash in storage; 6)storage; 7) mixing while loading potash on conveyor belts; 8) conveying and 9) mixing while placing the potash into the hold of ship. Mixing causes some surface particles to be

relocated from surface layers and placed within interior regions of piles or vessels. At the same time, some interior particles are taken and placed on the surface layers. Since surface layers are always exposed to the surrounding air they will pick up moisture from humid air. The exact distribution of potash in piles or vessels after these mixing processes depends on method of handling and is beyond the scope of this research. Nonetheless, the numerical model can now be used to predict the redistribution of moisture in potash after a moist layer has been mixed into the interior.

The problem of transient interior moisture diffusion is investigated for thin layers of hypothetical moist potash 15.2 mm thick periodically placed in a bed of dry potash. Each layer of potash is 60.8 mm from the adjacent parallel moist layers as shown in Figure 5.1. Such a hypothetical redistribution of moist potash into thin layers within a large pile may occur while a conveyor periodically dumps moist potash onto a pile where it flows down the surface of the pile which is at the angle of repose for that particular product.

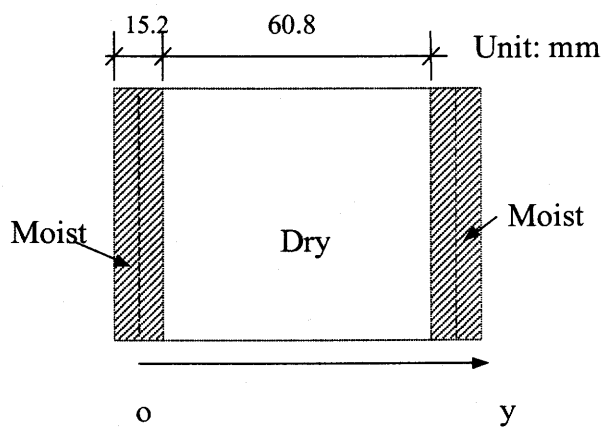

Figure 5.1 Schematic of the transient interior moisture distribution in the mixing process

5.2.1 BOUNDARY CONDITIONS AND INITIAL CONDITIONS

Due to symmetry, only a one-dimensional region which is 38 mm thick needs to be modeled. The initial conditions are assumed such that the high moisture content region (0<y<7.6 mm) has a moisture content of 1.0% while dry region (7.6 <y<38 mm) has the moisture content of 0.1%. The initial temperature is assumed uniform everywhere at 20°C. Mathematically, these initial conditions are:

$$T(t=0,\ 0<y^*<1.0)=20°C \tag{5.1}$$

$$X=1.0\%\ \ (t=0,\ 0\le y^*\le 0.2) \tag{5.2}$$

$$X=0.1\%\ \ (t=0,\ 0.2<y^*\le 1.0) \tag{5.3}$$

From symmetry, the boundary conditions at y=0 and 38 mm are adiabatic and impermeable (i.e. no heat or moisture diffusion). Mathematically, the boundary conditions are expressed as:

$$\frac{\partial T}{\partial y}=0 \quad (y^*=0,\ 1.0) \tag{5.4}$$

$$\frac{\partial \rho_\gamma}{\partial y}=0 \quad (y^*=0,\ 1.0) \tag{5.5}$$

5.2.2 SIMULATION RESULTS

Simulations were run for this moisture redistribution problem for a period of 3 hours. The process of moisture redistribution will continue as long as temperature and moisture content differences persist anywhere within the potash bed. Figure 5.2 shows that after 3 hours, the moisture content in the initially moist layer ($0 \leq y^* \leq 0.2$) decreases in moisture content from 1.0% to a maximum of 0.52% while the moisture content of the initially dry region increases significantly. As time increases indefinitely ($t \rightarrow \infty$) the moisture content will become uniform at 0.28%. The initially moist layer undergoes desorption and the dry region adsorption which causes the temperature to change from 20°C. Figure 5.3 shows the temperatures increased in both the dry region due to large heat release during moisture adsorption and in the moist layer where there was both desorption and heat gain by heat conduction.

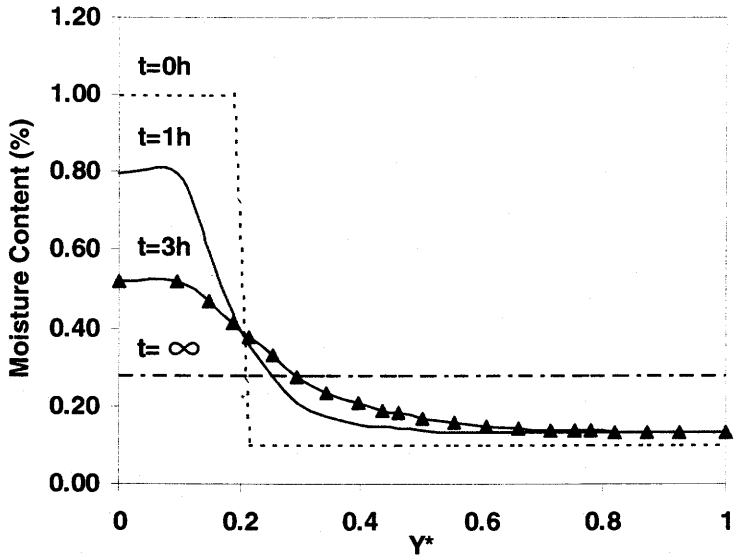

Figure 5.2 Spatial Moisture Content for a Thin Layer (0<y*<0.2) of Moist Potash (X=1% at t=0) in a Large Bed (0.2<y*<1.0) Dry Potash (X=0.1% at t=0)

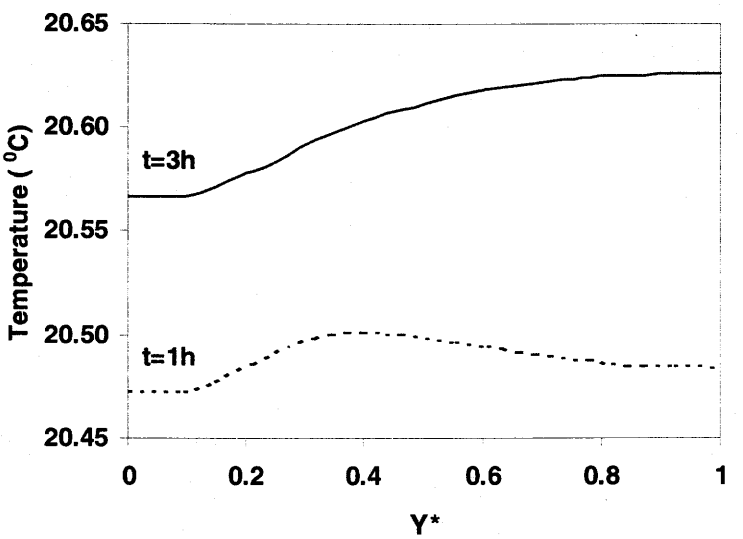

Figure 5.3 Spatial Temperature Distribution for a Layer (0<y*<0.2) of Moist Potash (X=1% at t=0) in a Bed (0.1<y*<1.0) of Dry Potash (X=0.1% at t=0)

5.3. MOISTURE ADSORPTION/DISSOLUTION DURING CONVEYING

When potash is loaded or unloaded from bulk carrier ships, it is put onto a conveyor belt to move the potash from warehouse to the ship or vice versa. During these processes, the cool potash, often at a lower temperature than the ambient air (i.e. as low as 5°C from a ship and 10°C from a warehouse), is suddenly exposed to a warm humid atmosphere (e.g. 22°C and 80% R.H). The conveyer belt moves at a significant speed (e.g. 1.5 m/s) and is often exposed to the ambient air wind speed. The typical duration for the conveying process is 5 to 15 minutes. Although this exposure time is very short, the risk of moisture gain on the exposed surface of potash is much higher than during storage and shipment in vessels due to the sudden exposure to a large temperature difference (e.g. perhaps 10°C) and high relative ambient air humidities (e.g. perhaps 80%) and the relative ambient air speed (e.g. 1.0m/s). An even larger risk will occur if the conveyer is stopped for some time while it is loaded or the conveyor belt loading and unloading process continues while it is raining.

This rapid moisture accumulation in cold potash on a conveyor belt is studied using the numerical model. The problem of transient moisture accumulation in cold potash, after it is placed on a conveyor belt in a warm humid atmosphere is investigated for a potash bed of 25 cm thick as shown in Figure 5.4. Later, the case of infrared heating of the surface layer of cold potash on the same belt will be considered as one method to prevent the rapid accumulation of moisture on the surface layer.

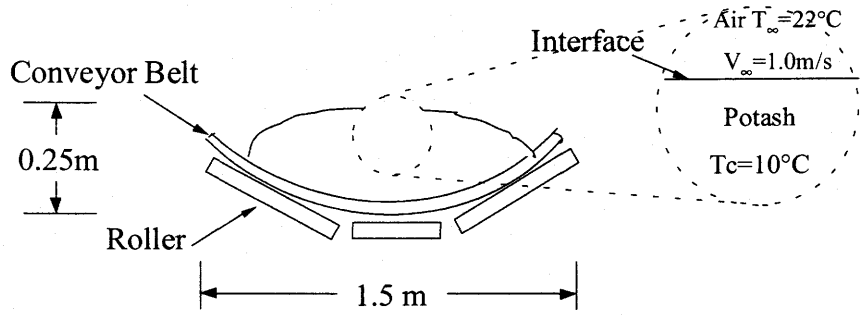

Figure 5.4. Schematic of the Transient Moisture Accumulation in Cold Potash Placed on Conveyor Belt

5.3.1 BOUNDARY CONDITIONS AND INITIAL CONDITIONS

The initial temperature of the interior grid nodes are set to 10°C except for the three grid nodes at the top which were set to 14°C, 13°C, and 12°C. This boundary conditions avoids condensation but permits adsorption and dissolution. The initial moisture content is set to about 7.0×10^{-5} corresponding to a local relative humidity of 10%. The ambient air is set to warm and humid conditions at 22°C and 80% relative humidity. Mathematically, the initial conditions are:

$$T(t=0,1)=14°C \tag{5.6}$$

$$T(t=0,2)=13°C \tag{5.7}$$

$$T(t=0,3)=12°C \tag{5.8}$$

$$T(t=0,i)=10°C\ (3<i<N) \tag{5.9}$$

$$\phi(I)=0.10\ (1<I<N) \tag{5.10}$$

Convective heat and moisture transfer occurs at y=0 where the heat and mass transfer coefficients are taken from the correlations used in Chapter 2. At y=25 cm the boundary conditions are assumed to be adiabatic and impermeable. Mathematically, these boundary conditions are:

1) at y=0

$$T_\infty=22°C,\ \phi_\infty=80\% \tag{5.11}$$

$$\delta_s \frac{\partial(\rho C_p T)}{\partial t} + \dot{m}''|_{x=0} \cdot Q = K_{eff} \frac{\partial T}{\partial y}|_{x=0} - h_h\left(T|_{y=0} - T_\infty\right) \tag{5.12}$$

$$\delta_s \frac{\partial(\rho')}{\partial t} + \dot{m}''|_{x=0} = D_{eff} \frac{\partial \rho_\gamma}{\partial y}|_{x=0} \tag{5.13}$$

where

$$\rho' = \varepsilon_\beta \rho_\beta + \varepsilon_\sigma \rho_\sigma X + \varepsilon_\gamma \rho_\gamma \tag{5.14}$$

2) at y=L (L=25 cm)

$$\frac{\partial \rho_\gamma}{\partial y}\Big|_{y=L} = 0 \tag{5.15}$$

$$\frac{\partial T}{\partial y}\Big|_{y=L} = 0 \tag{5.16}$$

5.3.2. SIMULATION OF COLD POTASH PLACED ON A CONVEYOR BELT

Figures 5.5 and 5.6 show the simulated spatial moisture content at several times from 0 to 30 minutes after the potash is placed on the conveyor belt. Moisture content near the surface ($0<y^*<0.1$) has increased from 0.075% to 1.24% in 5 minutes due to the rapid water vapor adsorption / dissolution caused by mostly initial cool surface temperature and the very high relative humidities that result. If the conveyor belt process takes even longer time (e.g. 15 to 30 minutes) then much more moisture will accumulate near the potash surface. This result also shows that the highest moisture content is expected to be right on the surface and the moisture content decreases rapidly with distance, y^*. It is found that the interior moisture content does not increase significantly during the conveyor belt exposure, implying that the rapid moisture accumulation is only significant for a narrow surface layer (e.g. the top 10%) when potash is placed on conveyor belt. Figure 5.8 shows the corresponding spatial temperature distribution within potash bed while it is on a moving conveyor belt. The potash surface temperatures ($0<y^*<0.2$) increase significantly due to their exposure to warm ambient air and the energy released by adsorption /dissolution and condensation. Significant temperature

increases are also found at interior nodes ($0.2<y^*<0.4$) due to the heat conduction and adsorption.

It is interesting to calculate the thermal boundary layer without moisture transfer. Using equation(1.1) the thermal penetration depth without moisture accumulation (δ_t) is calculated after 15 minutes as $\delta_t = 0.0022\sqrt{(15x60)} = 0.066$ m or 66 mm. Figure 5.8 gives a quite different distance for thermal penetration implying that equation (1.1) is not applicable for this case with strongly coupled moisture accumulation effects.

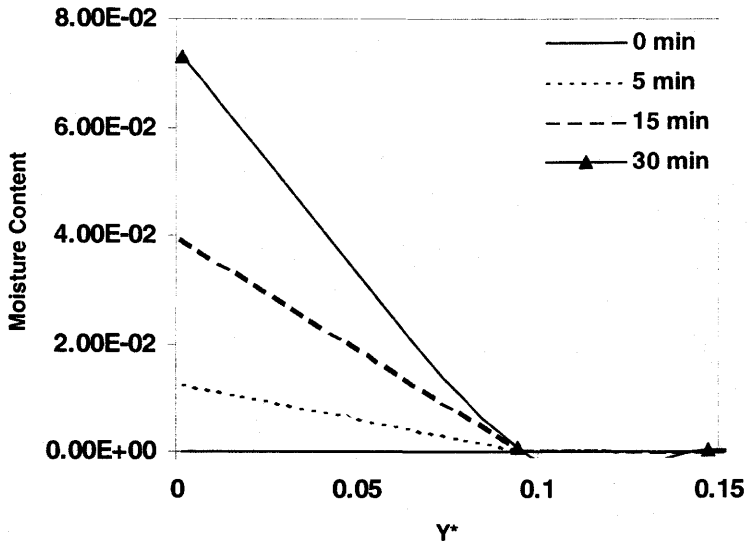

Figure 5.5(a) Spatial Moisture Content (0<y*<0.15) for Cold Potash (T=10°C at t=0)

Placed on Conveyor Belt Exposed to Humid Air (T_∞=22°C, RH=80%)

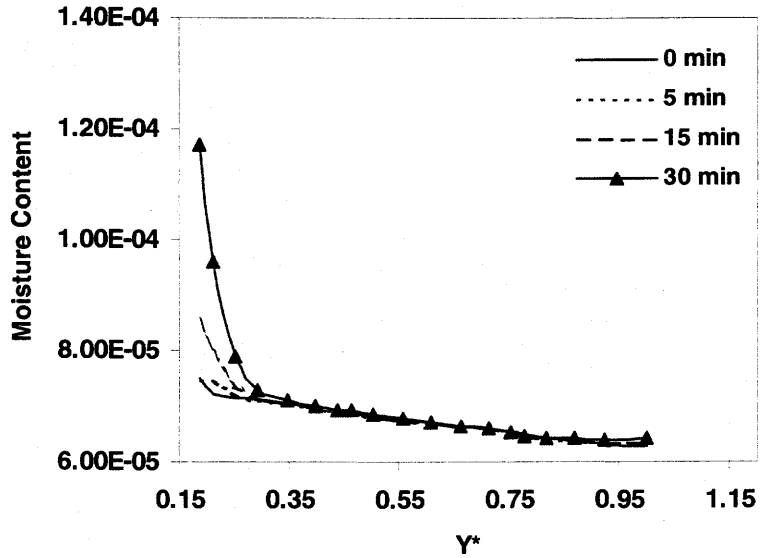

Figure 5.5(b) Spatial Moisture Content (0.15<y*<1.0) for Cold Potash (T=10°C at t=0)

Placed on Conveyor Belt Exposed to Humid Air (T_∞=22°C, RH=80%)

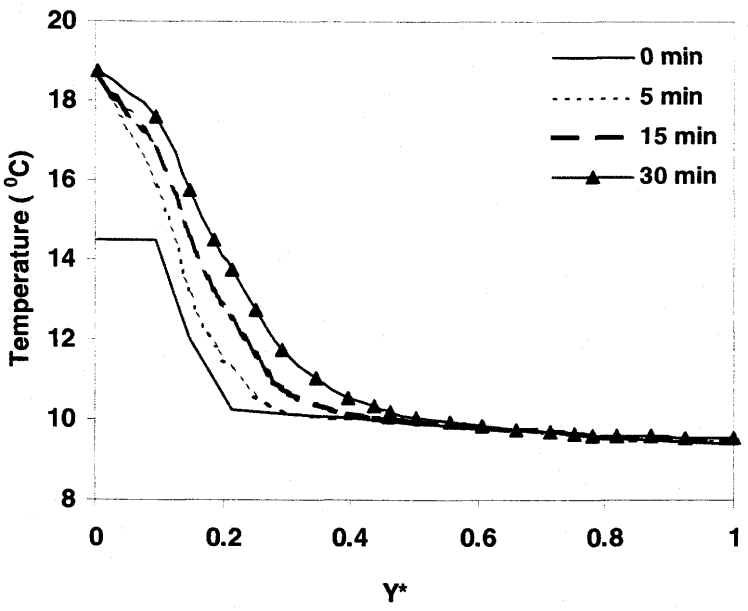

Figure 5.6. Spatial Temperature Distributions ($0.15<y^*<1.0$) for Cold Potash ($T=10°C$ at $t=0$) Placed on Conveyor Belt Exposed to Atmosphere ($T_\infty=22°C$, $RH=80\%$)

5.3.3. SIMULATION OF SURFACE WARMED POTASH PLACED ON CONVEYOR BELT

The rapid moisture accumulation only occurs near the exposed surface of potash placed on a conveyor belt. Now the moisture accumulation problem of section 5.3.2 is reconsidered when the surface is warmed up immediately after the potash is placed on conveyor belt and before it can adsorb moisture. Practically, the surface of potash could be heated by infrared radiation immediately after it is placed on the conveyor belt. The only changes of the initial conditions are assumed to be the four nodes near the top. Mathematically, they are:

$$T(t=0,1)=T(t=0,2)=22°C \tag{5.17}$$

$$T(t=0,3)=18°C \tag{5.18}$$

$$T(t=0,4)=15°C \tag{5.19}$$

$$T(t=0, i)= 10°C \tag{5.20}$$

Figure 5.7 shows the simulated spatial moisture contents from 0 to 30 minutes. It is found that significant moisture accumulation only happens near the surface layer ($0<y^*<0.2$). In this case the moisture content near the top is 20 times less than non-heated case after 5 minutes of exposure. With 30 minutes of exposure, the moisture content near the top will be increased to 0.42% which is also about 20 times lower than the non-heated case. Figure 5.8 shows the spatial temperature distribution. A significant temperature decrease near the top nodes ($0<y^*<0.2$) is noted while a significant temperature increase occurs for some of the interior nodes ($0.2<y^*<0.5$). No significant changes of either moisture content or temperature occur for $0.5<y^*<1.0$.

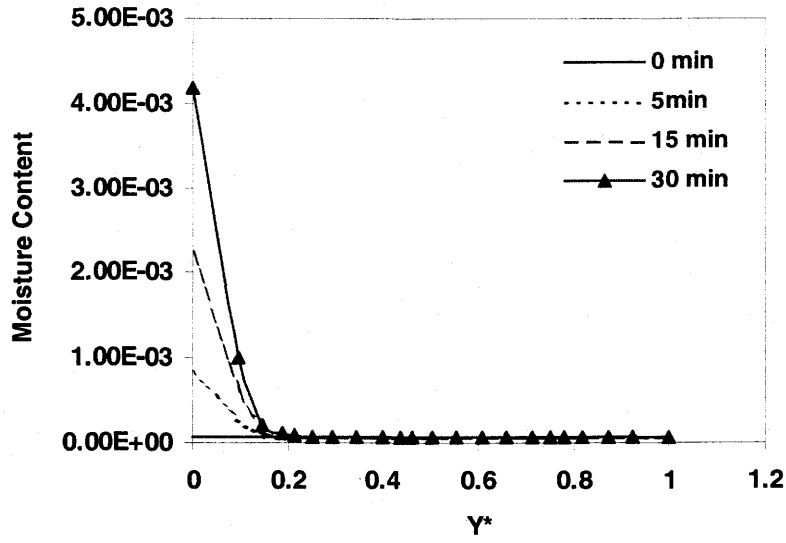

Figure 5.7. Spatial Moisture Content for a Preheated Surface Layer of Potash Placed on a Conveyor Belt Exposed to Air at T_∞=22°C, RH=80%

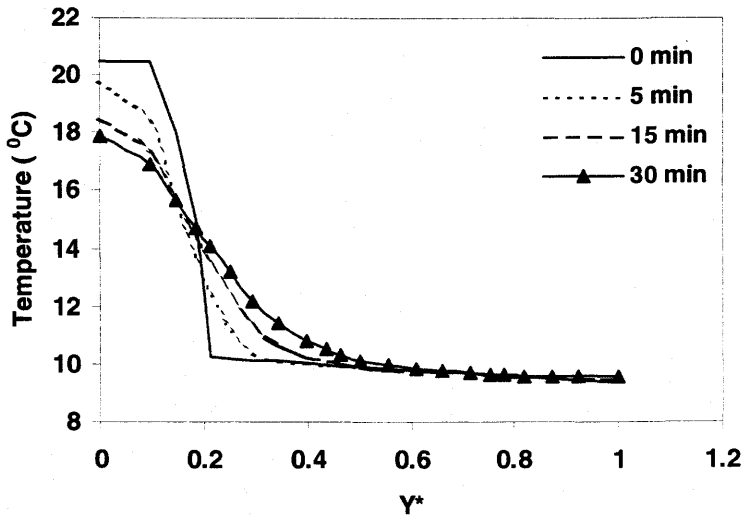

Figure 5.8. Spatial Temperature Distribution for a Preheated Surface Layer of Potash Placed on Conveyor Belt Exposed to Air at T_∞=22°C, RH=80%

Comparisons between the case of unheated and preheated potash illustrates how much moisture adsorption /dissolution may be reduced for the potash handling process – conveying cold potash from ship to shore or vice versa. Problems of moisture accumulation in potash will occur for all other storage and handling processes. They will be left for future research.

CHAPTER 6

SUMMARY, CONCLUSIONS, AND FUTURE WORK

6.1 SUMMARY

In this study, the effects of one-dimensional, transient, heat and moisture diffusion problem within the potash handling process and warehouse storage are investigated numerically and experimentally. The purpose of this study is to investigate the moisture accumulation in granular potash during handling and warehouse storage. The key objective was to develop and validate a numerical model to simulate the one-dimensional transient heat and moisture transfer process during a typical handling and storage period, then investigate typical alternative physical processes with typical bulk potash configurations.

Two types of granular potash, Rocanville Standard and Lanigan Granular, were investigated with warm humid airflow over the top and a cold or warm impermeable boundary at the bottom. The experimental and numerical temperature and moisture accumulation profiles were obtained and compared. The properties of bulk potash were measured including: permeability (K) and porosity (e), average particle size (Dp), specific surface area (Sv) and apparent thermal conductivity (K_{eff}).

The following points summarize the work carried out by this research:

1. A theoretical / numerical model was developed to describe the physical processes taking place within a bulk potash configuration subject to warm humid air over top and cold or warm temperature at the bottom. A Fortran program was developed based on the model and specified boundary conditions.

2. Temperature and moisture content profiles were measured in the potash bed subject to one-dimensional heat and moisture diffusion under specified boundary conditions. Two typical types of granular potash were tested.

3. The numerical model simulations were compared to the experimental data. Agreement was usually within uncertainty limits of the measured data. The good agreement with temperature data and simulations is considered to be a necessary but not sufficient condition. Good agreement between the moisture accumulation data and simulations is essential.

4. The numerical model was used to investigate the moisture redistribution in potash after mixing and rapid moisture accumulation for cold potash placed on conveyor belts exposed to warm humid air.

6.2 CONCLUSIONS

1. The model developed in this thesis for heat and water vapor one-dimensional transient diffusion through a layer of potash can accurately simulate the temperature

distribution and moisture accumulation process in potash but it does not include liquid capillary drainage through the potash bed. For moisture contents greater than 0.4%, the moisture distribution data differs from the simulation results at any point down from the surface but the total mass of accumulated water for the whole bed is accurately simulated. As a result of this deficiency, it is expected that the model should not be used for high moisture content (e.g. greater than 2%) and should not be used to predict the exact spatial distribution of moisture unless the moisture content is less than 0.4%.

2. The model developed can be used to simulate moisture redistribution inside a large potash bed or the rapid accumulation of moisture when cold potash is placed on a conveyor belt in a warm humid atmosphere.

6.3 FUTURE WORK

1. The theoretical / numerical model for air diffusion described and validated in this thesis is not able to accurately predict moisture content in any point with liquid capillary drainage when local potash moisture content is higher than 0.4%. Therefore, a numerical model including the drainage phenomena should be developed. New experiments should be done to verify such a model and to investigate any coupling between the heat and water vapor diffusion processes with liquid drainage.

2. Only two types of potash fertilizer, which have the same chemical compositions and similar specific surface areas, were investigated experimentally and numerically in this thesis. More research work should be done with other potash fertilizer products which have different surface chemical compositions (e.g. those with anti-caking additives) and specific surface areas (e.g.Cory soluble with Dp=0.22 mm and a specific surface area 10 times larger than Rocanville Standard.

3. Further research work should be done on the potash handling process and warehouse storage to fully understand the physical processes such as mixing and the effects that consolidation (shaking) and pressure may have on moisture diffusion, drainage, caking and dust formulation. The relationship among moisture content, pressure vibration, temperature, time and caking and dust formation needs to be more accurately correlated.

4. The model developed and verified needs to be applied to several processes in sequence from a mine in Saskatchewan to final delivery at a farm.

5. Research work should be done on preventive methods of protecting potash from moisture gain in potash fertilizers, such as the use of infrared heaters and wall jets, especially for conveyor belts and warehouse storage.

REFERENCES

Allen, T.1975, "Particle Size Measurement, 2nd Edition", London, Chapman and Hall

ANSI/ASME, 1985, "Measurement Uncertainty", ANSI/ASME PTC19.1-1985

Arpaci, V.S. and Larsen, P.S. 1984, "Convection Heat Transfer", Prentice-Hall. Inc

ASTM Standards, 1993, "Standard Test Method for Steady-State Heat Flux Measurements and Thermal Transmission Properties by Means of the Guarded-Hot-Plate Apparatus", Annual Book of ASTM Standards, C177- 85

Berner, R.A. 1978, "Rate of Mineral Dissolution under Earth Surface Condition", American J. Sci, 278, 1235-1252

Berner, R.A. 1980, "Early Diagenesis - a Theoretical Approach", Princeton University Press, Princeton, NJ

Berner, R.A. 1981, "Kinetics of Weathering and Diagenesis", Kinetics of Geochemical Processes, Reviews in Mineralogy,8, Ed. by Lasaga, A.C. and Kiskpatrick, R.J. 111-134

Carman, P.C. 1938, " The Determination of the Specific Surface. I ", Journal of the Society of Chemical Engineering, July, Page 225-234.

Carman, P.C. 1939, "The Determination of the Specific Surface. II", Journal of the Society of Chemical Engineering, January, Page 2-7.

Carman, P.C. 1956, " Flow of Gases Through Porous Media", London, Butterworths Scientific Publications

Chen, H. 1996, "Two-Dimensional Air Exfiltration / Infiltration and Heat Transfer through Fiberglass Insulation", M.Sc thesis, University of Saskatchewan.

Chen, H., Besant, R.W. and Tao, Y.-X. 1997, "Two-Dimensional Air Exfiltration and Heat Transfer through Fiberglass Insulation Part I. Numerical Model and Experimental Facility, Part II. Comparisons between Simulations and Experiments", Int.J.of HVAC & R Research V3(3) 197-232.

Chikazawa, M., Kaiho, M. and Kanazawa, T. 1972, " X-Ray Diffractometric Study of Hygroscopic Process in Alikali Halides", Nippon Kagaku Kaishi, No.5, pp.874-879.

Dullien, F.A.L. 1992, "Porous Media: Fluid Transport and Pore Structure", 2nd Edition, Academic Press.Inc

Hansen, L.D., Hoffmann, F., and Strathdee, G. 1998, "Effects if Anticaking Agents on the Thermodynamics and Kinetics of Water Sorption by Potash Fertilizers", Powder Technology, 98, 79-82

Incropera, F.P., Dewitt, D.P 1996, "Fundamental of Heat and Mass Transfer", 4th Ed, New York, John Willey & Sons

Kaviany, M. 1996, " Principle of Heat Transfer in Porous Media" 2nd edition, Springer-Verlag Book Co., New York

Kays, W.M., London, A.L. 1984, "Compact Heat Exchangers", 3rd Ed, McGraw-Hill Book Co., New York, NY

Kays, W.M. and Crawford ,M.E. 1988, "Convective Heat and Mass Transfer", McGraw-Hill Book Co., New York

Kennard, Earle.H. 1938, "Kinetic Theory of Gases", McGraw-Hill Book Company, Inc

Lee, Y.M., Haji-Sheikh, A., Fletcher, L.S., Peterson, G.P. 1994, "Effective Thermal Conductivity in Multidimensional Bodies", ASME JHT, Vol.116,17-27

Mao, Y.H., 1991, "The Measurement and Analysis of Frost Accumulation on a Flat Plate with Forced Convection", M.Sc thesis, University of Saskatchewan

Mitchell, D.R. 1993, " The Effects of Air Exfiltration / Infiltration on the Transient Thermal Response of A Glass-Fiber Insulation Slab", M.Sc Thesis, University of Saskatchewan

Mitchell, D.R., Tao, Y.-X. and Besant, R.W. 1995, "Air Filtration with Moisture and Frosting Phase Changes in Fiberglass Insulation Part I. Experiment Part II. Model Validation", Int.J. Heat Mass Transfer, V38 (9), 1587-1604

Nield, D.A., Bejan, A. 1992, "Convection in Porous Media", Springer-Verlag Book Co., New York

Patankar, Suhas V. 1980, " Numerical Heat Transfer and Fluid Flow" , McGRAW-HILL, Washington

Peng, S.W., Strathdee, G. and Besant, R.W. 1999, "Dissolution Reaction of Potash Fertilizer with Moisture", Can. JChE, V77(6),1127-1134.

Peng, S.W., Besant, R.W. and Strathdee, G. 2000a, "Measurement of Enthalpy Change during Potash-Moisture Interactions", submitted for review.

Peng, S.W., Besant, R.W. and Strathdee, G. 2000b, " Heat and Mass Transfer in Granular Potash Fertilizer with a Surface Dissolution Reaction", accepted for Can. JChE.

Peters, Steven.J and Ewing, George.E. 1997, " Thin Film Water on NaCl (100) Ambient Conditions: An Infrared Study", Laugmuir, V 13 (24), 6345-6348.

Pyne, M.T., Strathdee, G., Hansen, L.D. 1996, "Water Vapor Sorption by Potash Fertilizer Studied by a Kinetic Method", Thermochimica Act, 273, pp.277-285

Simonson, C.J. 1993. "Thermal Performance and Moisture Accumulation Within Fiberglass Insulation Subject to Transient Boundary Conditions", M.Sc thesis, University of Saskatchewan

Simonson, C.J., Tao, Y.-X. and Besant, R.W. 1996, "Simultaneous Heat and Moisture Transfer in Fiberglass Insulation with Transient Boundary Conditions", ASHRAE Transactions, V102(1) 315-327

Song, S., Yovanovich, M.M., Goodman, F.O. 1993, "Thermal Gap Conductance of Conforming Surfaces in Contact", Journal of Heat Transfer, August 1993, Vol.115 ,533-540

Tao, Y-X, Besant, R.W. and Rezkallah, K.S.,1991," Modeling of frost formation in a fibrous insulation slab and on an adjacent cold plate", Int.Comm. Heat mass Transfer 34, 1593-1603

Tao, Y-X., Besant, R.W. and Simonson, C.J. 1992, " Measurement of the Heat of Adsorption for a Typical Fibrous Insulation", ASHRAE Transactions: 98(1), 495-501

Thompson, D.C. 1972, "Fertilizer Caking and Its Prevention", Proceeding No.125, The Fertilizer Society of London.

Tien, C.L., Lienhard, J.H. 1971, "Statistical Thermodynamics", Rinehart and Winston, Inc

Walker, G.M., Megee, T.R.A., Holland, C.R., Ahmad, M.N., Moffat, N.A., and Kells, A.G. 1998, "Caking Process in Granular Potash NPK Fertilizer", Ind.Eng.Chem. Res., 37, pp.435-438.

Zhou, Q., Peng, S.W. and Besant, R.W. 1998, "Uncertainty in the Sieve Analysis of Granular Potash", Department of Mechanical Engineering, University of Saskatchewan, internal report.

Zhou, Q., Peng, S.W. and Besant, R.W. 1998, " Uncertainty in the Measurement of Permeability and Porosity of Granular Potash", Department of Mechanical Engineering, internal report.

Zhou, Q., Peng, S.W. and Besant, R.W. 1998, " Uncertainty in the Specific Surface Analysis of Granular Potash", Department of Mechanical Engineering, University of Saskatchewan, internal report

Zhou, Q., Peng, S.W. and Besant, R.W. 1999, " Uncertainty in the Measurement of apparent Thermal Conductivity of Granular Potash", Department of Mechanical Engineering, University of Saskatchewan, internal report

APPENDIX-A

PROPERTIES USED IN THE NUMERICAL MODEL

The properties used in the numerical model presented in Chapter 2 with simulation results in Chapter 4 are included in this appendix. These properties are either measured experimentally or taken from literature. Property values are taken at 300 K unless otherwise stated.

ROCANVIILE STANDARD POTASH PROPERTIES:

K_{eff}^{0}=0.597 W/(m•K) (New experimental data, 1999)

C_p^{0}=750.0 J/(kg•K) (Potash Corporation of Saskatchewan)

ε_σ^{0}=0.65 (New experimental data, 1998)

$\rho^{0}_{Sylvite}$=1987 kg/m^3 (Potash Corporation of Saskatchewan)

ρ^{0}_{Halite}=2163 kg/m^3 (Potash Corporation of Saskatchewan)

$\rho^{0}_{carnallite}$=1610 kg/m^3 (Potash Corporation of Saskatchewan)

M_{KCL}=74.5513 g/mol (Waser, Trueblood and Knobler 1980)

M_{NaCL}=58.4428 g/mol (Waser, Trueblood and Knobler 1980)

$M_{KMgCL•6H2O}$=277.85 g/mol (Waser, Trueblood and Knobler 1980)

GAS PROPERTIES:

ε_γ^{0}=0.35 (New experimental data, 1998)

Air:

ρ_a= Calculated

C_{pa}=1007 J/(kg•K) (Incropera and Dewiit 1996, p.839)

R_a=287 J/(kg•K) (Rogers and Mayhew 1988, p.24)

K_a=0.0263 W/(m•K) (Incropera and Dewiit 1996, p.839)

P_a=101325 Pa (Standard atmosphere pressure)

WATER VAPOR:

ρ_γ= Calculated

$C_{p\gamma}$=1872 J/(kg•K) (Incropera and Dewiit 1996, p.846)

R_γ= 462 J/(kg•K) (Calculated by $R_a \cdot \frac{29g/mol|_{air}}{18g/mol|_{H_2O}}$)

K_γ=0.0196 W/(m•K) (Incropera and Dewiit 1996, p.846)

LIQUID WATER PROPERTIES:

ρ_β= 997 kg/m^3 (Incropera and Dewiit 1996, p.846)

$C_{p\beta}$=4179 J/(kg•K) (Incropera and Dewiit 1996, p.846)

K_β=0.613 W/(m•K) (Incropera and Dewiit 1996, p.846)

OTHERS:

h_{fg}=2.502 x 10^6 J/kg (Incropera and Dewiit 1996, p.846) @273.15 K

$D = 2.6 \times 10^{-5}\ m^2/s$ (Incropera and Dewiit 1996, p.839)

$\tau = 1.10$ (Assumption based on the model of Peng et al. ,1999)

$X_m = 9.8 \times 10^{-4}$ (Peng et al. 1999)

$C = 1.54$ (Peng et al. 1999)

$h_a = 23.4253\ W/(m2 \bullet K)$ (Incropera and Dewiit 1996, p.314,p.445)

h_m= Calculated based on Stanton number correlation between heat transfer and mass transfer. Typical value is 5.0×10^{-5} m/s (Incropera and Dewiit 1996, p.320)

APPENDIX-B

CONTROL VOLUME FORMULATION FOR DISCRETIZATION OF GOVERNING EQUATIONS AND BOUNDARY COONDITIONS

In this study, the control volume formulation (Patankar,1980) is used for discretization of governing equations. Figure B.1 and B.2 show the typical control volume and solution domain used in the one-dimensional case.

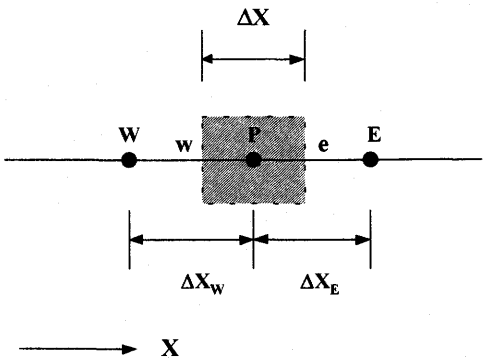

Figure B.1 Control Volume for One-Dimensional Diffusion at Node, P

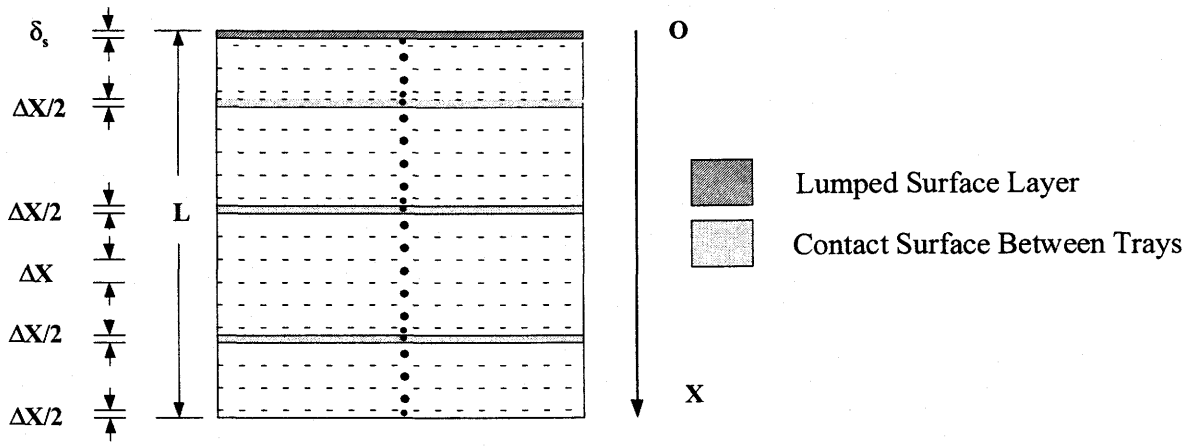

Figure B.2 Schematic of the Nodes in the Solution Domain for the Trays of Potash in the Test Bed

As described in Chapter 2, a lumped surface layer, which has a thickness of δ_s, is on the top surface. A uniform grid mesh is built below this layer and the total height is L. A special layer of the thickness of $\Delta X/2$, which has different thermal conductivity is used to simulate the screen and thermal contact resistance between the potash in adjacent trays.

DISCRETIZATION OF THE ENERGY EQUATION

The thermal energy equation is given as equation (2.8) and rewritten as below after integration over the control volume. The fully implicit scheme is employed for the transient term.

$$\left(\rho C_p T_p - \rho^0 C_p{}^0 T_p{}^0\right)\cdot \Delta x + \dot{m}\cdot Q\cdot \Delta x\cdot \Delta t = \left(K_{eff}^{e}\,\frac{T_E - T_P}{\Delta x_E} - K_{eff}^{w}\,\frac{T_p - T_W}{\Delta X_w}\right)\cdot \Delta t \qquad \text{(B1)}$$

Property values at the previous time step are denoted by ρ^0, $C_p{}^0$ and $T_p{}^0$. It is assumed that the properties T, ρ, C_p represent the average of each those properties over the control volume in Figure B.1. The value of apparent thermal conductivity at the interface of two control volumes is take by spatially averaging on each grid interfaces and is given as:

$$K_{eff}^{e} = \frac{K_{eff}^{E}\cdot K_{eff}^{P}}{r_P\cdot K_{eff}^{E} + r_E\cdot K_{eff}^{P}} \qquad \text{(B.2)}$$

$$K_{eff}^{w} = \frac{K_{eff}^{W} \cdot K_{eff}^{P}}{r_{w} K_{eff}^{P} + r_{P} \cdot K_{eff}^{W}} \tag{B.3}$$

where:

$$r_{E} = \frac{\Delta x_{E}}{\Delta x_{E} + \Delta x_{P}}$$

and

$$r_{p} = \frac{\Delta x_{P}}{\Delta x_{E} + \Delta x_{P}} \tag{B.4}$$

are equal to ½ for a uniform grid.

DISCRETIZATION OF GAS DIFFUSION EQUATION

Integrating the gas diffusion equation (2.6) over the control volume gives the following equation:

$$\left(\varepsilon_{\gamma} \rho_{\gamma,P} - \varepsilon_{\gamma}^{0} \rho_{\gamma,P}^{0}\right) \cdot \Delta x - \dot{m} \cdot \Delta x \cdot \Delta t = \left(D_{eff}^{e} \frac{\rho_{\gamma,E} - \rho_{\gamma,P}}{\Delta x_{E}} - D_{eff}^{w} \frac{\rho_{\gamma,P} - \rho_{\gamma,W}}{\Delta x_{W}} \right) \cdot \Delta t \tag{B.5}$$

The explanation of the terms in this equation is similar to the energy equation. The source term, $\dot{m}$, is defined by equation (2.39) and is linearized using the equation:

$$m = S = S_c + S_P \rho_{\gamma,P} \tag{B.6}$$

where the expressions for S_c and S_p are dependent on the local relative humidity ϕ. As described in Chapter 2, three different cases were given with equation (2.36), (2.37) and (2.38). That is :

(1) $0 \le \phi < 45\%$

$$S_c = \frac{(1-\phi)[1+(c-1)\phi]-\phi(c-2c\phi-2+2\phi)}{(1-\phi)^2[1+(c-1)\phi]^2} X_m \cdot X_c \cdot \rho_\sigma \tag{B.7}$$

$$S_P = -\frac{1}{\rho_{\gamma,S} \cdot \Delta t} \cdot \frac{(1-\phi)[1+(c-1)\phi]-\phi(c-2c\phi-2+2\phi)}{(1-\phi)^2[1+(c-1)\phi]^2} X_m \cdot X_c \cdot \rho_\sigma \tag{B.8}$$

(2) $45\% \le \phi < 53\%$

$$S_c = (2a\phi + b)\frac{\phi^0}{\Delta t}\rho_\sigma \tag{B.9}$$

$$S_P = -(2a\phi + b)\frac{1}{\rho_{\gamma,S} \cdot \Delta t}\rho_\sigma \tag{B.10}$$

(3) $53\% \le \phi < 85\%$

$$S_c = \frac{-(b + 2c\phi + 3d\phi^2)}{(a + b\phi + c\phi^2 + d\phi^3)^2} \cdot \frac{\phi^0}{\Delta t}\rho_\sigma \tag{B.11}$$

$$S_P = \frac{b + 2c\phi + 3d\phi^2}{\left(a + b\phi + c\phi^2 + d\phi^3\right)^2} \cdot \frac{1}{\rho_{\gamma,S} \cdot \Delta t} \cdot \rho_\sigma \qquad \text{(B.12)}$$

DISCRETIZATION OF CONTINUITY EQUATION

A. SOLID PHASE

$$\left(\varepsilon_\sigma - \varepsilon_\sigma{}^0\right) - \dot{m} \cdot \Omega_\sigma = 0 \qquad \text{(B.13)}$$

B. LIQUID PHASE

$$\left(\varepsilon_\beta - \varepsilon_\beta{}^0\right) - \dot{m} \cdot \Omega\beta = 0 \qquad \text{(B.14)}$$

C. GASEOUS PHASE

$$\varepsilon_\gamma = 1 - \varepsilon_\sigma - \varepsilon_\beta \qquad \text{(B.15)}$$

INTERGRAL OF AVERAGE MOISTURE CONTENT EQUATION

Integrating equation (2.25), the average moisture content by mass within potash could be expressed as:

$$\int_{t_0}^{t_1} \frac{\partial X}{\partial t} dt = \int_{t_0}^{t_1} \frac{\dot{m} \cdot \nu}{\left(1 - \varepsilon_\gamma{}^0\right)} dt \qquad \text{(B.16)}$$

BOUNDARY CONDITIONS

A. THERMAL BOUNDARY CONDITIONS

Thermal boundary conditions at x=0 and x=L are given by equations (2.26) and (2.31). The P.D.E equations are discretized by different methods at these two boundaries. The finite difference method is used at x=0 and at x=L where equation (2.8) and the control volume method is employed at x=L.

(1) at x=0

$$\delta_s \frac{\rho C_p T_P - \rho^0 C_P{}^0 T_P{}^0}{\Delta t} + \dot{m}\big|_{x=0} \cdot Q = K_{eff}^{x=0} \frac{T_E - T_P}{\Delta X_{E|_{x=0}}} - h_h (T_P - T_\infty) \qquad \text{(B.17)}$$

(2) at x=L

$$\left(\rho C_P T_Q - \rho^0 C_p{}^0 T_Q{}^0\right) \cdot \Delta X\Big|_{x=L} + \dot{m} \cdot Q \cdot \Delta t \cdot \Delta x\Big|_{x=L} = \left(-\dot{m}''\big|_{x=L} \cdot Q - \frac{T_Q - T_{bottom}}{R_{ct}} - \frac{T_W - T_Q}{\Delta x_W} \right) \cdot \Delta t$$

(B.18)

B. WATER VAPOR DIFFUSION BOUNDARY CONDITIONS

Water vapor diffusion boundary conditions are described in equation (2.27) and (2.32). Using the same method as in the thermal boundary condition equations, the discretized equations is presented as:

(1) at x=0

$$\delta_s \frac{\left(\varepsilon_\beta \rho_\beta + \varepsilon_\sigma \rho_\sigma X\big|_{x=0} + \varepsilon_\gamma \rho_\gamma\right) - \left(\varepsilon_\beta^0 \rho_\beta^0 + \varepsilon_\sigma^0 \rho_\sigma^0 X^0\big|_{x=0} + \varepsilon_\gamma{}^0 \rho_\gamma^0\right)}{\Delta t} + \dot{m} = D_{eff}^{x=0} \frac{\rho_{\gamma,E} - \rho_{\gamma,P}}{\Delta x_E} \tag{B.19}$$

(2) at x=L

$$\left(\varepsilon_\gamma \rho_{\gamma,Q} - \varepsilon_\gamma^0 \rho_{\gamma,Q}^0\right) \cdot \Delta x - \dot{m} \cdot \Delta t \cdot \Delta x\big|_{x=L} = \left(D_{eff}^{w} \frac{\rho_{\gamma,W} - \rho_{\gamma,Q}}{\Delta X_W} \right) \cdot \Delta t \tag{B.20}$$

APPENDIX C

EXPERIMENTAL MEASUREMENT OF PERMEABILITY AND POROSITY OF GRANULAR POTASH

Using a laboratory test facility, the permeability (K) and porosity (ε) of seven different types of commercial, granular potash were measured for a range of flow conditions. For each sample, these parameters are measured under two different particle configurations (consolidated and unconsolidated).

The measurement of permeability (K) is deduced from measuring the pressure difference, temperature and flow rate using the test facilities in the lab. A schematic of this test facility is shown in Figure C.1 showing the potash test container. Different permeabilities and porosities occur under different experimental conditions; i.e., unshaken (unconsolidated), or well-shaken (consolidated). These two states correspond to just placing particles in the test container before they are shaken and after they have been consolidated subject to vibratory disturbances to give a maximum density. Since dry potash is nearly pure Sylvite (KCl) with small fractions of other salts (Halite and Carnallite), the porosity (ε) can be deduced from a weight measurement with a very small uncertainty. This is the method of calculating porosity in these tests. Table C.1 identifies the seven different types of potash products tested and each average particle size (Zhou et al,1998).

The main assumptions for all the tests are:

1) The properties are uniform and isotropic throughout the test container

2) The Darcy equation for flow through a porous medium applies for the test conditions

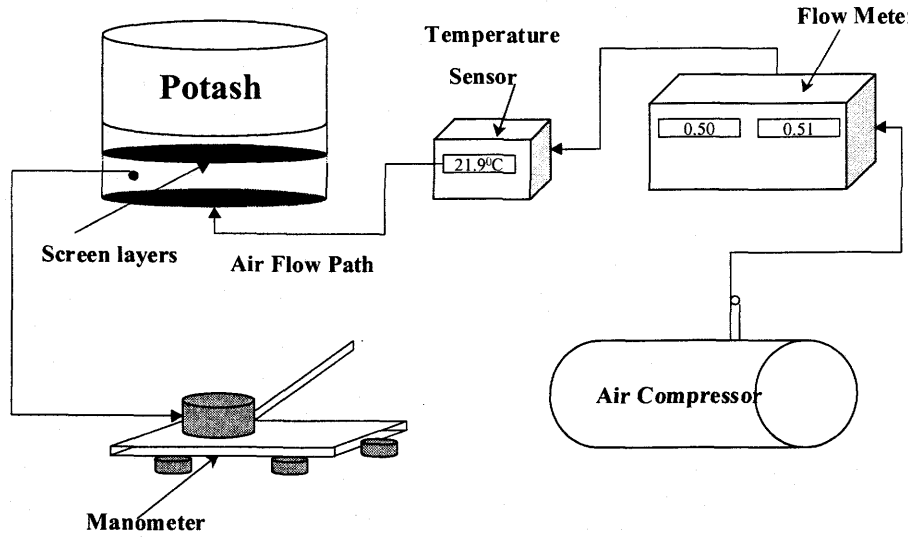

Figure C.1 The experimental Apparatus Used to Measure the Permeability and Porosity of Granular Potash

Table C.1 Reference List of Potash Material

Potash Category	Potash Identification	Average Particle Size (mm)
Type-A	Lanigan Untreated Granular#2	2.20
Type-B	Lanigan Untreated Standard	0.80
Type-C	R.Ville Untreated Granular	2.40
Type-D	R.Ville Untreated Standard	0.80
Type-E	Cory Untreated Soluable	0.22
Type-F	Cory Untreated White Granular	2.60
Type-G	Prills	2.30

GOVERNING EQUATIONS

1. For permeability (K)

The Darcy momentum equation is used to calculate the value of permeability (K) using the equation [Dullien 1991]:

$$u_D = \frac{K}{\mu} \cdot \frac{\Delta P}{\Delta X} \tag{C.1}$$

where

u_D is the Darcy velocity (m/s) can be expressed as $u_D = \frac{Q}{A} = \frac{4Q}{\pi \cdot D^2}$ (C.2)

Q = volume flow rate (m^3/s)

D= diameter of the test container (m)

K = permeability of potash (m^2)

μ = air viscosity (Pa • s)

ΔX= height of potash layer above the screen (m)

ΔP= pressure difference across potash layers (Pa)

Substituting equation (2) into equation (1) we get the equation for permeability calculation:

$$K = \frac{4}{\pi} \cdot \frac{\mu \cdot \Delta X \cdot Q}{\Delta P \cdot D^2} \tag{C.3}$$

2. For porosity (ε)

The porosity represents the volume fraction of air in the test container.

$$\varepsilon = \frac{V_{air}}{V_{cont}} \tag{C.4}$$

where

V_{cont}= internal volume of the container above the screen (m^3)

$$V_{cont} = \frac{\pi \cdot D^2}{4} \cdot \Delta X \tag{C.5}$$

V_{air}= volume of air within the container (m^3)

We can write

$$V_{air} = V_{cont} - V_{potash} = V_{cont} - \frac{\Delta M}{\rho_{potash}} \tag{C.6}$$

where

ΔM = net potash mass in the cylindrical container (kg)

ρ_{potash} = density of potash material (1987 kg/m^3)

The formula for porosity in term of the measured net mass of potash is:

$$\varepsilon = 1 - \frac{4\Delta M}{\rho_{potash} \cdot \pi \cdot D^2 \cdot \Delta X} \tag{C.7}$$

EXPERIMENTAL APPARATUS AND INSTRUMENTATION

1. Apparatus

For each test, we measure or calculate following parameters: supply air flow rate (Q_1), supply air temperature (T_1), air pressure difference (ΔP), and net potash mass in the

container (ΔM). The diameter of the cylinder (D) and the height of the cylinder (ΔX) are measured only once and used for all tests.

A schematic of the apparatus shown in Figure C-1 includes an air-compressor, air flow-rate control module with a valve and digital LED screen, manometer, digital LED temperature display and the cylindrical test container. The air compressor supplies a constant dry air flow-rate using a control module which controls the supply air flow rate. The air flows through potash with low pore size Reynolds number to satisfy the requirement of Darcy principle which requires a low internal flow momentum if the permeability is to be nearly independent of the Darcy velocity. i.e. $Re_{dp} < 10$ for well rounded particles ,where Re_{dp} = Reynolds number based on particle diameter $= \frac{\rho U_D \cdot dp}{\mu}$ (Kaviany,1996). Typical values for various types of potash range between $Re_{dp} = \frac{0.03x2.80x10^{-3}}{15.5x10^{-6}} \cong 5$ and $Re_{dp} = 0.5$. For particles with sharp (not well rounded) irregular surfaces on the particles, this range of Re_{dp} will be lower. Thus for large particles of irregular shape, we need to restrict the velocity to a lower value when computing the permeability.

Figure C.2 shows the detail drawing on the test container which has two important geometric parameters namely the diameter of the test container (D) and the depth of sample (ΔX). D and ΔX must be selected to be very large with respect to particle size so that the effect of surfaces on the container will not distort the interior particle alignments

and therefore the test data. Particle alignment near the sidewalls and on the bottom screen and at the top surface will differ from particle alignments far from these surfaces.

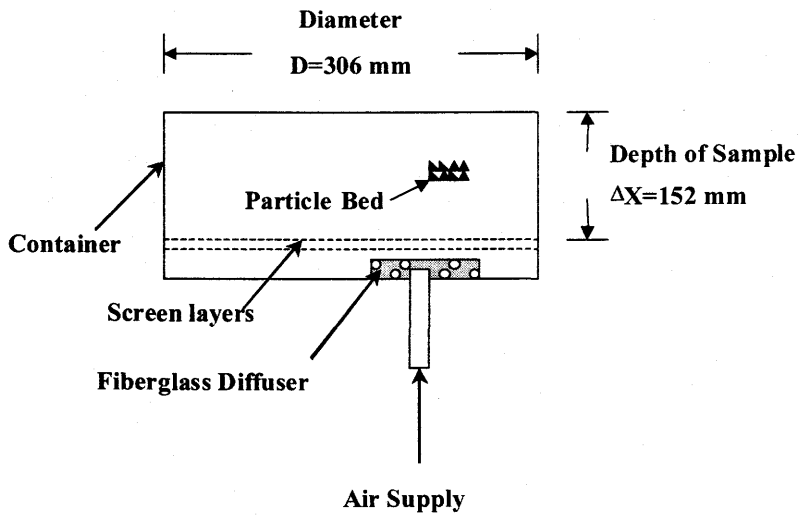

Figure C.2 Schematic of the Test Container Used to Measure the Permeability and Porosity

2. Test Procedure For Permeability (K) and Porosity (ε)

The test procedure used to measure both the permeability (K) and porosity (ε) for one test condition is as follows:

1) Measure geometry and calculate the volume (V_{cont}) of the test container
2) Measure the ambient air temperature (T_1)and atmosphere pressure (P_{bar})
3) Measure the air flow rate (Q_1) through potash using a calibrated volume flow meter.
4) Measure the pressure difference (ΔP) between potash and ambient air using an inclined manometer.

5) Measure the potash container mass difference ΔM with and without the potash for each test

6) Calculate the permeability (K) from Darcy equation (C.3)

7) Calculate the porosity (ε) from equation (C.7)

8) Estimate the measurement uncertainties for K and ε

The flow rate control model (MKS 1559A-200L-SV) has a range from 0 to 200 L/min and is calibrated with an uncertainty of 1% of the maximum flow rate.

Experimental Results and Analysis

1. Experimental Result

Seven types of potash have been measured in two different particle configurations: consolidated (shaken) and unconsolidated (unshaken). In the unconsolidated state the potash is pored into the test container without mixing the potash particles or shaking the container. In the consolidated state the full container of potash is vibrated for several minutes until the level of potash drops in the container to a final steady state. The container is then refilled to bring the level of potash to the top of the container and then the container is vibrated again. Finally the level of potash is carefully adjusted by a straight edge to exactly fill the container.

In each test, three measurements have been completed for every type of potash material to ensure the repeatability of the measurement. The experimental results for permeability (K) are listed in Table C.2 to Table C.8 for three repeated tests and 10 flow

rates for both unshaken (K_{11}, K_{12}, K_{13}) and shaken (K_{21}, K_{22}, K_{23}) permeabilities. The data for potash sample type-A is presented in graphical form for K versus U_D in Figure C.3 where the value of porosity is shown for the unshaken and shaken test conditions.

Table C.2 Experimental Data of Permeability for Type-A Potash

Darcy Velocity	Permeability (Unshaken)			Permeability (Shaken)		
U_D	K11	K12	K13	K21	K22	K23
(m / s)	(m^2)	(m^2)	(m^2)	(m^2)	(m^2)	(m^2)
5.13E-03	5.35E-08	5.35E-08	5.35E-08	3.89E-08	3.80E-08	3.89E-08
1.03E-02	5.70E-08	5.26E-08	5.35E-08	4.03E-08	4.03E-08	3.98E-08
1.53E-02	5.49E-08	5.26E-08	5.26E-08	3.95E-08	3.95E-08	3.95E-08
2.02E-02	5.48E-08	5.22E-08	5.22E-08	3.99E-08	3.99E-08	3.99E-08
2.51E-02	5.75E-08	5.25E-08	5.32E-08	4.04E-08	4.00E-08	3.98E-08
3.00E-02	5.56E-08	5.24E-08	5.24E-08	3.92E-08	3.94E-08	3.92E-08
3.48E-02	5.41E-08	5.17E-08	5.12E-08	3.94E-08	3.88E-08	3.86E-08
3.95E-02	5.36E-08	5.09E-08	5.03E-08	3.86E-08	3.81E-08	3.77E-08
4.43E-02	5.20E-08	5.03E-08	5.03E-08	3.79E-08	3.75E-08	3.74E-08
4.89E-02	5.05E-08	4.97E-08	4.97E-08	3.70E-08	3.70E-08	3.68E-08

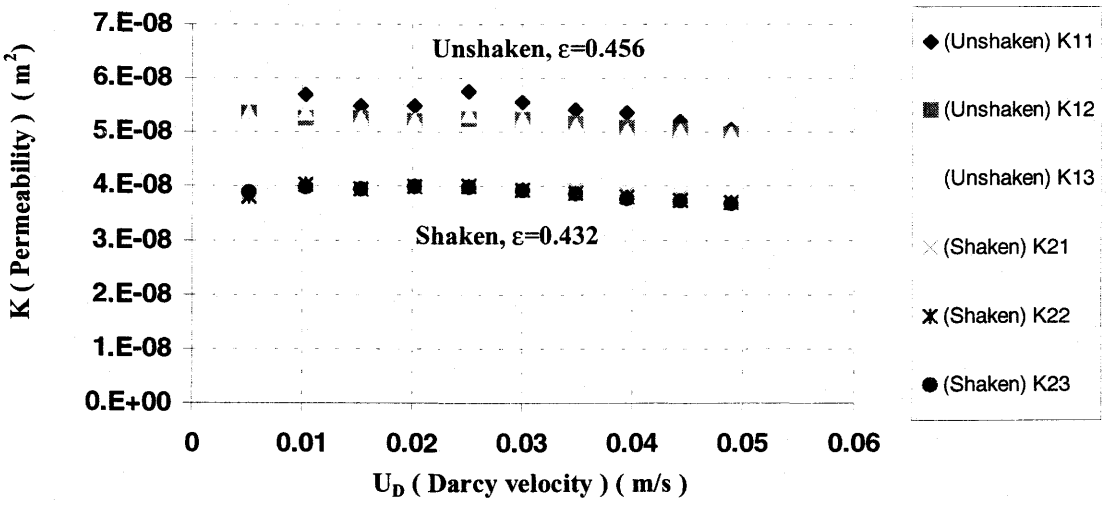

Figure C.3 Permeability and Porosity of Type-A Potash

Table C.3 Experimental Data of Permeability for Type-B Potash

Darcy Velocity	Permeability (Unshaken)			Permeability (Shaken)		
U_D	K11	K12	K13	K21	K22	K23
(m / s)	(m^2)	(m^2)	(m^2)	(m^2)	(m^{-2})	(m^2)
5.20E-03	4.78E-09	4.68E-09	4.68E-09	3.18E-09	3.18E-09	3.18E-09
1.04E-02	4.96E-09	4.89E-09	4.88E-09	3.31E-09	3.31E-09	3.31E-09
1.55E-02	4.92E-09	4.91E-09	4.88E-09	3.35E-09	3.35E-09	3.35E-09
2.05E-02	4.95E-09	4.93E-09	4.92E-09	3.33E-09	3.35E-09	3.35E-09
2.55E-02	4.90E-09	4.90E-09	4.90E-09	3.33E-09	3.33E-09	3.32E-09
3.04E-02	4.87E-09	4.87E-09	4.87E-09	3.30E-09	3.30E-09	3.30E-09
3.53E-02	4.80E-09	4.80E-09	4.80E-09	3.25E-09	3.25E-09	3.25E-09
4.01E-02	4.74E-09	4.74E-09	4.74E-09	3.21E-09	3.21E-09	3.21E-09
4.49E-02	4.66E-09	4.67E-09	4.66E-09	3.17E-09	3.17E-09	3.17E-09
4.95E-02	4.60E-09	4.62E-09	4.62E-09	3.12E-09	3.13E-09	3.12E-09

Table C.4 Experimental Data of Permeability for Type-C Potash

Darcy Velocity	Permeability (Unshaken)			Permeability (Shaken)		
U_D	K11	K12	K13	K21	K22	K23
(m / s)	(m^{-2})	(m^{-2})	(m^{-2})	(m^{-2})	(m^{-2})	(m^{-2})
5.14E-03	8.57E-08	7.45E-08	7.79E-08	5.71E-08	5.71E-08	5.71E-08
1.03E-02	8.57E-08	7.62E-08	7.62E-08	5.71E-08	5.53E-08	5.71E-08
1.53E-02	8.27E-08	7.77E-08	7.54E-08	5.69E-08	5.57E-08	5.69E-08
2.03E-02	8.13E-08	7.42E-08	7.42E-08	5.67E-08	5.49E-08	5.63E-08
2.52E-02	7.85E-08	7.36E-08	7.30E-08	5.63E-08	5.56E-08	5.63E-08
3.00E-02	7.83E-08	7.32E-08	7.32E-08	5.57E-08	5.45E-08	5.45E-08
3.49E-02	7.60E-08	7.41E-08	7.32E-08	5.56E-08	5.36E-08	5.39E-08
3.96E-02	7.51E-08	7.14E-08	7.14E-08	5.41E-08	5.28E-08	5.37E-08
4.44E-02	7.28E-08	7.21E-08	7.11E-08	5.36E-08	5.26E-08	5.26E-08
4.90E-02	7.13E-08	7.07E-08	7.01E-08	5.25E-08	5.21E-08	5.21E-08

Table C.5 Experimental Data of Permeability for Type-D Potash

Darcy Velocity	Permeability (Unshaken)			Permeability (Shaken)		
U_D	K11	K12	K13	K21	K22	K23
(m / s)	(m^2)	(m^2)	(m^2)	(m^2)	(m^2)	(m^2)
5.20E-03	6.77E-09	6.64E-09	6.64E-09	4.37E-09	4.37E-09	4.37E-09
1.04E-02	6.84E-09	6.84E-09	6.77E-09	4.64E-09	4.64E-09	4.64E-09
1.55E-02	6.86E-09	6.86E-09	6.81E-09	4.68E-09	4.66E-09	4.66E-09
2.05E-02	6.84E-09	6.80E-09	6.80E-09	4.68E-09	4.66E-09	4.66E-09
2.55E-02	6.82E-09	6.82E-09	6.82E-09	4.66E-09	4.65E-09	4.65E-09
3.04E-02	6.78E-09	6.76E-09	6.76E-09	4.60E-09	4.61E-09	4.61E-09
3.53E-02	6.72E-09	6.68E-09	6.70E-09	4.56E-09	4.55E-09	4.55E-09
4.01E-02	6.53E-09	6.53E-09	6.53E-09	4.49E-09	4.48E-09	4.49E-09
4.48E-02	6.48E-09	6.46E-09	6.48E-09	4.45E-09	4.44E-09	4.44E-09
4.95E-02	6.35E-09	6.35E-09	6.35E-09	4.38E-09	4.38E-09	4.38E-09

Table C.6 Experimental Data of Permeability for Type-E Potash

Darcy Velocity	Permeability (Unshaken)			Permeability (Shaken)		
U_D	K11	K12	K13	K21	K22	K23
(m / s)	(m^2)	(m^2)	(m^2)	(m^2)	(m^2)	(m^2)
5.11E-03	4.15E-11	4.09E-11	4.14E-11	2.61E-11	2.62E-11	2.62E-11
1.02E-02	4.06E-11	4.11E-11	4.12E-11	2.56E-11	2.60E-11	2.59E-11
1.52E-02	4.03E-11	4.07E-11	4.11E-11	2.53E-11	2.56E-11	2.56E-11
2.01E-02	4.14E-11	4.15E-11	4.15E-11			

Table C.7 Experimental Data of Permeability for Type-F Potash

Darcy Velocity	Permeability (Unshaken)			Permeability (Shaken)		
U_D	K11	K12	K13	K21	K22	K23
(m/s)	(m^2)	(m^2)	(m^2)	(m^2)	(m^2)	(m^2)
5.15E-03	5.21E-08	5.21E-08	5.21E-08	3.74E-08	3.74E-08	3.74E-08
1.03E-02	5.54E-08	5.46E-08	5.37E-08	3.86E-08	3.86E-08	3.86E-08
1.53E-02	5.56E-08	5.33E-08	5.28E-08	3.88E-08	3.88E-08	3.88E-08
2.03E-02	5.46E-08	5.29E-08	5.33E-08	3.91E-08	3.89E-08	3.89E-08
2.52E-02	5.59E-08	5.59E-08	5.28E-08	3.85E-08	3.85E-08	3.85E-08
3.01E-02	5.49E-08	5.29E-08	5.23E-08	3.87E-08	3.82E-08	3.82E-08
3.50E-02	5.40E-08	5.16E-08	5.12E-08	3.84E-08	3.79E-08	3.76E-08
3.97E-02	5.38E-08	5.17E-08	5.09E-08	3.84E-08	3.72E-08	3.70E-08
4.44E-02	5.24E-08	5.11E-08	5.04E-08	3.75E-08	3.70E-08	3.66E-08
4.91E-02	5.08E-08	5.02E-08	5.05E-08	3.67E-08	3.65E-08	3.67E-08

Table C.8 Experimental Data of Permeability for Type-G Potash

Darcy Velocity	Permeability (Unshaken)			Permeability (Shaken)		
U_D	K11	K12	K13	K21	K22	K23
(m/s)	(m^2)	(m^2)	(m^2)	(m^2)	(m^2)	(m^2)
5.20E-03	6.92E-08	6.92E-08	6.92E-08	5.41E-08	5.24E-08	5.24E-08
1.04E-02	7.21E-08	6.79E-08	6.79E-08	5.58E-08	5.49E-08	5.49E-08
1.55E-02	7.36E-08	6.70E-08	6.78E-08	5.48E-08	5.43E-08	5.49E-08
2.05E-02	7.18E-08	6.82E-08	6.75E-08	5.50E-08	5.50E-08	5.45E-08
2.55E-02	7.07E-08	6.78E-08	6.68E-08	5.65E-08	5.62E-08	5.51E-08
3.04E-02	7.03E-08	6.79E-08	6.75E-08	5.62E-08	5.53E-08	5.50E-08
3.53E-02	6.91E-08	6.75E-08	6.60E-08	5.59E-08	5.44E-08	5.39E-08
4.01E-02	6.84E-08	6.64E-08	6.61E-08	5.51E-08	5.40E-08	5.40E-08
4.49E-02	6.79E-08	6.67E-08	6.61E-08	5.51E-08	5.41E-08	5.35E-08
4.95E-02	6.67E-08	6.59E-08	6.59E-08	5.48E-08	5.41E-08	5.37E-08

2. General Observation for the Data

With the above experimental results we observed several phenomena:

a) The permeabilities (K) vary depending on the particles size and shape. The magnitude of K ranges from the order of 10^{-8} m^{-2} for the coarse grained potash to 10^{-11} m^{-2} for the smallest grained potash

b) The porosities (ε) don't vary greatly for the type A to F of potash. Type-G shows a high porosity because it is processed in a very different manner such that there are microscopic cracks in each sphere like particle

c) Comparison of the two different conditions (consolidated and unconsolidated) shows the change of value of potash permeability (K) is nearly 35 % , which is much bigger than the 9% change in the porosity (ε)

d) Potash permeability depends on particle size, shape and consolidation

e) Potash permeability is not the function of Darcy velocity except at the higher value of U_D for large particles

f) The repeatability of the experimental data is very good over low Darcy velocities for the consolidated test condition. But the unconsolidated material appeared to change in permeability slightly after the first test, perhaps due to the change of particles' resistance to the air flow after the first test.

Uncertainty Analysis

The uncertainty of measurement and calculation of permeability (K), porosity (ε) and Darcy velocity must be evaluated to show the confidence we can place these results. Since in our case the contribution by precision errors is small, we first consider the bias error.

1. General Equation For Bias Error and System Uncertainty

The basic equation of experimental uncertainty is given by:

$$U_{rss} = \sqrt{(B)^2 + (t \cdot S_{\bar{x}})^2} \qquad \text{(C.8)}$$

where the bias error is given by:

$$B = \sqrt{\sum_{i}^{N} \left(\frac{\partial B}{\partial X_i} \cdot B_{x_i}\right)^2} \qquad \text{(C.9)}$$

The precision error is given by the product of the Student t and the sample standard deviation $S_{\bar{x}}$. $S_{\bar{x}}$ is best evaluated using a large number of data that is available for all flow rates so that $t \cdot S_{\bar{x}}$ is replaced by $t \cdot SEE$ in equation(8).Bias errors are determined by calibration of each sensor and each measurement system. Sensor calibration studies were done for all the measurement devices used except the experimental test chamber. The experimental test chamber geometry was selected to minimize the effect of surface errors due to particles adjacent to each surface for a given large sample of about 10-kg.

2. Uncertainty of Parameters

Using equation (C.9) , the bias error can be estimated for each measurement. These are presented in the Table-9.

Table C.9. Bias Errors of the Measurement System

Error Category	Parameters	Bias Error Value
Bq	Flow Rate	1% of the Maximum Rate
Bv	Volume	0.5% of the value
Bx	Length (m)	1.00E-03
Bd	Length (m)	2.00E-04
Bp	Barometer	1% of the Max range
Bm	Mass Balance	1% of the Mass Difference
Br	Potash Density	0.05% of the density
$B(\varepsilon_{surface})$	Surface Error of Porosity	$0.0001<B(\varepsilon_{surface})<0.002$
$B(K_{surface})$	Surface Error of Permeability (m^2)	$6.6E\text{-}13<B(K_{surface})<1.2E\text{-}09$

The resulting typical bias values computed for permeability, Darcy velocity and porosity are computed for particle of small size and the results are presented in Table C.10. The uncertainty values presented in the table have considered the bias errors due to the bounding surface effect. The range of permeability uncertainties doesn't include the value of Type-E which is 7.15% caused by the very few experimental data.

Table C.10 Essential Bias Uncertainty of K, U_D and ε

Property	Uncertainty
Permeability (K)	1.96% to 3.54%
Darcy Velocity (u)	1%
Porosity (ε)	0.28% to 0.3%

Regression Uncertainty Analysis

1. Governing Equations

The permeability (K) of porous media is expected to be independent of the Darcy velocity over a certain range. In this part of study we examine the statistical relationship between the permeabilities (K) and Darcy velocity (u_D) in our experimental results. The equation describing the relationship should be a straight line in K versus u_D plane.

$$K_{ls} = a + b \cdot u_D \tag{C.10}$$

where "b" is the slope of the line defined by:

$$b = \frac{\sum_{k=1}^{n}(u_{D,k} - \bar{u}_D)(K_k - \bar{K})}{\sum_{k=1}^{n}(u_{D,k} - \bar{u}_D)^2} \tag{C.11}$$

and "a" is the intercept defined by:

$$a = \bar{K} - b \cdot \bar{u}_D \tag{C12}$$

where the mean value of each data for u_D and K are:

$$\bar{u}_D = \frac{1}{n}\sum_{k=1}^{n} u_{D,k} \tag{C.13}$$

$$\bar{K} = \frac{1}{n}\sum_{k=1}^{n} K_k \tag{C.14}$$

Here " K_k " represents the potash permeability (K) and " $U_{D,k}$ " represents the Darcy velocity for sample test k

2.Uncertainty of the Regression Results

The 95% uncertainty limits of K for the linear relationship between K and U_D is given by:

$$U_{rss} = \sqrt{(t \cdot SEE)^2 + B^2} \tag{C.15}$$

where

$$SEE = \left[\frac{\sum_{k=1}^{N}(K_k - K_{ls,k})^2}{N - C}\right]^{1/2} \tag{C.16}$$

t= the Student t which depends on the degrees of freedom. In our experiment

t=2.776 for most the potash types except for type-C which has t=3.182 and t=4.303 for type-E

C= the number of coefficients of equation(C.11) , C=2.

N= number of the experimental data.

B= bias error which has been calculated in the previous section

3. Regression Curve

Only the data for the consolidated potash particles is considered in this analysis of uncertainty. Figure C.9 presents the data and uncertainty in graphic form. The data are shown as points and the mid-line is the regression straight line. The upper and lower lines represent the uncertainty limits for this line at 95% confidence level. A linear relationship between K and U_D can be found with two constants a and b which are listed in the Table C.11.

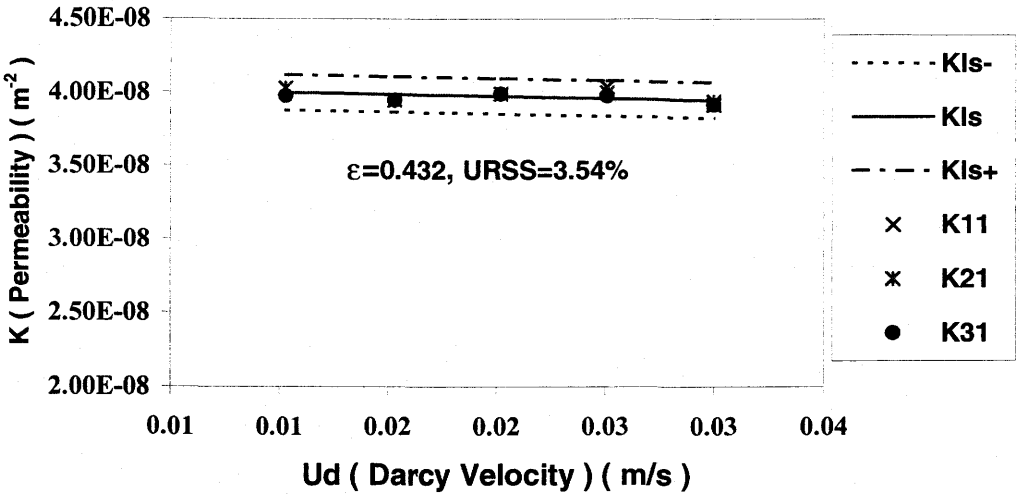

Figure C.4 Regression Curve of Selected Data for K versus Ud of Type-A Potash for the Consolidated State

Table C.11 Linear Regression Curve Constants a and b

Potash Type	Student t	a	b	U_D (m/s)
Type-A	2.776	4.03E-08	-2.65E-08	$0.01<U_D<0.03$
Type-B	2.776	3.30E-09	-9.85E-10	$0.01<U_D<0.03$
Type-C	3.182	5.74E-08	-6.78E-08	$0.005<U_D<0.02$
Type-D	2.776	4.68E-09	-1.78E-09	$0.01<U_D<0.03$
Type-E	4.303	2.63E-11	-9.94E-11	$0.005<U_D<0.02$
Type-F	2.776	3.90E-08	-1.52E-08	$0.01<U_D<0.03$
Type-G	2.776	5.56E-08	-2.51E-08	$0.01<U_D<0.0495$

APPENDIX D

SIEVE ANALYSIS OF GRANULAR POTASH

Using a sieve analysis, data for the mass fraction and cumulative mass fraction of seven different granular potash materials are measured. The sieve method is used to get the mass distribution for a range of particle sizes. Each type of potash material has a unique particle size distribution. A standard procedure has been followed for this measurement. An experimental uncertainty analysis has been performed for the mass fraction, cumulative mass fraction and particle diameter. It is assumed that the errors caused by the mass balance and sieve meshes belong to the bias error, and the error caused by sampling process belongs to the precision error. Table D.1 identifies the seven different types of potash tested.

Table D.1. Reference List of Potash Material

Potash Category	Potash Identification
Type-A	Lanigan Untreated Granular#2
Type-B	Lanigan Untreated Standard
Type-C	R.Ville Untreated Granular
Type-D	R.Ville Untreated Standard
Type-E	Cory Untreated Soluable
Type-F	Cory Untreated White Granular
Type-G	Prills

Governing Equations

Mass fraction in a certain particle size range is given by

$$MF_i = \frac{M_i}{M_{total}} (i = 1,2,.....n) \quad (D.1)$$

where MF_i = mass fraction of particles with size range $D_{i-1}>D>D_i$

M_i = mass of particle with size range $D_{i-1}>D>D_i$

M_{total} = total mass of the potash sample

D_i = the size of the i th sieve in the measurement

Cumulative mass fraction with sizes less than certain size is given by

$$CMF_i = \frac{\sum_{1}^{i} M_j}{M_{total}} (i = 1,2,.....n) \quad (D.2)$$

where CMF_i =cumulative mass fraction of particle with size $D< D_i$

ΣM_j= total mass of particle left in the sieves from D_1 to Di

M_{total} = total mass of the potash sample in the measurement

Experimental Apparatus and Instrumentation

1. Apparatus and Instrumentation

For the sieve analysis, the standard sieve series (Canadian and U.S) was used to sieve the granular potash materials which have a wide size distribution. The difference between Canadian and U.S sieve standards is small enough to be neglected. The sieve mesh size series include the numbers: #4, #5, #6, #7, #8, #10, #12, #16, #18, #20, #30, #40, #50, #60, #70, #100, #140, #200. Combinations of different size sieves were made

for each type of granular potash, and the packed sieves were put on the shaker for a certain time period. The electrical motor-driven testing sieve shaker (RO-TAP, Model-B, C-E Tyler product) causes both horizontal and vertical shaking. The time duration of shaking was long enough to have the particle distribution invariant with time.

The calibration data of sieve size are shown in Table D.2 where the mesh size is the clearance between adjacent wires in each sieve. The nominal mesh sizes listed in the table are the value claimed by the sieve manufacturer. These have been shown to be incorrect by our optical microscope calibration, especially for sieves less than 1 mm. For mesh size larger than 1 mm the error in mesh size (nominal to measured size with respect to measured value) range from 0.13 to 1.89 % but for mesh sizes lass than 1 mm these errors range from 1.82 % to 19.32 %. Generally, the sizes of these errors are proportional to the inverse of the mesh size and the measured values are, with the exception of one large mesh, bigger than the nominal value.

The calibration of the mesh screen for each sieve was done using an optical microscope (Model: ISOWA S.A, BIENNE-SWISSC) at 50X and a screw movable bed with a calibrated micrometer with scale of 10^{-4} inch or 0.00254 mm. Ten representative meshes from each sieve were selected to calibrate each sieve. Figure D.1 shows the sieve mesh calibration locations and Tables D.2 and D.3 presents the calibration results and uncertainties. The new mesh sizes have been calculated by the averaging the 10 representative values of each sieve.

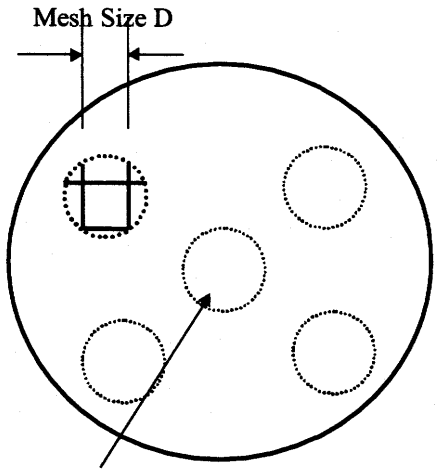

Figure D.1. Schematic of Selected Region for Mesh Calibration

Table D.2. Calibration Data for 15 Standard Sieves in the experiments

Sieve Number	Measurement Data										Nominal Mesh Size	Calib Mesh Size
	1	2	3	4	5	6	7	8	9	10	(mm)	(mm)
NO#4	4.750	4.800	4.825	4.700	4.750	4.725	4.800	4.800	4.800	4.800	4.760	4.775
NO#5	4.000	4.000	4.025	4.075	4.100	4.000	4.050	4.025	4.000	4.125	4.000	4.040
NO#6	3.325	3.250	3.350	3.340	3.350	3.250	3.400	3.300	3.375	3.000	3.350	3.294
NO#7	2.850	2.825	2.800	2.875	2.850	2.800	2.810	2.825	2.795	2.810	2.800	2.824
NO#8	2.350	2.340	2.425	2.375	2.425	2.350	2.375	2.375	2.350	2.350	2.360	2.372
NO#10	2.050	2.025	1.980	2.050	2.050	1.990	2.100	2.050	1.990	2.025	2.000	2.031
NO#12	1.700	1.725	1.700	1.750	1.750	1.700	1.700	1.750	1.600	1.600	1.700	1.698
NO#16	1.150	1.180	1.225	1.185	1.200	1.185	1.150	1.150	1.190	1.200	1.180	1.182
NO#18	1.000	1.025	1.050	1.050	0.998	0.995	1.000	1.000	1.025	1.050	1.000	1.019
NO#20	0.881	0.881	0.919	0.904	0.869	0.899	0.889	0.914	0.907	0.876	0.850	0.894
NO#30	0.655	0.632	0.640	0.648	0.632	0.610	0.622	0.625	0.660	0.660	0.595	0.639
NO#40	0.447	0.447	0.432	0.439	0.432	0.437	0.447	0.434	0.432	0.439	0.425	0.439
NO#50	0.305	0.305	0.297	0.300	0.305	0.305	0.305	0.300	0.305	0.330	0.300	0.306
NO#60	0.267	0.269	0.269	0.259	0.279	0.267	0.274	0.269	0.267	0.269	0.250	0.269
NO#70	0.239	0.239	0.239	0.241	0.244	0.244	0.229	0.236	0.246	0.246	0.212	0.240
NO#100	0.175	0.163	0.168	0.165	0.163	0.178	0.165	0.170	0.168	0.170	0.149	0.168
NO#140	0.124	0.122	0.121	0.122	0.124	0.127	0.127	0.122	0.127	0.117	0.106	0.123
NO#200	0.099	0.089	0.091	0.089	0.091	0.094	0.094	0.091	0.097	0.094	0.075	0.093

Table D.3 Experimental Uncertainty in Sieves Calibration

Sieve Number	Nominal Mesh Size (mm)	Calib Mesh Size (mm)	Microscope Bias Error (mm)	Mesh Size Uncertainty (%)
NO#4	4.760	4.775	0.00254	0.61%
NO#5	4.000	4.040	0.00254	0.82%
NO#6	3.350	3.294	0.00254	2.48%
NO#7	2.800	2.824	0.00254	0.68%
NO#8	2.360	2.372	0.00254	0.94%
NO#10	2.000	2.031	0.00254	1.30%
NO#12	1.700	1.698	0.00254	2.36%
NO#16	1.180	1.182	0.00254	1.53%
NO#18	1.000	1.019	0.00254	1.69%
NO#20	0.850	0.894	0.00254	1.40%
NO#30	0.595	0.639	0.00254	1.98%
NO#40	0.425	0.439	0.00254	1.20%
NO#50	0.300	0.306	0.00254	2.29%
NO#60	0.250	0.269	0.00254	1.69%
NO#70	0.212	0.240	0.00254	1.92%
NO#100	0.149	0.168	0.00254	2.64%
NO#140	0.106	0.123	0.00254	2.81%
NO#200	0.075	0.093	0.00254	3.68%

2. Experimental Procedure of the Size Distribution

The procedure used to obtain the particle size distribution was as follows:

1. Clean-up the sieves and potash container and zero the mass balance
2. Measure the mass of the empty glass potash container
3. Put each potash sample into the potash container and measure the mass of container with granular potash (M_{total}) for each sample
4. Carefully fill the granular potash into the top of the stacked sieves, then put the sieves into the shaker and set the shaking time and start the shaking process
5. When the shaker stops, weight the mass of potash left in each sieve (M_i) after pouring the sample from M_i into the glass container and record the data
6. Put the potash from all the sieves together and mix them well

7. Repeat the process from step 1) to step 5) with the same sample

8. Repeat the process from step1) to step7) with two other potash samples

Experimental Results and Analysis

1. Experiment Results

For each type of granular potash we use three samples. For each sample, two particle size distribution measurements have been done to examine the repeatability of the test procedure and to collect more data. The experimental data for the seven types of granular potash are presented for mass fraction and cumulative mass fraction in Tables D.4 to D.10. The uncertainty for each of these is presented. The results of Type-D, Roconville Standard, for mass fraction (MF) and cumulative mass fraction (CMF) are presented graphically for distribution and accumulated distribution as a function of particle diameter in Figures D.2 to D.3.

An analytical normal particle size distribution curve (prediction) has been selected to compare with the data. This curve has been selected to minimize the error between the discontinuous data and the smooth curve. The equations for these curvefits are given in Table D.11 and D.12 for each type of potash. The best-fit smooth curves have also been provided together with the cumulative mass fraction data. The formulae for these curves are listed in the Tables D.13 and 14.

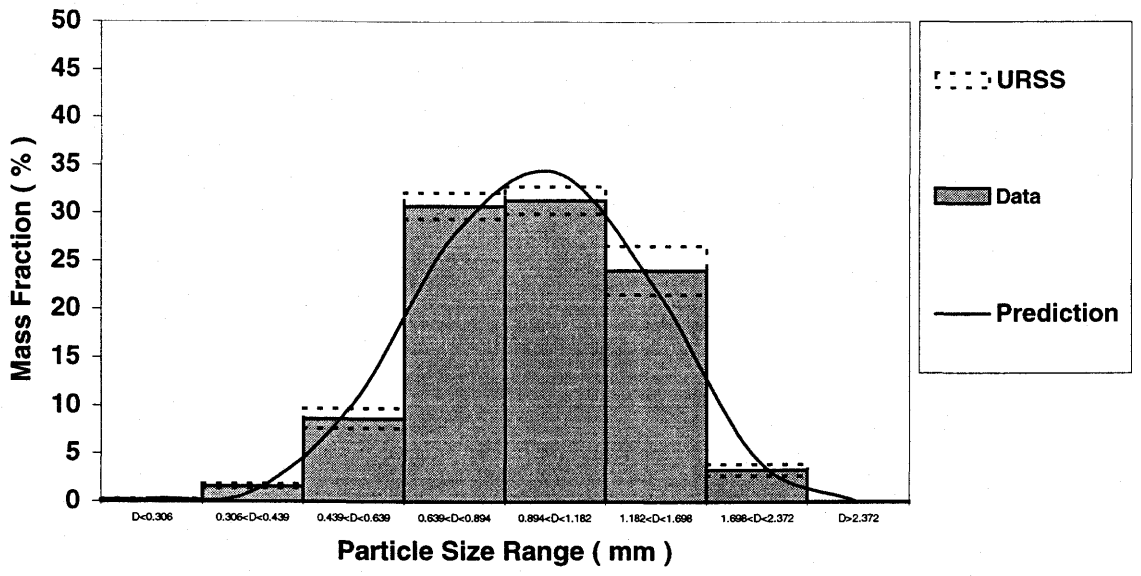

Figure D.2. Mass Fraction as a Function of Particle Size for Rocanville Standard

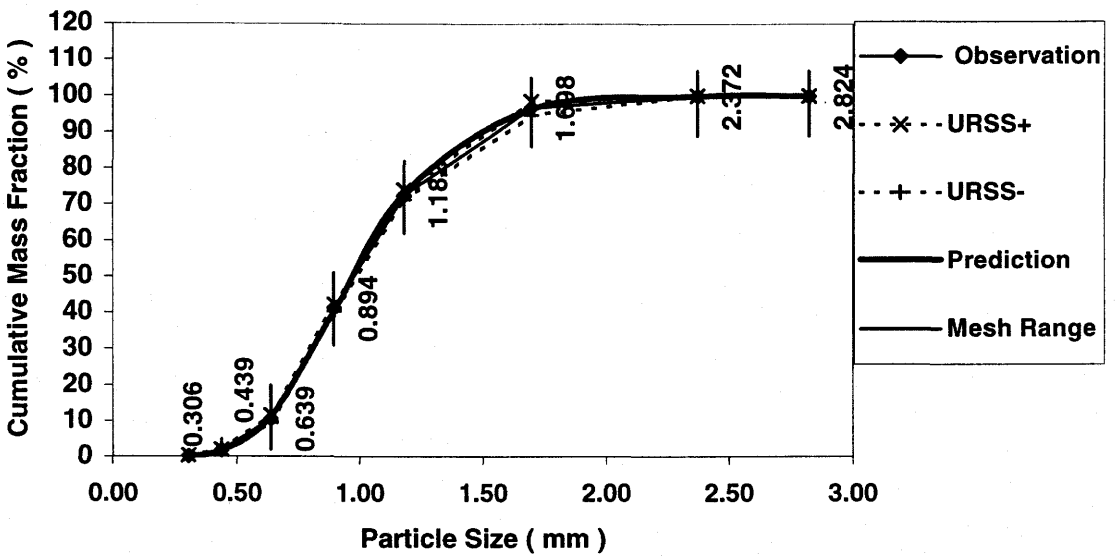

Figure D.3 Cumulative Mass Fraction versus Particle Size for Rocanville Standard

Table D.4 Particle Size Distribution/Uncertainty of Type-A Potash

Sieve Number	Particle Size Less Than	Mass Fraction	Uncertainty of MF at 95% Coverage	Cumulative Mass Fraction	Uncertainty of CMF at 95% Coverage
(mm)	(mm)	(%)	(%)	(%)	(%)
< #18	1.019	0.13	0.10%	0.13	0.10%
#18	1.698	8.57	1.06%	8.7	0.89%
#12	2.031	16.63	0.95%	25.33	0.70%
#10	2.372	28.76	2.54%	54.08	2.31%
#8	2.824	24.85	2.41%	78.94	2.10%
#7	3.294	18.7	2.53%	97.64	1.36%
#6	4.04	2.45	0.80%	100	0.42%

Table D.5 Particle Size Distribution/Uncertainty of Type-B Potash

Sieve Number	Particle Size Less Than	Mass Fraction	Uncertainty of MF at 95% Coverage	Cumulative Mass Fraction	Uncertainty of CMF at 95% Coverage
(mm)	(mm)	(%)	(%)	(%)	(%)
<#50	0.306	0.43	0.11%	0.43	0.11%
#50	0.439	6.29	0.73%	6.71	0.62%
#40	0.639	8.07	0.32%	14.79	0.18%
#30	0.894	21.95	0.43%	36.84	0.36%
#20	1.182	28.21	0.98%	64.95	0.75%
#16	1.698	26.66	1.30%	91.61	1.16%
#12	2.031	6.59	0.29%	98.2	0.29%
#10	2.372	1.87	0.26%	99.98	0.04%
#8	2.824	0.04	0.01%	100	0.01%

Table D.6 Particle Size Distribution/Uncertainty of Type-C Potash

Sieve Number	Particle Size Less Than	Mass Fraction	Uncertainty of MF at 95% Coverage	Cumulative Mass Fraction	Uncertainty of CMF at 95% Coverage
(mm)	(mm)	(%)	(%)	(%)	(%)
<#18	1.019	0.24	0.10%	0.24	0.10%
#18	1.698	1.89	0.41%	2.13	0.40%
#12	2.031	5.37	0.67%	7.51	0.65%
#10	2.372	20.9	0.94%	28.41	0.62%
#8	2.824	27.64	2.46%	56.05	2.22%
#7	3.294	29.12	2.21%	85.17	1.84%
#6	4.04	14.36	1.00%	99.53	0.28%
#5	4.775	0.51	0.32%	100	0.18%

Table D.7 Particle Size Distribution/Uncertainty of Type-D Potash

Sieve Number	Particle Size Less Than	Mass Fraction	Uncertainty of MF at 95% Coverage	Cumulative Mass Fraction	Uncertainty of CMF at 95% Coverage
(mm)	(mm)	(%)	(%)	(%)	(%)
<#50	0.306	0.21	0.08%	0.21	0.08%
#50	0.439	1.64	0.21%	1.84	0.05%
#40	0.639	8.66	1.04%	10.5	1.04%
#30	0.894	30.76	1.38%	41.26	0.90%
#20	1.182	31.35	1.45%	72.6	1.33%
#16	1.698	24.04	2.52%	96.64	1.92%
#12	2.372	3.35	0.61%	99.95	0.06%
#8	2.824	0.04	0.01%	100	0.03%

Table D.8 Particle Size Distribution/Uncertainty of Type-E Potash

Sieve Number	Particle Size Less Than	Mass Fraction	Uncertainty of MF at 95% Coverage	Cumulative Mass Fraction	Uncertainty of CMF at 95% Coverage
(mm)	(mm)	(%)	(%)	(%)	(%)
<#200	0.093	1.57	0.25%	1.57	0.25%
#200	0.123	2.98	0.27%	4.55	0.27%
#140	0.168	8.13	1.37%	12.68	1.05%
#100	0.24	29.31	4.59%	41.99	2.29%
#70	0.306	28.57	2.65%	70.55	0.36%
#50	0.439	20.51	3.10%	91.06	1.75%
#40	0.639	5.38	0.54%	96.45	0.14%
#30	0.894	3.57	0.16%	99.97	0.11%
#20	1.019	0.1	0.03%	100	0.03%

Table D.9 Particle Size Distribution/Uncertainty of Type-F Potash

Sieve Number	Particle Size Less Than	Mass Fraction	Uncertainty of MF at 95% Coverage	Cumulative Mass Fraction	Uncertainty of CMF at 95% Coverage
(mm)	(mm)	(%)	(%)	(%)	(%)
<#12	1.698	0.52	0.12	0.52	0.12
#12	2.031	2.75	0.47	3.27	0.51
#10	2.372	13.22	1.14	16.49	1.38
#8	2.824	28.47	0.69	44.96	1.92
#7	3.294	42.07	1.27	87.04	0.89
#6	4.04	12.58	1.27	99.62	1.37
#5	4.775	0.31	0.26	100	1.38

Table D.10 Particle Size Distribution/Uncertainty of Type-G Potash

Sieve Number	Particle Size Less Than	Mass Fraction	Uncertainty of MF at 95% Coverage	Cumulative Mass Fraction	Uncertainty of CMF at 95% Coverage
(mm)	(mm)	(%)	(%)	(%)	(%)
<#16	1.182	0.28	0.24%	0.28	0.24%
#16	1.698	0.5	0.09%	0.78	0.05%
#12	2.031	8.07	1.14%	8.85	0.98%
#10	2.372	28.33	2.20%	37.18	0.57%
#8	2.824	43.23	4.75%	80.41	4.38%
#7	3.294	17.34	1.89%	97.75	1.03%
#6	4.04	2.08	0.44%	99.82	0.23%
#5	4.775	0.14	0.04%	100	0.02%

Table D.11 Curvefit Formulae for Mass Fraction, MF (y) versus Particle Size, D(x(mm))

Potash Type	Formula
A	y=a+blnx+c(lnx)^2+d(lnx)^3+e(lnx)^4
B	lny=a+bx+cx^2+dx^3+ex^4
C	lny=a+bx+cx^2+dx^3+ex^4+fx^5
D	y=a+blnx+c(lnx)^2+d(lnx)^3+e(lnx)^4+f(lnx)^5+g(lnx)^6
E	lny=a+bx+cx^2+dx^3+ex^4+fx^5
F	y=a+bx+c/x+dx^2+e/x^2+fx^3+g/x^3
G	lny=a+bx+cx^2+dx^3

Table D12. Constants In the Analytical Formulae of Table D.11

Potash Type	a	b	c	d	e	f	g	r2
A	0.15	-118.92	416.34	-356.19	85.57			0.98
B	-1.81	12.52	-12.43	6.28	-1.34			0.97
C	-33.58	37.51	-11.58	0.07	0.54	-0.07		0.99
D	33.09	20.96	-76.21	-37.86	58.19	16.37	-14.46	0.98
E	-132.95	207.71	-128.74	40.03	-6.15	0.37		1.00
F	936.95	-2198.44	-167.83	2264.9	13.14	-848.34	-0.37	0.98
G	-27.77	27.08	-7.16	0.54				1.00

Table D.13 Curvefit Formulae for Cumulative Mass Fraction, CMF (Y) versus Particle Size, D (x(mm))

Potash Type	Formula
A	Y=(a+cx+ex^2)/(1+bx+dx^2)
B	Y=(a+cx+ex^2)/(1+bx+dx^2)
C	Y=(a+cx+ex^2)/(1+bx+dx^2)
D	Y=a+blnx+c(lnx)^2+d(lnx)^3+e(lnx)^4+f(lnx)^5
E	Y=(a+cx+ex^2)/(1+bx+dx^2+fx^3)
F	Y=a+blnx+c(lnx)^2+d(lnx)^3+e(lnx)^4+f(lnx)^5+g(lnx)^6+h(lnx)^7
G	Y=(a+cx+ex^2+gx^3)/(1+bx+dx^2+fx^3)

Table D.14. Constants In the Analytical Formulae of Table D.13

Potash Type	a	b	c	d	e	f	g	h	r2
A	13.251	-0.682	-23.23	0.1584	10.018				1.00
B	0.4	-0.88	-9.24	0.6	44.68				1.00
C	11.61	-0.59	-18.42	0.12	6.98				1.00
D	57.04	101.81	-14.91	-81.84	8.61	29.06			1.00
E	3.93	-0.72	-5.52	0.17	1.92	-0.01			1.00
F	100.06	-4.72	-57.87	-132.5	-143.67	-51.39	-1.49	1.41	1.00
G	-9.02	-0.56	22.22	0.01	-17.7	0.03	4.6		1.00

2. Observations

1) Each sieve mesh size must be calibrated to avoid large error in the size distribution of particles.

2) The best curve fit equation for mass fraction is not the well-known Gaussian normal equation for probability density, y, as a function of the independent variable, x :

$$y = \frac{1}{\sqrt{2\pi}\sigma} e^{-\frac{1}{2}(\frac{x-\mu}{\omega})^2}$$

where σ= standard deviation, μ= the mean value of x

3) Granular potash materials have a wide range of particle sizes for each type. A mass fraction of 25% to 40% was found for the sieve with the largest mass of potash and this coincides with the largest uncertainty in mass fraction.

4) No single set of sieves could be used to obtain the mass fraction of all the types granular potash. The sieves were selected for each measurement to minimize the uncertainty in the results.

Experimental Uncertainty

Both bias and precision errors influence the accuracy of the result for mass fraction, cumulative mass fraction and particle size. The sampling error is included in the precision error. The fixed or bias uncertainties are errors caused by the mass balance and sieves. Calculating the root-sum-squared uncertainty, we get the experimental uncertainty at 95 % confidence level.

It was assumed that the six tests for each type of potash are statistically independent when only three samples were taken and each one was repeated twice. For samples taken from potash types A to F, the repetition of the mass fraction measurements showed a maximum difference with the same sample of 0.5% while the maximum difference between the mean value and the peak value for the same sample of potash was 1.25%. Other test results showed smaller variations of these two comparisons for type A to F. These results imply that the assumption of the statistical independence is reasonable.

For type G, prills, were processed from fine particles and the repetition of the mass fraction analysis in the sieve tests appeared to cause a slight systematic shift in the mass fraction distributions of up to 2.5%. It appears that prills are more fragile than the other types of potash which results in some of larger particles broken into smaller pieces as a result of the sieving process. As a consequence, we conclude that all sieve analysis with the prills will cause some deterioration of the sample. This lead us to conclude that the assumption of statistical independence for type G is not fully justified.

Governing Equations

1) The 95% confidence level uncertainty (root-squared-sum uncertainty) for mass fraction and cumulative mass fraction

$$U_{rss}(MF) = [(t \cdot S_{\bar{x}})^2 + B_{mf}{}^2]^{1/2} \tag{D.3}$$

$$U_{rssc}(CMF) = [(t \cdot S_{\bar{cx}})^2 + B_{cmf}{}^2]^{1/2} \tag{D.4}$$

where the sample standard deviation of the mean values for the mass fraction and the cumulative mass fraction are:

$$S_{\bar{x}} = \frac{S_x}{\sqrt{N}} \tag{D.5}$$

$$S_{\bar{cx}} = \frac{S_{cx}}{\sqrt{N}} \tag{D.6}$$

$U_{rss}(MF)$= uncertainty of the mass fraction

$U_{rssc}(CMF)$= uncertainty of the cumulative mass fraction

$S_{\bar{x}}$ = precision index of mass fraction

$S_{\bar{cx}}$ = precision index of cumulative mass fraction

S_x = standard deviation of mass fraction

S_{cx} = standard deviation of cumulative mass fraction

t = Student t for each experiment.

2) Bias error in the mass fraction:

Another bias error is due to the mass balance B_{mbal} which is used to weigh the potash particles left in each sieve and has the value of 0.05 g .

3) Precision errors for mass fraction and cumulative mass fraction:

The sample standard deviation for the mass in screen i is :

$$S_x = [\frac{\sum_{i}^{N} (M_i - \bar{M})^2}{N-1}]^{1/2} \quad \text{(D.7)}$$

where N = the number of the samples

$\bar{M}$ = the mean value of mass in sieve i

$$\bar{M} = \frac{\sum_{i=1}^{N} M_i}{N} \quad \text{(D.8)}$$

the sample standard deviation for cumulative mass up to sieve i is :

$$S_{cx} = [\frac{\sum_{i}^{N} (M_{cui} - \bar{M}_{cu})^2}{N-1}]^{1/2} \quad \text{(D.9)}$$

where the average cumulative mass up to sieve i is :

$$\bar{M}_{cu} = \frac{\sum_{i=1}^{N} M_{cui}}{N} \quad \text{(D.10)}$$

where S_x , S_{cx}= the precision index (g)

M_i = the mass left in the D_i sieve (g)

$\bar{M}, \bar{M}_{cu}$ = the average mass left in the D_i sieve (g)

N= the number of the repeating measurement, it equals to 6 or 4 in this report

Observations and Conclusions:

As a result of these tests and analysis, several observations can be made:

1. The precision error due to random variations between samples is the most important source of uncertainty in the results. These precision errors ranged from 0.01% to 4.75%. Increasing the number of samples is unlikely to alter mass fraction uncertainty significantly.
2. Even after calibration, uncertainty in the calibrated mesh size was the second largest cause of uncertainty with a range of 0.61% for the largest mesh to 3.68% for the smallest mesh. This uncertainty can not be neglected as it can be the dominant cause of uncertainty.
3. The uncertainty in the mass fraction is somewhat higher than the cumulative mass fraction (i.e. 2.8% average maximum for mass fraction and 2.0% average maximum for the cumulative mass fraction) because the uncertainty in the totals for accumulated masses decreases with sample size.

APPENDIX E

Uncertainty in the Specific Surface Analysis of Granular Potash

The specific surface of a particle bed is the surface area of the particles per unit mass or per unit volume of bed. Using the measured value of permeability, porosity and particle size distribution the specific surface of these seven types of granular potash is calculated based on the permeability of a bed of particles using the formula by Carman (1938).

In his research, Carman independently investigated each parameter that might change the result in his equation for specific surface. These include particle size, shape, size range, porosity, fluid density, fluid viscosity and permeability. For the full range of parameter variations, Carman estimated the accuracy of the computed specific surface to be such that the errors were less than 4%. Since the range of parameters investigated for the seven types of potash studied nearly all lie within the ranges investigated by Carman, we will assume the uncertainty of the Carman's equation for specific surface is ±4%. There are, however, a few concerns with Carman's permeability method of the computing specific surface of granular potash. Carman discussed one of these.

The range of pore space size in a powder bed is a factor that could have an impact on the validity of this equation. According to Carman's research, large capillaries give disproportionately high rate of flow which swamp the effect of the small capillaries for fluid flow through a powder bed. Since the range of particle sizes of the potash samples is

not too large with respect to the mean value, the set of results for permeability should be satisfactory using the Carman equation provided that the granular potash is in the shaken or consolidated condition. In the unshaken condition, large pore sizes will exist along with some small pore sizes.

A second concern with the use of Carman's equation is closely related to the problem that may occur with large range of capillary pore sizes. Prills, which are typically 2.3 mm diameter, are manufactured by the accretion of large number of small particles, which are typically less than 0.22 mm diameter. Consequently, the Prill particles contain large microscopic surface areas within each particle. The capillary pore sizes within the Prills particles are expected to be one to two orders of magnitude smaller than the pore sizes between the Prills particles. Therefore, the specific surface can not be accurately calculated for Prills using Carman's equation.

GOVERNING EQUATION

The specific surface is calculated from the Carmen equation (1938)as below:

$$S_p = \left[\frac{1}{k \cdot \mu \cdot \rho_s{}^2 \cdot u} \cdot \frac{\varepsilon^3}{(1-\varepsilon)^2} \cdot \frac{\Delta P}{L} \right]^{1/2} \qquad \text{(E.1)}$$

where

S_p = the permeability specific surface of the powder (m^2/kg)

k = aspect factor , $k = k_0 \cdot k_1$

where

k_0 is a factor which depends on the shape and size of the cross-sectional areas of the capillaries hence of particles which make up the bed

k_1 is the tortusity factor

According to Carman's research, the aspect factor k is assumed to be 5

ρ_s = the powder density of potash (1987 kg/m^3)

ε = the porosity of the powder bed

ΔP = pressure difference across the powder bed (Pa)

u = the Darcy velocity (m/s)

μ = fluid viscosity (Pa•s)

L = the height of the powder bed (m)

We can also express the equation (1) using permeability and it takes the simple form:

$$S_p = [\frac{1}{k \cdot \rho_s^{\,2}} \cdot \frac{\varepsilon^3}{(1-\varepsilon)^2} \cdot \frac{1}{K}]^{1/2} \qquad \text{(E.2)}$$

where

K = the permeability of powder bed which is derived from the Darcy momentum equation [Dullien !991]:

$$u = \frac{K}{\mu} \cdot \frac{\Delta P}{L} \tag{E.3}$$

Experimental Results and Analysis

1. Experimental Results

In the permeability measurement, data were taken for each type of granular potash to calculate permeability under two different conditions: consolidated (shaken) and unconsolidated (unshaken). Each type was measured three times under these two conditions. To calculate the specific surface, we substitute the permeability experimental data into equation (E.2).

The permeability data reported by Carman (1938) compare well with the data in this thesis. Carman's permeability data was from 10^{-10} to 10^{-8} m^2 which is almost the same range of our experiment data from 10^{-11} to 10^{-8} m^2. The range of particle average size tested by Carman was from 0.25 mm to 1.025 mm, while data in this thesis is from 0.80 mm to 2.60 mm. So we conclude that : 1) the range of K found by Carman was similar to our tests, and 2) the particle sizes were slightly smaller than, but not significantly different from, this thesis.

The values of specific surface for the seven granular potash range from 0.56 m^2/kg to 19.7 m^2/kg. The representative particle sizes of the seven granular potash range from 0.80 mm to 2.60 mm except for the type-E which has a value of 0.22 mm. Since the granular potash size falls in a specific range, we define the particle size distribution range as the ratio of the very top limit of the size distribution to the very low limit. For these seven types of granular potash, their particle size distribution ranges were about 4:1.

Table E.1 to E.7 present the calculated specific surface per unit mass using the permeability data presented in the report by Zhou, Peng and Besant (1998) " Uncertainty in the Measurement of Permeability and Porosity of Granular Potash". S_p (u) represents the specific surface under the unconsolidated condition, while S_p (s) represents the value under the consolidated (shaken) condition.

Table E.1. Experimental Data of the Specific Surface for Type-A Granular Potash (Average Particle Size 2.20 mm)

Ud	Unshaken			Shaken		
	S_p(u1)	S_p(u2)	S_p(u3)	S_p(s1)	S_p(s2)	S_p(s3)
(m/s)	(m^2/kg)	(m^2/kg)	(m^2/kg)	(m^2/kg)	(m^2/kg)	(m^2/kg)
0.005	0.55	0.55	0.55	0.57	0.58	0.57
0.010	0.53	0.56	0.55	0.56	0.56	0.56
0.015	0.54	0.56	0.56	0.57	0.57	0.57
0.020	0.54	0.56	0.56	0.56	0.56	0.56
0.025	0.53	0.56	0.55	0.56	0.56	0.56
0.030	0.54	0.56	0.56	0.57	0.57	0.57
0.035	0.55	0.56	0.56	0.57	0.57	0.57
0.040	0.55	0.57	0.57	0.57	0.58	0.58
0.044	0.56	0.57	0.57	0.58	0.58	0.58
0.049	0.57	0.57	0.57	0.59	0.59	0.59

Table E.2. Experimental Data of the Specific Surface for Type-B Granular Potash (Average Particle Size 0.80 mm)

Ud	Unshaken			Shaken		
	S_p (u1)	S_p (u2)	S_p (u3)	S_p (s1)	S_p (s2)	S_p (s3)
(m/s)	(m^2/kg)	(m^2/kg)	(m^2/kg)	(m^2/kg)	(m^2/kg)	(m^2/kg)
0.005	1.54	1.55	1.55	1.55	1.55	1.55
0.010	1.51	1.52	1.52	1.52	1.52	1.52
0.016	1.51	1.52	1.52	1.51	1.51	1.51
0.021	1.51	1.51	1.51	1.51	1.51	1.51
0.026	1.52	1.52	1.52	1.51	1.51	1.52
0.030	1.52	1.52	1.52	1.52	1.52	1.52
0.035	1.53	1.53	1.53	1.53	1.53	1.53
0.040	1.54	1.54	1.54	1.54	1.54	1.54
0.045	1.56	1.56	1.55	1.55	1.55	1.55
0.050	1.57	1.56	1.56	1.57	1.56	1.57

Table E.3. Experimental Data of the Specific Surface for Type-C Granular Potash (Average Particle Size 2.40 mm)

Ud	Unshaken			Shaken		
	S_p(u1)	S_p(u2)	S_p(u3)	S_p(s1)	S_p(s2)	S_p(s3)
(m/s)	(m^2/kg)	(m^2/kg)	(m^2/kg)	(m^2/kg)	(m^2/kg)	(m^2/kg)
0.005	0.47	0.50	0.49	0.50	0.50	0.50
0.010	0.47	0.50	0.50	0.50	0.51	0.50
0.015	0.48	0.49	0.50	0.50	0.51	0.50
0.020	0.48	0.50	0.50	0.50	0.51	0.51
0.025	0.49	0.50	0.51	0.51	0.51	0.51
0.030	0.49	0.51	0.51	0.51	0.51	0.51
0.035	0.50	0.50	0.51	0.51	0.52	0.52
0.040	0.50	0.51	0.51	0.52	0.52	0.52
0.044	0.51	0.51	0.51	0.52	0.52	0.52
0.049	0.51	0.52	0.52	0.52	0.53	0.53

Table E.4. Experimental Data of the Specific Surface for Type-D Granular Potash

(Average Particle Size 0.80 mm)

Ud	Unshaken			Shaken		
	S_p(u1)	S_p(u2)	S_p(u3)	S_p(s1)	S_p(s2)	S_p(s3)
(m/s)	(m^2/kg)	(m^2/kg)	(m^2/kg)	(m^2/kg)	(m^2/kg)	(m^2/kg)
0.005	1.49	1.50	1.50	1.53	1.53	1.53
0.010	1.48	1.48	1.49	1.49	1.49	1.49
0.016	1.48	1.48	1.48	1.48	1.48	1.48
0.021	1.48	1.48	1.48	1.48	1.48	1.48
0.026	1.48	1.48	1.48	1.48	1.48	1.48
0.030	1.48	1.49	1.49	1.49	1.49	1.49
0.035	1.49	1.50	1.49	1.50	1.50	1.50
0.040	1.51	1.51	1.51	1.51	1.51	1.51
0.045	1.52	1.52	1.52	1.52	1.52	1.52
0.050	1.53	1.53	1.53	1.53	1.53	1.53

Table E.5. Experimental Data of the Specific Surface for Type-E Granular Potash
(Average Particle Size 0.22 mm)

Ud	Unshaken			Shaken		
	S_p(u1)	S_p(u2)	S_p(u3)	S_p(s1)	S_p(s2)	S_p(s3)
(m/s)	(m^2/kg)	(m^2/kg)	(m^2/kg)	(m^2/kg)	(m^2/kg)	(m^2/kg)
0.005	17.65	17.78	17.67	19.39	19.36	19.36
0.010	17.84	17.73	17.71	19.58	19.43	19.47
0.015	17.91	17.82	17.73	19.70	19.58	19.58

Table E.6. Experimental Data of the Specific Surface for Type-F Granular Potash

(Average Particle Size 2.60 mm)

Ud	Unshaken			Shaken		
	S_p(u1)	S_p(u2)	S_p(u3)	S_p(s1)	S_p(s2)	S_p(s3)
(m/s)	(m^2/kg)	(m^2/kg)	(m^2/kg)	(m^2/kg)	(m^2/kg)	(m^2/kg)
0.005	0.57	0.57	0.57	0.59	0.59	0.59
0.010	0.56	0.56	0.56	0.58	0.58	0.58
0.015	0.55	0.57	0.57	0.58	0.58	0.58
0.020	0.56	0.57	0.57	0.58	0.58	0.58
0.025	0.55	0.55	0.57	0.58	0.58	0.58
0.030	0.56	0.57	0.57	0.58	0.58	0.58
0.035	0.56	0.58	0.58	0.58	0.58	0.59
0.040	0.56	0.58	0.58	0.58	0.59	0.59
0.044	0.57	0.58	0.58	0.59	0.59	0.59
0.049	0.58	0.58	0.58	0.59	0.60	0.59

Table E.7. Experimental Data of the Specific Surface for Type-G Granular Potash (Average Particle Size 2.30 mm)

Ud	Unshaken			Shaken		
	S_p(u1)	S_p(u2)	S_p(u3)	S_p(s1)	S_p(s2)	S_p(s3)
(m/s)	(m^2/kg)	(m^2/kg)	(m^2/kg)	(m^2/kg)	(m^2/kg)	(m^2/kg)
0.005	1.07	1.07	1.07	1.14	1.16	1.16
0.010	1.04	1.08	1.08	1.12	1.13	1.13
0.016	1.03	1.08	1.08	1.13	1.14	1.13
0.021	1.05	1.07	1.08	1.13	1.13	1.14
0.026	1.06	1.08	1.09	1.12	1.12	1.13
0.030	1.06	1.08	1.08	1.12	1.13	1.13
0.035	1.07	1.08	1.09	1.12	1.14	1.14
0.040	1.07	1.09	1.09	1.13	1.14	1.14
0.045	1.08	1.09	1.09	1.13	1.14	1.15
0.050	1.09	1.09	1.09	1.13	1.14	1.15

2. Some General Observations

a) It was shown that the range of the porosity values (ε) at 0.385 to 0.603 is small but the range of permeability (K) is large. The permeability of the seven types of grained potash ranges from 10^{-8} m^2 for the coarse grained potash to 10^{-11} m^2 for the smallest grained potash. The corresponding value of the specific surface range from 0.56 m^2/kg for coarse grained potash to 19.7 m^2/kg for the smallest grained potash.

b) The specific surface of granular potash appears to vary inversely with the average particle diameter. The calculated specific surface appears to be strongly dependent on the average particle size of potash. FigureE.1 presents the calculated specific surface (under two different definitions of average particle size) versus the inverse of the particle diameter and compares the results to the equation by Dullien (1979) :

$$S_p = \frac{6}{\rho \cdot dp}$$

Figure E.1-a defines the average particle size as the value of 50% cumulative mass fraction according to the report by Zhou, Peng and Besant (1998) " Uncertainty in the Sieve Analysis of Granular Potash " . Figure E.1-b defines the average particle size on the basis of 90% cumulative mass fraction. In both of these conditions, type-E , which is powder-like granular potash, shows poor agreement between this equation and experimental results.

(a) S_p With Average Particle Size of 50% CMF

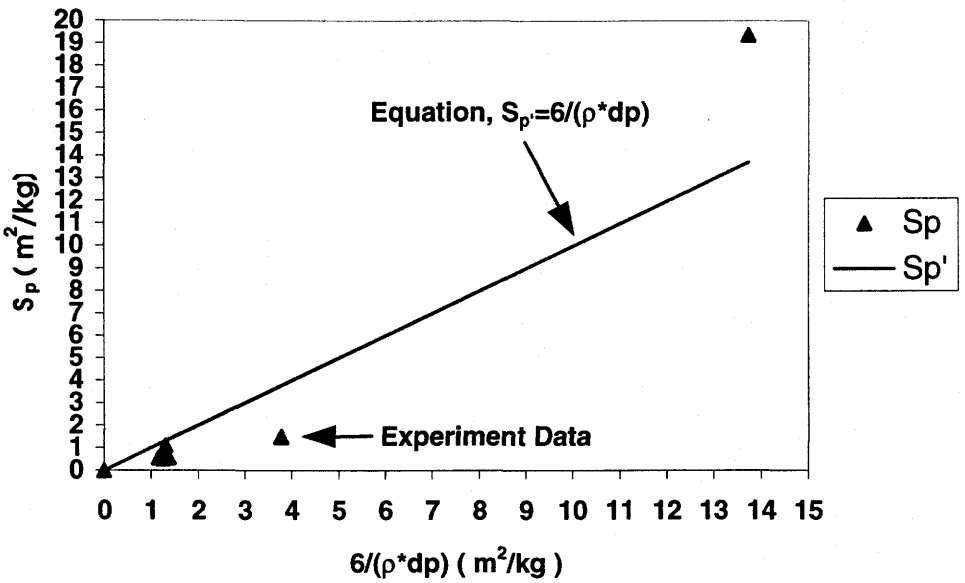

(b) S_p with Average Particle Size of 90% CMF

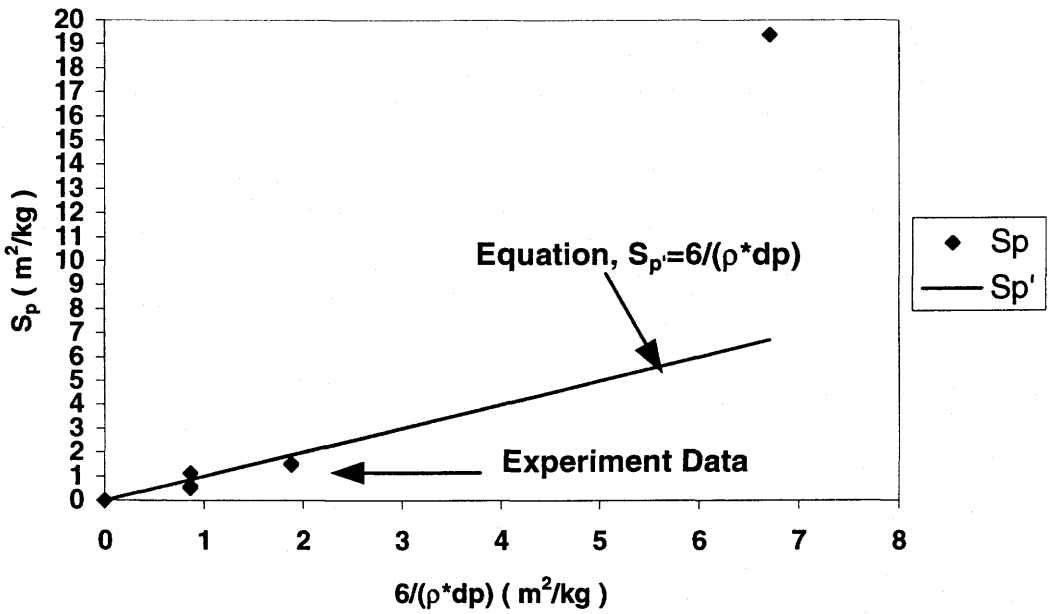

c) Comparison of the two different test conditions (consolidated and unconsolidated) shows that the change of specific surface is from 3.5% to 8.8% with the consolidated (shaken) value always larger.

d) Type-G potash (Prills), which is a coarse sphere-like particle with a much higher porosity inside each particle, appears to give specific surface results that are in considerable doubt because the range of capillary pore sizes for air flow in the permeability tests is too large.

e) The specific surface is almost independent on the Darcy velocity

UNCERTAINTY ANALYSIS

1. Uncertainty of Parameters

Since the data used for specific surface (S_p) calculation are derived from the permeability and porosity measurement, the uncertainty of the specific surface includes the uncertainties of permeability (K) and porosity (ε).

The bias errors of relative parameters for specific surface calculation are presented in Table-8. These bias errors are for the properties listed but they don't give the uncertainty bias in Sp. This bias uncertainty must be obtained from the correlation of how well the equation for Sp represents the data as measured by an independent method.

Table E.8. Bias Errors of the Specific Surface Calculation

Bias Error Category	Parameters	Bias Error Value
Br	Potash Powder Density	0.99 kg/m3
Bk'	Aspect Factor	0.1
BK	Ganular Potash Permeability	1.04E-12 m2<BK<1.32E-09 m2
Be	Granular Potash Porosity	7.55E-04<Be<1.9E-03

3. Bias error of the Carman equation

In Carman's equation for specific surface, the particles used in the experiments are uniform and sphere-like which is quite different from the non-uniform, irregular shape particles in practice. This would contribute an inherent bias error to the Carman equation which could be expressed by the aspect factor k in equation E.1 or E.2. Following Carman's uncertainty analysis, a 4% bias error has been included into the uncertainty analysis. Errors from other parameters have been treated as precision errors.

The uncertainty values for these seven types of potash are presented in TableE.9.

Table E.9. Uncertainty of the Specific Surface of the Seven Types of Granular Potash

Potash Type	Uncertainty of the Specific Surface (%)
Type-A	4.50%
Type-B	4.32%
Type-C	4.67%
Type-D	4.32%
Type-E	5.10%
Type-F	4.23%
Type-G	4.24%

REGRESSION UNCERTAINTY ANALYSIS

1. Governing Equations

Since the permeability (K) of porous media is independent of the Darcy velocity (U_D), the weight specific surface of granular potash, which is calculated from permeability and porosity, should also be independent on the Darcy velocity. Some data of the specific surface have been selected over a certain range of Darcy velocity to examine the relationship and have been presented graphically in the form of regression straight line which could be expressed as :

$$SP_{ls} = a + b \cdot u_D \tag{E.4}$$

where b is the slope of the line defined by:

$$b = \frac{\sum_{i=1}^{n}(u_{D,i} - \bar{u}_D)(SP_i - \bar{SP})}{\sum_{i=1}^{n}(u_{D,i} - \bar{u}_D)^2} \tag{E.5}$$

and a is the intercept defined by:

$$a = \bar{SP} - b \cdot \bar{u}_D \tag{E.6}$$

where the mean value of each data for u_D and SP are given by:

$$\bar{u}_D = \frac{1}{n}\sum_{i=1}^{n} u_{D,i} \tag{E.7}$$

$$\bar{SP} = \frac{1}{n}\sum_{i=1}^{n} SP_i \tag{E.8}$$

Here the u_D represents the Darcy velocity of the sample test and SP represents the Specific surface of the sample test

2. Uncertainty of the Regression Results

The 95% uncertainty limits of SP for linear relationship between SP and u_D is given by :

$$U_{rss} = [(t \cdot SEE)^2 + B^2]^{1/2} \tag{E.9}$$

where " SEE " is the standard error of estimate which could be expressed as:

$$SEE = [\frac{\sum_{i=1}^{N}(SP_i - SP_{ls,i})^2}{N - C}]^{1/2} \tag{E.10}$$

t= student number which depends on the degree of freedom

C= the number of coefficients of equation E.5 (C=2)

N= number of the data in each calculation

B= bias error of the specific surface (Presented in TableE.9)

3. Regression Curve

Since the permeability method for calculating the specific surface is most accurate for consolidated condition, we just show the regression curve in this condition with Type-D in Figure E.2. In the analysis of the uncertainty, we consider only data in the middle range of Darcy velocity and have excluded the data point at the lowest Darcy velocity and few points at the highest Darcy velocity. In the figure, the data are shown as points and the mid-line is the regression straight line. The upper and lower lines represent the uncertainty limits for this line at the 95% confidence level.

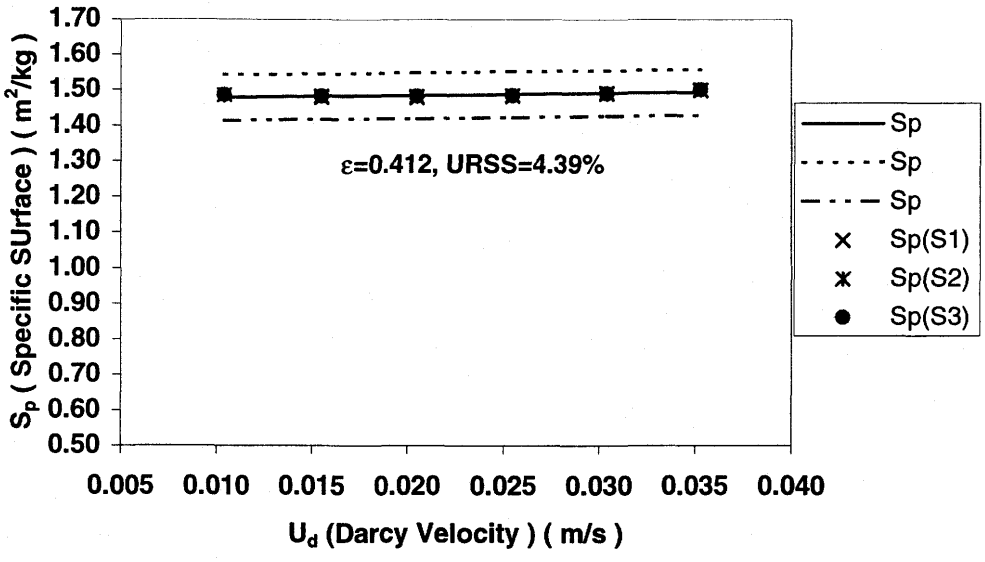

Figure E.2. Regression Curve of Selected Data for Sp versus Ud of Type-D Potash for the Consolidated State

A linear relationship between *Sp* and U_D can be found with two constants a and b which are listed in the Table E.10

TableE.10. Linear Regression Curve Constant a and b

Potash Type	Student t	a	b	U_D (m/s)
Type-A	2.776	0.56	0.19	$0.01<U_D<0.03$
Type-B	2.571	1.50	0.62	$0.01<U_D<0.035$
Type-C	2.776	0.47	0.28	$0.01<U_D<0.03$
Type-D	2.571	1.47	0.61	$0.01<U_D<0.035$
Type-E	4.303	19.25	30.17	$0.005<U_D<0.015$
Type-F	2.571	0.57	0.25	$0.01<U_D<0.035$
Type-G	2.776	1.14	-0.13	$0.01<U_D<0.03$

APPENDIX F

UNCERTAINTY IN THE MEASUREMENT OF APPARENT THERMAL CONDUCTIVITY OF GRANULAR POTASH

Several methods have been used to measure the apparent thermal conductivity of granular materials. Generally, these methods can be classified as transient or steady state tests. We have chosen a steady state method to measure the apparent thermal conductivity of granular potash because it results in the least uncertainty. In this method, we attempted to minimize the heat flux interactions with the surroundings and correct for these calculated heat losses or gains.

INTRODUCTION

In this experiment we measured the apparent thermal conductivity (k) of four different types of granular potash fertilizer product by using a special test facility. To prepare samples for testing, the granular potash was put into an oven at 100°C to dry for more than 24 hours and then allowed to cool to room temperature for 24 hours before each measurement. This is called the dry condition.

The apparent thermal conductivity was measured with constant heat input from the top and heat removal at the bottom as shown in the schematic and photo in Figure F.1. The depth of potash test sample was 132 mm giving a test sample of 599.6 x 280x 132 mm. During each test, heat was supplied at the top and removed at the bottom of

each sample such that the lid temperature was 10 to 15°C above room ambient air temperature and the cold plate at the heat flux meter was 10 to 15°C below room temperature. The electrical heat input and temperatures were recorded from sensors shown in Figure F.2. A calibrated heat flux meter at the test section bottom was used to measure the heat flux through potash.

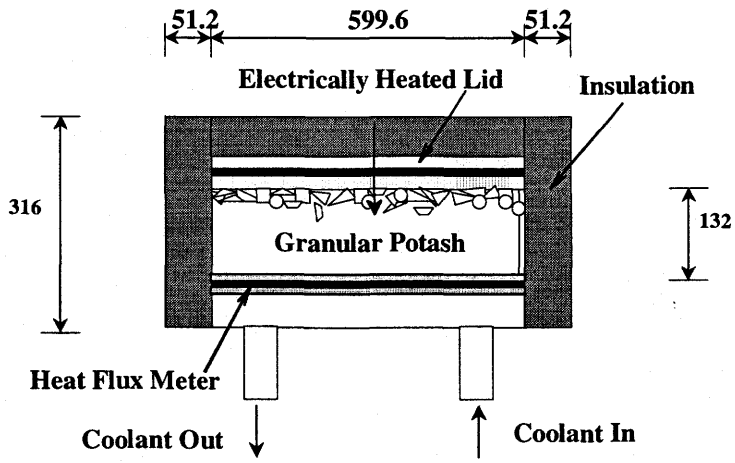

(a)

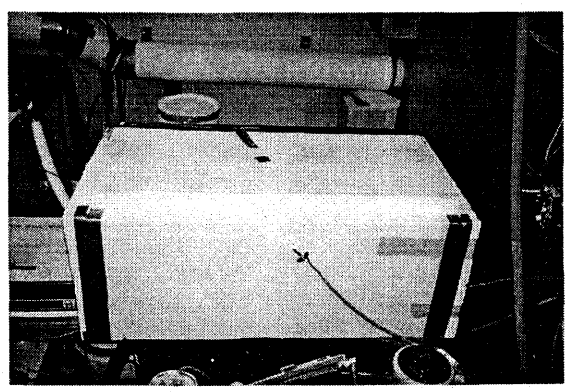

(b)

Figure F.1. Schematic of the Apparent Thermal Conductivity Test Facility (a) and Measurement Apparatus Photo (b)

Two types of tests were done to measure the apparent thermal conductivity. In the first set of tests, it shows how the apparent thermal conductivity of several types of dry potash vary with their consolidation (shaken) condition. In the second set of tests it shows how the thermal conductivity of one type of potash varies with moisture content and caking.

For each sample in the first set of tests, the conductivity was measured under two different conditions: consolidated or shaken, and unconsolidated or unshaken. The unshaken test condition was taken to exist after the potash was pored into the test facility and leveled. The shaken test condition was achieved after applying a surface vibrator (a hand held electrical sander) to the top surface after the unshaken test. This shaking would cause the potash to decrease in level 6 to 15% depending on the potash type. The void space at the top was then refilled and the shaking process was repeated until the test sample filled the test facility. The difference in thermal conductivity between these two conditions range from 2.7% to 43.6% depending on the granular particle size distribution while the porosity differences of each potash bed range from 6% to 15%. The test facility for these tests are shown in Figure F.2.

In the second set of tests using one type of granular potash, Rocanville Standard, the apparent thermal conductivity was measured in the in the dry, moist and caked condition. That is, a sample of potash was first tested in the dry and shaken condition. Then this same sample was exposed to a forced parallel flow of humid air at about 85 %

RH for 48 hours (24 hours in one direction followed by 24 hours in the opposite direction) as shown in Figure F.3 and then tested again for thermal conductivity.

The moisture content of the moist potash was measured taking small samples from the top surface. This moist condition indicated an apparent thermal conductivity much higher than the corresponding dry sample. This moist potash layer was then dried over 48 hours with a flow of dry air at a relative humidity of 7% RH. After retesting the dried layer, the apparent thermal conductivity was higher than the first dry case but lower than the moist sample test. Final inspection of this sample showed that it was somewhat uniformly caked.

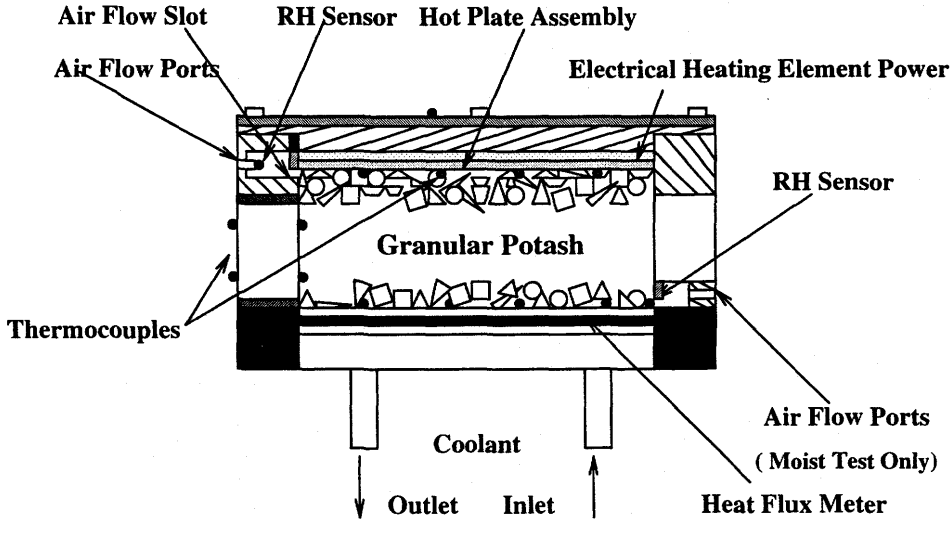

Figure F.2. Schematic of Thermocouple Locations In The Test Section

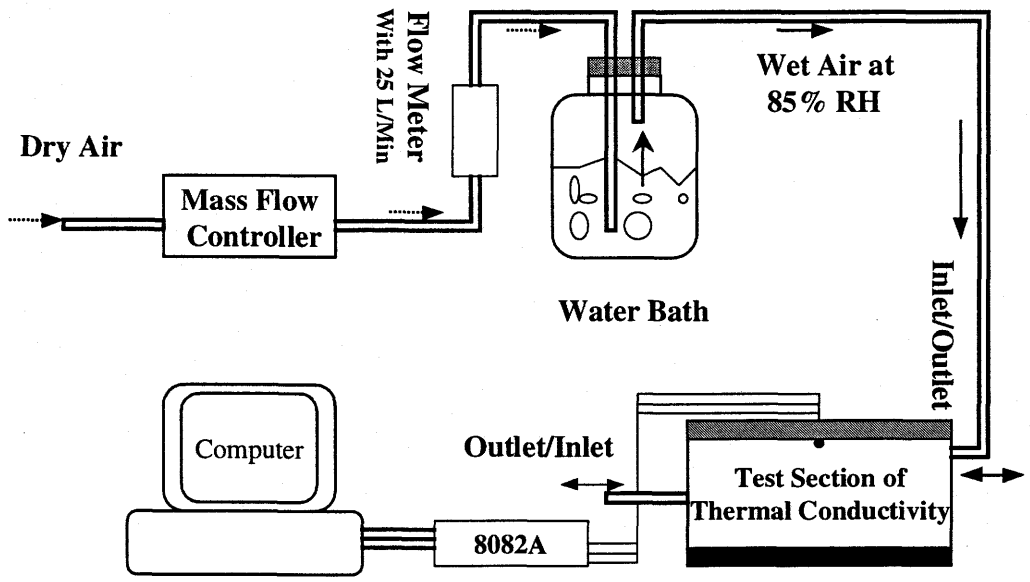

Figure F.3. Schematic of the Wetting Process Apparent Thermal Conductivity Measurement

GOVERNING EQUATIONS

1) Apparent Thermal Conductivity (k)

After the system reaches steady state, the apparent thermal conductivity is calculated with the equation:

$$k = \frac{L/A}{\frac{\Delta T}{\dot{Q}_{net}} - Rct_1 - Rct_2} \tag{F.1}$$

where

L = Height of potash bed in the test facility (m)

A = Area of the top lid or bottom the test cell (m^2)

ΔT = Temperature difference between top lid and bottom plate (K)

Q_{net} = Net heat transfer from the top to the bottom excluding the heat

losses or gains(W)

Rct1 = Contact resistance between top lid and surface potash layer (K/W)

Rct2 = Contact resistance between bottom plate and potash layer at the bottom of the test cell (K/W)

2) Heat Loss / gain from the System

Figure F.4 shows a schematic of the heat flows at steady state in our test facility. The electrical heating elements inside the top lid provide a constant heat input, Q_{input}, to granular potash particles in the vertical direction. The heat loss and gain from the chamber includes such elements as: heat loss from the top, Q_1, heat loss from the corner and edge of adjoining walls Q_{1a} and Q_{1b}, heat loss and gain from the side walls and end walls, Q_{2a} & Q_{2b}, heat gain from the bottom heat flux meter, Q_3. There is a neutral line elevation on both the side walls and end walls where the heat loss to the environment will change to heat gain from the environment.

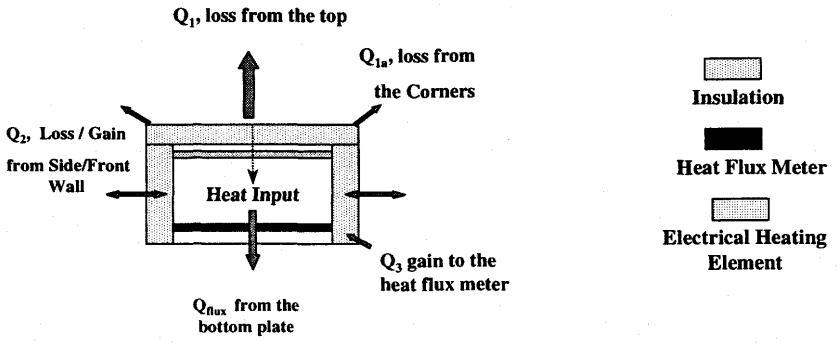

Figure F.4. Schematic of Energy Balance in the Test Facility

2-a. Heat input to the electrical heating elements (Q_{input})

$$Q_{input} = V \cdot I \tag{F.2}$$

where

V = voltage (V)

I = electrical current (A)

A typical electrical heat input is 14.75 W

2-b. Heat loss from the top lid to the envirnment (Q_1)

$$Q_1 = k_s \cdot \frac{(T_{lid,i} - T_{lid,o})}{\Delta hc} \cdot A_{top} \tag{F.3}$$

where

k_s = the thermal conductivity of the insulation material

(k_s=0.029 W/K• m)

T_{lid} = lid temperature at the interface with the insulation material (K)

$T_{lid,o}$ = lid temperature of the insulation material at the interface with surrounding air(K)

Δh_c = thickness of the lid insulation material (m)

A_{top} = area of the lid insulation material (m^2)

A typical heat flow from the top lid is 7.46×10^{-1} W

2-c. Heat loss from the top corners (Q_{1a})

The heat transfer at the four top corners is calculated with equation:

$$Q_{1a} = s \cdot k_s \cdot (T_{lid} - T_{lid,o}) \tag{F.4}$$

where

s = shape factor for a two-dimensional corner

$$s=0.15 \bullet \Delta hc \bullet 4 \text{ (m)} \tag{F.5}$$

2-d. Heat loss from the top edges of adjoining walls (Q_{1b})

$$s = 0.54 \cdot (l_a + l_b) \cdot 2 \text{ (m)} \tag{F.6}$$

A typical value of the heat loss Q_{1a} +Q_{1b} is 1.57×10^{-1} W

2-e. Heat loss / gain from the side wall (Q_{2a}) and end wall (Q_{2b})

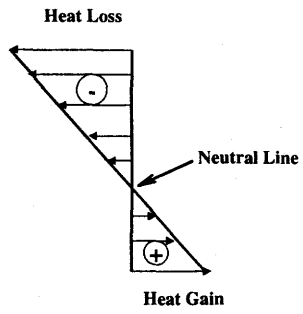

Figure F.5. Schematic of Heat transfer at the Side / End Walls

The heat transfer at the side walls and end walls are divided into heat gain and heat loss by the neutral line as shown in Figure-5.

$$Q_2 = Q_{2a} + Q_{2b} \tag{F.7}$$

$$Q_{2a} = \sum_{i=1}^{n} k_s \cdot (T_{f,i} - T_{o,i}) \cdot A_f \cdot 2 \tag{F.8}$$

$$Q_{2b} = \sum_{j=1}^{n} k_s \cdot (T_{s,j} - T_{o,j}) \cdot A_s \cdot 2 \tag{F.9}$$

where

$T_{f,i}$, $T_{o,i}$ = the i_{th} temeprature of inside and outside end wall (K)

$T_{s,j}$, $T_{o,j}$ = the j_{th} temeprature of inside and outside side wall (K)

A_f, A_s = the surface area of end wall and side wall respectively (m^2)

Typical maximum and minimum values of this heat loss/gain are 2.42×10^{-2} / -3.97×10^{-2} W.

2-f. Heat gain near the bottom flux meter (Q_3)

Due to the temperature difference between the cool bottom plate and warm outside insulation material, the heat gain to heat flux meter,Q_3, is subtracted from the flux meter reading.

$$Q_3 = \frac{k_s \cdot A_{flux} \cdot (T_{ins} - T_{pl})}{\Delta h_a} \tag{F.10}$$

where

A_{flux} = the effective contact area between flux meter and insulation (m^2).

$$A_{flux} = p \cdot \Delta X \tag{F.11}$$

where

p = the perimeter of the flux meter (m)

ΔX= thickness of the flux meter (m), $\Delta X=6x10^{-3}$ m

A typical value of this heat gain is $7.22x10^{-2}$ W

3) Heat transfer from the bottom flux meter (Q_{flux})

A heat flux meter is made up of a polystyrene layer sandwiched between two aluminum plates with many thermocouples distributed on both sides of the polystyrene layer and is used to measure the heat flux.

$$Q_{flux} = S_{poly} \cdot (T_{up} - T_{low}) \cdot A_{flux} \tag{F.12}$$

where

S_{poly} = thermal conductance of the polystyrene, calibrated to be

9.2 ± 0.37 W/m^2 •K

T_{up}, T_{low} = the thermocouple readings on the upper and lower side of the polystyrene layer (K)

A typical value of this heat rate is 16.39 W

4) Net heat transfer in vertical direction from the top to bottom (Q_{net})

In this test, we recorded both the temperature readings at the bottom flux meter and electrical input into the top lid. Both of these values are modified for the heat gain or loss within the test facility. To minimize the uncertainty for the net heat transfer, we introduce two weighting factors, f_1 & f_2, in our calculation.

$$Q_{net} = f_1 \cdot (Q_{input} - Q_1 - Q_{1a,b}) + f_2 \cdot (Q_{flux} - Q_3) \mp Q_{2a,b} \quad \text{(F.13)}$$

where

f_1,f_2= weighting factors ,and f_1+f_2=1.0

A typical net heat rate is 15.99 W

5) Contact resistance (Rct)

$$Rct = \frac{\Delta T'}{Q_{net}} \quad \text{(F.14)}$$

where

ΔT' = the temperature difference between the top lid and top surface layer of potash (K)

A typical value of their heat flow contact resistance is 2.5×10^{-2} K/W

6) Moisture Content (M)

$$M = \frac{M_{wet} - M_{dry}}{M_{dry}} \quad \text{(F.15)}$$

where

M = Moisture content (kg wet / kg dry)
M_{dry} = The mass of potash sample in the dry condition (kg)
M_{wet} = The mass of potash sample in the wet condition (kg)

7) Porosity of Potash Bed (ε)

$$\varepsilon = 1 - \frac{M_{potash} / \rho_{potash}}{V_{cont}} \quad \text{(F.16)}$$

where

ε = Porosity of potash bed

M_{potash} = the potash mass in the test container (kg)

V_{cont} = the volume of the test container (m^3)

EXPERIMENTAL APPARATUS AND PROCEDURE

A. Parameter and Apparatus

For each test, we measured or calculated the following parameters: input voltage and electrical current, the mass of potash filled in the test facility, thickness of the potash bed, dimension of test facility, thickness of the insulation and the effective surface area, thermal contact resistance, different temperatures inside the facility: inside temperature of the top lid, temperature of surface layer potash, temperatures at the top insulation material inside/outside walls, temperatures at the side wall insulation material inside/outside, temperatures at the end wall insulation material inside/outside, temperatures of the heat flux meter at the top and bottom, temperature of the bottom cold plate temperature, ambient air temperature. For the moist condition and re-dried condition, we also measured supply air flow rate and relative humidity for each test and calculate the moisture content.

A schematic of the apparatus used for the potash in the dry condition is shown in Figure F.1. The test section is made up of polystyrene sheets surrounded by thin Plexiglas walls. The side walls and end walls are constructed by polystyrene sheets surrounded by thin Plexiglas walls, thereby reducing the heat loss to the surroundings and protecting against the moisture transfer. The top hot plate assembly is a sandwich-like construction with a polystyrene sheet placed between an aluminum plate and a sheet of Plexiglas. The

electrical heating elements are in direct contact with the aluminum plate. An adjustable DC power supply provides the electrical power to the heating elements. The temperature of lid was maintained at 25 ^{0}C higher than that of the cold bottom plate. The test section is bounded by an aluminum cold plate at the bottom which is connected to a big glycol coolant reservoir tank located inside an environment chamber (Model: C812, Refrigerant: R502, Controlled Environment Ltd, Canada) which could create a wide range of temperatures (eg. –40 ^{0}C to +40 ^{0}C) . The low temperature glycol coolant was pumped into the bottom plate from this large reservoir. The setpoint of the environment chamber is always above the freezing point of the glycol for all the tests. A heat-flux meter is mounted within the cold plate for the measurement of heat flux through it. The heat-flux meter is made up of a 6.4 mm polystyrene layer sandwiched between two aluminum plates with 21 thermocouples spread out on each side of the polystyrene layer. The connection between the top cover-lid and test chamber is fixed by 6 bolts at the four corners and two central points of the longer side. A 40-kg heavy load is put on the top of the lid to reduce the contact resistance between granular potash and lid. The side and bottom edges of the test section are sealed with silicon caulking to create an air tight box. The test section is surrounded with Styrofoam material for insulation and sealed by tape at the adjoining edges.

Figure F.2 shows more details on the thermocouples location inside and outside this section to record the different temperatures. Four thermocouples were put at such places as: top lid inside face, top layer of potash surface, bottom cold plate, side walls / end wall inside face. There are still several thermocouples put between the insulation

materials. Thermocouples at the top layer of particle surface are held in place by a 1-inch x 1-inch aluminum foil tape which has the sticky side faced to particles. Figure F.6 shows the detail of thermocouples placement on potash top surface layer. The tape helps shield the thermocouples to protect them from the warm lid radiation transfer. The radiation transfer from the warm lid to the particles is quite small and can be taken to be negligible.

The equipment for wetting and re-drying is shown in Figure F.3. Additional apparatus employed by these two tests include a compressor, flow mass control and water bath. Two rectangular slots, 335 mm x 10 mm, were used as the water vapor and air entrance and exit at the two end walls. Two fine screens were put on the slot entrance inside to prevent particles from blocking the air supply. The water vapor was first diffused in from the top entrance on the end wall for more than 24 hours, then diffused from the bottom entrance on the other end wall for another 24 hours. The supply airflow rate was set to 25 L/min prior to the moist tests. One humidity sensor placed behind each slot entrance to record the supply air relative humidity. The moisture contents in both of these two conditions are sampled from the surface layer of particles because it's impractical to measure the test section weight each time. Only the samples from particle surface layer were used to estimate the moisture content inside the section. A high uncertainty in the moisture content may exist below the top surface where the density may be slightly higher.

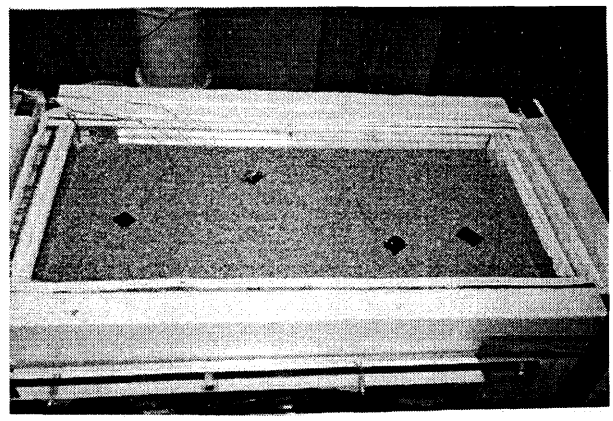

Figure F.6. Thermocouple Placement on the Top Surface Layer

B. Data Acquisition

The data acquisition system consists of a 286 microcomputer and a Scientific Instruments 8082A Electronic Measurement System analogue to digital (A/D) board. The data acquisition system consists of 64 A/D channels. One is used as a reference temperature for the board, the remaining 63 channels are used to measure analogue voltage signals from the thermocouples used in the test section. During the experiment, temperature readings are taken through the A/D board at 30 minutes intervals. Data is then stored in the hard drive of the computer.

C. Temperature Measurement

Type T thermocouples with a temperature difference accuracy of $\pm 0.1\ ^{0}C$ are used to measure temperature. Each channel of the 8082A board is calibrated using an

Ectron 1100 Thermocouple Simulator where the squared approximate curve fit at the 99.8% confidence level is used to adjust each thermocouples curve fit. The heat flux meter at the bottom was calibrated previously with a 4.3% uncertainty by Gartner (1996).

D. Experimental Procedure for Testing Samples in the Dry Condition

1) Measure geometry and calculate the volume of the test cell for the potash.
2) Put the granular potash into the drying oven at 100 ^{0}C for more than 24 hours, then put the potash material into a sealed container to cool to room temperature for at least 24 hours.
3) Position the thermocouples at the bottom plate, side walls and end walls within the test cell with alunimium tape.
4) Carefully pour the potash material into the test facility and level the surface of potash bed with straight edge. Measure the mass difference (ΔM) of container before and after filling with potash, calculate the porosity (ε) of the potash bed. For the shaken or consolidated test condition, a mechanical vibration (mechanical hand sander) was applied over the top surface for about 10 minutes and the test cell was filled again with potash and then vibrated until no further height changes in the potash were observed .
5) Using reflective aluminium tape, fix the thermocouples on the top surface layer of granular particles and on the lid of the test cell.

6) Put the lid onto the test facility and tighten the bolts. Insulate the top of the test cell and seal all adjoining edges with tape. Put the 40-kg heavy load on the top of the test section.

7) Position the thermocouples on the outside surfaces of insulation material with tape.

8) Start the electrical power supply to heat the lid, start the environment chamber and select the cold plate temperature. Open the coolant pipe valve connected to the bottom cold plate, then start the coolant pump.

9) Operate the system for more than 48 hours and record the transient temperatures at 30 minutes intervals. After all the thermocouples reach steady state, record more than 30 temperature readings in each channel over a period of 1 hour at 90 seconds intervals.

10) Shut down the power supply to both the electrical heaters in the lid and environment chamber. Shut down the coolant pump and close the coolant valve.

11) Record the transient temperature back to room temperature with 30 minutes intervals

12) Process the experimental data and calculate the apparent thermal conductvity (k)

13) Compare experimental and simulated temperature profiles during the transient periods

14) Calculate the measurement uncertainty for k

E. Experimental Procedure for Testing a Sample in the Moist Condition

This experimental procedure was the same as for the dry condition for the first past of the test. The following additional steps were used to prepare the sample.

1) Remove the insulation material from the test section lid. Open the slot entrance on the two end walls and connect the air supply pipe to the slot entrances. Tightly seal the test facility at each adjoining edge.
2) Open the valve to supply compressor air to the water bath and adjust the mass flow controller to the desired flow rate.
3) Supply the moist air at RH 85% 25 L/min and 22°C into test section from the top slot entrance for 24 hours. Reverse the air flow direction in the test cell by supplying the moist air to the bottom slot entrance for another 24 hours.
4) Disconnect the water vapor supply and seal both of these two air slots on the test cell. Open the lid, then fix the thermocouples at the top surface layer of granular particles and lid
5) Repeat experimental procedure steps D 6) –14)
6) Open the lid to take particle samples from the potash top surface layer using aluminium foil tape and measure their mass. Put these samples into the oven at 100 ^{0}C for more than 24 hours and measure their mass again and calculate the moisture content of the moist potash.

Experimental Procedure for the Re-dried Condition

Again this test procedure is somewhat similar to those above. The new sample preparation steps are:

1) After testing sample in the moist condition, remove the insulation material from the test section. Open the slot entrance on two end walls, connect the air supply pipe with slot entrances. Tightly seal the test facility at each adjoining edge.
2) Supply the dry air at RH 7% 25 L/min and 22 °C into test section from the top slot entrance for more than 24 hours. Reverse the air flow direction in the test cell by supplying air to the bottom slot entrance for another 24 hours.
3) Disconnect the dry air supply and seal both two slots. Open the lid, then fix the thermocouples at the top surface layer of granular particles and the lid
4) Repeat experimental procedure D 6)-14)

EXPERIMENTAL RESULTS AND ANALYSIS

1. Experimental Results

Following the test procedure prescribed above, we measured data to calculate the apparent thermal conductivity (k) for four different types of commercial potash listed in Table F.1. Each type of potash has been measured under two different conditions: consolidated (shaken) and unconsolidated (unshaken). The experimental data have been presented in Table F.2 to F.5.

Table F.1. Reference List of Potash Material

Potash Category	Potash Identifiction	Average Particle Size (mm)
Type-A	Lanigan Untreated Granular#2	2.2
Type-D	R.Ville Untreated Standard	0.8
Type-E	Cory Untreated Soluable	0.22
Type-F	Cory Untreated White Granular	2.6

Table F.2. Experimental Data of Apparent Thermal Conductivity ($W \bullet K^{-1} \bullet m^{-1}$) for Type-A Potash

Data	Apparent Thermal Conductivity		Data	Apparent Thermal Conductivity	
	k_u (unshaken)	k_s (shaken)		k_u (unshaken)	k_s (shaken)
1	4.77E-01	6.85E-01	18	4.75E-01	6.84E-01
2	4.77E-01	6.85E-01	19	4.76E-01	6.81E-01
3	4.78E-01	6.83E-01	20	4.76E-01	6.82E-01
4	4.77E-01	6.84E-01	21	4.76E-01	6.83E-01
5	4.77E-01	6.84E-01	22	4.76E-01	6.81E-01
6	4.78E-01	6.85E-01	23	4.76E-01	6.82E-01
7	4.77E-01	6.85E-01	24	4.77E-01	6.83E-01
8	4.78E-01	6.86E-01	25	4.76E-01	6.86E-01
9	4.77E-01	6.85E-01	26	4.76E-01	6.84E-01
10	4.77E-01	6.85E-01	27	4.77E-01	6.82E-01
11	4.78E-01	6.87E-01	28	4.76E-01	6.86E-01
12	4.75E-01	6.82E-01	29	4.77E-01	6.89E-01
13	4.77E-01	6.86E-01	30	4.77E-01	6.85E-01
14	4.76E-01	6.84E-01	31	4.77E-01	6.87E-01
15	4.76E-01	6.86E-01	32	4.77E-01	6.83E-01
16	4.76E-01	6.84E-01	33	4.77E-01	6.78E-01
17	4.74E-01	6.82E-01	34	4.77E-01	6.75E-01

Table F.3. Experimental Data of Apparent Thermal Conductivity $W \bullet K^{-1} \bullet m^{-1}$) for Type-D Potash

Data	Apparent Thermal Conductivity		Data	Apparent Thermal Conductivity	
	k_u (unshaken)	k_s (shaken)		k_u (unshaken)	k_s (shaken)
1	5.93E-01	6.49E-01	17	5.94E-01	6.52E-01
2	5.96E-01	6.52E-01	18	5.93E-01	6.50E-01
3	5.96E-01	6.50E-01	19	5.97E-01	6.48E-01
4	5.96E-01	6.53E-01	20	5.96E-01	6.48E-01
5	5.97E-01	6.52E-01	21	5.95E-01	6.48E-01
6	5.96E-01	6.52E-01	22	5.95E-01	6.48E-01
7	5.96E-01	6.50E-01	23	5.95E-01	6.49E-01
8	5.94E-01	6.49E-01	24	5.95E-01	6.49E-01
9	5.94E-01	6.47E-01	25	5.95E-01	6.49E-01
10	5.95E-01	6.49E-01	26	5.96E-01	6.50E-01
11	5.94E-01	6.50E-01	27	5.95E-01	6.49E-01
12	5.96E-01	6.51E-01	28	5.96E-01	6.51E-01
13	5.97E-01	6.52E-01	29	5.96E-01	6.52E-01
14	5.96E-01	6.51E-01	30	5.95E-01	6.50E-01
15	5.96E-01	6.53E-01	31	5.95E-01	6.50E-01
16	5.95E-01	6.53E-01			

Table-4. Experimental Data of Apparent Thermal Conductivity($W \bullet K^{-1} \bullet m^{-1}$) for Type-E Potash

Data	Apparent Thermal Conductivity		Data	Apparent Thermal Conductivity	
	k_u (unshaken)	k_s (shaken)		k_u (unshaken)	k_s (shaken)
1	5.56E-01	7.25E-01	17	5.38E-01	7.44E-01
2	5.38E-01	7.29E-01	18	5.37E-01	7.43E-01
3	5.38E-01	7.31E-01	19	5.38E-01	7.43E-01
4	5.38E-01	7.32E-01	20	5.38E-01	7.45E-01
5	5.39E-01	7.34E-01	21	5.37E-01	7.51E-01
6	5.39E-01	7.35E-01	22	5.38E-01	7.45E-01
7	5.37E-01	7.35E-01	23	5.39E-01	7.47E-01
8	5.39E-01	7.36E-01	24	5.38E-01	7.48E-01
9	5.38E-01	7.39E-01	25	5.38E-01	7.49E-01
10	5.39E-01	7.37E-01	26	5.40E-01	7.48E-01
11	5.38E-01	7.40E-01	27	5.39E-01	7.47E-01
12	5.37E-01	7.40E-01	28	5.40E-01	7.50E-01
13	5.38E-01	7.40E-01	29	5.41E-01	7.49E-01
14	5.38E-01	7.42E-01	30	5.39E-01	7.49E-01
15	5.37E-01	7.42E-01	31	5.39E-01	7.49E-01
16	5.36E-01	7.41E-01	32	5.40E-01	7.51E-01

Table F.5. Experimental Data of Apparent Thermal Conductivity ($W \bullet K^{-1} \bullet m^{-1}$) for Type-F Potash

Data	Apparent Thermal Conductivity		Data	Apparent Thermal Conductivity	
	k_u (unshaken)	k_s (shaken)		k_u (unshaken)	k_s (shaken)
1	4.71E-01	4.75E-01	19	4.71E-01	4.74E-01
2	4.69E-01	4.76E-01	20	4.71E-01	4.74E-01
3	4.69E-01	4.74E-01	21	4.70E-01	4.74E-01
4	4.71E-01	4.75E-01	22	4.71E-01	4.73E-01
5	4.71E-01	4.76E-01	23	4.71E-01	4.74E-01
6	4.69E-01	4.76E-01	24	4.72E-01	4.74E-01
7	4.69E-01	4.77E-01	25	4.71E-01	4.74E-01
8	4.71E-01	4.75E-01	26	4.72E-01	4.74E-01
9	4.69E-01	4.74E-01	27	4.71E-01	4.74E-01
10	4.69E-01	4.74E-01	28	4.71E-01	4.75E-01
11	4.70E-01	4.75E-01	29	4.72E-01	4.73E-01
12	4.72E-01	4.74E-01	30	4.72E-01	4.74E-01
13	4.71E-01	4.77E-01	31	4.71E-01	4.73E-01
14	4.69E-01	4.77E-01	32	4.72E-01	4.74E-01
15	4.70E-01	4.77E-01	33	4.71E-01	4.73E-01
16	4.70E-01	4.74E-01	34	4.71E-01	4.74E-01
17	4.72E-01	4.74E-01	35	4.71E-01	4.73E-01
18	4.70E-01	4.73E-01	36	4.72E-01	4.73E-01

Rocanville standard (Type-D) was tested under dry, moist and re-dried conditions. An average value of 0.66% moisture content was found by taking different samples from the potash top surface layer during the moist test. The moist and re-dried tests are measured under a consolidated condition with a porosity value of 0.380. The data for these tests are shown in Table F.6

Table F.6. Experimental Data of Apparent Thermal Conductivity ($W \bullet K^{-1} \bullet m^{-1}$) for Moist and Re-dried Tests

Data	Apparent Thermal Conductivity		Data	Apparent Thermal Conductivity	
	k_w (Moist)	$k_{re\text{-}dry}$ (Re-dried)		k_w (Moist)	$k_{re\text{-}dry}$ (Re-dried)
1	1.3397	7.81E-01	18	1.3377	7.82E-01
2	1.3420	7.82E-01	19	1.3400	7.81E-01
3	1.3413	7.81E-01	20	1.3400	7.82E-01
4	1.3385	7.84E-01	21	1.3400	7.81E-01
5	1.3403	7.84E-01	22	1.3432	7.83E-01
6	1.3417	7.83E-01	23	1.3377	7.84E-01
7	1.3396	7.83E-01	24	1.3406	7.84E-01
8	1.3424	7.84E-01	25	1.3437	7.84E-01
9	1.3399	7.84E-01	26	1.3408	7.85E-01
10	1.3408	7.85E-01	27	1.3411	7.86E-01
11	1.3486	7.85E-01	28	1.3415	7.86E-01
12	1.3383	7.81E-01	29	1.3381	7.85E-01
13	1.3414	7.83E-01	30	1.3372	7.85E-01
14	1.3426	7.81E-01	31	1.3426	7.86E-01
15	1.3377	7.82E-01	32	1.3406	7.86E-01

2. General Observations for the Data

1) Typical values of k, apparent thermal conductivity, for four types of granular potash range from 0.471 $W.K^{-1}.m^{-1}$ for the coarse grained potash to 0.781 $W.K^{-1}.m^{-1}$ for the smallest grained potash in the dry condition

2) Comparison of the two different test conditions, shaken and unshaken, in the dry condition shows that the change of apparent thermal conductivity (k) ranges from 2.7% to 44% while the change of porosity (ε) is just 6% to 15 %

3) The apparent thermal conductivity of granular potash will be changed after it picks up moisture. A 106% increase of the thermal conductivity was found for Rocanville Standard potash when the average moisture content was 0.66% on the top surface after the moist test

4) There is a 20 % increase in the apparent thermal conductivity between dry and re-dried experimental results. Re-drying creates caking between the granular particles which increases the contact between particles and enhances heat conduction between the particles.

5) The apparent thermal conductivity depends on particle size, size distribution, consolidation of particles in the test cell, moisture content and the existence of caking

UNCERTAINTY ANALYSIS

The bias error for each element in the measurement has been presented in Table F.7. The dominant bias error in Table F.7 is due to the calibration of the heat flux meter. The uncertainty values have been presented in Table F.8. This uncertainty in the apparent conductivity in Table F.8 is dominated by the calibration of the heat flux meter. That is, the precision error and other bias errors only contribute to about 10% of the uncertainty.

Table F.7. Bias Errors of the Measurement System

Error Category	Parameter	Bias Error Value
B_v	Electrical Voltage Reading	1%
B_I	Electrical Current Reading	1%
B_{flux}	Thermal Conductance of The Heat Flux Meter	4.30%
B_{sty}	Thermal Conductivity of Styrofoam Material	2%
B_{air}	Thermal Conductivity of Air	1%
B_L	Height of Potash Bed	1 mm
B_x	Length Measurement	1 mm
B_T	Temperature Measurement	0.1 K
B_f	Weighting Factor in Equaion(13)	0.1 or 10%

Table F.8. Uncertainty of k and ε

Property	Uncertainty
Apparent Thermal Conductivity (k)	4.55% to 4.90%
Porosity (e)	0.50%

APPENDIX G

INSTRUMENTATION AND CALIBRATION INCLUDING THE DATA ACQUISITION SYSTEM AND HEAT FLUX METER

CALIBRATION OF THE DATA ACQUISITION SYSTEM

The data acquisition system, Scientific Instruments 641 Electronic Measurement system analog to digital (A/D) board connected to sensors, was calibrated for both temperature and relative humidity measurement.

An Ectron 1100 Thermocouple Simulator was used to calibrate all the 62 channels on the 641 board. One of these channel, channel 58, is used as the internal reference channel. All others are used to measure the temperature except channel 58 which was used for relative humdity measurement. The calibrated readings from these channels have been corrected by a formula expressed as $: y = a + bx + cx^2$. The coefficients for each channel have been presented in Table G-1. Figure G.1 shows the correlation between reading and true value from one of the 64 channels. The readings were within ±0.3°C of the curve fit.

The humidity sensor calibration was performed by Peng et al. (1999). The VAISALA HMP 233 Humidity Sensor was calibrated using a General Eastern Hgro-M2

Dew Point Monitor with model 1211H sensor and a General Eastern Model C-1 Percent Relative Humidity Generator. The reading were within ±2% R.H.

Table G-1. Channel Reading Correction Coefficients

Chanel	a	b	c	r2	Chanel	a	b	c	r2
1	-0.19170	0.99290	0.00021	0.99998	32	-0.73920	1.01142	-0.00021	0.99999
2	0.07800	0.99270	0.00021	0.99999	33	-0.70489	1.01191	0.00002	0.99999
3	0.10445	0.99230	0.00020	0.99998	34	-0.67300	1.01779	-0.00013	0.99997
4	0.19110	0.99380	0.00020	1.00000	35	-0.66770	1.01790	-0.00009	1.00000
5	0.18056	0.99196	0.00025	1.00000	36	0.27170	0.99020	0.00035	1.00000
6	0.05070	0.99900	0.00014	1.00000	37	0.24150	0.99250	0.00017	1.00000
7	0.05150	0.99680	0.00024	0.99999	38	0.49180	0.96980	0.00060	0.99999
8	0.16332	0.99436	0.00027	0.99999	39	0.22640	0.99240	0.00021	1.00000
9	0.00470	0.99925	0.00017	0.99999	40	0.16600	0.99310	0.00019	1.00000
10	-0.00828	0.99950	-0.00017	0.99999	41	-0.48220	1.01197	0.00005	1.00000
11	-0.22350	1.00780	0.00007	1.00000	42	-0.50830	1.01677	-0.00003	0.99999
12	-0.26430	1.00945	-0.14070	1.00000	43	-0.45505	1.01741	-0.00005	0.99995
13	-0.21150	1.00780	0.00003	1.00000	44	-0.16898	1.00769	0.00005	0.99999
14	-0.34630	1.00106	0.00023	1.00000	45	-0.28690	1.00880	0.00007	0.99999
15	-0.33860	1.00018	0.00012	1.00000	46	-0.36870	1.00265	0.00015	1.00000
16	-0.70600	1.00047	0.00020	1.00000	47	-0.60570	1.00496	0.00008	1.00000
17	-0.68980	1.01022	-0.19870	1.00000	48	-0.31187	0.99935	0.00001	1.00000
18	-0.54890	1.00924	0.00009	1.00000	49	-0.25940	1.00402	0.00000	1.00000
19	-0.35940	0.96400	0.00095	1.00000	50	-0.21894	1.00514	0.00002	1.00000
20	-0.21630	1.00195	0.00017	1.00000	51	-0.16457	1.00560	0.00002	0.99999
21	-0.43640	0.99736	0.00028	1.00000	52	-0.12859	1.00479	0.00004	0.99996
22	-0.46800	0.99800	0.00029	1.00000	53	-0.29099	1.00789	0.00004	1.00000
23	-0.52410	1.00008	0.00020	0.99999	54	-0.39009	1.01105	0.00003	0.99999
24	-0.41229	0.99880	0.00026	0.99998	55	-0.69550	1.01140	0.00017	0.99999
25	-0.37370	0.99984	0.00017	1.00000	56	-0.32930	1.00395	0.00016	0.99999
26	-0.79060	1.00079	0.00022	1.00000	57	-0.57260	1.00799	0.00010	1.00000
27	-0.69950	1.00139	0.00020	0.99999	58	-0.62530	1.01030	0.00007	0.99999
28	-0.50480	0.99620	0.00027	1.00000	59	-0.60800	1.00990	0.00004	1.00000
29	-0.55410	0.99750	0.00025	0.99998	60	-0.19200	1.00058	0.00019	1.00000
30	-0.68575	1.00381	0.00011	1.00000	61	-0.26020	1.01565	-0.00025	1.00000
31	-0.84480	1.00356	0.00017	0.99999	62	-0.23190	1.01282	-0.00019	0.99998

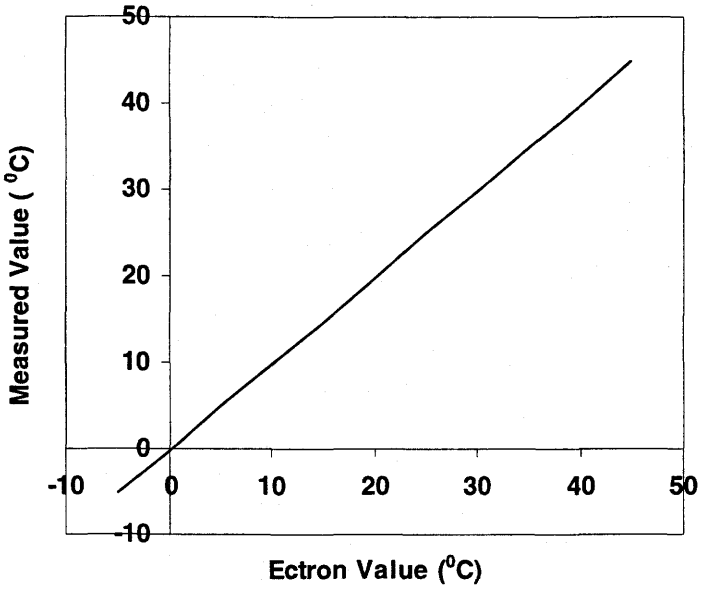

Figure G.1 Correlation between Readings and Ectron Simulation Value for Thermocouples (Type T)

HEAT FLUX MEASUREMENT AND CALIBRATION

The heat flux was measured in each experiment using a heat flux meter designed and calibrated by Mao et al (1991). The heat flux meter is composed of a high thermal resistance polyethylene sheet (3.25-mm thickness) with a thermal conductivity of 0.2177 W/m• K, as given by the manufacturer. The polyethylene sheet is sandwiched between the aluminum test plate and cooling device which is mentioned in Chapter 3. The heat

flux meter was calibrated at a series of temperatures as low as –50 °C and gave an uncertainty of less than 6%. The thermocouple used in the calibration gave an uncertainty of ±0.1 °C.

In Mao's calibration, the major uncertainty in the calibration came from the temperature difference across the polyethylene sheet, ΔT, which gave a high error for a small value. The experimental data shows that the ΔT is always higher than 1°C. Unfortunately, most of our experiments data give a very small temperature difference across the heat flux meter with a typical reading of 0.1°C which is right in the uncertainty limit for thermocouples and could cause very high uncertainty in the heat flux. A very large discrepancy between experimental data and simulation results was found in the heat flux data.

APPENDIX H

EXPERIMENTAL DATA FOR AIR DIFFUSION OVER POTASH BED

ROCANVILLE STANDARD POTASH

1. MOISTURE CONTENT DATA

RH=45%, Tair=22^{0}C, Tc=2^{0}C, Q=9.33L/s

time (h)	MC#1 (kg/kg-dry)	MC#2 (kg/kg-dry)	MC#3 (kg/kg-dry)	MC#4 (kg/kg-dry)
1	1.18E-03	3.00E-04	7.00E-04	5.00E-04
2	1.28E-03	8.00E-04	1.60E-03	8.25E-04
3	1.54E-03	2.00E-03	1.43E-03	9.39E-04
8	5.55E-03	3.90E-03	5.30E-03	3.26E-03

RH=45%, Tair=22^{0}C, Tc=21^{0}C, Q=9.33L/s

time (h)	MC#1 (kg/kg-dry)	MC#2 (kg/kg-dry)	MC#3 (kg/kg-dry)	MC#4 (kg/kg-dry)
8	1.50E-03	7.90E-04	7.11E-04	6.64E-04

RH=65%, Tair=22^{0}C, Tc=2^{0}C, Q=9.33L/s

time (h)	MC#1 (kg/kg-dry)	MC#2 (kg/kg-dry)	MC#3 (kg/kg-dry)	MC#4 (kg/kg-dry)
1	3.50E-03	1.74E-03	1.34E-03	1.26E-03
2	5.26E-03	3.09E-03	1.80E-03	1.50E-03
3	6.06E-03	4.20E-03	2.60E-03	1.84E-03
8	1.50E-02	1.02E-02	1.01E-02	9.79E-03

RH=65%, Tair=22^{0}C, Tc=21^{0}C, Q=9.33L/s

time (h)	MC#1 (kg/kg-dry)	MC#2 (kg/kg-dry)	MC#3 (kg/kg-dry)	MC#4 (kg/kg-dry)
8	2.12E-03	9.79E-04	5.31E-04	2.02E-04

RH=80%, Tair=22^{0}C, Tc=2^{0}C, Q=9.17L/s

time (h)	MC#1 (kg/kg-dry)	MC#2 (kg/kg-dry)	MC#3 (kg/kg-dry)	MC#4 (kg/kg-dry)
1	9.06E-03	1.97E-03	8.00E-04	7.00E-04
2	1.79E-02		1.05E-03	7.00E-04
3	2.91E-02		2.20E-03	1.17E-03
8	6.68E-02	1.65E-02	1.07E-02	9.86E-03

RH=80%, Tair=22^{0}C, Tc=21^{0}C, Q=9.17L/s

time (h)	MC#1 (kg/kg-dry)	MC#2 (kg/kg-dry)	MC#3 (kg/kg-dry)	MC#4 (kg/kg-dry)
8	2.15E-03	9.70E-04	4.69E-03	4.56E-04

2. TEMPERATURE DATA

RH=45%, Tair=22^{0}C, Tc=2^{0}C, Q=9.33 L/s

Time (s)	Tray#1 (^{0}C)	Tray#2 (^{0}C)	Tray#3 (^{0}C)	Tray#4 (^{0}C)	Time (s)	Tray#1 (^{0}C)	Tray#2 (^{0}C)	Tray#3 (^{0}C)	Tray#4 (^{0}C)	Time (s)	Tray#1 (^{0}C)	Tray#2 (^{0}C)	Tray#3 (^{0}C)	Tray#4 (^{0}C)	Time (s)	Tray#1 (^{0}C)	Tray#2 (^{0}C)	Tray#3 (^{0}C)	Tray#4 (^{0}C)
0	22.42	21.52	14.87	16.17	0.94	16.34	12.62	6.68	7.98	1.86	15.62	12.05	6.1	7.4	2.78	15.28	11.73	5.81	7.11
0.04	22.37	20.81	13.27	14.57	0.96	16.29	12.62	6.64	7.94	1.88	15.62	12.05	6.1	7.4	2.8	15.28	11.71	5.81	7.11
0.06	22.32	20.52	12.8	14.1	0.98	16.25	12.57	6.63	7.93	1.9	15.58	12.03	6.07	7.37	2.82	15.28	11.71	5.81	7.11
0.08	22.2	20.17	12.35	13.65	1	16.24	12.57	6.58	7.88	1.92	15.57	12	6.05	7.35	2.83	15.28	11.66	5.81	7.11
0.1	22.1	19.77	11.95	13.25	1.02	16.19	12.52	6.58	7.88	1.93	15.57	12	6.05	7.35	2.85	15.32	11.75	5.85	7.15
0.12	21.95	19.33	11.59	12.89	1.04	16.18	12.52	6.53	7.83	1.95	15.56	12	6.05	7.35	2.87	15.31	11.75	5.84	7.14
0.14	21.76	18.93	11.29	12.59	1.05	16.17	12.48	6.56	7.86	1.97	15.52	12	6.05	7.35	2.89	15.29	11.75	5.84	7.14
0.15	21.59	18.56	11.04	12.34	1.07	16.17	12.5	6.56	7.86	1.99	15.52	11.98	6	7.3	2.91	15.28	11.75	5.85	7.15
0.17	21.39	18.14	10.79	12.09	1.09	16.12	12.5	6.55	7.85	2.01	15.55	11.99	6.03	7.33	2.93	15.23	11.7	5.8	7.1
0.19	21.14	17.76	10.54	11.84	1.11	16.12	12.45	6.51	7.81	2.03	15.55	11.98	6.03	7.33	2.95	15.27	11.75	5.84	7.14
0.21	20.91	17.39	10.29	11.59	1.13	16.08	12.45	6.51	7.81	2.04	15.55	11.98	6.03	7.33	2.96	15.27	11.73	5.81	7.11
0.23	20.72	17.04	10.08	11.38	1.15	16.07	12.43	6.47	7.77	2.06	15.55	11.98	6.03	7.33	2.98	15.28	11.74	5.8	7.1
0.25	20.48	16.68	9.91	11.21	1.16	16.03	12.4	6.46	7.76	2.08	15.52	11.98	6.03	7.33	3	15.27	11.74	5.83	7.13
0.26	20.26	16.42	9.71	11.01	1.18	16.02	12.4	6.46	7.76	2.1	15.5	11.98	6.03	7.33	3.02	15.28	11.74	5.8	7.1
0.28	20.04	16.12	9.54	10.84	1.2	16.02	12.36	6.41	7.71	2.12	15.5	11.94	6.01	7.31	3.04	15.27	11.68	5.8	7.1
0.3	19.85	15.91	9.4	10.7	1.22	15.97	12.35	6.41	7.71	2.14	15.5	11.93	5.98	7.28	3.06	15.27	11.73	5.8	7.1
0.32	19.65	15.66	9.25	10.55	1.24	15.97	12.35	6.41	7.71	2.16	15.5	11.93	5.98	7.28	3.07	15.27	11.72	5.8	7.1
0.34	19.4	15.41	9.09	10.39	1.26	15.96	12.32	6.4	7.7	2.17	15.47	11.93	5.98	7.28	3.09	15.27	11.71	5.8	7.1
0.36	19.14	15.16	8.89	10.19	1.27	15.92	12.3	6.36	7.66	2.19	15.46	11.93	5.98	7.28	3.11	15.27	11.7	5.8	7.1
0.37	19.01	15.01	8.79	10.09	1.29	15.92	12.3	6.36	7.66	2.21	15.45	11.9	5.98	7.28	3.13	15.27	11.7	5.8	7.1
0.39	18.81	14.81	8.64	9.94	1.31	15.92	12.3	6.36	7.66	2.23	15.45	11.88	5.97	7.27	3.15	15.3	11.73	5.83	7.13
0.41	18.66	14.66	8.54	9.84	1.33	15.89	12.3	6.36	7.66	2.25	15.45	11.88	5.97	7.27	3.17	15.3	11.73	5.83	7.13
0.43	18.49	14.54	8.41	9.71	1.35	15.87	12.28	6.34	7.64	2.27	15.42	11.88	5.95	7.25	3.18	15.27	11.73	5.83	7.13
0.45	18.32	14.36	8.31	9.61	1.37	15.87	12.26	6.32	7.62	2.28	15.41	11.88	5.93	7.23	3.2	15.21	11.68	5.78	7.08
0.47	18.19	14.26	8.21	9.51	1.38	15.87	12.25	6.31	7.61	2.3	15.4	11.88	5.93	7.23	3.22	15.25	11.7	5.83	7.13
0.48	18.04	14.12	8.14	9.44	1.4	15.86	12.25	6.31	7.61	2.32	15.4	11.85	5.93	7.23	3.24	15.2	11.65	5.78	7.08
0.5	17.9	14.01	8.03	9.33	1.42	15.82	12.25	6.28	7.58	2.34	15.4	11.83	5.93	7.23	3.26	15.2	11.63	5.76	7.06
0.52	17.79	13.87	7.93	9.23	1.44	15.82	12.25	6.3	7.6	2.36	15.35	11.78	5.88	7.18	3.28	15.25	11.68	5.79	7.09
0.54	17.67	13.77	7.83	9.13	1.46	15.82	12.25	6.28	7.58	2.38	15.32	11.78	5.87	7.17	3.29	15.25	11.68	5.78	7.08
0.56	17.6	13.7	7.76	9.06	1.48	15.82	12.24	6.25	7.55	2.39	15.35	11.83	5.89	7.19	3.31	15.19	11.63	5.73	7.03
0.58	17.5	13.59	7.69	8.99	1.49	15.78	12.21	6.24	7.54	2.41	15.35	11.83	5.88	7.18	3.33	15.23	11.68	5.78	7.08
0.59	17.4	13.54	7.61	8.91	1.51	15.77	12.2	6.25	7.55	2.43	15.35	11.79	5.88	7.18	3.35	15.2	11.67	5.78	7.08
0.61	17.3	13.44	7.52	8.82	1.53	15.77	12.2	6.25	7.55	2.45	15.35	11.81	5.88	7.18	3.37	15.2	11.64	5.78	7.08
0.63	17.21	13.39	7.46	8.76	1.55	15.76	12.18	6.21	7.51	2.47	15.35	11.78	5.88	7.18	3.39	15.2	11.64	5.78	7.08
0.65	17.14	13.29	7.4	8.7	1.57	15.72	12.15	6.21	7.51	2.49	15.38	11.81	5.91	7.21	3.4	15.15	11.58	5.72	7.02
0.67	17.05	13.24	7.3	8.6	1.59	15.72	12.15	6.2	7.5	2.5	15.38	11.81	5.91	7.21	3.42	15.2	11.63	5.77	7.07
0.69	16.99	13.19	7.25	8.55	1.6	15.72	12.15	6.2	7.5	2.52	15.35	11.81	5.91	7.21	3.44	15.18	11.61	5.75	7.05
0.7	16.9	13.14	7.2	8.5	1.62	15.69	12.14	6.2	7.5	2.54	15.33	11.81	5.89	7.19	3.46	15.21	11.66	5.77	7.07
0.72	16.85	13.09	7.15	8.45	1.64	15.67	12.1	6.2	7.5	2.56	15.33	11.81	5.87	7.17	3.48	15.18	11.66	5.79	7.09
0.74	16.8	13.04	7.1	8.4	1.66	15.67	12.12	6.17	7.47	2.58	15.33	11.79	5.86	7.16	3.5	15.19	11.66	5.77	7.07
0.76	16.79	13.03	7.09	8.39	1.68	15.67	12.1	6.15	7.45	2.6	15.33	11.79	5.86	7.16	3.51	15.18	11.63	5.76	7.06
0.78	16.72	12.98	7.04	8.34	1.7	15.67	12.1	6.15	7.45	2.61	15.28	11.73	5.81	7.11	3.53	15.18	11.63	5.76	7.06
0.8	16.65	12.93	6.99	8.29	1.71	15.67	12.1	6.15	7.45	2.63	15.28	11.72	5.86	7.16	3.55	15.18	11.62	5.75	7.05
0.81	16.59	12.88	6.94	8.24	1.73	15.66	12.1	6.15	7.45	2.65	15.28	11.72	5.81	7.11	3.57	15.13	11.57	5.71	7.01
0.83	16.54	12.83	6.9	8.2	1.75	15.63	12.1	6.13	7.43	2.67	15.28	11.72	5.81	7.11	3.59	15.18	11.61	5.76	7.06
0.85	16.54	12.83	6.86	8.16	1.77	15.62	12.07	6.12	7.42	2.69	15.28	11.71	5.81	7.11	3.61	15.18	11.61	5.76	7.06
0.87	16.49	12.78	6.84	8.14	1.79	15.62	12.08	6.1	7.4	2.71	15.33	11.76	5.86	7.16	3.62	15.17	11.56	5.75	7.05
0.89	16.44	12.73	6.78	8.08	1.81	15.62	12.07	6.1	7.4	2.72	15.29	11.76	5.85	7.15	3.64	15.18	11.61	5.73	7.03
0.91	16.39	12.73	6.73	8.03	1.82	15.62	12.06	6.1	7.4	2.74	15.29	11.76	5.82	7.12	3.66	15.18	11.61	5.74	7.04
0.92	16.35	12.68	6.73	8.03	1.84	15.62	12.05	6.1	7.4	2.76	15.23	11.71	5.76	7.06	3.68	15.18	11.61	5.74	7.04

RH=45%, Tair=22°C, Tc=2°C, Q=9.33 L/s

Time (s)	Tray#1 (°C)	Tray#2 (°C)	Tray#3 (°C)	Tray#4 (°C)	Time (s)	Tray#1 (°C)	Tray#2 (°C)	Tray#3 (°C)	Tray#4 (°C)	Time (s)	Tray#1 (°C)	Tray#2 (°C)	Tray#3 (°C)	Tray#4 (°C)	Time (s)	Tray#1 (°C)	Tray#2 (°C)	Tray#3 (°C)	Tray#4 (°C)
3.7	15.15	11.61	5.73	7.03	4.58	14.98	11.46	5.66	6.96	5.46	14.93	11.46	5.66	6.96	6.34	14.8	11.35	5.62	6.92
3.72	15.14	11.61	5.71	7.01	4.6	14.98	11.46	5.65	6.95	5.48	14.93	11.45	5.64	6.94	6.36	14.8	11.35	5.62	6.92
3.73	15.14	11.61	5.71	7.01	4.62	14.98	11.46	5.64	6.94	5.5	14.98	11.5	5.69	6.99	6.38	14.8	11.35	5.62	6.92
3.75	15.18	11.61	5.73	7.03	4.63	14.98	11.45	5.64	6.94	5.52	14.93	11.45	5.67	6.97	6.4	14.8	11.35	5.63	6.93
3.77	15.18	11.61	5.71	7.01	4.65	14.97	11.46	5.63	6.93	5.53	14.98	11.51	5.7	7	6.42	14.81	11.35	5.62	6.92
3.79	15.16	11.61	5.71	7.01	4.67	14.98	11.44	5.66	6.96	5.55	14.98	11.51	5.71	7.01	6.44	14.78	11.32	5.59	6.89
3.81	15.17	11.61	5.72	7.02	4.69	14.98	11.45	5.65	6.95	5.57	14.93	11.46	5.66	6.96	6.45	14.85	11.4	5.67	6.97
3.83	15.14	11.61	5.71	7.01	4.71	14.97	11.45	5.66	6.96	5.59	14.93	11.45	5.66	6.96	6.47	14.82	11.37	5.63	6.93
3.85	15.14	11.61	5.73	7.03	4.73	14.96	11.45	5.62	6.92	5.61	14.93	11.45	5.65	6.95	6.49	14.82	11.37	5.63	6.93
3.86	15.14	11.61	5.73	7.03	4.74	14.94	11.44	5.64	6.94	5.63	14.93	11.46	5.65	6.95	6.51	14.77	11.32	5.58	6.88
3.88	15.13	11.61	5.71	7.01	4.76	14.94	11.44	5.65	6.95	5.65	14.98	11.5	5.7	7	6.53	14.77	11.32	5.58	6.88
3.9	15.13	11.61	5.73	7.03	4.78	14.98	11.47	5.69	6.99	5.66	14.93	11.46	5.66	6.96	6.55	14.78	11.32	5.58	6.88
3.92	15.13	11.6	5.73	7.03	4.8	14.98	11.46	5.67	6.97	5.68	14.93	11.46	5.66	6.96	6.56	14.82	11.32	5.59	6.89
3.94	15.09	11.56	5.68	6.98	4.82	14.93	11.43	5.62	6.92	5.7	14.93	11.46	5.65	6.95	6.58	14.82	11.32	5.58	6.88
3.96	15.08	11.56	5.68	6.98	4.84	14.93	11.43	5.64	6.94	5.72	14.93	11.46	5.66	6.96	6.6	14.82	11.36	5.6	6.9
3.97	15.13	11.59	5.73	7.03	4.86	14.93	11.43	5.65	6.95	5.74	14.98	11.51	5.7	7	6.62	14.82	11.37	5.6	6.9
3.99	15.08	11.52	5.66	6.96	4.87	14.98	11.46	5.68	6.98	5.76	14.93	11.46	5.65	6.95	6.64	14.87	11.4	5.67	6.97
4.01	15.08	11.51	5.69	6.99	4.89	14.93	11.43	5.64	6.94	5.77	14.93	11.45	5.66	6.96	6.66	14.87	11.4	5.65	6.95
4.03	15.08	11.51	5.68	6.98	4.91	14.93	11.43	5.64	6.94	5.79	14.92	11.44	5.66	6.96	6.67	14.82	11.37	5.59	6.89
4.05	15.05	11.51	5.66	6.96	4.93	14.93	11.43	5.63	6.93	5.81	14.93	11.44	5.65	6.95	6.69	14.87	11.4	5.66	6.96
4.07	15.03	11.51	5.66	6.96	4.95	14.93	11.44	5.63	6.93	5.83	14.93	11.44	5.66	6.96	6.71	14.87	11.4	5.67	6.97
4.08	15.03	11.51	5.66	6.96	4.97	14.99	11.47	5.69	6.99	5.85	14.93	11.44	5.66	6.96	6.73	14.82	11.37	5.63	6.93
4.1	15.08	11.56	5.69	6.99	4.98	14.98	11.5	5.69	6.99	5.87	14.98	11.48	5.7	7	6.75	14.87	11.4	5.67	6.97
4.12	15.08	11.55	5.7	7	5	14.95	11.45	5.64	6.94	5.88	14.93	11.44	5.66	6.96	6.77	14.82	11.37	5.6	6.9
4.14	15.03	11.51	5.64	6.94	5.02	14.93	11.46	5.62	6.92	5.9	14.93	11.43	5.66	6.96	6.78	14.83	11.33	5.63	6.93
4.16	15.08	11.54	5.71	7.01	5.04	14.94	11.45	5.64	6.94	5.92	14.97	11.46	5.71	7.01	6.8	14.78	11.33	5.58	6.88
4.18	15.03	11.46	5.65	6.95	5.06	14.97	11.46	5.62	6.92	5.94	14.91	11.43	5.66	6.96	6.82	14.79	11.33	5.59	6.89
4.19	15	11.46	5.65	6.95	5.08	15.01	11.5	5.67	6.97	5.96	14.94	11.46	5.71	7.01	6.84	14.81	11.33	5.6	6.9
4.21	15.01	11.46	5.68	6.98	5.09	14.98	11.46	5.65	6.95	5.98	14.89	11.43	5.66	6.96	6.86	14.8	11.33	5.61	6.91
4.23	14.99	11.46	5.64	6.94	5.11	14.97	11.46	5.62	6.92	5.99	14.9	11.43	5.66	6.96	6.88	14.79	11.33	5.61	6.91
4.25	14.98	11.46	5.64	6.94	5.13	14.97	11.46	5.64	6.94	6.01	14.9	11.43	5.66	6.96	6.89	14.8	11.34	5.59	6.89
4.27	14.98	11.46	5.62	6.92	5.15	14.98	11.46	5.66	6.96	6.03	14.88	11.43	5.66	6.96	6.91	14.8	11.34	5.6	6.9
4.29	15.03	11.51	5.7	7	5.17	14.97	11.46	5.64	6.94	6.05	14.93	11.46	5.71	7.01	6.93	14.8	11.34	5.6	6.9
4.3	14.99	11.46	5.67	6.97	5.19	14.96	11.46	5.65	6.95	6.07	14.88	11.43	5.66	6.96	6.95	14.81	11.33	5.6	6.9
4.32	14.98	11.46	5.66	6.96	5.2	14.95	11.46	5.63	6.93	6.09	14.88	11.42	5.66	6.96	6.97	14.82	11.34	5.6	6.9
4.34	14.98	11.46	5.64	6.94	5.22	14.94	11.46	5.65	6.95	6.1	14.88	11.41	5.66	6.96	6.99	14.83	11.35	5.6	6.9
4.36	15.03	11.51	5.68	6.98	5.24	14.96	11.46	5.64	6.94	6.12	14.85	11.36	5.62	6.92	7	14.88	11.41	5.65	6.95
4.38	15.03	11.51	5.68	6.98	5.26	14.96	11.46	5.65	6.95	6.14	14.88	11.38	5.65	6.95	7.02	14.83	11.35	5.61	6.91
4.4	14.98	11.46	5.63	6.93	5.28	15.01	11.51	5.69	6.99	6.16	14.85	11.36	5.62	6.92	7.04	14.83	11.35	5.59	6.89
4.41	14.98	11.46	5.62	6.92	5.3	14.96	11.46	5.66	6.96	6.18	14.85	11.35	5.58	6.88	7.06	14.83	11.35	5.6	6.9
4.43	14.98	11.46	5.62	6.92	5.31	14.98	11.51	5.72	7.02	6.2	14.9	11.4	5.68	6.98	7.08	14.81	11.34	5.6	6.9
4.45	14.98	11.46	5.64	6.94	5.33	14.98	11.51	5.7	7	6.21	14.85	11.35	5.62	6.92	7.1	14.87	11.39	5.65	6.95
4.47	15.03	11.51	5.7	7	5.35	14.98	11.51	5.7	7	6.23	14.85	11.36	5.61	6.91	7.11	14.82	11.35	5.6	6.9
4.49	14.98	11.46	5.65	6.95	5.37	14.93	11.46	5.64	6.94	6.25	14.85	11.35	5.61	6.91	7.13	14.83	11.4	5.65	6.95
4.51	15.03	11.51	5.7	7	5.39	14.98	11.49	5.7	7	6.27	14.85	11.35	5.63	6.93	7.15	14.79	11.34	5.59	6.89
4.52	14.98	11.46	5.66	6.96	5.41	14.93	11.5	5.66	6.96	6.29	14.88	11.4	5.67	6.97	7.17	14.8	11.34	5.65	6.95
4.54	14.98	11.46	5.65	6.95	5.42	14.93	11.45	5.64	6.94	6.31	14.89	11.4	5.68	6.98	7.19	14.81	11.35	5.6	6.9
4.56	15.03	11.51	5.7	7	5.44	14.93	11.46	5.66	6.96	6.32	14.87	11.4	5.67	6.97	7.21	14.87	11.4	5.65	6.95

RH=65%, Tair=22°C, Tc=2°C, Q=9.33 L/s

Time (s)	Tray#1 (°C)	Tray#2 (°C)	Tray#3 (°C)	Tray#4 (°C)	Time (s)	Tray#1 (°C)	Tray#2 (°C)	Tray#3 (°C)	Tray#4 (°C)	Time (s)	Tray#1 (°C)	Tray#2 (°C)	Tray#3 (°C)	Tray#4 (°C)	Time (s)	Tray#1 (°C)	Tray#2 (°C)	Tray#3 (°C)	Tray#4 (°C)
0	20.88	19.1	19.99	19.7	0.9	13.98	11.27	12.625	11.87	1.8	13.16	10.14	11.65	10.74	2.7	12.68	9.51	11.095	10.11
0.02	20.47	18.63	19.55	19.23	0.92	13.93	11.24	12.585	11.84	1.82	13.11	10.09	11.6	10.69	2.72	12.64	9.48	11.06	10.08
0.04	20.14	18.23	19.185	18.83	0.94	13.93	11.19	12.56	11.79	1.84	13.11	10.04	11.575	10.64	2.74	12.64	9.46	11.05	10.06
0.06	19.84	17.91	18.875	18.51	0.96	13.91	11.21	12.56	11.81	1.86	13.08	10.03	11.555	10.63	2.76	12.64	9.46	11.05	10.06
0.08	19.48	17.58	18.53	18.18	0.98	13.91	11.17	12.54	11.77	1.87	13.06	10.03	11.545	10.63	2.78	12.64	9.46	11.05	10.06
0.1	19.13	17.22	18.175	17.82	0.99	13.86	11.12	12.49	11.72	1.89	13.06	9.98	11.52	10.58	2.79	12.64	9.46	11.05	10.06
0.11	18.91	16.97	17.94	17.57	1.01	13.82	11.11	12.465	11.71	1.91	13.06	9.98	11.52	10.58	2.81	12.61	9.46	11.035	10.06
0.13	18.62	16.67	17.645	17.27	1.03	13.81	11.09	12.45	11.69	1.93	13.11	10.06	11.585	10.66	2.83	12.61	9.42	11.015	10.02
0.15	18.33	16.36	17.345	16.96	1.05	13.77	11.06	12.415	11.66	1.95	13.05	9.97	11.51	10.57	2.85	12.6	9.43	11.015	10.03
0.17	18.11	16.07	17.09	16.67	1.07	13.79	11.07	12.43	11.67	1.97	13.04	9.96	11.5	10.56	2.87	12.59	9.41	11	10.01
0.19	17.84	15.77	16.805	16.37	1.09	13.74	11.02	12.38	11.62	1.98	13.04	9.96	11.5	10.56	2.89	12.59	9.41	11	10.01
0.21	17.6	15.54	16.57	16.14	1.1	13.74	10.97	12.355	11.57	2	13.04	9.93	11.485	10.53	2.9	12.59	9.41	11	10.01
0.22	17.39	15.24	16.315	15.84	1.12	13.69	10.93	12.31	11.53	2.02	13	9.92	11.46	10.52	2.92	12.59	9.4	10.995	10
0.24	17.17	14.99	16.08	15.59	1.14	13.69	10.9	12.295	11.5	2.04	13.03	9.94	11.485	10.54	2.94	12.59	9.39	10.99	9.99
0.26	17	14.77	15.885	15.37	1.16	13.64	10.87	12.255	11.47	2.06	13.02	9.94	11.48	10.54	2.96	12.56	9.36	10.96	9.96
0.28	16.75	14.47	15.61	15.07	1.18	13.68	10.86	12.27	11.46	2.08	13.02	9.94	11.48	10.54	2.98	12.54	9.36	10.95	9.96
0.3	16.6	14.27	15.435	14.87	1.2	13.63	10.81	12.22	11.41	2.09	13.02	9.89	11.455	10.49	3	12.54	9.36	10.95	9.96
0.32	16.38	14.04	15.21	14.64	1.21	13.63	10.8	12.215	11.4	2.11	12.98	9.89	11.435	10.49	3.01	12.54	9.36	10.95	9.96
0.33	16.23	13.87	15.05	14.47	1.23	13.58	10.76	12.17	11.36	2.13	12.97	9.89	11.43	10.49	3.03	12.54	9.36	10.95	9.96
0.35	16.03	13.62	14.825	14.22	1.25	13.58	10.71	12.145	11.31	2.15	12.97	9.84	11.405	10.44	3.05	12.54	9.34	10.94	9.94
0.37	15.88	13.42	14.65	14.02	1.27	13.53	10.7	12.115	11.3	2.17	12.92	9.84	11.38	10.44	3.07	12.54	9.31	10.925	9.91
0.39	15.76	13.25	14.505	13.85	1.29	13.52	10.66	12.09	11.26	2.19	12.92	9.82	11.37	10.42	3.09	12.51	9.32	10.915	9.92
0.41	15.61	13.1	14.355	13.7	1.31	13.51	10.64	12.075	11.24	2.21	12.88	9.79	11.335	10.39	3.11	12.5	9.31	10.905	9.91
0.43	15.46	12.95	14.205	13.55	1.32	13.51	10.62	12.065	11.22	2.22	12.87	9.79	11.33	10.39	3.12	12.49	9.31	10.9	9.91
0.44	15.35	12.82	14.085	13.42	1.34	13.46	10.59	12.025	11.19	2.24	12.87	9.76	11.315	10.36	3.14	12.49	9.31	10.9	9.91
0.46	15.25	12.69	13.97	13.29	1.36	13.46	10.54	12	11.14	2.26	12.86	9.78	11.32	10.38	3.16	12.49	9.29	10.89	9.89
0.48	15.1	12.54	13.82	13.14	1.38	13.42	10.54	11.98	11.14	2.28	12.86	9.78	11.32	10.38	3.18	12.49	9.26	10.875	9.86
0.5	15	12.41	13.705	13.01	1.4	13.41	10.49	11.95	11.09	2.3	12.82	9.73	11.275	10.33	3.2	12.49	9.23	10.86	9.83
0.52	14.9	12.29	13.595	12.89	1.42	13.37	10.47	11.92	11.07	2.32	12.81	9.73	11.27	10.33	3.22	12.46	9.23	10.845	9.83
0.54	14.83	12.22	13.525	12.82	1.43	13.39	10.47	11.93	11.07	2.33	12.81	9.68	11.245	10.28	3.23	12.45	9.23	10.84	9.83
0.55	14.73	12.12	13.425	12.72	1.45	13.39	10.44	11.915	11.04	2.35	12.81	9.68	11.245	10.28	3.25	12.43	9.23	10.83	9.83
0.57	14.66	12.02	13.34	12.62	1.47	13.34	10.42	11.88	11.02	2.37	12.81	9.68	11.245	10.28	3.27	12.41	9.23	10.82	9.83
0.59	14.58	11.96	13.27	12.56	1.49	13.34	10.38	11.86	10.98	2.39	12.86	9.7	11.28	10.3	3.29	12.41	9.22	10.815	9.82
0.61	14.55	11.89	13.22	12.49	1.51	13.29	10.37	11.83	10.97	2.41	12.81	9.65	11.23	10.25	3.31	12.41	9.2	10.805	9.8
0.63	14.47	11.84	13.155	12.44	1.53	13.29	10.34	11.815	10.94	2.43	12.81	9.64	11.225	10.24	3.33	12.41	9.19	10.8	9.79
0.65	14.41	11.78	13.095	12.38	1.54	13.27	10.32	11.795	10.92	2.44	12.77	9.63	11.2	10.23	3.35	12.41	9.19	10.8	9.79
0.66	14.36	11.71	13.035	12.31	1.56	13.24	10.29	11.765	10.89	2.46	12.79	9.66	11.225	10.26	3.36	12.41	9.18	10.795	9.78
0.68	14.37	11.69	13.03	12.29	1.58	13.24	10.27	11.755	10.87	2.48	12.76	9.6	11.18	10.2	3.38	12.39	9.18	10.785	9.78
0.7	14.32	11.63	12.975	12.23	1.6	13.25	10.28	11.765	10.88	2.5	12.76	9.59	11.175	10.19	3.4	12.41	9.18	10.795	9.78
0.72	14.27	11.59	12.93	12.19	1.62	13.23	10.26	11.745	10.86	2.52	12.76	9.61	11.185	10.21	3.42	12.4	9.18	10.79	9.78
0.74	14.22	11.55	12.885	12.15	1.64	13.23	10.25	11.74	10.85	2.54	12.74	9.6	11.17	10.2	3.44	12.39	9.18	10.785	9.78
0.76	14.17	11.5	12.835	12.1	1.65	13.22	10.21	11.715	10.81	2.55	12.74	9.57	11.155	10.17	3.46	12.4	9.18	10.79	9.78
0.77	14.15	11.51	12.83	12.11	1.67	13.18	10.21	11.695	10.81	2.57	12.72	9.56	11.14	10.16	3.47	12.39	9.18	10.785	9.78
0.79	14.12	11.46	12.79	12.06	1.69	13.18	10.18	11.68	10.78	2.59	12.69	9.56	11.125	10.16	3.49	12.38	9.17	10.775	9.77
0.81	14.09	11.41	12.75	12.01	1.71	13.18	10.16	11.67	10.76	2.61	12.69	9.56	11.125	10.16	3.51	12.38	9.12	10.75	9.72
0.83	14.05	11.37	12.71	11.97	1.73	13.13	10.14	11.635	10.74	2.63	12.66	9.53	11.095	10.13	3.53	12.37	9.12	10.745	9.72
0.85	14.03	11.37	12.7	11.97	1.75	13.16	10.14	11.65	10.74	2.65	12.69	9.51	11.1	10.11	3.55	12.37	9.12	10.745	9.72
0.87	14.03	11.34	12.685	11.94	1.76	13.16	10.14	11.65	10.74	2.66	12.69	9.51	11.1	10.11	3.57	12.36	9.12	10.74	9.72
0.88	13.98	11.29	12.635	11.89	1.78	13.11	10.1	11.605	10.7	2.68	12.69	9.51	11.1	10.11	3.58	12.36	9.12	10.74	9.72

RH=65%, Tair=22°C, Tc=2°C, Q=9.33 L/s

Time (s)	Tray#1 (°C)	Tray#2 (°C)	Tray#3 (°C)	Tray#4 (°C)	Time (s)	Tray#1 (°C)	Tray#2 (°C)	Tray#3 (°C)	Tray#4 (°C)	Time (s)	Tray#1 (°C)	Tray#2 (°C)	Tray#3 (°C)	Tray#4 (°C)	Time (s)	Tray#1 (°C)	Tray#2 (°C)	Tray#3 (°C)	Tray#4 (°C)
3.6	12.37	9.12	10.745	9.72	4.5	12.26	9.02	10.64	9.62	5.4	12.2	9.07	10.635	9.67	6.31	12.13	8.98	10.555	9.58
3.62	12.36	9.12	10.74	9.72	4.52	12.25	9.02	10.635	9.62	5.42	12.2	9.07	10.635	9.67	6.33	12.12	8.98	10.55	9.58
3.64	12.4	9.12	10.76	9.72	4.54	12.23	9.02	10.625	9.62	5.44	12.2	9.07	10.635	9.67	6.34	12.12	8.94	10.53	9.54
3.66	12.38	9.12	10.75	9.72	4.56	12.22	9.02	10.62	9.62	5.46	12.2	9.06	10.63	9.66	6.36	12.12	8.88	10.5	9.48
3.68	12.38	9.12	10.75	9.72	4.58	12.22	9.02	10.62	9.62	5.48	12.2	9.07	10.635	9.67	6.38	12.09	8.94	10.515	9.54
3.69	12.36	9.12	10.74	9.72	4.6	12.24	9.06	10.65	9.66	5.5	12.2	9.07	10.635	9.67	6.4	12.07	8.94	10.505	9.54
3.71	12.36	9.12	10.74	9.72	4.61	12.24	9.06	10.65	9.66	5.51	12.2	9.06	10.63	9.66	6.42	12.07	8.9	10.485	9.5
3.73	12.36	9.12	10.74	9.72	4.63	12.25	9.06	10.655	9.66	5.53	12.24	9.11	10.675	9.71	6.44	12.07	8.92	10.495	9.52
3.75	12.36	9.12	10.74	9.72	4.65	12.24	9.06	10.65	9.66	5.55	12.2	9.07	10.635	9.67	6.45	12.07	8.89	10.48	9.49
3.77	12.36	9.12	10.74	9.72	4.67	12.24	9.06	10.65	9.66	5.57	12.24	9.11	10.675	9.71	6.47	12.07	8.87	10.47	9.47
3.79	12.36	9.12	10.74	9.72	4.69	12.24	9.06	10.65	9.66	5.59	12.24	9.11	10.675	9.71	6.49	12.07	8.9	10.485	9.5
3.8	12.37	9.13	10.75	9.73	4.71	12.24	9.06	10.65	9.66	5.61	12.24	9.11	10.675	9.71	6.51	12.07	8.87	10.47	9.47
3.82	12.36	9.12	10.74	9.72	4.72	12.24	9.06	10.65	9.66	5.63	12.24	9.09	10.665	9.69	6.53	12.06	8.91	10.485	9.51
3.84	12.36	9.12	10.74	9.72	4.74	12.24	9.06	10.65	9.66	5.64	12.24	9.07	10.655	9.67	6.55	12.04	8.87	10.455	9.47
3.86	12.36	9.12	10.74	9.72	4.76	12.24	9.06	10.65	9.66	5.66	12.23	9.07	10.65	9.67	6.56	12.03	8.88	10.455	9.48
3.88	12.39	9.16	10.775	9.76	4.78	12.23	9.06	10.645	9.66	5.68	12.2	9.06	10.63	9.66	6.58	12.06	8.94	10.5	9.54
3.9	12.39	9.16	10.775	9.76	4.8	12.22	9.06	10.64	9.66	5.7	12.2	9.07	10.635	9.67	6.6	12.06	8.83	10.445	9.43
3.92	12.39	9.16	10.775	9.76	4.82	12.21	9.06	10.635	9.66	5.72	12.19	9.06	10.625	9.66	6.62	12.07	8.85	10.46	9.45
3.93	12.39	9.16	10.775	9.76	4.83	12.21	9.06	10.635	9.66	5.74	12.19	9.06	10.625	9.66	6.64	12.07	8.86	10.465	9.46
3.95	12.39	9.16	10.775	9.76	4.85	12.25	9.1	10.675	9.7	5.75	12.19	9.06	10.625	9.66	6.66	12.07	8.95	10.51	9.55
3.97	12.39	9.16	10.775	9.76	4.87	12.23	9.1	10.665	9.7	5.77	12.16	9.03	10.595	9.63	6.67	12.07	8.9	10.485	9.5
3.99	12.39	9.16	10.775	9.76	4.89	12.24	9.1	10.67	9.7	5.79	12.15	9.04	10.595	9.64	6.69	12.07	8.89	10.48	9.49
4.01	12.39	9.16	10.775	9.76	4.91	12.24	9.1	10.67	9.7	5.81	12.14	9.02	10.58	9.62	6.71	12.07	8.86	10.465	9.46
4.03	12.39	9.16	10.775	9.76	4.93	12.23	9.09	10.66	9.69	5.83	12.14	9.01	10.575	9.61	6.73	12.05	8.84	10.445	9.44
4.04	12.39	9.16	10.775	9.76	4.95	12.23	9.1	10.665	9.7	5.85	12.14	9.01	10.575	9.61	6.75	12.04	8.87	10.455	9.47
4.06	12.39	9.16	10.775	9.76	4.96	12.23	9.1	10.665	9.7	5.86	12.13	9.01	10.57	9.61	6.77	12.05	8.96	10.505	9.56
4.08	12.39	9.16	10.775	9.76	4.98	12.23	9.09	10.66	9.69	5.88	12.12	8.97	10.545	9.57	6.79	12.09	8.93	10.51	9.53
4.1	12.39	9.16	10.775	9.76	5	12.23	9.08	10.655	9.68	5.9	12.11	8.97	10.54	9.57	6.8	12.08	8.95	10.515	9.55
4.12	12.35	9.16	10.755	9.76	5.02	12.23	9.08	10.655	9.68	5.92	12.11	8.97	10.54	9.57	6.82	12.07	9.03	10.55	9.63
4.14	12.37	9.16	10.765	9.76	5.04	12.23	9.09	10.66	9.69	5.94	12.09	8.95	10.52	9.55	6.84	12.09	8.94	10.515	9.54
4.15	12.37	9.14	10.755	9.74	5.06	12.23	9.06	10.645	9.66	5.96	12.1	8.96	10.53	9.56	6.86	12.07	8.87	10.47	9.47
4.17	12.37	9.14	10.755	9.74	5.07	12.23	9.06	10.645	9.66	5.98	12.1	8.96	10.53	9.56	6.88	12.07	8.95	10.51	9.55
4.19	12.34	9.14	10.74	9.74	5.09	12.23	9.05	10.64	9.65	5.99	12.1	8.96	10.53	9.56	6.9	12.07	8.97	10.52	9.57
4.21	12.32	9.14	10.73	9.74	5.11	12.22	9.05	10.635	9.65	6.01	12.12	8.96	10.54	9.56	6.91	12.09	8.95	10.52	9.55
4.23	12.32	9.11	10.715	9.71	5.13	12.2	9.06	10.63	9.66	6.03	12.11	8.96	10.535	9.56	6.93	12.06	8.93	10.495	9.53
4.25	12.32	9.08	10.7	9.68	5.15	12.23	9.05	10.64	9.65	6.05	12.15	8.98	10.565	9.58	6.95	12.06	8.95	10.505	9.55
4.27	12.27	9.08	10.675	9.68	5.17	12.23	9.05	10.64	9.65	6.07	12.17	8.99	10.58	9.59	6.97	12.06	8.94	10.5	9.54
4.28	12.27	9.08	10.675	9.68	5.18	12.24	9.07	10.655	9.67	6.09	12.17	8.99	10.58	9.59	6.99	12.06	8.96	10.51	9.56
4.3	12.27	9.08	10.675	9.68	5.2	12.25	9.07	10.66	9.67	6.1	12.17	8.99	10.58	9.59	7.01	12.07	8.96	10.515	9.56
4.32	12.27	9.03	10.65	9.63	5.22	12.24	9.07	10.655	9.67	6.12	12.17	8.99	10.58	9.59	7.02	12.06	8.95	10.505	9.55
4.34	12.26	9.03	10.645	9.63	5.24	12.22	9.07	10.645	9.67	6.14	12.17	8.98	10.575	9.58	7.04	12.06	8.97	10.515	9.57
4.36	12.25	9.03	10.64	9.63	5.26	12.22	9.07	10.645	9.67	6.16	12.17	8.99	10.58	9.59	7.06	12.06	8.97	10.515	9.57
4.38	12.25	9.03	10.64	9.63	5.28	12.22	9.07	10.645	9.67	6.18	12.17	8.99	10.58	9.59	7.08	12.06	8.99	10.525	9.59
4.39	12.29	9.08	10.685	9.68	5.29	12.2	9.07	10.635	9.67	6.2	12.17	8.99	10.58	9.59	7.1	12.06	8.96	10.51	9.56
4.41	12.28	9.08	10.68	9.68	5.31	12.2	9.07	10.635	9.67	6.21	12.17	8.99	10.58	9.59	7.12	12.06	8.97	10.515	9.57
4.43	12.27	9.06	10.665	9.66	5.33	12.2	9.07	10.635	9.67	6.23	12.15	8.99	10.57	9.59	7.13	12.06	9	10.53	9.6
4.45	12.26	9.06	10.66	9.66	5.35	12.22	9.07	10.645	9.67	6.25	12.13	8.99	10.56	9.59	7.15	12.06	9.05	10.555	9.65
4.47	12.26	9.04	10.65	9.64	5.37	12.2	9.07	10.635	9.67	6.27	12.14	8.98	10.56	9.58	7.17	12.06	8.93	10.495	9.53
4.49	12.26	9.02	10.64	9.62	5.39	12.21	9.07	10.64	9.67	6.29	12.14	8.99	10.565	9.59	7.19	12.11	9.05	10.58	9.65

RH=80%, Tair=22°C, Tc=2°C, Q=9.17 L/s

Time (s)	Tray#1 (°C)	Tray#2 (°C)	Tray#3 (°C)	Tray#4 (°C)	Time (s)	Tray#1 (°C)	Tray#2 (°C)	Tray#3 (°C)	Tray#4 (°C)	Time (s)	Tray#1 (°C)	Tray#2 (°C)	Tray#3 (°C)	Tray#4 (°C)	Time (s)	Tray#1 (°C)	Tray#2 (°C)	Tray#3 (°C)	Tray#4 (°C)
0	21.3	20.295	17.2	4.21	0.87	14.86	10.31	4.44	1.65	1.75	14.5	9.79	4.17	1.68	2.62	14.45	9.675	4.14	1.72
0.02	20.7	19.105	14.5	3.93	0.89	14.86	10.28	4.42	1.65	1.76	14.46	9.775	4.16	1.68	2.63	14.45	9.67	4.12	1.72
0.04	20.01	17.93	12.4	3.26	0.91	14.81	10.245	4.42	1.65	1.78	14.46	9.765	4.16	1.68	2.65	14.45	9.67	4.14	1.72
0.06	19.77	17.285	9.57	2.31	0.93	14.85	10.265	4.42	1.67	1.8	14.5	9.78	4.16	1.68	2.67	14.45	9.69	4.14	1.72
0.08	19.49	16.885	9.16	2.27	0.95	14.8	10.23	4.41	1.66	1.82	14.49	9.75	4.17	1.68	2.72	14.45	9.665	4.11	1.72
0.09	19.21	16.485	8.78	2.22	0.96	14.8	10.19	4.4	1.65	1.83	14.46	9.75	4.15	1.68	2.74	14.48	9.69	4.16	1.76
0.11	18.96	16.105	8.45	2.2	0.98	14.75	10.18	4.36	1.65	1.85	14.45	9.75	4.16	1.68	2.76	14.48	9.685	4.14	1.76
0.13	18.71	15.73	8.11	2.16	1	14.75	10.155	4.36	1.64	1.87	14.45	9.75	4.15	1.68	2.78	14.48	9.675	4.14	1.76
0.15	18.52	15.395	7.86	2.11	1.02	14.73	10.14	4.36	1.67	1.89	14.45	9.75	4.15	1.68	2.79	14.48	9.67	4.13	1.76
0.16	18.35	15.08	7.61	2.11	1.03	14.7	10.12	4.36	1.64	1.91	14.45	9.75	4.15	1.68	2.81	14.48	9.67	4.13	1.75
0.18	18.11	14.745	7.36	2.06	1.05	14.7	10.105	4.32	1.65	1.92	14.45	9.745	4.16	1.68	2.83	14.48	9.67	4.13	1.76
0.2	17.93	14.49	7.13	2.08	1.07	14.7	10.065	4.31	1.63	1.94	14.45	9.745	4.15	1.68	2.85	14.46	9.67	4.13	1.71
0.22	17.77	14.2	6.93	2.06	1.09	14.65	10.055	4.31	1.64	1.96	14.45	9.745	4.15	1.68	2.87	14.43	9.67	4.11	1.7
0.23	17.59	13.95	6.76	2.04	1.11	14.65	10.045	4.29	1.64	1.98	14.46	9.735	4.15	1.68	2.88	14.44	9.665	4.11	1.7
0.25	17.43	13.715	6.57	2.04	1.12	14.68	10.035	4.29	1.61	1.99	14.45	9.735	4.15	1.68	2.9	14.43	9.67	4.11	1.7
0.27	17.28	13.485	6.42	2	1.14	14.67	10.035	4.29	1.63	2.01	14.46	9.735	4.15	1.69	2.92	14.43	9.67	4.11	1.69
0.29	17.13	13.28	6.27	1.98	1.16	14.63	9.995	4.29	1.61	2.03	14.45	9.73	4.15	1.69	2.94	14.43	9.65	4.09	1.67
0.31	16.98	13.055	6.12	1.94	1.18	14.63	9.985	4.27	1.61	2.05	14.45	9.73	4.15	1.69	2.95	14.43	9.635	4.09	1.65
0.32	16.88	12.875	6.01	1.95	1.19	14.58	9.94	4.23	1.6	2.07	14.46	9.73	4.15	1.69	2.97	14.43	9.645	4.08	1.65
0.34	16.73	12.675	5.86	1.91	1.21	14.58	9.935	4.23	1.59	2.08	14.45	9.725	4.15	1.68	2.99	14.43	9.62	4.08	1.65
0.36	16.59	12.52	5.76	1.88	1.23	14.58	9.93	4.19	1.59	2.1	14.45	9.725	4.15	1.69	3.01	14.43	9.62	4.07	1.65
0.38	16.48	12.36	5.66	1.85	1.25	14.6	9.95	4.22	1.61	2.12	14.45	9.725	4.15	1.7	3.03	14.43	9.62	4.07	1.64
0.39	16.38	12.215	5.57	1.87	1.27	14.57	9.93	4.23	1.64	2.14	14.45	9.725	4.15	1.69	3.04	14.42	9.62	4.06	1.62
0.41	16.28	12.09	5.46	1.84	1.28	14.57	9.925	4.22	1.64	2.15	14.45	9.725	4.16	1.68	3.06	14.4	9.615	4.02	1.61
0.43	16.18	11.96	5.4	1.83	1.3	14.57	9.925	4.22	1.65	2.17	14.45	9.725	4.14	1.68	3.08	14.39	9.615	4.03	1.6
0.45	16.12	11.85	5.34	1.84	1.32	14.57	9.925	4.22	1.65	2.19	14.45	9.715	4.13	1.7	3.1	14.38	9.6	4.02	1.6
0.47	15.98	11.71	5.21	1.78	1.34	14.57	9.905	4.22	1.65	2.21	14.45	9.705	4.15	1.68	3.11	14.38	9.595	4.02	1.6
0.48	15.92	11.625	5.19	1.81	1.35	14.57	9.9	4.22	1.65	2.23	14.45	9.725	4.15	1.69	3.13	14.38	9.595	4.02	1.6
0.5	15.82	11.515	5.14	1.79	1.37	14.57	9.9	4.22	1.65	2.24	14.45	9.685	4.13	1.68	3.15	14.38	9.59	4.02	1.6
0.52	15.77	11.42	5.08	1.78	1.39	14.57	9.9	4.22	1.66	2.26	14.45	9.68	4.13	1.68	3.17	14.38	9.57	4.03	1.6
0.54	15.67	11.33	5.02	1.78	1.41	14.56	9.88	4.22	1.65	2.28	14.45	9.675	4.12	1.68	3.19	14.38	9.575	4.02	1.57
0.55	15.62	11.245	4.98	1.77	1.43	14.53	9.865	4.19	1.65	2.3	14.45	9.675	4.11	1.69	3.2	14.38	9.57	4.01	1.57
0.57	15.57	11.165	4.93	1.77	1.44	14.52	9.845	4.19	1.65	2.31	14.45	9.675	4.12	1.68	3.22	14.38	9.56	3.98	1.56
0.59	15.5	11.08	4.88	1.76	1.46	14.52	9.86	4.22	1.65	2.33	14.45	9.675	4.12	1.68	3.24	14.38	9.55	3.98	1.55
0.61	15.43	11.015	4.86	1.74	1.48	14.52	9.845	4.18	1.65	2.35	14.42	9.675	4.11	1.68	3.26	14.38	9.545	3.97	1.55
0.63	15.37	10.935	4.82	1.74	1.5	14.52	9.845	4.18	1.65	2.37	14.44	9.675	4.12	1.68	3.27	14.38	9.545	3.98	1.55
0.64	15.32	10.865	4.78	1.73	1.51	14.51	9.83	4.17	1.65	2.39	14.45	9.675	4.13	1.69	3.29	14.38	9.545	3.97	1.55
0.66	15.27	10.815	4.75	1.71	1.53	14.48	9.815	4.17	1.65	2.4	14.45	9.675	4.14	1.7	3.31	14.38	9.54	3.98	1.56
0.68	15.22	10.745	4.7	1.72	1.55	14.47	9.805	4.17	1.64	2.42	14.45	9.675	4.12	1.69	3.33	14.42	9.585	4.01	1.59
0.7	15.17	10.7	4.67	1.72	1.57	14.47	9.8	4.17	1.64	2.44	14.45	9.675	4.11	1.71	3.35	14.38	9.54	3.97	1.55
0.71	15.14	10.655	4.66	1.7	1.59	14.47	9.795	4.17	1.65	2.46	14.47	9.705	4.15	1.72	3.36	14.38	9.54	3.97	1.55
0.73	15.1	10.62	4.62	1.7	1.6	14.47	9.79	4.16	1.65	2.47	14.45	9.7	4.14	1.72	3.38	14.42	9.55	4.01	1.59
0.75	15.09	10.565	4.61	1.7	1.62	14.47	9.785	4.17	1.65	2.49	14.45	9.71	4.14	1.72	3.4	14.42	9.54	4	1.59
0.77	15.04	10.515	4.57	1.7	1.64	14.47	9.775	4.16	1.65	2.51	14.45	9.685	4.13	1.72	3.42	14.42	9.54	4	1.59
0.79	15.02	10.51	4.57	1.7	1.66	14.5	9.8	4.19	1.68	2.53	14.45	9.68	4.15	1.72	3.43	14.42	9.54	3.99	1.6
0.8	14.99	10.465	4.52	1.69	1.67	14.5	9.8	4.16	1.68	2.55	14.45	9.715	4.15	1.73	3.45	14.4	9.55	4.01	1.63
0.82	14.96	10.415	4.52	1.68	1.69	14.5	9.795	4.16	1.68	2.56	14.45	9.685	4.13	1.72	3.47	14.39	9.545	4.01	1.61
0.84	14.92	10.37	4.47	1.64	1.71	14.5	9.795	4.17	1.68	2.58	14.45	9.68	4.13	1.72	3.49	14.41	9.56	4.01	1.62
0.86	14.91	10.36	4.47	1.67	1.73	14.49	9.79	4.16	1.68	2.6	14.45	9.67	4.13	1.72	3.51	14.42	9.535	4.01	1.62

RH=80%, Tair=22°C, Tc=2°C, Q=9.17 L/s

Time (s)	Tray#1 (°C)	Tray#2 (°C)	Tray#3 (°C)	Tray#4 (°C)	Time (s)	Tray#1 (°C)	Tray#2 (°C)	Tray#3 (°C)	Tray#4 (°C)	Time (s)	Tray#1 (°C)	Tray#2 (°C)	Tray#3 (°C)	Tray#4 (°C)	Time (s)	Tray#1 (°C)	Tray#2 (°C)	Tray#3 (°C)	Tray#4 (°C)
3.52	14.42	9.565	4.01	1.64	4.39	14.34	9.495	4.02	1.72	5.27	14.39	9.45	3.9	1.71	6.14	14.35	9.425	3.88	1.75
3.54	14.42	9.55	4.01	1.64	4.41	14.34	9.495	3.99	1.71	5.28	14.39	9.45	3.91	1.7	6.15	14.35	9.42	3.85	1.76
3.56	14.42	9.55	4.01	1.64	4.43	14.34	9.49	3.99	1.72	5.3	14.38	9.45	3.92	1.71	6.17	14.37	9.425	3.89	1.76
3.58	14.38	9.54	3.99	1.63	4.45	14.34	9.5	4	1.72	5.32	14.39	9.455	3.92	1.71	6.19	14.35	9.42	3.89	1.75
3.59	14.37	9.53	3.99	1.64	4.47	14.34	9.495	4	1.71	5.34	14.39	9.45	3.93	1.71	6.21	14.35	9.425	3.87	1.76
3.61	14.37	9.535	3.99	1.64	4.48	14.34	9.5	3.99	1.72	5.35	14.39	9.455	3.94	1.71	6.22	14.35	9.42	3.88	1.77
3.63	14.37	9.53	3.97	1.64	4.5	14.34	9.475	3.99	1.71	5.37	14.43	9.455	3.93	1.71	6.24	14.35	9.42	3.9	1.78
3.65	14.37	9.55	3.97	1.64	4.52	14.3	9.435	3.95	1.64	5.39	14.43	9.46	3.93	1.71	6.26	14.37	9.425	3.88	1.78
3.67	14.37	9.52	3.99	1.64	4.54	14.34	9.485	3.99	1.69	5.41	14.43	9.46	3.95	1.71	6.28	14.35	9.425	3.88	1.78
3.68	14.37	9.52	3.97	1.64	4.55	14.34	9.49	3.99	1.72	5.43	14.43	9.48	3.93	1.71	6.3	14.35	9.425	3.91	1.78
3.7	14.37	9.51	3.96	1.64	4.57	14.34	9.485	3.99	1.72	5.44	14.43	9.46	3.93	1.71	6.31	14.35	9.42	3.89	1.78
3.72	14.37	9.505	3.97	1.64	4.59	14.34	9.49	3.99	1.71	5.46	14.43	9.46	3.92	1.71	6.33	14.35	9.42	3.87	1.78
3.74	14.35	9.5	3.96	1.64	4.61	14.34	9.495	3.99	1.72	5.48	14.4	9.435	3.9	1.69	6.35	14.36	9.425	3.91	1.78
3.75	14.35	9.505	3.96	1.64	4.63	14.32	9.47	3.95	1.68	5.5	14.4	9.44	3.91	1.68	6.37	14.35	9.42	3.91	1.78
3.77	14.34	9.51	3.97	1.64	4.64	14.3	9.445	3.95	1.68	5.51	14.4	9.435	3.91	1.68	6.38	14.35	9.42	3.93	1.78
3.79	14.37	9.51	3.97	1.64	4.66	14.35	9.475	3.96	1.69	5.53	14.4	9.42	3.9	1.68	6.4	14.35	9.42	3.92	1.78
3.81	14.34	9.51	3.98	1.65	4.68	14.35	9.495	4	1.7	5.55	14.4	9.445	3.87	1.69	6.42	14.36	9.42	3.89	1.79
3.83	14.33	9.48	3.93	1.62	4.7	14.35	9.47	4	1.68	5.57	14.4	9.445	3.92	1.7	6.44	14.35	9.42	3.89	1.78
3.84	14.29	9.465	3.94	1.65	4.71	14.35	9.495	4	1.69	5.59	14.4	9.445	3.9	1.71	6.46	14.35	9.42	3.87	1.79
3.86	14.31	9.47	3.95	1.64	4.73	14.35	9.465	4	1.69	5.6	14.4	9.445	3.94	1.72	6.47	14.35	9.42	3.89	1.78
3.88	14.32	9.455	3.95	1.65	4.75	14.35	9.505	4	1.69	5.62	14.4	9.445	3.91	1.73	6.49	14.35	9.42	3.89	1.78
3.9	14.28	9.46	3.96	1.65	4.77	14.35	9.5	4	1.73	5.64	14.4	9.45	3.93	1.73	6.51	14.35	9.42	3.89	1.79
3.91	14.31	9.475	3.97	1.65	4.79	14.35	9.5	4.01	1.73	5.66	14.4	9.46	3.9	1.73	6.53	14.35	9.42	3.88	1.83
3.93	14.31	9.45	3.97	1.65	4.8	14.35	9.5	4	1.72	5.67	14.4	9.445	3.9	1.73	6.54	14.35	9.42	3.9	1.8
3.95	14.28	9.455	3.97	1.65	4.82	14.35	9.495	4	1.73	5.69	14.4	9.445	3.9	1.72	6.56	14.36	9.425	3.9	1.8
3.97	14.27	9.45	3.97	1.65	4.84	14.37	9.495	4.01	1.73	5.71	14.4	9.445	3.89	1.73	6.58	14.35	9.425	3.89	1.79
3.99	14.28	9.45	3.97	1.68	4.86	14.37	9.495	3.99	1.71	5.73	14.4	9.445	3.9	1.73	6.6	14.36	9.42	3.9	1.8
4	14.3	9.46	3.97	1.67	4.87	14.38	9.495	3.99	1.73	5.75	14.4	9.445	3.9	1.72	6.62	14.35	9.425	3.9	1.79
4.02	14.29	9.46	3.97	1.68	4.89	14.37	9.495	4	1.73	5.76	14.39	9.445	3.9	1.73	6.63	14.35	9.425	3.9	1.8
4.04	14.3	9.465	3.97	1.69	4.91	14.36	9.495	3.97	1.72	5.78	14.4	9.445	3.91	1.74	6.65	14.35	9.42	3.9	1.79
4.06	14.31	9.465	3.97	1.7	4.93	14.35	9.495	3.97	1.71	5.8	14.38	9.445	3.88	1.73	6.67	14.36	9.44	3.9	1.8
4.07	14.31	9.475	3.97	1.7	4.95	14.35	9.475	3.98	1.72	5.82	14.38	9.445	3.88	1.72	6.69	14.35	9.435	3.9	1.8
4.09	14.32	9.485	3.97	1.7	4.96	14.35	9.485	3.97	1.72	5.83	14.37	9.445	3.9	1.72	6.7	14.35	9.44	3.88	1.79
4.11	14.33	9.48	3.98	1.7	4.98	14.35	9.48	3.99	1.73	5.85	14.37	9.445	3.89	1.73	6.72	14.35	9.445	3.89	1.78
4.13	14.33	9.485	3.98	1.7	5	14.35	9.46	3.93	1.7	5.87	14.37	9.445	3.88	1.73	6.74	14.35	9.44	3.9	1.78
4.15	14.29	9.46	3.97	1.67	5.02	14.32	9.445	3.93	1.7	5.89	14.38	9.445	3.89	1.73	6.76	14.35	9.44	3.9	1.79
4.16	14.29	9.46	3.97	1.67	5.03	14.32	9.45	3.93	1.7	5.91	14.37	9.44	3.89	1.73	6.78	14.35	9.445	3.89	1.78
4.18	14.29	9.46	3.98	1.69	5.05	14.32	9.45	3.94	1.71	5.92	14.36	9.44	3.9	1.74	6.79	14.35	9.445	3.88	1.78
4.2	14.29	9.46	3.99	1.69	5.07	14.33	9.445	3.94	1.71	5.94	14.36	9.445	3.89	1.73	6.81	14.35	9.43	3.89	1.79
4.22	14.29	9.46	3.99	1.69	5.09	14.33	9.445	3.93	1.7	5.96	14.36	9.44	3.89	1.73	6.83	14.35	9.455	3.93	1.82
4.23	14.29	9.46	3.99	1.7	5.11	14.37	9.455	3.95	1.71	5.98	14.35	9.435	3.88	1.73	6.85	14.35	9.435	3.9	1.79
4.25	14.3	9.46	4	1.69	5.12	14.39	9.46	3.94	1.71	5.99	14.35	9.425	3.88	1.74	6.86	14.38	9.465	3.95	1.81
4.27	14.29	9.46	4	1.7	5.14	14.42	9.465	3.95	1.73	6.01	14.35	9.43	3.89	1.73	6.88	14.35	9.425	3.9	1.79
4.29	14.32	9.46	3.99	1.7	5.16	14.42	9.465	3.93	1.73	6.03	14.36	9.425	3.89	1.75	6.9	14.38	9.445	3.93	1.82
4.31	14.33	9.46	3.99	1.7	5.18	14.42	9.45	3.94	1.71	6.05	14.35	9.425	3.89	1.75	6.92	14.38	9.435	3.92	1.81
4.32	14.34	9.46	4	1.7	5.19	14.42	9.46	3.93	1.73	6.06	14.35	9.425	3.9	1.76	6.94	14.38	9.44	3.93	1.81
4.34	14.34	9.465	3.99	1.69	5.21	14.42	9.485	3.95	1.74	6.08	14.36	9.42	3.89	1.75	6.95	14.38	9.44	3.93	1.81
4.36	14.32	9.47	3.98	1.68	5.23	14.42	9.49	3.98	1.74	6.1	14.35	9.42	3.88	1.75	6.97	14.38	9.435	3.93	1.81
4.38	14.34	9.48	3.99	1.72	5.25	14.38	9.45	3.92	1.71	6.12	14.35	9.425	3.89	1.75	6.99	14.38	9.425	3.92	1.82

RH=45%, Tair=22°C, Tc=21°C, Q=9.33 L/s

Time (s)	Tray#1 (°C)	Tray#2 (°C)	Tray#3 (°C)	Tray#4 (°C)	Time (s)	Tray#1 (°C)	Tray#2 (°C)	Tray#3 (°C)	Tray#4 (°C)	Time (s)	Tray#1 (°C)	Tray#2 (°C)	Tray#3 (°C)	Tray#4 (°C)	Time (s)	Tray#1 (°C)	Tray#2 (°C)	Tray#3 (°C)	Tray#4 (°C)
0	22.02	21.98	21.64	21.14	0.95	21.59	21.59	21.3	21.05	1.85	21.38	21.43	21.24	21.01	2.75	21.29	21.34	21.2	20.98
0.08	22.17	21.98	21.53	21.14	0.97	21.59	21.59	21.3	21.04	1.87	21.38	21.43	21.24	20.96	2.77	21.29	21.34	21.2	20.93
0.09	22.25	22.01	21.55	21.08	0.99	21.59	21.59	21.25	21	1.89	21.38	21.42	21.2	20.96	2.79	21.29	21.34	21.2	20.99
0.11	22.25	22.01	21.52	21.07	1.01	21.57	21.57	21.28	21.03	1.91	21.38	21.39	21.19	21.01	2.8	21.29	21.34	21.18	20.98
0.13	22.23	22.01	21.5	21.06	1.03	21.57	21.57	21.28	21.03	1.93	21.38	21.38	21.19	21.01	2.82	21.29	21.3	21.16	20.98
0.15	22.23	21.99	21.5	21.1	1.05	21.57	21.57	21.28	21.03	1.94	21.38	21.38	21.19	20.96	2.84	21.29	21.3	21.15	20.98
0.17	22.21	22.02	21.48	21.1	1.06	21.52	21.52	21.24	20.98	1.96	21.38	21.38	21.19	20.96	2.86	21.29	21.29	21.15	20.98
0.19	22.16	22.02	21.48	21.08	1.08	21.56	21.56	21.27	21.02	1.98	21.38	21.41	21.22	21.04	2.88	21.29	21.29	21.15	20.98
0.2	22.15	22	21.46	21.11	1.1	21.56	21.56	21.27	21.02	2	21.36	21.41	21.22	21	2.9	21.29	21.29	21.15	20.93
0.22	22.12	21.98	21.44	21.05	1.12	21.56	21.56	21.27	21.02	2.02	21.36	21.41	21.22	20.99	2.91	21.28	21.29	21.15	20.98
0.24	22.13	21.98	21.44	21.1	1.14	21.55	21.54	21.3	21	2.04	21.36	21.41	21.22	20.94	2.93	21.28	21.29	21.15	20.98
0.26	22.08	21.98	21.44	21.1	1.16	21.54	21.54	21.26	21.04	2.05	21.36	21.38	21.19	20.99	2.95	21.29	21.29	21.15	20.98
0.28	22.06	21.96	21.47	21.09	1.17	21.54	21.54	21.25	21	2.07	21.36	21.36	21.18	20.94	2.97	21.24	21.29	21.15	20.93
0.3	22.1	22	21.46	21.12	1.19	21.51	21.53	21.25	21	2.09	21.36	21.36	21.17	20.94	2.99	21.25	21.29	21.15	20.98
0.31	22.08	21.98	21.49	21.1	1.21	21.52	21.52	21.28	21.03	2.11	21.33	21.36	21.18	20.99	3.01	21.29	21.33	21.19	21.02
0.33	22.03	21.96	21.44	21.06	1.23	21.52	21.52	21.28	21.03	2.13	21.37	21.4	21.21	21.03	3.02	21.28	21.33	21.19	21.02
0.35	22.05	21.96	21.47	21.13	1.25	21.52	21.52	21.26	21.03	2.15	21.36	21.4	21.21	20.98	3.04	21.28	21.33	21.19	21.02
0.37	22.01	21.91	21.43	21.13	1.27	21.47	21.52	21.24	21.02	2.16	21.36	21.4	21.21	20.98	3.06	21.28	21.33	21.19	21.02
0.39	21.96	21.91	21.43	21.09	1.28	21.47	21.48	21.24	20.99	2.18	21.35	21.4	21.21	21.01	3.08	21.28	21.33	21.19	21.01
0.41	21.9	21.84	21.36	21.06	1.3	21.51	21.51	21.28	21.03	2.2	21.35	21.4	21.21	20.98	3.1	21.28	21.32	21.19	21.01
0.42	21.89	21.83	21.36	21.05	1.32	21.51	21.51	21.28	21.03	2.22	21.35	21.37	21.21	20.98	3.12	21.28	21.31	21.19	21
0.44	21.88	21.83	21.4	21.05	1.34	21.49	21.51	21.28	20.98	2.24	21.35	21.35	21.21	20.98	3.13	21.28	21.33	21.19	21.01
0.46	21.87	21.82	21.35	21.05	1.36	21.46	21.5	21.25	21.03	2.26	21.35	21.35	21.18	20.98	3.15	21.28	21.33	21.19	21
0.48	21.86	21.81	21.38	21.08	1.38	21.49	21.49	21.26	21.04	2.27	21.31	21.35	21.17	20.98	3.17	21.28	21.32	21.19	20.97
0.5	21.85	21.82	21.39	21.03	1.39	21.49	21.49	21.26	21.03	2.29	21.34	21.38	21.19	21.01	3.19	21.28	21.31	21.19	21.02
0.52	21.84	21.79	21.36	21.01	1.41	21.49	21.49	21.26	21.01	2.31	21.33	21.38	21.19	21.01	3.21	21.28	21.32	21.19	21.02
0.53	21.79	21.77	21.36	21.01	1.43	21.44	21.49	21.26	21.01	2.33	21.34	21.38	21.19	21.01	3.23	21.28	21.3	21.19	21
0.55	21.82	21.77	21.34	21.06	1.45	21.44	21.47	21.26	20.96	2.35	21.33	21.38	21.19	20.96	3.24	21.28	21.29	21.19	21.02
0.57	21.77	21.73	21.34	21.04	1.47	21.44	21.44	21.22	21.01	2.37	21.33	21.38	21.19	20.96	3.26	21.28	21.29	21.18	20.92
0.59	21.8	21.75	21.37	21.07	1.49	21.47	21.47	21.24	21.02	2.38	21.33	21.37	21.19	21.01	3.28	21.28	21.28	21.15	20.98
0.61	21.75	21.72	21.32	21.06	1.5	21.47	21.47	21.24	21.01	2.4	21.33	21.35	21.19	21	3.3	21.28	21.28	21.16	20.92
0.63	21.71	21.7	21.32	21.02	1.52	21.44	21.47	21.24	20.99	2.42	21.33	21.33	21.19	21.01	3.32	21.28	21.28	21.15	20.97
0.64	21.74	21.72	21.35	21.01	1.54	21.42	21.47	21.24	20.96	2.44	21.33	21.33	21.19	20.97	3.34	21.28	21.28	21.18	20.97
0.66	21.73	21.7	21.32	21.06	1.56	21.42	21.43	21.24	20.99	2.46	21.3	21.33	21.19	20.97	3.35	21.28	21.28	21.15	20.97
0.68	21.7	21.7	21.31	21.01	1.58	21.42	21.42	21.24	20.99	2.47	21.32	21.37	21.21	21.01	3.37	21.27	21.28	21.17	20.93
0.7	21.73	21.68	21.34	21.04	1.6	21.45	21.45	21.22	21.02	2.49	21.32	21.37	21.18	21.01	3.39	21.27	21.28	21.14	20.93
0.72	21.76	21.76	21.37	21.06	1.61	21.42	21.45	21.22	21.02	2.51	21.32	21.37	21.18	21.01	3.41	21.26	21.28	21.15	20.97
0.73	21.71	21.66	21.32	21.02	1.63	21.41	21.45	21.22	21.02	2.53	21.32	21.37	21.19	21.01	3.43	21.25	21.28	21.14	20.97
0.75	21.67	21.66	21.32	21.02	1.65	21.4	21.45	21.22	21.01	2.55	21.32	21.37	21.19	20.98	3.45	21.25	21.28	21.14	20.92
0.77	21.7	21.7	21.33	21.06	1.67	21.4	21.4	21.22	20.99	2.57	21.32	21.34	21.18	20.96	3.46	21.25	21.28	21.14	20.92
0.79	21.7	21.65	21.31	21.06	1.69	21.4	21.4	21.22	20.99	2.58	21.32	21.34	21.18	21.01	3.48	21.25	21.28	21.14	20.92
0.81	21.65	21.65	21.31	21.04	1.71	21.4	21.4	21.24	20.99	2.6	21.32	21.33	21.18	21.01	3.5	21.25	21.28	21.14	20.97
0.83	21.68	21.64	21.33	21.04	1.72	21.44	21.44	21.26	21.03	2.62	21.32	21.32	21.18	21.01	3.52	21.29	21.31	21.17	21
0.84	21.65	21.63	21.29	21.04	1.74	21.42	21.44	21.23	20.98	2.64	21.32	21.32	21.18	21.01	3.54	21.29	21.31	21.17	21
0.86	21.63	21.63	21.29	21.04	1.76	21.4	21.44	21.21	20.98	2.66	21.31	21.32	21.18	21	3.56	21.29	21.31	21.17	21
0.88	21.63	21.59	21.29	21.01	1.78	21.4	21.44	21.21	21.03	2.68	21.29	21.32	21.18	20.94	3.57	21.29	21.31	21.17	20.95
0.9	21.63	21.61	21.32	21.02	1.8	21.4	21.41	21.21	21.02	2.69	21.28	21.32	21.18	20.99	3.59	21.29	21.31	21.17	20.95
0.92	21.61	21.61	21.27	21.02	1.82	21.4	21.4	21.21	21.01	2.71	21.27	21.32	21.18	20.98	3.61	21.29	21.31	21.17	21
0.94	21.64	21.63	21.3	21	1.83	21.4	21.4	21.21	20.98	2.73	21.3	21.34	21.2	20.96	3.63	21.29	21.31	21.17	21

RH=45%, Tair=22°C, Tc=21°C, Q=9.33 L/s

Time (s)	Tray#1 (°C)	Tray#2 (°C)	Tray#3 (°C)	Tray#4 (°C)	Time (s)	Tray#1 (°C)	Tray#2 (°C)	Tray#3 (°C)	Tray#4 (°C)	Time (s)	Tray#1 (°C)	Tray#2 (°C)	Tray#3 (°C)	Tray#4 (°C)	Time (s)	Tray#1 (°C)	Tray#2 (°C)	Tray#3 (°C)	Tray#4 (°C)
3.65	21.29	21.3	21.17	21	4.54	21.28	21.29	21.16	20.99	5.44	21.25	21.28	21.16	20.99	6.34	21.26	21.31	21.19	21
3.67	21.29	21.3	21.17	21	4.56	21.28	21.29	21.16	20.94	5.46	21.24	21.28	21.16	20.99	6.36	21.26	21.31	21.16	20.97
3.68	21.29	21.29	21.17	21	4.58	21.28	21.32	21.16	20.99	5.48	21.27	21.28	21.16	20.99	6.38	21.26	21.31	21.17	20.96
3.7	21.29	21.29	21.17	21	4.6	21.28	21.31	21.16	20.94	5.5	21.24	21.28	21.16	20.94	6.4	21.26	21.3	21.17	21.01
3.72	21.29	21.29	21.17	21	4.62	21.28	21.3	21.16	20.99	5.52	21.25	21.28	21.16	20.99	6.41	21.26	21.3	21.15	20.96
3.74	21.29	21.29	21.17	21	4.64	21.28	21.31	21.16	20.94	5.53	21.24	21.28	21.16	20.99	6.43	21.26	21.3	21.14	20.95
3.76	21.29	21.29	21.17	21	4.65	21.28	21.31	21.16	20.99	5.55	21.24	21.28	21.16	20.99	6.45	21.26	21.27	21.15	20.98
3.78	21.29	21.29	21.17	20.95	4.67	21.28	21.29	21.16	20.99	5.57	21.25	21.28	21.16	20.99	6.47	21.26	21.27	21.15	20.99
3.79	21.29	21.29	21.17	20.95	4.69	21.28	21.28	21.16	20.99	5.59	21.27	21.28	21.16	20.99	6.49	21.26	21.27	21.15	20.98
3.81	21.29	21.29	21.17	21	4.71	21.28	21.29	21.16	20.99	5.61	21.26	21.28	21.16	20.94	6.51	21.26	21.27	21.14	20.97
3.83	21.29	21.29	21.17	21	4.73	21.28	21.29	21.16	20.99	5.63	21.28	21.28	21.16	20.94	6.52	21.26	21.27	21.15	20.97
3.85	21.29	21.29	21.17	20.95	4.75	21.28	21.29	21.16	20.99	5.64	21.27	21.28	21.16	20.99	6.54	21.26	21.28	21.14	20.97
3.87	21.29	21.29	21.16	21	4.76	21.28	21.28	21.16	20.99	5.66	21.26	21.28	21.16	20.99	6.56	21.26	21.28	21.14	20.94
3.89	21.26	21.29	21.16	20.95	4.78	21.28	21.28	21.16	20.99	5.68	21.25	21.28	21.16	20.99	6.58	21.26	21.27	21.14	20.92
3.9	21.27	21.29	21.15	20.95	4.8	21.24	21.25	21.12	20.9	5.7	21.23	21.28	21.16	20.94	6.6	21.26	21.27	21.14	20.97
3.92	21.26	21.29	21.17	20.98	4.82	21.28	21.29	21.16	20.99	5.72	21.23	21.28	21.16	20.99	6.62	21.26	21.27	21.14	20.96
3.94	21.25	21.29	21.15	20.97	4.84	21.28	21.3	21.16	20.99	5.74	21.24	21.28	21.16	20.94	6.63	21.26	21.26	21.14	20.92
3.96	21.27	21.29	21.16	20.96	4.86	21.28	21.3	21.16	20.94	5.75	21.24	21.28	21.16	20.99	6.65	21.26	21.26	21.14	20.92
3.98	21.29	21.29	21.17	20.94	4.87	21.28	21.29	21.16	20.99	5.77	21.24	21.28	21.16	20.99	6.67	21.26	21.26	21.14	20.92
4	21.25	21.29	21.15	20.94	4.89	21.28	21.28	21.16	20.99	5.79	21.24	21.28	21.16	20.94	6.69	21.26	21.26	21.14	20.97
4.01	21.26	21.29	21.15	20.99	4.91	21.28	21.28	21.16	20.99	5.81	21.23	21.28	21.16	20.94	6.71	21.26	21.26	21.14	20.97
4.03	21.25	21.29	21.14	20.96	4.93	21.28	21.28	21.16	20.94	5.83	21.25	21.28	21.16	20.94	6.73	21.26	21.26	21.14	20.97
4.05	21.25	21.29	21.15	20.99	4.95	21.28	21.28	21.16	20.99	5.85	21.24	21.28	21.16	20.99	6.74	21.26	21.26	21.14	20.92
4.07	21.25	21.29	21.14	20.97	4.97	21.28	21.28	21.16	20.99	5.86	21.23	21.28	21.16	20.99	6.76	21.26	21.26	21.14	20.92
4.09	21.24	21.29	21.13	20.96	4.98	21.28	21.28	21.16	20.94	5.88	21.23	21.28	21.16	20.99	6.78	21.26	21.26	21.14	20.97
4.11	21.24	21.29	21.14	20.97	5	21.28	21.29	21.16	20.94	5.9	21.24	21.28	21.16	20.99	6.8	21.26	21.26	21.14	20.97
4.12	21.24	21.29	21.12	20.97	5.02	21.28	21.28	21.16	20.94	5.92	21.23	21.28	21.16	20.99	6.82	21.26	21.26	21.14	20.96
4.14	21.24	21.29	21.13	20.96	5.04	21.28	21.28	21.16	20.99	5.94	21.23	21.28	21.16	20.99	6.84	21.26	21.26	21.14	20.92
4.16	21.24	21.29	21.14	20.95	5.06	21.28	21.28	21.16	20.99	5.96	21.25	21.28	21.16	20.99	6.85	21.26	21.26	21.14	20.97
4.18	21.24	21.29	21.12	20.92	5.08	21.28	21.28	21.16	20.94	5.97	21.24	21.28	21.16	20.99	6.87	21.26	21.26	21.14	20.97
4.2	21.24	21.29	21.12	20.91	5.09	21.28	21.28	21.16	20.94	5.99	21.24	21.28	21.16	20.94	6.89	21.25	21.26	21.14	20.97
4.21	21.24	21.29	21.13	20.95	5.11	21.28	21.28	21.16	20.94	6.01	21.24	21.28	21.16	20.94	6.91	21.26	21.26	21.14	20.97
4.23	21.24	21.29	21.14	20.96	5.13	21.27	21.28	21.16	20.94	6.03	21.23	21.28	21.16	20.94	6.93	21.26	21.26	21.14	20.97
4.25	21.24	21.29	21.12	20.95	5.15	21.28	21.28	21.16	20.99	6.05	21.23	21.28	21.16	20.99	6.95	21.26	21.26	21.14	20.92
4.27	21.24	21.29	21.12	20.9	5.17	21.28	21.28	21.16	20.99	6.07	21.23	21.28	21.16	20.99	6.96	21.29	21.3	21.18	21.01
4.29	21.24	21.29	21.12	20.95	5.19	21.28	21.28	21.16	20.94	6.08	21.23	21.28	21.16	20.99	6.98	21.29	21.3	21.18	21.01
4.31	21.24	21.29	21.12	20.95	5.2	21.28	21.28	21.16	20.94	6.1	21.23	21.28	21.16	20.99	7	21.27	21.3	21.18	21.01
4.32	21.24	21.29	21.12	20.95	5.22	21.28	21.28	21.16	20.94	6.12	21.23	21.28	21.16	20.98	7.02	21.28	21.3	21.18	21.01
4.34	21.24	21.29	21.12	20.9	5.24	21.28	21.28	21.16	20.99	6.14	21.23	21.28	21.16	20.99	7.04	21.27	21.3	21.18	20.96
4.36	21.24	21.29	21.12	21	5.26	21.28	21.28	21.16	20.99	6.16	21.24	21.28	21.16	20.98	7.06	21.25	21.3	21.18	21.01
4.38	21.24	21.29	21.12	20.95	5.28	21.27	21.28	21.16	20.94	6.18	21.23	21.28	21.16	20.94	7.07	21.25	21.3	21.18	21.01
4.4	21.24	21.29	21.12	20.91	5.3	21.27	21.28	21.16	20.99	6.19	21.23	21.28	21.16	20.94	7.09	21.26	21.3	21.18	21.01
4.42	21.28	21.33	21.16	20.99	5.31	21.25	21.28	21.16	20.99	6.21	21.23	21.28	21.16	20.94	7.11	21.27	21.3	21.18	21.01
4.43	21.28	21.33	21.16	20.99	5.33	21.25	21.28	21.16	20.99	6.23	21.23	21.28	21.16	20.94	7.13	21.25	21.3	21.18	20.96
4.45	21.28	21.33	21.16	20.99	5.35	21.24	21.28	21.16	20.99	6.25	21.23	21.28	21.16	20.99	7.15	21.25	21.3	21.18	21.01
4.47	21.28	21.31	21.16	20.99	5.37	21.24	21.28	21.16	20.99	6.27	21.23	21.28	21.15	20.99	7.17	21.26	21.3	21.18	21.01
4.49	21.28	21.31	21.16	20.99	5.39	21.27	21.28	21.16	20.99	6.29	21.23	21.28	21.14	20.99	7.18	21.25	21.3	21.18	21.01
4.51	21.28	21.31	21.16	20.99	5.41	21.27	21.28	21.16	20.94	6.3	21.23	21.28	21.15	20.98	7.2	21.25	21.3	21.18	21.01
4.53	21.28	21.29	21.16	20.99	5.42	21.26	21.28	21.16	20.94	6.32	21.23	21.28	21.14	20.97	7.22	21.25	21.3	21.18	21.01

RH=65%, Tair=22°C, Tc=21°C, Q=9.33 L/s

Time (s)	Tray#1 (°C)	Tray#2 (°C)	Tray#3 (°C)	Tray#4 (°C)	Time (s)	Tray#1 (°C)	Tray#2 (°C)	Tray#3 (°C)	Tray#4 (°C)	Time (s)	Tray#1 (°C)	Tray#2 (°C)	Tray#3 (°C)	Tray#4 (°C)	Time (s)	Tray#1 (°C)	Tray#2 (°C)	Tray#3 (°C)	Tray#4 (°C)
0	21.545	21.6	21.4	20.42	0.94	20.665	20.65	20.59	20.28	1.84	20.58	20.59	20.51	20.33	2.73	20.615	20.59	20.515	20.33
0.06	21.59	21.37	21.1	20.41	0.96	20.67	20.64	20.57	20.31	1.85	20.575	20.58	20.5	20.3	2.75	20.615	20.59	20.515	20.33
0.07	21.54	21.36	21.445	20.34	0.97	20.645	20.67	20.565	20.28	1.87	20.615	20.55	20.48	20.3	2.77	20.615	20.59	20.515	20.33
0.09	21.495	21.3	21.49	20.32	0.99	20.64	20.63	20.57	20.29	1.89	20.615	20.58	20.475	20.24	2.79	20.615	20.59	20.515	20.33
0.11	21.45	21.32	21.44	20.35	1.01	20.65	20.62	20.545	20.29	1.91	20.615	20.58	20.515	20.34	2.81	20.61	20.59	20.515	20.33
0.13	21.35	21.31	21.395	20.35	1.03	20.625	20.65	20.54	20.29	1.93	20.595	20.58	20.515	20.28	2.83	20.605	20.59	20.515	20.33
0.15	21.325	21.26	21.35	20.33	1.05	20.625	20.62	20.55	20.29	1.95	20.62	20.58	20.515	20.28	2.84	20.62	20.59	20.51	20.36
0.17	21.295	21.24	21.25	20.37	1.07	20.635	20.6	20.525	20.3	1.96	20.605	20.61	20.495	20.35	2.86	20.62	20.62	20.505	20.36
0.18	21.25	21.23	21.225	20.32	1.08	20.63	20.63	20.525	20.26	1.98	20.6	20.61	20.52	20.32	2.88	20.625	20.62	20.52	20.32
0.2	21.19	21.18	21.195	20.34	1.1	20.65	20.63	20.535	20.26	2	20.595	20.57	20.505	20.32	2.9	20.625	20.62	20.52	20.31
0.22	21.13	21.15	21.15	20.29	1.12	20.65	20.62	20.53	20.29	2.02	20.595	20.56	20.5	20.36	2.92	20.62	20.62	20.525	20.36
0.24	21.105	21.1	21.09	20.32	1.14	20.63	20.61	20.55	20.27	2.04	20.59	20.56	20.495	20.29	2.94	20.62	20.62	20.525	20.36
0.26	21.085	21.12	21.03	20.33	1.16	20.635	20.61	20.55	20.31	2.06	20.615	20.56	20.495	20.35	2.96	20.615	20.62	20.52	20.36
0.28	21.06	21.11	21.005	20.3	1.18	20.63	20.64	20.53	20.28	2.07	20.61	20.59	20.49	20.32	2.97	20.625	20.62	20.52	20.32
0.29	21.05	21.1	20.985	20.29	1.19	20.63	20.6	20.535	20.28	2.09	20.61	20.59	20.515	20.29	2.99	20.605	20.62	20.515	20.31
0.31	21.05	21.05	20.96	20.32	1.21	20.645	20.59	20.53	20.31	2.11	20.6	20.59	20.51	20.3	3.01	20.6	20.62	20.525	20.32
0.33	21.035	21.03	20.95	20.35	1.23	20.63	20.63	20.53	20.29	2.13	20.595	20.59	20.51	20.3	3.03	20.595	20.61	20.505	20.31
0.35	20.985	21.01	20.95	20.34	1.25	20.625	20.63	20.545	20.26	2.15	20.585	20.57	20.5	20.3	3.05	20.595	20.59	20.5	20.31
0.37	20.965	21	20.935	20.33	1.27	20.62	20.59	20.53	20.3	2.17	20.625	20.56	20.495	20.34	3.07	20.595	20.58	20.495	20.31
0.39	20.92	20.99	20.885	20.33	1.29	20.645	20.59	20.525	20.28	2.18	20.625	20.58	20.485	20.34	3.08	20.635	20.59	20.495	20.3
0.4	20.94	20.94	20.865	20.32	1.3	20.63	20.61	20.52	20.25	2.2	20.625	20.58	20.525	20.34	3.1	20.635	20.64	20.495	20.3
0.42	20.895	20.92	20.82	20.31	1.32	20.62	20.61	20.545	20.32	2.22	20.62	20.58	20.525	20.34	3.12	20.585	20.63	20.535	20.3
0.44	20.875	20.92	20.84	20.34	1.34	20.64	20.61	20.53	20.32	2.24	20.605	20.58	20.525	20.34	3.14	20.635	20.58	20.535	20.35
0.46	20.845	20.9	20.795	20.3	1.36	20.635	20.63	20.52	20.31	2.26	20.61	20.58	20.52	20.34	3.16	20.635	20.62	20.485	20.35
0.48	20.855	20.85	20.775	20.34	1.38	20.63	20.59	20.54	20.33	2.28	20.625	20.58	20.505	20.31	3.18	20.635	20.63	20.535	20.35
0.5	20.84	20.88	20.745	20.3	1.4	20.615	20.59	20.535	20.31	2.29	20.63	20.61	20.51	20.28	3.19	20.635	20.62	20.535	20.35
0.51	20.835	20.86	20.755	20.3	1.41	20.63	20.59	20.53	20.33	2.31	20.63	20.61	20.525	20.33	3.21	20.635	20.62	20.535	20.35
0.53	20.815	20.83	20.74	20.34	1.43	20.615	20.62	20.515	20.29	2.33	20.625	20.61	20.53	20.32	3.23	20.635	20.62	20.535	20.35
0.55	20.805	20.85	20.735	20.33	1.45	20.61	20.58	20.53	20.32	2.35	20.61	20.61	20.53	20.32	3.25	20.635	20.62	20.535	20.35
0.57	20.765	20.8	20.715	20.31	1.47	20.61	20.57	20.515	20.27	2.37	20.605	20.59	20.525	20.32	3.27	20.635	20.62	20.535	20.35
0.59	20.78	20.8	20.705	20.3	1.49	20.645	20.6	20.51	20.29	2.39	20.605	20.58	20.51	20.32	3.29	20.635	20.62	20.535	20.3
0.61	20.745	20.78	20.665	20.3	1.51	20.625	20.61	20.51	20.27	2.4	20.605	20.56	20.505	20.32	3.3	20.635	20.62	20.535	20.3
0.63	20.765	20.78	20.68	20.31	1.52	20.61	20.61	20.545	20.34	2.42	20.605	20.56	20.505	20.32	3.32	20.635	20.62	20.535	20.35
0.64	20.745	20.77	20.645	20.31	1.54	20.63	20.6	20.525	20.36	2.44	20.635	20.56	20.505	20.35	3.34	20.635	20.62	20.535	20.35
0.66	20.765	20.77	20.665	20.34	1.56	20.63	20.6	20.51	20.36	2.46	20.635	20.59	20.505	20.35	3.36	20.635	20.62	20.535	20.35
0.68	20.745	20.75	20.645	20.29	1.58	20.615	20.6	20.53	20.35	2.48	20.635	20.59	20.535	20.35	3.38	20.63	20.62	20.535	20.35
0.7	20.75	20.78	20.665	20.27	1.6	20.61	20.6	20.53	20.34	2.5	20.635	20.59	20.535	20.3	3.4	20.63	20.62	20.535	20.35
0.72	20.71	20.73	20.645	20.32	1.62	20.625	20.6	20.515	20.33	2.51	20.63	20.59	20.535	20.35	3.41	20.635	20.62	20.53	20.35
0.73	20.735	20.73	20.65	20.31	1.63	20.61	20.6	20.51	20.32	2.53	20.615	20.59	20.535	20.35	3.43	20.63	20.62	20.53	20.35
0.75	20.7	20.71	20.61	20.3	1.65	20.61	20.6	20.525	20.37	2.55	20.61	20.59	20.53	20.35	3.45	20.62	20.62	20.535	20.35
0.77	20.715	20.71	20.635	20.3	1.67	20.605	20.58	20.51	20.32	2.57	20.61	20.59	20.515	20.34	3.47	20.635	20.62	20.53	20.35
0.79	20.69	20.7	20.6	20.29	1.69	20.635	20.58	20.51	20.31	2.59	20.61	20.59	20.51	20.31	3.49	20.635	20.62	20.52	20.3
0.81	20.665	20.69	20.615	20.28	1.71	20.615	20.61	20.505	20.3	2.61	20.6	20.59	20.51	20.3	3.51	20.635	20.62	20.535	20.3
0.83	20.69	20.69	20.59	20.29	1.73	20.605	20.61	20.535	20.32	2.62	20.62	20.59	20.51	20.33	3.52	20.625	20.62	20.535	20.35
0.85	20.65	20.67	20.565	20.3	1.74	20.595	20.59	20.515	20.33	2.64	20.615	20.62	20.5	20.33	3.54	20.63	20.62	20.535	20.35
0.86	20.675	20.67	20.59	20.29	1.76	20.625	20.57	20.505	20.36	2.66	20.615	20.6	20.52	20.33	3.56	20.635	20.62	20.525	20.35
0.88	20.67	20.65	20.55	20.28	1.78	20.62	20.59	20.495	20.35	2.68	20.62	20.59	20.515	20.31	3.58	20.625	20.62	20.53	20.35
0.9	20.69	20.65	20.575	20.27	1.8	20.61	20.59	20.525	20.34	2.7	20.615	20.61	20.515	20.28	3.6	20.625	20.62	20.535	20.35
0.92	20.67	20.69	20.57	20.31	1.82	20.6	20.59	20.52	20.33	2.72	20.615	20.61	20.52	20.33	3.62	20.63	20.62	20.525	20.35

RH=65%, Tair=22°C, Tc=21°C, Q=9.33 L/s

Time (s)	Tray#1 (°C)	Tray#2 (°C)	Tray#3 (°C)	Tray#4 (°C)	Time (s)	Tray#1 (°C)	Tray#2 (°C)	Tray#3 (°C)	Tray#4 (°C)	Time (s)	Tray#1 (°C)	Tray#2 (°C)	Tray#3 (°C)	Tray#4 (°C)	Time (s)	Tray#1 (°C)	Tray#2 (°C)	Tray#3 (°C)	Tray#4 (°C)
3.63	20.63	20.62	20.525	20.35	4.53	20.625	20.63	20.535	20.36	5.43	20.625	20.64	20.525	20.39	6.33	20.635	20.63	20.485	20.4
3.65	20.62	20.62	20.53	20.35	4.55	20.62	20.63	20.525	20.36	5.45	20.625	20.61	20.53	20.39	6.35	20.635	20.64	20.535	20.4
3.67	20.605	20.62	20.53	20.25	4.57	20.615	20.63	20.525	20.36	5.47	20.625	20.61	20.525	20.39	6.37	20.635	20.61	20.535	20.4
3.69	20.635	20.62	20.52	20.3	4.59	20.6	20.63	20.52	20.36	5.49	20.625	20.6	20.525	20.34	6.39	20.635	20.62	20.535	20.4
3.71	20.585	20.62	20.505	20.25	4.61	20.61	20.63	20.515	20.32	5.51	20.625	20.6	20.525	20.34	6.4	20.635	20.61	20.535	20.4
3.73	20.635	20.57	20.535	20.35	4.62	20.605	20.63	20.5	20.32	5.52	20.655	20.6	20.525	20.42	6.42	20.63	20.62	20.535	20.4
3.74	20.635	20.62	20.485	20.35	4.64	20.6	20.63	20.51	20.36	5.54	20.655	20.63	20.525	20.38	6.44	20.62	20.61	20.535	20.4
3.76	20.635	20.62	20.535	20.35	4.66	20.64	20.63	20.505	20.41	5.56	20.655	20.64	20.555	20.37	6.46	20.625	20.61	20.53	20.4
3.78	20.585	20.62	20.535	20.3	4.68	20.64	20.66	20.5	20.38	5.58	20.655	20.64	20.555	20.42	6.48	20.625	20.61	20.52	20.35
3.8	20.635	20.57	20.535	20.35	4.7	20.595	20.66	20.54	20.31	5.6	20.65	20.64	20.555	20.42	6.5	20.635	20.61	20.525	20.35
3.82	20.585	20.62	20.485	20.3	4.72	20.595	20.59	20.54	20.36	5.62	20.65	20.64	20.555	20.41	6.51	20.58	20.61	20.525	20.35
3.84	20.635	20.57	20.535	20.35	4.73	20.64	20.58	20.495	20.39	5.63	20.65	20.63	20.55	20.41	6.53	20.635	20.56	20.535	20.4
3.85	20.635	20.62	20.485	20.31	4.75	20.64	20.62	20.495	20.39	5.65	20.65	20.64	20.55	20.41	6.55	20.585	20.62	20.48	20.35
3.87	20.635	20.62	20.535	20.3	4.77	20.64	20.62	20.54	20.37	5.67	20.64	20.63	20.55	20.41	6.57	20.58	20.56	20.535	20.35
3.89	20.635	20.62	20.535	20.3	4.79	20.64	20.62	20.54	20.36	5.69	20.635	20.63	20.55	20.35	6.59	20.63	20.56	20.485	20.4
3.91	20.635	20.62	20.535	20.36	4.81	20.595	20.63	20.54	20.29	5.71	20.58	20.63	20.54	20.33	6.61	20.615	20.61	20.48	20.4
3.93	20.63	20.62	20.535	20.35	4.83	20.59	20.58	20.54	20.31	5.73	20.585	20.58	20.535	20.34	6.62	20.62	20.61	20.53	20.4
3.95	20.625	20.62	20.535	20.35	4.84	20.59	20.57	20.495	20.32	5.74	20.585	20.58	20.48	20.32	6.64	20.615	20.61	20.515	20.4
3.96	20.58	20.62	20.53	20.3	4.86	20.635	20.57	20.49	20.37	5.76	20.63	20.58	20.485	20.4	6.66	20.63	20.61	20.52	20.4
3.98	20.58	20.57	20.525	20.31	4.88	20.635	20.62	20.49	20.31	5.78	20.63	20.63	20.485	20.38	6.68	20.63	20.61	20.515	20.35
4	20.625	20.57	20.48	20.35	4.9	20.62	20.62	20.535	20.31	5.8	20.59	20.63	20.53	20.36	6.7	20.63	20.61	20.53	20.35
4.02	20.615	20.62	20.48	20.35	4.92	20.615	20.62	20.535	20.36	5.82	20.63	20.58	20.53	20.38	6.72	20.63	20.61	20.53	20.4
4.04	20.635	20.62	20.525	20.35	4.94	20.615	20.62	20.52	20.36	5.84	20.63	20.63	20.49	20.37	6.74	20.63	20.61	20.53	20.4
4.06	20.635	20.62	20.515	20.31	4.95	20.61	20.62	20.515	20.36	5.85	20.62	20.63	20.53	20.37	6.75	20.62	20.61	20.53	20.4
4.07	20.635	20.62	20.535	20.35	4.97	20.605	20.62	20.515	20.36	5.87	20.62	20.63	20.53	20.37	6.77	20.63	20.61	20.53	20.4
4.09	20.635	20.62	20.535	20.3	4.99	20.6	20.62	20.51	20.29	5.89	20.62	20.63	20.52	20.32	6.79	20.63	20.61	20.52	20.4
4.11	20.615	20.62	20.535	20.35	5.01	20.645	20.6	20.505	20.39	5.91	20.62	20.63	20.52	20.37	6.81	20.625	20.62	20.53	20.4
4.13	20.625	20.62	20.535	20.35	5.03	20.63	20.65	20.5	20.39	5.93	20.61	20.63	20.52	20.31	6.83	20.625	20.61	20.53	20.4
4.15	20.615	20.62	20.515	20.35	5.05	20.635	20.65	20.545	20.39	5.95	20.63	20.61	20.52	20.38	6.85	20.62	20.61	20.525	20.4
4.17	20.62	20.62	20.525	20.35	5.07	20.635	20.65	20.53	20.39	5.96	20.625	20.63	20.51	20.37	6.86	20.62	20.61	20.525	20.4
4.18	20.61	20.62	20.515	20.35	5.08	20.625	20.65	20.535	20.34	5.98	20.62	20.63	20.53	20.37	6.88	20.63	20.57	20.52	20.35
4.2	20.56	20.62	20.52	20.3	5.1	20.625	20.65	20.535	20.34	6	20.605	20.63	20.525	20.37	6.9	20.635	20.61	20.52	20.35
4.22	20.56	20.57	20.51	20.3	5.12	20.625	20.65	20.525	20.39	6.02	20.56	20.63	20.52	20.32	6.92	20.64	20.62	20.53	20.4
4.24	20.61	20.57	20.46	20.3	5.14	20.575	20.65	20.525	20.34	6.04	20.615	20.58	20.505	20.37	6.94	20.64	20.62	20.535	20.4
4.26	20.59	20.62	20.46	20.33	5.16	20.625	20.6	20.525	20.39	6.06	20.61	20.63	20.46	20.37	6.96	20.64	20.61	20.54	20.4
4.28	20.63	20.6	20.51	20.38	5.18	20.59	20.65	20.475	20.29	6.07	20.57	20.63	20.515	20.37	6.97	20.63	20.61	20.54	20.4
4.29	20.63	20.65	20.49	20.33	5.19	20.625	20.6	20.525	20.39	6.09	20.635	20.58	20.51	20.35	6.99	20.635	20.61	20.54	20.4
4.31	20.625	20.65	20.53	20.38	5.21	20.625	20.65	20.49	20.39	6.11	20.645	20.66	20.47	20.35	7.01	20.63	20.62	20.53	20.4
4.33	20.62	20.65	20.53	20.38	5.23	20.625	20.65	20.525	20.39	6.13	20.595	20.66	20.535	20.3	7.03	20.63	20.61	20.535	20.4
4.35	20.62	20.64	20.525	20.38	5.25	20.625	20.65	20.525	20.39	6.15	20.64	20.61	20.545	20.4	7.05	20.635	20.61	20.53	20.4
4.37	20.565	20.63	20.52	20.32	5.27	20.625	20.63	20.525	20.39	6.17	20.64	20.66	20.495	20.4					
4.39	20.565	20.56	20.52	20.31	5.29	20.625	20.65	20.525	20.34	6.18	20.635	20.66	20.54	20.4					
4.4	20.565	20.55	20.465	20.29	5.3	20.575	20.65	20.525	20.29	6.2	20.64	20.64	20.54	20.4					
4.42	20.565	20.56	20.465	20.27	5.32	20.625	20.58	20.525	20.39	6.22	20.635	20.64	20.535	20.4					
4.44	20.615	20.55	20.465	20.34	5.34	20.625	20.61	20.475	20.39	6.24	20.635	20.64	20.54	20.4					
4.46	20.645	20.6	20.465	20.36	5.36	20.625	20.61	20.525	20.34	6.26	20.635	20.62	20.535	20.4					
4.48	20.635	20.63	20.515	20.35	5.38	20.625	20.62	20.525	20.39	6.28	20.585	20.62	20.535	20.37					
4.5	20.635	20.63	20.545	20.32	5.4	20.625	20.63	20.525	20.39	6.29	20.585	20.59	20.535	20.3					
4.51	20.625	20.63	20.535	20.36	5.41	20.63	20.6	20.525	20.39	6.31	20.635	20.59	20.485	20.35					

RH=80%, Tair=22°C, Tc=21°C, Q=9.17L/s

Time (s)	Tray#1 (°C)	Tray#2 (°C)	Tray#3 (°C)	Tray#4 (°C)	Time (s)	Tray#1 (°C)	Tray#2 (°C)	Tray#3 (°C)	Tray#4 (°C)	Time (s)	Tray#1 (°C)	Tray#2 (°C)	Tray#3 (°C)	Tray#4 (°C)	Time (s)	Tray#1 (°C)	Tray#2 (°C)	Tray#3 (°C)	Tray#4 (°C)
0	22.27	21.93	22	20.88	0.93	21.15	21.28	20.95	20.71	1.83	20.98	21.03	20.87	20.62	2.73	20.94	20.97	20.83	20.65
0.05	22.19	21.89	21.8	20.8	0.95	21.13	21.23	20.97	20.67	1.85	21.02	21.07	20.86	20.66	2.74	20.94	20.95	20.83	20.65
0.07	22.13	21.87	21.6	20.77	0.96	21.16	21.26	20.93	20.7	1.86	20.99	21.07	20.83	20.66	2.76	20.94	20.94	20.83	20.65
0.08	22.09	21.9	21.4	20.72	0.98	21.13	21.22	20.93	20.7	1.88	20.99	21.04	20.83	20.64	2.78	20.93	20.94	20.83	20.65
0.1	22.04	21.94	21.35	20.79	1	21.11	21.21	20.96	20.69	1.9	20.98	21.03	20.83	20.64	2.8	20.91	20.94	20.83	20.65
0.12	21.94	21.89	21.31	20.75	1.02	21.11	21.21	20.93	20.65	1.92	20.97	21.03	20.83	20.66	2.82	20.94	20.97	20.83	20.68
0.14	21.87	21.92	21.27	20.77	1.04	21.13	21.19	20.92	20.68	1.94	20.97	21.03	20.87	20.66	2.84	20.94	20.97	20.83	20.68
0.16	21.85	21.9	21.22	20.77	1.06	21.09	21.19	20.95	20.68	1.96	21	21.06	20.87	20.67	2.85	20.94	20.97	20.8	20.68
0.18	21.76	21.85	21.2	20.75	1.07	21.12	21.22	20.91	20.66	1.97	21	21.06	20.87	20.67	2.87	20.94	20.97	20.78	20.68
0.19	21.73	21.83	21.2	20.78	1.09	21.12	21.21	20.9	20.62	1.99	20.98	21.02	20.85	20.67	2.89	20.94	20.97	20.78	20.63
0.21	21.71	21.82	21.19	20.76	1.11	21.1	21.17	20.9	20.66	2.01	20.96	21.01	20.83	20.67	2.91	20.94	20.97	20.81	20.68
0.23	21.66	21.81	21.17	20.76	1.13	21.07	21.17	20.92	20.66	2.03	20.96	21.01	20.82	20.67	2.93	20.94	20.97	20.81	20.68
0.25	21.65	21.8	21.15	20.75	1.15	21.11	21.2	20.89	20.7	2.05	20.96	21.01	20.85	20.67	2.95	20.94	20.97	20.81	20.66
0.27	21.63	21.78	21.15	20.74	1.17	21.11	21.16	20.91	20.68	2.07	20.96	21.01	20.85	20.67	2.96	20.94	20.95	20.81	20.65
0.29	21.61	21.76	21.13	20.74	1.18	21.07	21.16	20.91	20.66	2.08	20.99	21.04	20.85	20.65	2.98	20.94	20.94	20.81	20.64
0.3	21.56	21.71	21.14	20.75	1.2	21.06	21.16	20.91	20.65	2.1	20.94	20.99	20.85	20.6	3	20.94	20.92	20.81	20.64
0.32	21.54	21.74	21.11	20.78	1.22	21.09	21.14	20.86	20.68	2.12	20.99	21.01	20.85	20.69	3.02	20.94	20.92	20.81	20.64
0.34	21.51	21.69	21.13	20.73	1.24	21.09	21.14	20.9	20.68	2.14	20.96	20.99	20.85	20.66	3.04	20.94	20.92	20.81	20.63
0.36	21.52	21.72	21.12	20.76	1.26	21.04	21.14	20.9	20.64	2.16	20.94	20.99	20.83	20.65	3.06	20.97	20.95	20.81	20.66
0.38	21.47	21.67	21.13	20.72	1.28	21.07	21.17	20.9	20.62	2.18	20.94	20.99	20.83	20.65	3.07	20.97	20.95	20.81	20.65
0.4	21.46	21.67	21.1	20.75	1.29	21.07	21.13	20.86	20.61	2.19	20.89	20.94	20.78	20.6	3.09	20.97	20.95	20.8	20.61
0.41	21.45	21.62	21.12	20.74	1.31	21.07	21.12	20.88	20.66	2.21	20.94	20.99	20.83	20.65	3.11	20.95	20.95	20.78	20.66
0.43	21.44	21.64	21.08	20.73	1.33	21.07	21.12	20.88	20.66	2.23	20.97	21.02	20.83	20.68	3.13	20.94	20.95	20.78	20.66
0.45	21.39	21.59	21.06	20.73	1.35	21.06	21.15	20.88	20.69	2.25	20.97	21.02	20.83	20.68	3.15	20.92	20.95	20.82	20.66
0.47	21.42	21.57	21.06	20.72	1.37	21.05	21.13	20.91	20.68	2.27	20.97	21.02	20.83	20.68	3.17	20.92	20.95	20.82	20.66
0.49	21.4	21.56	21.06	20.7	1.39	21.05	21.1	20.89	20.64	2.29	20.97	21.01	20.78	20.63	3.18	20.92	20.95	20.8	20.66
0.51	21.4	21.55	21.05	20.74	1.4	21.05	21.1	20.86	20.64	2.3	20.97	20.97	20.83	20.68	3.2	20.92	20.95	20.79	20.66
0.52	21.41	21.53	21.03	20.75	1.42	21.03	21.1	20.86	20.64	2.32	20.96	20.97	20.84	20.68	3.22	20.92	20.95	20.79	20.66
0.54	21.38	21.52	21.06	20.73	1.44	21.03	21.13	20.89	20.67	2.34	20.94	20.97	20.84	20.65	3.24	20.92	20.95	20.79	20.66
0.56	21.36	21.51	21.06	20.76	1.46	21.03	21.1	20.89	20.67	2.36	20.92	20.97	20.81	20.63	3.26	20.92	20.95	20.79	20.66
0.58	21.31	21.46	21.04	20.71	1.48	21.03	21.08	20.86	20.62	2.38	20.92	20.97	20.81	20.63	3.28	20.92	20.95	20.79	20.63
0.6	21.34	21.49	21.04	20.74	1.5	21.03	21.08	20.85	20.62	2.4	20.95	21	20.81	20.66	3.29	20.92	20.92	20.79	20.61
0.62	21.29	21.44	21.02	20.74	1.51	21.03	21.08	20.84	20.63	2.41	20.95	21	20.81	20.66	3.31	20.92	20.92	20.79	20.66
0.63	21.25	21.39	21.02	20.69	1.53	21.03	21.12	20.87	20.66	2.43	20.95	21	20.81	20.66	3.33	20.92	20.92	20.79	20.66
0.65	21.28	21.43	21.05	20.73	1.55	21.02	21.08	20.87	20.66	2.45	20.95	21	20.81	20.66	3.35	20.92	20.9	20.79	20.66
0.67	21.27	21.41	21.01	20.72	1.57	21.02	21.08	20.87	20.66	2.47	20.95	20.98	20.81	20.66	3.37	20.92	20.91	20.79	20.65
0.69	21.26	21.41	21.04	20.67	1.59	21.02	21.07	20.87	20.66	2.49	20.95	20.98	20.84	20.61	3.39	20.92	20.9	20.79	20.66
0.71	21.24	21.36	20.99	20.71	1.61	21.02	21.07	20.84	20.66	2.51	20.95	20.95	20.83	20.66	3.4	20.9	20.9	20.79	20.63
0.73	21.25	21.37	20.99	20.74	1.63	21	21.07	20.87	20.63	2.52	20.95	20.95	20.8	20.66	3.42	20.88	20.9	20.79	20.63
0.74	21.22	21.35	21.02	20.7	1.64	21.01	21.1	20.86	20.66	2.54	20.95	20.95	20.82	20.66	3.44	20.9	20.9	20.79	20.61
0.76	21.23	21.37	21.01	20.72	1.66	21	21.06	20.86	20.64	2.56	20.94	20.95	20.81	20.66	3.46	20.88	20.9	20.79	20.61
0.78	21.23	21.33	21.01	20.72	1.68	21	21.06	20.86	20.6	2.58	20.97	20.99	20.81	20.7	3.48	20.95	20.94	20.78	20.62
0.8	21.18	21.33	20.97	20.68	1.7	21	21.05	20.86	20.59	2.6	20.94	20.99	20.79	20.68	3.5	20.91	20.94	20.78	20.61
0.82	21.21	21.31	20.99	20.7	1.72	21	21.05	20.83	20.64	2.62	20.94	20.99	20.8	20.66	3.51	20.91	20.94	20.76	20.65
0.84	21.16	21.31	20.99	20.7	1.74	21.03	21.08	20.84	20.67	2.63	20.94	20.99	20.79	20.66	3.53	20.91	20.94	20.75	20.65
0.85	21.16	21.26	20.97	20.7	1.75	21	21.08	20.84	20.67	2.65	20.94	20.99	20.79	20.65	3.55	20.91	20.94	20.82	20.65
0.87	21.19	21.29	20.97	20.68	1.77	20.98	21.04	20.84	20.65	2.67	20.94	20.99	20.83	20.65	3.57	20.91	20.94	20.83	20.65
0.89	21.14	21.25	20.95	20.63	1.79	20.98	21.03	20.84	20.65	2.69	20.94	20.99	20.83	20.61	3.59	20.91	20.91	20.8	20.65
0.91	21.18	21.28	20.95	20.72	1.81	20.98	21.03	20.84	20.62	2.71	20.94	20.98	20.83	20.65	3.61	20.91	20.94	20.81	20.65

RH=80%, Tair=22°C, Tc=21°C, Q=9.17 L/s

Time (s)	Tray#1 (°C)	Tray#2 (°C)	Tray#3 (°C)	Tray#4 (°C)	Time (s)	Tray#1 (°C)	Tray#2 (°C)	Tray#3 (°C)	Tray#4 (°C)	Time (s)	Tray#1 (°C)	Tray#2 (°C)	Tray#3 (°C)	Tray#4 (°C)	Time (s)	Tray#1 (°C)	Tray#2 (°C)	Tray#3 (°C)	Tray#4 (°C)
3.62	20.91	20.91	20.78	20.65	4.52	20.8	20.85	20.71	20.58	5.42	20.8	20.83	20.69	20.58	6.32	20.86	20.91	20.74	20.64
3.64	20.86	20.87	20.78	20.6	4.54	20.8	20.85	20.71	20.58	5.44	20.79	20.83	20.74	20.58	6.34	20.86	20.91	20.73	20.6
3.66	20.91	20.9	20.78	20.65	4.56	20.8	20.85	20.76	20.58	5.46	20.79	20.83	20.69	20.57	6.36	20.81	20.86	20.77	20.6
3.68	20.91	20.91	20.78	20.6	4.58	20.8	20.85	20.71	20.58	5.48	20.83	20.88	20.69	20.57	6.38	20.86	20.91	20.75	20.64
3.7	20.91	20.89	20.78	20.6	4.6	20.8	20.85	20.7	20.58	5.5	20.83	20.88	20.69	20.56	6.4	20.86	20.91	20.77	20.64
3.72	20.86	20.87	20.78	20.6	4.62	20.84	20.9	20.67	20.63	5.51	20.83	20.88	20.69	20.61	6.41	20.86	20.91	20.77	20.64
3.73	20.91	20.89	20.73	20.65	4.63	20.84	20.9	20.68	20.63	5.53	20.78	20.83	20.69	20.56	6.43	20.86	20.91	20.76	20.64
3.75	20.9	20.89	20.78	20.65	4.65	20.8	20.85	20.67	20.53	5.55	20.83	20.88	20.69	20.61	6.45	20.9	20.95	20.72	20.69
3.77	20.86	20.89	20.78	20.65	4.67	20.84	20.9	20.67	20.58	5.57	20.78	20.83	20.74	20.56	6.47	20.9	20.95	20.77	20.64
3.79	20.86	20.89	20.78	20.65	4.69	20.84	20.9	20.66	20.58	5.59	20.83	20.88	20.73	20.56	6.49	20.9	20.95	20.77	20.64
3.81	20.86	20.89	20.73	20.65	4.71	20.84	20.9	20.73	20.63	5.61	20.83	20.88	20.7	20.61	6.5	20.9	20.95	20.77	20.64
3.83	20.86	20.89	20.78	20.64	4.73	20.8	20.83	20.72	20.58	5.62	20.86	20.91	20.65	20.64	6.52	20.85	20.9	20.77	20.59
3.84	20.86	20.89	20.78	20.65	4.74	20.8	20.84	20.67	20.58	5.64	20.86	20.91	20.73	20.64	6.54	20.9	20.95	20.76	20.69
3.86	20.86	20.89	20.75	20.63	4.76	20.8	20.82	20.71	20.58	5.66	20.86	20.91	20.68	20.64	6.56	20.9	20.95	20.81	20.69
3.88	20.86	20.89	20.74	20.59	4.78	20.8	20.85	20.71	20.58	5.68	20.86	20.91	20.71	20.6	6.58	20.85	20.9	20.81	20.64
3.9	20.86	20.89	20.73	20.6	4.8	20.8	20.8	20.71	20.58	5.7	20.81	20.86	20.72	20.55	6.6	20.9	20.95	20.81	20.69
3.92	20.86	20.89	20.73	20.64	4.82	20.8	20.82	20.66	20.58	5.72	20.81	20.86	20.74	20.6	6.62	20.9	20.95	20.76	20.69
3.94	20.86	20.89	20.73	20.63	4.84	20.84	20.89	20.66	20.58	5.73	20.86	20.91	20.74	20.64	6.63	20.9	20.95	20.81	20.69
3.95	20.86	20.89	20.73	20.63	4.85	20.84	20.88	20.66	20.63	5.75	20.81	20.86	20.68	20.6	6.65	20.9	20.95	20.81	20.69
3.97	20.86	20.89	20.73	20.63	4.87	20.84	20.88	20.66	20.63	5.77	20.81	20.86	20.73	20.55	6.67	20.85	20.9	20.76	20.69
3.99	20.86	20.89	20.73	20.62	4.89	20.84	20.87	20.66	20.58	5.79	20.86	20.91	20.68	20.64	6.69	20.9	20.95	20.81	20.64
4.01	20.86	20.88	20.73	20.62	4.91	20.8	20.81	20.66	20.57	5.81	20.81	20.86	20.68	20.6	6.71	20.85	20.9	20.81	20.59
4.03	20.86	20.88	20.73	20.62	4.93	20.84	20.86	20.71	20.63	5.83	20.86	20.89	20.72	20.64	6.73	20.9	20.95	20.81	20.64
4.05	20.86	20.88	20.73	20.6	4.95	20.84	20.85	20.71	20.63	5.84	20.81	20.85	20.69	20.6	6.74	20.9	20.95	20.81	20.69
4.07	20.83	20.88	20.73	20.56	4.96	20.84	20.85	20.71	20.62	5.86	20.86	20.9	20.68	20.64	6.76	20.9	20.95	20.76	20.69
4.08	20.81	20.86	20.73	20.54	4.98	20.84	20.85	20.71	20.61	5.88	20.86	20.89	20.72	20.6	6.78	20.9	20.95	20.81	20.69
4.1	20.81	20.83	20.73	20.52	5	20.8	20.82	20.66	20.57	5.9	20.86	20.9	20.67	20.6	6.8	20.85	20.9	20.76	20.64
4.12	20.81	20.84	20.73	20.56	5.02	20.84	20.86	20.71	20.58	5.92	20.81	20.84	20.72	20.6	6.82	20.85	20.87	20.81	20.64
4.14	20.81	20.83	20.7	20.56	5.04	20.8	20.81	20.71	20.58	5.94	20.81	20.83	20.67	20.6	6.84	20.9	20.92	20.81	20.69
4.16	20.81	20.82	20.73	20.55	5.06	20.8	20.81	20.71	20.57	5.95	20.86	20.9	20.72	20.6	6.85	20.9	20.9	20.81	20.69
4.17	20.81	20.82	20.68	20.56	5.07	20.88	20.88	20.71	20.61	5.97	20.86	20.88	20.72	20.6	6.87	20.9	20.9	20.8	20.64
4.19	20.81	20.82	20.68	20.55	5.09	20.8	20.8	20.66	20.52	5.99	20.86	20.88	20.72	20.64	6.89	20.9	20.92	20.73	20.64
4.21	20.85	20.87	20.68	20.6	5.11	20.88	20.88	20.71	20.66	6.01	20.86	20.91	20.67	20.64	6.91	20.9	20.91	20.73	20.64
4.23	20.86	20.87	20.68	20.61	5.13	20.83	20.83	20.66	20.59	6.03	20.81	20.83	20.67	20.6	6.93	20.85	20.86	20.76	20.64
4.25	20.8	20.82	20.68	20.55	5.15	20.82	20.83	20.66	20.6	6.05	20.86	20.88	20.72	20.64	6.95	20.9	20.91	20.71	20.69
4.27	20.81	20.82	20.68	20.53	5.17	20.88	20.88	20.74	20.63	6.06	20.86	20.84	20.72	20.64	6.96	20.89	20.91	20.76	20.69
4.29	20.81	20.82	20.68	20.5	5.18	20.83	20.83	20.66	20.59	6.08	20.81	20.82	20.72	20.55	6.98	20.87	20.9	20.76	20.69
4.3	20.81	20.82	20.73	20.5	5.2	20.83	20.83	20.74	20.55	6.1	20.86	20.87	20.72	20.6	7	20.87	20.9	20.76	20.69
4.32	20.81	20.82	20.73	20.55	5.22	20.83	20.83	20.69	20.56	6.12	20.86	20.87	20.67	20.64	7.02	20.87	20.91	20.71	20.69
4.34	20.81	20.82	20.68	20.56	5.24	20.83	20.83	20.69	20.6	6.14	20.81	20.85	20.72	20.6	7.04	20.82	20.85	20.76	20.64
4.36	20.79	20.82	20.68	20.55	5.26	20.83	20.83	20.74	20.58	6.16	20.81	20.85	20.67	20.55					
4.38	20.8	20.82	20.68	20.55	5.28	20.87	20.88	20.69	20.65	6.17	20.86	20.9	20.67	20.64					
4.4	20.82	20.87	20.68	20.6	5.29	20.81	20.83	20.69	20.54	6.19	20.86	20.91	20.72	20.64					
4.41	20.83	20.87	20.68	20.6	5.31	20.87	20.88	20.69	20.63	6.21	20.86	20.9	20.73	20.64					
4.43	20.77	20.82	20.68	20.55	5.33	20.78	20.83	20.69	20.57	6.23	20.86	20.91	20.68	20.64					
4.45	20.85	20.9	20.68	20.6	5.35	20.85	20.88	20.74	20.62	6.25	20.81	20.85	20.69	20.6					
4.47	20.84	20.9	20.68	20.53	5.37	20.78	20.83	20.74	20.57	6.27	20.86	20.91	20.73	20.64					
4.49	20.8	20.85	20.71	20.53	5.39	20.81	20.83	20.69	20.56	6.28	20.86	20.91	20.74	20.6					
4.51	20.81	20.85	20.7	20.53	5.4	20.8	20.83	20.74	20.55	6.3	20.86	20.91	20.74	20.6					

LANIGAN GRANULAR POTASH

1. MOISTURE CONTENT DATA

RH=45%, Tair=22^{0}C, Tc=2^{0}C, Q=9.33L/s

time (h)	MC#1 (kg/kg-dry)	MC#2 (kg/kg-dry)	MC#3 (kg/kg-dry)	MC#4 (kg/kg-dry)
1	2.70E-04	2.29E-04	2.00E-04	1.80E-04
2	4.10E-04	3.11E-04	3.42E-04	2.50E-04
8	5.96E-03	9.80E-04	5.76E-04	4.19E-04

RH=45%, Tair=22^{0}C, Tc=21^{0}C, Q=9.33L/s

time (h)	MC#1 (kg/kg-dry)	MC#2 (kg/kg-dry)	MC#3 (kg/kg-dry)	MC#4 (kg/kg-dry)
8	1.03E-03	9.90E-04	1.74E-04	3.50E-05

RH=65%, Tair=22^{0}C, Tc=2^{0}C, Q=9.33L/s

time (h)	MC#1 (kg/kg-dry)	MC#2 (kg/kg-dry)	MC#3 (kg/kg-dry)	MC#4 (kg/kg-dry)
1	1.88E-03	4.50E-04	8.20E-04	1.15E-03
2	3.84E-03	1.31E-03	8.34E-04	1.25E-03
8	8.77E-03	1.90E-03	1.00E-03	1.80E-03

RH=65%, Tair=22^{0}C, Tc=21^{0}C, Q=9.33L/s

time (h)	MC#1 (kg/kg-dry)	MC#2 (kg/kg-dry)	MC#3 (kg/kg-dry)	MC#4 (kg/kg-dry)
8	1.10E-03	9.95E-04	1.31E-04	8.00E-05

RH=85%, Tair=22^{0}C, Tc=2^{0}C, Q=9.17L/s

time (h)	MC#1 (kg/kg-dry)	MC#2 (kg/kg-dry)	MC#3 (kg/kg-dry)	MC#4 (kg/kg-dry)
1	6.70E-03	1.40E-04	1.10E-04	5.00E-05
2	1.99E-02	4.10E-04	4.00E-04	3.00E-04
3	2.06E-02	1.74E-03	6.00E-04	5.23E-04
8	8.50E-02	3.35E-03	2.03E-03	4.48E-03

RH=85%, Tair=22^{0}C, Tc=21^{0}C, Q=9.17L/s

time (h)	MC#1 (kg/kg-dry)	MC#2 (kg/kg-dry)	MC#3 (kg/kg-dry)	MC#4 (kg/kg-dry)
8	5.72E-03	2.90E-04	2.47E-04	9.68E-05

2. TEMPERATURE DATA

RH=80%, Tair=22^{0}C, Tc=2^{0}C, Q=9.33 L/s

Time (s)	Tray#1 (^{0}C)	Tray#2 (^{0}C)	Tray#3 (^{0}C)	Tray#4 (^{0}C)	Time (s)	Tray#1 (^{0}C)	Tray#2 (^{0}C)	Tray#3 (^{0}C)	Tray#4 (^{0}C)	Time (s)	Tray#1 (^{0}C)	Tray#2 (^{0}C)	Tray#3 (^{0}C)	Tray#4 (^{0}C)	Time (s)	Tray#1 (^{0}C)	Tray#2 (^{0}C)	Tray#3 (^{0}C)	Tray#4 (^{0}C)
0	19.89	19.80	17.82	4.66	0.9	11.23	9.60	6.16	3.54	1.8	11.19	9.40	5.99	3.50	2.69	11.27	9.44	5.96	3.45
0.02	19.67	19.60	15.60	4.49	0.92	11.23	9.58	6.15	3.53	1.81	11.18	9.41	5.99	3.52	2.71	11.27	9.44	5.96	3.45
0.04	19.56	18.76	13.97	4.27	0.94	11.26	9.58	6.14	3.61	1.83	11.18	9.40	5.99	3.51	2.73	11.33	9.50	5.96	3.44
0.06	19.32	18.23	12.78	3.98	0.95	11.26	9.61	6.13	3.57	1.85	11.18	9.40	5.99	3.51	2.75	11.24	9.44	5.96	3.46
0.07	18.96	17.76	11.88	3.90	0.97	11.26	9.56	6.12	3.52	1.87	11.18	9.40	5.98	3.46	2.77	11.27	9.44	5.96	3.51
0.09	18.67	16.98	11.18	3.88	0.99	11.25	9.56	6.11	3.50	1.89	11.21	9.43	5.98	3.50	2.79	11.25	9.49	5.96	3.57
0.11	18.43	16.39	10.62	3.93	1.01	11.28	9.56	6.10	3.52	1.91	11.17	9.43	5.98	3.46	2.8	11.33	9.49	5.96	3.53
0.13	17.70	15.00	10.16	3.88	1.03	11.23	9.55	6.09	3.45	1.92	11.17	9.41	5.98	3.41	2.82	11.29	9.46	5.96	3.57
0.15	16.76	14.49	9.77	3.88	1.05	11.23	9.50	6.09	3.49	1.94	11.16	9.34	5.98	3.49	2.84	11.35	9.52	5.96	3.59
0.17	16.00	14.12	9.44	3.84	1.06	11.23	9.50	6.08	3.47	1.96	11.17	9.39	5.98	3.54	2.86	11.30	9.46	5.96	3.61
0.18	15.34	13.68	9.15	3.84	1.08	11.26	9.49	6.07	3.49	1.98	11.17	9.40	5.98	3.54	2.88	11.30	9.46	5.96	3.57
0.2	14.75	13.30	8.89	3.83	1.1	11.21	9.48	6.07	3.45	2	11.13	9.34	5.98	3.53	2.9	11.27	9.45	5.96	3.63
0.22	14.24	12.94	8.66	3.83	1.12	11.19	9.48	6.06	3.44	2.02	11.16	9.41	5.98	3.53	2.91	11.32	9.51	5.96	3.67
0.24	13.83	12.65	8.46	3.83	1.14	11.16	9.43	6.06	3.52	2.03	11.20	9.47	5.98	3.54	2.93	11.33	9.50	5.96	3.64
0.26	13.52	12.36	8.27	3.83	1.16	11.19	9.46	6.06	3.49	2.05	11.20	9.43	5.98	3.48	2.95	11.33	9.55	5.96	3.74
0.28	13.22	12.12	8.10	3.78	1.17	11.19	9.42	6.05	3.50	2.07	11.20	9.42	5.98	3.51	2.97	11.38	9.58	5.96	3.67
0.29	12.97	11.90	7.94	3.76	1.19	11.19	9.41	6.05	3.48	2.09	11.20	9.42	5.98	3.50	2.99	11.38	9.60	5.96	3.64
0.31	12.76	11.67	7.80	3.76	1.21	11.18	9.45	6.04	3.50	2.11	11.20	9.42	5.98	3.52	3.01	11.43	9.65	5.96	3.67
0.33	12.57	11.47	7.66	3.77	1.23	11.18	9.43	6.04	3.47	2.13	11.15	9.37	5.98	3.48	3.02	11.45	9.65	5.96	3.69
0.35	12.42	11.30	7.54	3.74	1.25	11.17	9.40	6.04	3.47	2.14	11.20	9.41	5.98	3.52	3.04	11.44	9.66	5.96	3.68
0.37	12.30	11.18	7.43	3.74	1.27	11.14	9.40	6.04	3.46	2.16	11.20	9.41	5.98	3.52	3.06	11.44	9.66	5.96	3.65
0.39	12.14	11.01	7.32	3.77	1.28	11.17	9.40	6.03	3.50	2.18	11.23	9.44	5.97	3.45	3.08	11.48	9.69	5.95	3.65
0.4	12.07	10.93	7.22	3.73	1.3	11.16	9.38	6.03	3.46	2.2	11.23	9.43	5.97	3.51	3.1	11.49	9.71	5.95	3.69
0.42	11.97	10.78	7.13	3.76	1.32	11.15	9.38	6.03	3.47	2.22	11.20	9.40	5.97	3.49	3.12	11.47	9.68	5.95	3.65
0.44	11.87	10.68	7.05	3.74	1.34	11.11	9.37	6.02	3.49	2.24	11.19	9.40	5.97	3.48	3.13	11.51	9.72	5.95	3.55
0.46	11.81	10.59	6.97	3.72	1.36	11.15	9.41	6.02	3.48	2.25	11.13	9.35	5.97	3.49	3.15	11.51	9.73	5.95	3.60
0.48	11.76	10.49	6.90	3.74	1.38	11.15	9.39	6.02	3.49	2.27	11.18	9.40	5.97	3.50	3.17	11.51	9.73	5.95	3.63
0.5	11.72	10.45	6.84	3.66	1.39	11.17	9.38	6.02	3.50	2.29	11.18	9.40	5.97	3.48	3.19	11.46	9.69	5.95	3.57
0.51	11.64	10.34	6.77	3.67	1.41	11.15	9.37	6.01	3.49	2.31	11.18	9.40	5.97	3.51	3.21	11.46	9.69	5.95	3.62
0.53	11.59	10.24	6.72	3.70	1.43	11.15	9.37	6.01	3.47	2.33	11.18	9.40	5.97	3.50	3.23	11.46	9.69	5.95	3.61
0.55	11.57	10.22	6.67	3.70	1.45	11.17	9.39	6.01	3.46	2.35	11.18	9.40	5.97	3.55	3.24	11.46	9.73	5.95	3.69
0.57	11.52	10.13	6.62	3.69	1.47	11.17	9.39	6.01	3.49	2.36	11.18	9.40	5.97	3.49	3.26	11.45	9.71	5.95	3.71
0.59	11.50	10.10	6.57	3.65	1.48	11.17	9.38	6.01	3.49	2.38	11.21	9.44	5.97	3.54	3.28	11.48	9.71	5.95	3.64
0.61	11.49	10.05	6.53	3.64	1.5	11.17	9.36	6.01	3.45	2.4	11.22	9.44	5.97	3.50	3.3	11.48	9.74	5.95	3.60
0.62	11.50	10.02	6.49	3.63	1.52	11.13	9.34	6.00	3.45	2.42	11.22	9.45	5.97	3.50	3.32	11.54	9.81	5.95	3.57
0.64	11.46	9.93	6.45	3.64	1.54	11.18	9.38	6.00	3.48	2.44	11.17	9.40	5.97	3.51	3.34	11.58	9.81	5.95	3.55
0.66	11.40	9.88	6.42	3.62	1.56	11.16	9.38	6.00	3.45	2.46	11.22	9.45	5.97	3.56	3.35	11.54	9.77	5.95	3.55
0.68	11.40	9.87	6.39	3.62	1.58	11.18	9.38	6.00	3.49	2.47	11.17	9.43	5.97	3.51	3.37	11.48	9.73	5.95	3.54
0.7	11.37	9.82	6.36	3.58	1.59	11.16	9.38	6.00	3.50	2.49	11.17	9.44	5.97	3.49	3.39	11.44	9.78	5.95	3.59
0.72	11.38	9.80	6.34	3.58	1.61	11.16	9.38	6.00	3.51	2.51	11.22	9.49	5.97	3.49	3.41	11.41	9.72	5.95	3.59
0.73	11.36	9.76	6.31	3.60	1.63	11.14	9.36	6.00	3.51	2.53	11.22	9.49	5.97	3.48	3.43	11.41	9.72	5.95	3.57
0.75	11.33	9.78	6.29	3.64	1.65	11.18	9.41	6.00	3.50	2.55	11.24	9.49	5.97	3.52	3.45	11.45	9.73	5.95	3.56
0.77	11.34	9.73	6.27	3.63	1.67	11.14	9.39	5.99	3.49	2.57	11.22	9.44	5.97	3.49	3.46	11.48	9.73	5.95	3.55
0.79	11.31	9.70	6.25	3.60	1.69	11.16	9.39	5.99	3.50	2.58	11.25	9.49	5.96	3.51	3.48	11.50	9.73	5.95	3.52
0.81	11.28	9.68	6.23	3.63	1.7	11.17	9.39	5.99	3.44	2.6	11.27	9.45	5.96	3.50	3.5	11.51	9.73	5.95	3.55
0.83	11.30	9.67	6.21	3.59	1.72	11.14	9.37	5.99	3.48	2.62	11.33	9.54	5.96	3.46	3.52	11.49	9.73	5.95	3.53
0.84	11.30	9.67	6.20	3.58	1.74	11.14	9.37	5.99	3.52	2.64	11.27	9.46	5.96	3.44	3.54	11.52	9.74	5.95	3.50
0.86	11.26	9.62	6.18	3.60	1.76	11.14	9.36	5.99	3.52	2.66	11.33	9.53	5.96	3.49	3.56	11.52	9.74	5.95	3.48
0.88	11.28	9.65	6.17	3.58	1.78	11.14	9.40	5.99	3.52	2.68	11.32	9.50	5.96	3.42	3.57	11.52	9.74	5.95	3.51

RH=80%, Tair=22°C, Tc=2°C, Q=9.33 L/s

Time (s)	Tray#1 (°C)	Tray#2 (°C)	Tray#3 (°C)	Tray#4 (°C)	Time (s)	Tray#1 (°C)	Tray#2 (°C)	Tray#3 (°C)	Tray#4 (°C)	Time (s)	Tray#1 (°C)	Tray#2 (°C)	Tray#3 (°C)	Tray#4 (°C)	Time (s)	Tray#1 (°C)	Tray#2 (°C)	Tray#3 (°C)	Tray#4 (°C)
3.59	11.55	9.80	5.95	3.51	4.49	11.43	9.73	5.93	3.45	5.39	11.38	9.70	5.92	3.43	6.29	11.38	9.66	5.90	3.41
3.61	11.57	9.80	5.95	3.52	4.51	11.44	9.73	5.93	3.44	5.41	11.39	9.70	5.92	3.42	6.3	11.38	9.66	5.90	3.50
3.63	11.56	9.77	5.94	3.54	4.53	11.43	9.74	5.93	3.50	5.42	11.39	9.70	5.91	3.43	6.32	11.38	9.67	5.90	3.47
3.65	11.58	9.77	5.94	3.54	4.54	11.41	9.74	5.93	3.45	5.44	11.39	9.68	5.91	3.48	6.34	11.38	9.66	5.90	3.49
3.67	11.60	9.78	5.94	3.53	4.56	11.44	9.74	5.93	3.44	5.46	11.39	9.68	5.91	3.49	6.36	11.38	9.66	5.90	3.45
3.68	11.60	9.81	5.94	3.47	4.58	11.44	9.73	5.93	3.41	5.48	11.39	9.71	5.91	3.40	6.38	11.38	9.70	5.90	3.42
3.7	11.61	9.83	5.94	3.48	4.6	11.44	9.73	5.93	3.47	5.5	11.40	9.72	5.91	3.49	6.4	11.38	9.70	5.90	3.43
3.72	11.60	9.83	5.94	3.51	4.62	11.41	9.73	5.93	3.45	5.52	11.40	9.72	5.91	3.42	6.41	11.38	9.71	5.90	3.48
3.74	11.60	9.83	5.94	3.42	4.64	11.41	9.73	5.93	3.42	5.53	11.40	9.72	5.91	3.50	6.43	11.38	9.71	5.90	3.53
3.76	11.56	9.78	5.94	3.40	4.65	11.41	9.71	5.93	3.46	5.55	11.36	9.68	5.91	3.43	6.45	11.38	9.71	5.90	3.51
3.77	11.56	9.78	5.94	3.47	4.67	11.41	9.70	5.93	3.43	5.57	11.41	9.73	5.91	3.41	6.47	11.39	9.71	5.90	3.58
3.79	11.56	9.78	5.94	3.48	4.69	11.41	9.68	5.93	3.45	5.59	11.38	9.68	5.91	3.42	6.49	11.38	9.71	5.90	3.52
3.81	11.53	9.75	5.94	3.49	4.71	11.41	9.68	5.93	3.48	5.61	11.41	9.69	5.91	3.47	6.51	11.42	9.76	5.90	3.49
3.83	11.53	9.75	5.94	3.52	4.73	11.41	9.68	5.93	3.48	5.63	11.41	9.72	5.91	3.44	6.52	11.38	9.71	5.90	3.47
3.85	11.53	9.75	5.94	3.49	4.75	11.41	9.68	5.93	3.56	5.64	11.37	9.70	5.91	3.41	6.54	11.41	9.76	5.90	3.48
3.87	11.55	9.77	5.94	3.52	4.76	11.41	9.68	5.93	3.45	5.66	11.37	9.70	5.91	3.45	6.56	11.38	9.71	5.90	3.47
3.89	11.56	9.77	5.94	3.48	4.78	11.41	9.69	5.93	3.48	5.68	11.37	9.70	5.91	3.47	6.58	11.38	9.71	5.90	3.46
3.9	11.58	9.79	5.94	3.51	4.8	11.41	9.68	5.92	3.46	5.7	11.37	9.70	5.91	3.43	6.6	11.34	9.66	5.90	3.43
3.92	11.58	9.79	5.94	3.50	4.82	11.45	9.68	5.92	3.36	5.72	11.37	9.70	5.91	3.43	6.62	11.34	9.66	5.90	3.47
3.94	11.58	9.80	5.94	3.51	4.84	11.41	9.70	5.92	3.45	5.74	11.41	9.70	5.91	3.46	6.63	11.34	9.66	5.90	3.44
3.96	11.54	9.76	5.94	3.49	4.86	11.38	9.66	5.92	3.46	5.75	11.42	9.70	5.91	3.46	6.65	11.34	9.66	5.90	3.45
3.98	11.54	9.77	5.94	3.55	4.87	11.38	9.68	5.92	3.50	5.77	11.39	9.70	5.91	3.42	6.67	11.37	9.66	5.90	3.48
3.99	11.55	9.77	5.94	3.57	4.89	11.38	9.70	5.92	3.51	5.79	11.41	9.70	5.91	3.43	6.69	11.37	9.67	5.90	3.51
4.01	11.59	9.78	5.94	3.56	4.91	11.38	9.70	5.92	3.47	5.81	11.39	9.67	5.91	3.44	6.71	11.36	9.66	5.90	3.49
4.03	11.59	9.81	5.94	3.54	4.93	11.38	9.70	5.92	3.45	5.83	11.38	9.67	5.91	3.47	6.72	11.37	9.66	5.89	3.49
4.05	11.59	9.81	5.94	3.54	4.95	11.39	9.70	5.92	3.51	5.85	11.39	9.67	5.91	3.55	6.74	11.37	9.68	5.89	3.51
4.07	11.59	9.81	5.94	3.56	4.97	11.38	9.70	5.92	3.47	5.86	11.39	9.68	5.91	3.47	6.76	11.37	9.68	5.89	3.50
4.09	11.59	9.81	5.94	3.56	4.98	11.38	9.70	5.92	3.47	5.88	11.39	9.68	5.91	3.46	6.78	11.37	9.69	5.89	3.45
4.1	11.56	9.78	5.94	3.57	5	11.43	9.70	5.92	3.51	5.9	11.39	9.68	5.91	3.44	6.8	11.36	9.68	5.89	3.45
4.12	11.56	9.78	5.94	3.56	5.02	11.43	9.70	5.92	3.52	5.92	11.45	9.76	5.91	3.42	6.82	11.37	9.69	5.89	3.52
4.14	11.56	9.78	5.94	3.52	5.04	11.43	9.71	5.92	3.51	5.94	11.39	9.72	5.91	3.47	6.83	11.36	9.70	5.89	3.51
4.16	11.56	9.82	5.94	3.50	5.06	11.40	9.71	5.92	3.47	5.96	11.36	9.69	5.91	3.43	6.85	11.37	9.72	5.89	3.53
4.18	11.56	9.82	5.94	3.54	5.08	11.40	9.72	5.92	3.50	5.97	11.36	9.69	5.91	3.44	6.87	11.37	9.72	5.89	3.51
4.2	11.56	9.78	5.93	3.55	5.09	11.40	9.72	5.92	3.52	5.99	11.36	9.69	5.91	3.44	6.89	11.37	9.72	5.89	3.46
4.21	11.56	9.78	5.93	3.54	5.11	11.40	9.72	5.92	3.51	6.01	11.36	9.68	5.91	3.43	6.91	11.42	9.77	5.89	3.54
4.23	11.55	9.78	5.93	3.52	5.13	11.40	9.72	5.92	3.54	6.03	11.36	9.69	5.91	3.44	6.93	11.37	9.72	5.89	3.52
4.25	11.56	9.78	5.93	3.55	5.15	11.40	9.72	5.92	3.49	6.05	11.37	9.69	5.91	3.43	6.95	11.37	9.72	5.89	3.51
4.27	11.55	9.80	5.93	3.49	5.17	11.40	9.72	5.92	3.45	6.07	11.37	9.69	5.90	3.44	6.96	11.37	9.72	5.89	3.51
4.29	11.54	9.80	5.93	3.44	5.19	11.40	9.72	5.92	3.51	6.08	11.36	9.69	5.90	3.47	6.98	11.42	9.77	5.89	3.52
4.31	11.53	9.75	5.93	3.46	5.2	11.41	9.72	5.92	3.48	6.1	11.36	9.69	5.90	3.48	7	11.37	9.72	5.89	3.51
4.32	11.58	9.82	5.93	3.42	5.22	11.39	9.68	5.92	3.48	6.12	11.36	9.69	5.90	3.43	7.02	11.37	9.72	5.89	3.55
4.34	11.48	9.75	5.93	3.45	5.24	11.41	9.71	5.92	3.45	6.14	11.37	9.69	5.90	3.41	7.04	11.37	9.72	5.89	3.55
4.36	11.48	9.75	5.93	3.39	5.26	11.41	9.71	5.92	3.47	6.16	11.40	9.69	5.90	3.41	7.05	11.39	9.72	5.89	3.54
4.38	11.48	9.74	5.93	3.44	5.28	11.41	9.73	5.92	3.47	6.18	11.41	9.69	5.90	3.44	7.07	11.39	9.72	5.89	3.53
4.4	11.48	9.75	5.93	3.41	5.3	11.41	9.72	5.92	3.49	6.19	11.41	9.69	5.90	3.41	7.09	11.37	9.72	5.89	3.58
4.42	11.48	9.75	5.93	3.44	5.31	11.41	9.73	5.92	3.43	6.21	11.38	9.66	5.90	3.41	7.11	11.38	9.72	5.89	3.59
4.43	11.44	9.71	5.93	3.46	5.33	11.38	9.70	5.92	3.47	6.23	11.37	9.66	5.90	3.46	7.13	11.38	9.72	5.89	3.54
4.45	11.44	9.71	5.93	3.42	5.35	11.38	9.70	5.92	3.50	6.25	11.38	9.67	5.90	3.43	7.15	11.37	9.72	5.89	3.54
4.47	11.44	9.71	5.93	3.47	5.37	11.38	9.70	5.92	3.43	6.27	11.38	9.66	5.90	3.47	7.16	11.37	9.72	5.89	3.54

RH=65%, Tair=22^{0}C, Tc=2^{0}C, Q=9.33 L/s

Time (s)	Tray#1 (^{0}C)	Tray#2 (^{0}C)	Tray#3 (^{0}C)	Tray#4 (^{0}C)	Time (s)	Tray#1 (^{0}C)	Tray#2 (^{0}C)	Tray#3 (^{0}C)	Tray#4 (^{0}C)	Time (s)	Tray#1 (^{0}C)	Tray#2 (^{0}C)	Tray#3 (^{0}C)	Tray#4 (^{0}C)	Time (s)	Tray#1 (^{0}C)	Tray#2 (^{0}C)	Tray#3 (^{0}C)	Tray#4 (^{0}C)
0	20.25	20.02	17.86	10.63	0.9	14.89	11.36	7.56	4.22	1.8	14.77	11.27	7.26	4.21	2.69	14.86	11.38	7.20	4.19
0.02	20.35	19.80	15.66	7.97	0.92	14.84	11.35	7.54	4.27	1.81	14.76	11.27	7.25	4.21	2.71	14.86	11.38	7.20	4.18
0.04	20.33	19.40	14.09	6.87	0.93	14.85	11.31	7.53	4.27	1.83	14.75	11.27	7.25	4.15	2.73	14.81	11.38	7.20	4.12
0.05	20.25	19.00	13.00	6.08	0.95	14.84	11.31	7.51	4.21	1.85	14.71	11.27	7.25	4.16	2.75	14.81	11.38	7.20	4.19
0.07	20.45	18.60	12.22	5.82	0.97	14.84	11.31	7.50	4.25	1.87	14.71	11.27	7.25	4.17	2.77	14.81	11.38	7.20	4.13
0.09	20.15	18.20	11.65	5.53	0.99	14.82	11.27	7.48	4.26	1.89	14.70	11.26	7.25	4.22	2.79	14.81	11.38	7.20	4.16
0.11	19.95	17.90	11.21	5.07	1.01	14.84	11.26	7.47	4.17	1.91	14.66	11.22	7.25	4.17	2.8	14.81	11.38	7.20	4.15
0.13	19.75	17.48	10.86	4.87	1.03	14.79	11.26	7.46	4.22	1.92	14.65	11.22	7.24	4.15	2.82	14.84	11.38	7.20	4.18
0.15	19.55	17.10	10.57	4.76	1.04	14.84	11.26	7.45	4.18	1.94	14.70	11.22	7.24	4.15	2.84	14.86	11.38	7.20	4.19
0.16	19.15	16.50	10.33	4.70	1.06	14.79	11.26	7.44	4.22	1.96	14.75	11.22	7.24	4.15	2.86	14.82	11.38	7.20	4.12
0.18	18.55	15.90	10.12	4.59	1.08	14.79	11.26	7.43	4.17	1.98	14.70	11.22	7.24	4.18	2.88	14.86	11.38	7.20	4.19
0.2	18.35	15.45	9.93	4.56	1.1	14.79	11.25	7.42	4.18	2	14.70	11.22	7.24	4.13	2.9	14.86	11.38	7.19	4.13
0.22	18.07	15.15	9.76	4.55	1.12	14.79	11.23	7.41	4.17	2.02	14.70	11.22	7.24	4.18	2.91	14.86	11.40	7.19	4.13
0.24	17.80	14.85	9.61	4.48	1.14	14.74	11.21	7.40	4.21	2.03	14.70	11.22	7.24	4.18	2.93	14.87	11.43	7.19	4.14
0.26	17.55	14.57	9.47	4.51	1.15	14.77	11.24	7.39	4.20	2.05	14.75	11.24	7.23	4.13	2.95	14.86	11.43	7.19	4.20
0.27	17.31	14.25	9.35	4.47	1.17	14.77	11.24	7.38	4.20	2.07	14.75	11.27	7.23	4.18	2.97	14.86	11.43	7.19	4.14
0.29	17.14	14.03	9.23	4.40	1.19	14.77	11.24	7.38	4.20	2.09	14.75	11.26	7.23	4.13	2.99	14.86	11.43	7.19	4.12
0.31	16.94	13.78	9.12	4.39	1.21	14.77	11.24	7.37	4.25	2.11	14.75	11.27	7.23	4.13	3.01	14.86	11.43	7.19	4.14
0.33	16.79	13.58	9.01	4.42	1.23	14.81	11.24	7.36	4.25	2.13	14.75	11.27	7.23	4.18	3.02	14.86	11.43	7.19	4.14
0.35	16.59	13.38	8.91	4.42	1.25	14.77	11.24	7.36	4.20	2.14	14.75	11.27	7.23	4.13	3.04	14.86	11.43	7.19	4.19
0.37	16.44	13.17	8.82	4.37	1.26	14.77	11.24	7.35	4.25	2.16	14.75	11.27	7.23	4.18	3.06	14.86	11.43	7.19	4.14
0.38	16.34	13.02	8.73	4.37	1.28	14.77	11.24	7.34	4.25	2.18	14.76	11.27	7.23	4.13	3.08	14.86	11.43	7.19	4.13
0.4	16.19	12.87	8.65	4.40	1.3	14.77	11.24	7.34	4.21	2.2	14.75	11.27	7.23	4.19	3.1	14.86	11.43	7.19	4.13
0.42	16.13	12.76	8.57	4.34	1.32	14.76	11.24	7.33	4.15	2.22	14.75	11.27	7.22	4.12	3.12	14.86	11.43	7.19	4.19
0.44	16.03	12.66	8.50	4.36	1.34	14.77	11.24	7.33	4.25	2.24	14.75	11.27	7.22	4.18	3.13	14.86	11.43	7.19	4.17
0.46	15.93	12.51	8.43	4.41	1.36	14.77	11.24	7.32	4.22	2.25	14.75	11.27	7.22	4.13	3.15	14.86	11.43	7.19	4.13
0.48	15.83	12.41	8.37	4.36	1.37	14.77	11.24	7.32	4.16	2.27	14.75	11.27	7.22	4.18	3.17	14.84	11.43	7.18	4.19
0.49	15.73	12.31	8.31	4.41	1.39	14.77	11.24	7.32	4.17	2.29	14.75	11.27	7.22	4.14	3.19	14.81	11.43	7.18	4.14
0.51	15.63	12.21	8.25	4.33	1.41	14.77	11.24	7.31	4.20	2.31	14.75	11.27	7.22	4.19	3.21	14.81	11.43	7.18	4.14
0.53	15.58	12.15	8.19	4.32	1.43	14.77	11.24	7.31	4.16	2.33	14.77	11.26	7.22	4.16	3.23	14.86	11.43	7.18	4.21
0.55	15.48	12.06	8.14	4.37	1.45	14.80	11.27	7.30	4.18	2.35	14.77	11.27	7.22	4.11	3.24	14.86	11.43	7.18	4.24
0.57	15.43	11.97	8.09	4.36	1.47	14.80	11.27	7.30	4.18	2.36	14.77	11.27	7.22	4.11	3.26	14.86	11.43	7.18	4.19
0.59	15.38	11.91	8.05	4.30	1.48	14.80	11.27	7.30	4.23	2.38	14.77	11.29	7.22	4.17	3.28	14.88	11.44	7.18	4.19
0.61	15.33	11.85	8.00	4.30	1.5	14.80	11.27	7.29	4.19	2.4	14.78	11.29	7.22	4.18	3.3	14.86	11.47	7.18	4.25
0.62	15.28	11.80	7.96	4.27	1.52	14.80	11.27	7.29	4.24	2.42	14.79	11.27	7.21	4.09	3.32	14.86	11.43	7.18	4.25
0.64	15.20	11.75	7.92	4.26	1.54	14.80	11.27	7.29	4.18	2.44	14.79	11.31	7.21	4.11	3.34	14.83	11.46	7.18	4.23
0.66	15.16	11.70	7.89	4.29	1.56	14.80	11.27	7.28	4.18	2.46	14.79	11.31	7.21	4.11	3.35	14.83	11.44	7.18	4.26
0.68	15.11	11.67	7.85	4.29	1.58	14.79	11.27	7.28	4.23	2.47	14.84	11.31	7.21	4.17	3.37	14.87	11.45	7.18	4.21
0.7	15.11	11.61	7.82	4.27	1.59	14.80	11.27	7.28	4.24	2.49	14.84	11.33	7.21	4.17	3.39	14.87	11.45	7.18	4.21
0.71	15.06	11.58	7.79	4.30	1.61	14.80	11.27	7.28	4.23	2.51	14.85	11.36	7.21	4.17	3.41	14.88	11.45	7.18	4.27
0.73	15.04	11.53	7.76	4.24	1.63	14.80	11.27	7.27	4.23	2.53	14.87	11.36	7.21	4.17	3.43	14.88	11.45	7.18	4.29
0.75	15.01	11.48	7.73	4.29	1.65	14.80	11.27	7.27	4.17	2.55	14.85	11.36	7.21	4.17	3.45	14.89	11.48	7.17	4.25
0.77	15.01	11.48	7.71	4.24	1.67	14.77	11.27	7.27	4.22	2.57	14.86	11.38	7.21	4.18	3.46	14.90	11.50	7.17	4.26
0.79	15.01	11.43	7.68	4.23	1.69	14.75	11.27	7.27	4.18	2.58	14.86	11.37	7.21	4.09	3.48	14.88	11.50	7.17	4.26
0.81	14.96	11.43	7.66	4.22	1.7	14.75	11.27	7.26	4.18	2.6	14.86	11.40	7.21	4.18	3.5	14.88	11.51	7.17	4.29
0.82	14.91	11.40	7.64	4.25	1.72	14.75	11.27	7.26	4.18	2.62	14.88	11.38	7.21	4.10	3.52	14.83	11.46	7.17	4.26
0.84	14.90	11.38	7.62	4.19	1.74	14.75	11.27	7.26	4.21	2.64	14.86	11.38	7.20	4.19	3.54	14.85	11.46	7.17	4.27
0.86	14.91	11.38	7.60	4.20	1.76	14.75	11.27	7.26	4.17	2.66	14.89	11.41	7.20	4.16	3.56	14.88	11.46	7.17	4.28
0.88	14.90	11.33	7.58	4.19	1.78	14.75	11.27	7.26	4.22	2.68	14.86	11.38	7.20	4.12	3.58	14.88	11.47	7.17	4.28

RH=65%, Tair=22°C, Tc=2°C, Q=9.33 L/s

Time (s)	Tray#1 (°C)	Tray#2 (°C)	Tray#3 (°C)	Tray#4 (°C)	Time (s)	Tray#1 (°C)	Tray#2 (°C)	Tray#3 (°C)	Tray#4 (°C)	Time (s)	Tray#1 (°C)	Tray#2 (°C)	Tray#3 (°C)	Tray#4 (°C)	Time (s)	Tray#1 (°C)	Tray#2 (°C)	Tray#3 (°C)	Tray#4 (°C)
3.59	14.88	11.49	7.17	4.27	4.49	14.89	11.57	7.14	4.44	5.39	14.97	11.71	7.12	4.62	6.29	14.98	11.68	7.09	4.34
3.61	14.88	11.51	7.17	4.32	4.51	14.90	11.59	7.14	4.39	5.41	14.98	11.73	7.12	4.67	6.31	14.97	11.68	7.09	4.39
3.63	14.92	11.51	7.17	4.35	4.53	14.92	11.59	7.14	4.38	5.43	14.99	11.73	7.12	4.69	6.33	14.96	11.68	7.09	4.39
3.65	14.90	11.51	7.17	4.32	4.55	14.93	11.60	7.14	4.39	5.45	15.01	11.73	7.12	4.65	6.34	14.96	11.68	7.09	4.39
3.67	14.88	11.51	7.17	4.32	4.57	14.93	11.60	7.14	4.39	5.46	15.01	11.73	7.12	4.65	6.36	14.93	11.65	7.09	4.36
3.69	14.88	11.51	7.17	4.37	4.58	14.94	11.60	7.14	4.43	5.48	15.01	11.73	7.12	4.70	6.38	14.96	11.68	7.09	4.39
3.7	14.88	11.51	7.17	4.33	4.6	14.94	11.60	7.14	4.44	5.5	15.01	11.73	7.11	4.65	6.4	14.96	11.68	7.09	4.33
3.72	14.88	11.51	7.17	4.39	4.62	14.89	11.60	7.14	4.39	5.52	15.01	11.73	7.11	4.80	6.42	14.93	11.65	7.09	4.36
3.74	14.88	11.51	7.17	4.40	4.64	14.88	11.60	7.14	4.41	5.54	15.01	11.73	7.11	4.70	6.44	14.93	11.65	7.09	4.35
3.76	14.88	11.51	7.16	4.36	4.66	14.93	11.60	7.14	4.43	5.56	15.01	11.73	7.11	4.60	6.45	14.93	11.65	7.09	4.31
3.78	14.88	11.51	7.16	4.33	4.68	14.94	11.61	7.14	4.44	5.57	15.01	11.73	7.11	4.66	6.47	14.96	11.68	7.09	4.34
3.8	14.88	11.52	7.16	4.42	4.69	14.93	11.61	7.14	4.51	5.59	15.01	11.73	7.11	4.65	6.49	14.93	11.65	7.09	4.30
3.81	14.88	11.53	7.16	4.42	4.71	14.93	11.61	7.14	4.49	5.61	15.01	11.73	7.11	4.59	6.51	14.96	11.68	7.09	4.39
3.83	14.88	11.53	7.16	4.36	4.73	14.93	11.61	7.14	4.45	5.63	15.00	11.73	7.11	4.60	6.53	14.93	11.65	7.09	4.30
3.85	14.93	11.58	7.16	4.41	4.75	14.93	11.60	7.14	4.46	5.65	15.01	11.73	7.11	4.61	6.55	14.93	11.65	7.09	4.36
3.87	14.94	11.60	7.16	4.41	4.77	14.93	11.60	7.13	4.50	5.67	14.99	11.73	7.11	4.55	6.56	14.93	11.65	7.09	4.35
3.89	14.93	11.60	7.16	4.41	4.79	14.93	11.62	7.13	4.49	5.68	15.01	11.73	7.11	4.56	6.58	14.93	11.65	7.09	4.34
3.91	14.97	11.60	7.16	4.41	4.8	14.93	11.60	7.13	4.50	5.7	15.01	11.73	7.11	4.50	6.6	14.93	11.65	7.09	4.30
3.92	14.94	11.60	7.16	4.40	4.82	14.93	11.60	7.13	4.53	5.72	15.01	11.73	7.11	4.49	6.62	14.93	11.65	7.09	4.36
3.94	14.95	11.60	7.16	4.45	4.84	14.93	11.60	7.13	4.41	5.74	15.01	11.73	7.11	4.56	6.64	14.93	11.65	7.09	4.31
3.96	14.98	11.60	7.16	4.40	4.86	14.93	11.61	7.13	4.42	5.76	15.01	11.73	7.11	4.49	6.66	14.93	11.65	7.09	4.35
3.98	14.96	11.60	7.16	4.44	4.88	14.93	11.60	7.13	4.44	5.78	15.01	11.73	7.11	4.55	6.67	14.93	11.65	7.08	4.31
4	14.93	11.60	7.16	4.41	4.9	14.93	11.62	7.13	4.41	5.79	15.01	11.73	7.11	4.48	6.69	14.93	11.65	7.08	4.29
4.02	14.93	11.60	7.16	4.40	4.91	14.93	11.60	7.13	4.47	5.81	15.01	11.73	7.11	4.54	6.71	14.93	11.65	7.08	4.36
4.03	14.93	11.60	7.16	4.46	4.93	14.94	11.60	7.13	4.46	5.83	15.00	11.73	7.11	4.51	6.73	14.93	11.65	7.08	4.33
4.05	14.93	11.60	7.16	4.41	4.95	14.93	11.62	7.13	4.57	5.85	15.01	11.73	7.11	4.49	6.75	14.93	11.65	7.08	4.35
4.07	14.93	11.60	7.16	4.41	4.97	14.93	11.62	7.13	4.44	5.87	15.01	11.73	7.11	4.45	6.77	14.92	11.65	7.08	4.28
4.09	14.93	11.60	7.15	4.41	4.99	14.93	11.63	7.13	4.41	5.89	15.01	11.73	7.10	4.45	6.78	14.90	11.65	7.08	4.35
4.11	14.93	11.60	7.15	4.46	5.01	14.93	11.60	7.13	4.46	5.9	15.01	11.73	7.10	4.44	6.8	14.88	11.65	7.08	4.30
4.13	14.93	11.60	7.15	4.41	5.02	14.93	11.63	7.13	4.41	5.92	15.01	11.73	7.10	4.43	6.82	14.88	11.65	7.08	4.35
4.14	14.93	11.60	7.15	4.41	5.04	14.97	11.64	7.13	4.42	5.94	15.01	11.73	7.10	4.47	6.84	14.88	11.65	7.08	4.35
4.16	14.93	11.60	7.15	4.41	5.06	14.97	11.68	7.13	4.47	5.96	15.01	11.73	7.10	4.47	6.86	14.90	11.62	7.08	4.30
4.18	14.93	11.60	7.15	4.40	5.08	14.97	11.68	7.13	4.48	5.98	15.01	11.73	7.10	4.47	6.88	14.90	11.65	7.08	4.28
4.2	14.93	11.60	7.15	4.44	5.1	14.96	11.68	7.13	4.47	6	15.01	11.73	7.10	4.40	6.89	14.90	11.65	7.08	4.30
4.22	14.93	11.60	7.15	4.44	5.12	14.96	11.68	7.12	4.55	6.01	15.01	11.73	7.10	4.39	6.91	14.92	11.65	7.08	4.29
4.24	14.93	11.59	7.15	4.46	5.13	14.97	11.68	7.12	4.52	6.03	15.01	11.73	7.10	4.45	6.93	14.93	11.65	7.08	4.31
4.25	14.93	11.60	7.15	4.40	5.15	14.97	11.68	7.12	4.55	6.05	15.01	11.73	7.10	4.39	6.95	14.93	11.65	7.08	4.29
4.27	14.93	11.60	7.15	4.39	5.17	15.01	11.68	7.12	4.56	6.07	15.01	11.73	7.10	4.39	6.97	14.93	11.65	7.08	4.30
4.29	14.93	11.60	7.15	4.44	5.19	14.99	11.68	7.12	4.53	6.09	15.01	11.73	7.10	4.39	6.99	14.93	11.65	7.08	4.36
4.31	14.93	11.60	7.15	4.39	5.21	15.00	11.68	7.12	4.57	6.11	15.01	11.73	7.10	4.44	7	14.93	11.65	7.08	4.36
4.33	14.93	11.60	7.15	4.44	5.23	15.01	11.68	7.12	4.49	6.12	14.99	11.71	7.10	4.37	7.02	14.93	11.65	7.08	4.36
4.35	14.93	11.60	7.15	4.38	5.24	15.01	11.68	7.12	4.56	6.14	14.96	11.69	7.10	4.43	7.04	14.93	11.65	7.08	4.28
4.36	14.92	11.60	7.15	4.36	5.26	15.01	11.68	7.12	4.55	6.16	14.96	11.68	7.10	4.41	7.06	14.93	11.65	7.08	4.28
4.38	14.91	11.59	7.15	4.38	5.28	15.01	11.68	7.12	4.55	6.18	14.96	11.69	7.10	4.39	7.08	14.93	11.65	7.08	4.28
4.4	14.89	11.60	7.15	4.37	5.3	15.01	11.69	7.12	4.55	6.2	14.96	11.68	7.10	4.41	7.1	14.93	11.65	7.07	4.30
4.42	14.88	11.56	7.14	4.44	5.32	15.01	11.68	7.12	4.60	6.22	14.96	11.68	7.10	4.34	7.11	14.92	11.65	7.07	4.30
4.44	14.88	11.55	7.14	4.42	5.34	14.97	11.69	7.12	4.76	6.23	14.96	11.68	7.10	4.39	7.13	14.89	11.65	7.07	4.33
4.46	14.88	11.57	7.14	4.38	5.35	14.97	11.69	7.12	4.67	6.25	14.96	11.68	7.10	4.39	7.15	14.88	11.65	7.07	4.34
4.47	14.88	11.58	7.14	4.40	5.37	14.96	11.69	7.12	4.66	6.27	14.97	11.68	7.09	4.34	7.17	14.88	11.65	7.07	4.30

RH=45%, Tair=22°C, Tc=2°C, Q=9.33 L/s

Time (s)	Tray#1 (°C)	Tray#2 (°C)	Tray#3 (°C)	Tray#4 (°C)	Time (s)	Tray#1 (°C)	Tray#2 (°C)	Tray#3 (°C)	Tray#4 (°C)	Time (s)	Tray#1 (°C)	Tray#2 (°C)	Tray#3 (°C)	Tray#4 (°C)	Time (s)	Tray#1 (°C)	Tray#2 (°C)	Tray#3 (°C)	Tray#4 (°C)
0	19.4	16.079	15.64	5.17	0.9	14.47	9.78	5.24	2.59	1.79	14.37	9.54	4.94	2.34	2.69	14.3	9.46	4.86	2.18
0.02	18.56	15.55	8.95	4.47	0.91	14.47	9.73	5.21	2.57	1.81	14.38	9.54	4.94	2.3	2.71	14.25	9.41	4.81	2.17
0.04	18.31	15.14	8.70	3.77	0.93	14.44	9.73	5.20	2.57	1.83	14.32	9.49	4.89	2.3	2.73	14.3	9.46	4.86	2.16
0.05	18.09	14.79	8.44	3.57	0.95	14.42	9.73	5.19	2.6	1.85	14.29	9.47	4.89	2.27	2.75	14.3	9.46	4.84	2.14
0.07	17.86	14.46	8.21	3.37	0.97	14.37	9.63	5.13	2.6	1.87	14.4	9.55	4.98	2.27	2.76	14.3	9.46	4.84	2.18
0.09	17.64	14.16	8.01	3.17	0.99	14.46	9.72	5.18	2.57	1.88	14.33	9.49	4.93	2.29	2.78	14.3	9.44	4.81	2.16
0.11	17.43	13.86	7.86	3.12	1.01	14.46	9.72	5.18	2.56	1.9	14.32	9.49	4.93	2.3	2.8	14.28	9.4	4.79	2.18
0.13	17.22	13.62	7.68	2.93	1.02	14.42	9.72	5.18	2.55	1.92	14.37	9.53	4.97	2.26	2.82	14.28	9.4	4.79	2.13
0.14	17.02	13.32	7.49	2.93	1.04	14.42	9.72	5.18	2.55	1.94	14.32	9.48	4.90	2.24	2.84	14.28	9.4	4.79	2.17
0.16	16.85	13.06	7.33	2.88	1.06	14.36	9.62	5.12	2.54	1.96	14.37	9.53	4.94	2.19	2.85	14.28	9.39	4.79	2.16
0.18	16.69	12.85	7.21	2.87	1.08	14.44	9.7	5.17	2.47	1.98	14.37	9.53	4.93	2.29	2.87	14.28	9.39	4.79	2.17
0.2	16.49	12.6	7.06	2.86	1.1	14.44	9.7	5.16	2.54	1.99	14.37	9.53	4.93	2.24	2.89	14.28	9.39	4.79	2.17
0.22	16.34	12.4	6.94	2.84	1.12	14.44	9.68	5.16	2.54	2.01	14.37	9.53	4.93	2.28	2.91	14.28	9.39	4.79	2.13
0.24	16.22	12.2	6.85	2.84	1.13	14.43	9.65	5.16	2.52	2.03	14.37	9.53	4.93	2.29	2.93	14.33	9.44	4.84	2.13
0.25	16.07	12.03	6.70	2.82	1.15	14.41	9.65	5.12	2.54	2.05	14.37	9.53	4.93	2.24	2.95	14.26	9.39	4.75	2.12
0.27	15.92	11.83	6.61	2.78	1.17	14.35	9.6	5.05	2.48	2.07	14.37	9.53	4.93	2.31	2.96	14.31	9.44	4.79	2.1
0.29	15.77	11.64	6.45	2.83	1.19	14.39	9.65	5.11	2.52	2.09	14.32	9.48	4.88	2.28	2.98	14.24	9.39	4.74	2.11
0.31	15.7	11.5	6.41	2.77	1.21	14.39	9.65	5.11	2.53	2.1	14.32	9.48	4.88	2.29	3	14.3	9.44	4.79	2.1
0.33	15.6	11.35	6.30	2.77	1.23	14.34	9.58	5.05	2.53	2.12	14.37	9.52	4.93	2.3	3.02	14.3	9.44	4.79	2.1
0.35	15.45	11.2	6.21	2.77	1.24	14.42	9.64	5.14	2.52	2.14	14.37	9.53	4.93	2.29	3.04	14.28	9.41	4.79	2.15
0.36	15.37	11.09	6.13	2.75	1.26	14.42	9.63	5.13	2.51	2.16	14.37	9.52	4.93	2.27	3.06	14.28	9.41	4.79	2.1
0.38	15.33	10.98	6.06	2.75	1.28	14.42	9.63	5.09	2.45	2.18	14.37	9.53	4.93	2.3	3.08	14.24	9.38	4.74	2.15
0.4	15.23	10.88	6.01	2.74	1.3	14.42	9.63	5.09	2.48	2.2	14.37	9.51	4.92	2.24	3.09	14.23	9.37	4.74	2.07
0.42	15.14	10.78	5.91	2.73	1.32	14.37	9.58	5.03	2.47	2.21	14.32	9.43	4.86	2.21	3.11	14.28	9.39	4.79	2.14
0.44	15.11	10.71	5.89	2.72	1.33	14.4	9.63	5.09	2.41	2.23	14.37	9.5	4.89	2.26	3.13	14.28	9.39	4.75	2.11
0.46	15.01	10.56	5.79	2.68	1.35	14.38	9.62	5.08	2.5	2.25	14.37	9.48	4.88	2.26	3.15	14.23	9.34	4.70	2.12
0.47	15	10.53	5.76	2.68	1.37	14.37	9.59	5.04	2.5	2.27	14.37	9.49	4.91	2.24	3.17	14.23	9.34	4.69	2.11
0.49	14.92	10.48	5.68	2.71	1.39	14.37	9.58	5.03	2.48	2.29	14.4	9.51	4.92	2.25	3.18	14.23	9.34	4.69	2.08
0.51	14.84	10.36	5.61	2.66	1.41	14.4	9.61	5.07	2.47	2.31	14.35	9.46	4.87	2.26	3.2	14.23	9.34	4.69	2.05
0.53	14.84	10.36	5.62	2.66	1.43	14.4	9.61	5.07	2.42	2.32	14.4	9.51	4.91	2.18	3.22	14.28	9.39	4.74	2.1
0.55	14.8	10.31	5.57	2.69	1.44	14.37	9.56	5.07	2.45	2.34	14.37	9.48	4.88	2.24	3.24	14.23	9.34	4.69	2.12
0.57	14.76	10.23	5.56	2.64	1.46	14.4	9.61	5.07	2.42	2.36	14.38	9.51	4.91	2.21	3.26	14.28	9.39	4.74	2.04
0.58	14.78	10.21	5.55	2.66	1.48	14.4	9.61	5.06	2.43	2.38	14.3	9.46	4.86	2.24	3.28	14.23	9.33	4.69	2.04
0.6	14.73	10.15	5.50	2.64	1.5	14.4	9.61	5.03	2.4	2.4	14.35	9.51	4.91	2.26	3.29	14.23	9.34	4.69	2.05
0.62	14.63	10.05	5.47	2.62	1.52	14.4	9.59	5.01	2.43	2.42	14.3	9.46	4.86	2.21	3.31	14.28	9.38	4.73	2.05
0.64	14.68	10.08	5.45	2.65	1.54	14.35	9.53	4.96	2.42	2.43	14.3	9.46	4.86	2.26	3.33	14.23	9.32	4.68	2.08
0.66	14.66	10.08	5.44	2.62	1.55	14.38	9.56	5.01	2.43	2.45	14.35	9.5	4.91	2.24	3.35	14.28	9.35	4.69	2.04
0.68	14.65	10.03	5.43	2.62	1.57	14.36	9.56	5.01	2.42	2.47	14.3	9.42	4.86	2.26	3.37	14.28	9.35	4.69	2.1
0.69	14.61	9.98	5.38	2.66	1.59	14.35	9.56	4.99	2.39	2.49	14.3	9.44	4.86	2.2	3.39	14.28	9.34	4.69	2.05
0.71	14.57	9.95	5.38	2.65	1.61	14.38	9.59	5.00	2.38	2.51	14.29	9.42	4.86	2.24	3.4	14.23	9.29	4.66	2.03
0.73	14.56	9.92	5.33	2.63	1.63	14.33	9.54	4.94	2.39	2.53	14.33	9.46	4.88	2.18	3.42	14.23	9.29	4.66	2.09
0.75	14.53	9.87	5.33	2.62	1.65	14.33	9.53	4.99	2.32	2.54	14.27	9.41	4.84	2.2	3.44	14.26	9.34	4.69	2.01
0.77	14.54	9.9	5.32	2.64	1.66	14.38	9.57	4.99	2.38	2.56	14.25	9.41	4.81	2.25	3.46	14.21	9.29	4.66	2.05
0.79	14.54	9.85	5.31	2.64	1.68	14.38	9.55	4.99	2.36	2.58	14.25	9.41	4.81	2.18	3.48	14.23	9.34	4.69	2.07
0.8	14.49	9.84	5.28	2.64	1.7	14.38	9.54	4.99	2.34	2.6	14.25	9.41	4.81	2.19	3.5	14.25	9.33	4.71	2.07
0.82	14.49	9.8	5.26	2.6	1.72	14.38	9.54	4.99	2.37	2.62	14.25	9.41	4.81	2.19	3.51	14.21	9.29	4.66	2.01
0.84	14.52	9.83	5.29	2.6	1.74	14.33	9.49	4.93	2.28	2.64	14.25	9.41	4.81	2.23	3.53	14.25	9.33	4.70	2.01
0.86	14.48	9.81	5.26	2.59	1.76	14.38	9.54	4.96	2.35	2.65	14.3	9.46	4.86	2.19	3.55	14.25	9.33	4.70	2.06
0.88	14.47	9.78	5.24	2.62	1.77	14.37	9.54	4.94	2.3	2.67	14.28	9.46	4.81	2.16	3.57	14.27	9.38	4.72	1.99

RH=45%, Tair=22°C, Tc=2°C, Q=9.33 L/s

Time (s)	Tray#1 (°C)	Tray#2 (°C)	Tray#3 (°C)	Tray#4 (°C)	Time (s)	Tray#1 (°C)	Tray#2 (°C)	Tray#3 (°C)	Tray#4 (°C)	Time (s)	Tray#1 (°C)	Tray#2 (°C)	Tray#3 (°C)	Tray#4 (°C)	Time (s)	Tray#1 (°C)	Tray#2 (°C)	Tray#3 (°C)	Tray#4 (°C)
3.59	14.25	9.33	4.66	2.03	4.49	14.16	9.19	4.56	1.99	5.38	14.25	9.31	4.66	1.97	6.28	14.23	9.27	4.59	1.93
3.61	14.27	9.36	4.71	2.04	4.5	14.18	9.19	4.56	1.91	5.4	14.2	9.26	4.63	1.99	6.3	14.18	9.2	4.56	1.89
3.62	14.27	9.36	4.71	2	4.52	14.2	9.2	4.56	1.94	5.42	14.2	9.26	4.63	1.97	6.32	14.23	9.24	4.59	1.95
3.64	14.25	9.28	4.65	2.03	4.54	14.21	9.25	4.60	1.94	5.44	14.2	9.26	4.63	1.97	6.34	14.18	9.23	4.56	1.9
3.66	14.25	9.29	4.65	2.02	4.56	14.21	9.24	4.59	1.96	5.46	14.2	9.26	4.63	2	6.35	14.18	9.22	4.56	1.92
3.68	14.25	9.28	4.65	2.07	4.58	14.17	9.19	4.56	1.9	5.48	14.2	9.26	4.63	2	6.37	14.18	9.22	4.56	1.96
3.7	14.25	9.28	4.65	2.04	4.6	14.22	9.24	4.61	1.89	5.49	14.2	9.26	4.63	2.06	6.39	14.18	9.23	4.56	1.96
3.72	14.25	9.28	4.65	2.07	4.61	14.2	9.19	4.55	1.89	5.51	14.2	9.27	4.63	2.01	6.41	14.18	9.23	4.56	1.9
3.73	14.27	9.34	4.71	2.08	4.63	14.21	9.24	4.61	1.9	5.53	14.2	9.26	4.63	2.02	6.43	14.18	9.23	4.56	1.9
3.75	14.25	9.28	4.65	2.03	4.65	14.17	9.19	4.56	1.94	5.55	14.2	9.26	4.63	2.01	6.45	14.18	9.24	4.56	1.9
3.77	14.23	9.28	4.65	2.03	4.67	14.21	9.24	4.61	1.95	5.57	14.2	9.26	4.63	1.97	6.46	14.23	9.29	4.59	1.92
3.79	14.24	9.28	4.65	2.02	4.69	14.21	9.24	4.61	1.93	5.59	14.2	9.26	4.63	1.99	6.48	14.18	9.24	4.56	1.94
3.81	14.25	9.28	4.65	2.02	4.71	14.21	9.19	4.61	1.95	5.6	14.2	9.26	4.63	2	6.5	14.18	9.24	4.56	1.93
3.83	14.27	9.33	4.71	1.99	4.72	14.21	9.25	4.61	1.93	5.62	14.2	9.26	4.63	1.99	6.52	14.18	9.24	4.56	1.9
3.84	14.26	9.33	4.71	2.07	4.74	14.18	9.2	4.56	1.96	5.64	14.2	9.26	4.63	1.99	6.54	14.23	9.29	4.59	1.95
3.86	14.21	9.28	4.65	2.04	4.76	14.18	9.2	4.56	1.92	5.66	14.2	9.26	4.63	1.99	6.56	14.18	9.24	4.56	1.94
3.88	14.21	9.28	4.63	2.01	4.78	14.17	9.21	4.56	1.95	5.68	14.2	9.26	4.63	1.98	6.57	14.19	9.24	4.56	2
3.9	14.23	9.28	4.65	2	4.8	14.21	9.26	4.61	1.99	5.69	14.18	9.24	4.60	1.97	6.59	14.23	9.29	4.60	1.95
3.92	14.21	9.28	4.65	1.99	4.82	14.16	9.19	4.56	1.99	5.71	14.22	9.26	4.63	1.98	6.61	14.23	9.29	4.60	1.96
3.94	14.21	9.28	4.65	2.04	4.83	14.19	9.2	4.56	1.98	5.73	14.22	9.26	4.63	1.97	6.63	14.19	9.24	4.58	1.94
3.95	14.26	9.33	4.69	2.03	4.85	14.18	9.21	4.56	1.94	5.75	14.2	9.23	4.60	1.98	6.65	14.22	9.24	4.59	2.02
3.97	14.26	9.33	4.68	1.98	4.87	14.19	9.21	4.56	1.95	5.77	14.21	9.23	4.60	1.97	6.67	14.23	9.24	4.59	1.94
3.99	14.26	9.33	4.65	1.99	4.89	14.21	9.23	4.58	1.95	5.79	14.19	9.24	4.60	1.97	6.68	14.2	9.21	4.55	1.94
4.01	14.24	9.28	4.60	1.99	4.91	14.21	9.23	4.61	2	5.8	14.21	9.23	4.59	1.93	6.7	14.2	9.21	4.55	2
4.03	14.26	9.32	4.65	1.98	4.93	14.21	9.24	4.61	1.97	5.82	14.21	9.23	4.59	1.98	6.72	14.2	9.21	4.55	1.99
4.05	14.26	9.33	4.65	1.96	4.94	14.21	9.24	4.61	1.95	5.84	14.21	9.23	4.57	1.98	6.74	14.2	9.22	4.55	1.96
4.06	14.25	9.33	4.65	2.04	4.96	14.21	9.24	4.61	1.98	5.86	14.21	9.23	4.57	1.93	6.76	14.2	9.23	4.55	1.98
4.08	14.25	9.32	4.65	2.01	4.98	14.23	9.29	4.66	1.97	5.88	14.22	9.25	4.60	1.95	6.78	14.2	9.23	4.55	1.97
4.1	14.23	9.28	4.60	2.02	5	14.23	9.29	4.66	2.01	5.9	14.22	9.27	4.59	1.95	6.79	14.2	9.24	4.55	1.95
4.12	14.25	9.32	4.65	1.97	5.02	14.21	9.24	4.61	1.99	5.91	14.22	9.28	4.59	1.94	6.81	14.19	9.23	4.55	1.95
4.14	14.21	9.28	4.60	2.02	5.04	14.21	9.24	4.61	1.99	5.93	14.22	9.24	4.60	1.92	6.83	14.2	9.26	4.55	1.95
4.16	14.25	9.33	4.65	2.02	5.05	14.21	9.24	4.61	1.99	5.95	14.22	9.26	4.59	1.93	6.85	14.25	9.3	4.61	1.93
4.17	14.25	9.32	4.65	2.03	5.07	14.23	9.29	4.66	2.02	5.97	14.22	9.26	4.60	1.95	6.87	14.2	9.26	4.55	1.92
4.19	14.2	9.26	4.60	2.01	5.09	14.21	9.24	4.61	2.05	5.99	14.22	9.23	4.60	1.93	6.89	14.2	9.26	4.55	1.92
4.21	14.2	9.27	4.60	1.96	5.11	14.21	9.24	4.66	2.05	6.01	14.22	9.27	4.59	1.94	6.9	14.2	9.26	4.55	1.92
4.23	14.25	9.3	4.65	2	5.13	14.21	9.26	4.66	2	6.02	14.22	9.26	4.59	1.94	6.92	14.2	9.26	4.55	1.92
4.25	14.2	9.24	4.60	1.96	5.15	14.21	9.28	4.66	2.01	6.04	14.22	9.28	4.60	1.92	6.94	14.2	9.26	4.55	1.95
4.27	14.2	9.24	4.60	2.01	5.16	14.21	9.29	4.66	2.03	6.06	14.22	9.25	4.60	1.93	6.96	14.2	9.26	4.55	2.01
4.28	14.25	9.28	4.65	2.01	5.18	14.18	9.26	4.63	2.06	6.08	14.22	9.28	4.60	1.96	6.98	14.2	9.26	4.55	1.96
4.3	14.26	9.3	4.65	1.96	5.2	14.18	9.26	4.63	2.04	6.1	14.22	9.28	4.60	1.96	7	14.21	9.26	4.55	1.95
4.32	14.21	9.24	4.60	1.96	5.22	14.18	9.26	4.63	2.03	6.12	14.22	9.28	4.60	1.94	7.01	14.21	9.26	4.55	1.95
4.34	14.25	9.31	4.65	1.99	5.24	14.18	9.26	4.63	2.04	6.13	14.22	9.28	4.60	1.94	7.03	14.26	9.31	4.61	1.94
4.36	14.25	9.3	4.65	1.96	5.26	14.18	9.26	4.63	2.02	6.15	14.21	9.26	4.60	1.95	7.05	14.21	9.26	4.55	1.96
4.38	14.26	9.28	4.65	1.96	5.27	14.18	9.26	4.63	2.03	6.17	14.2	9.26	4.60	1.95	7.07	14.27	9.31	4.62	1.96
4.39	14.21	9.2	4.56	2	5.29	14.19	9.26	4.63	2	6.19	14.15	9.21	4.56	1.97	7.09	14.24	9.26	4.55	1.97
4.41	14.22	9.26	4.61	2.01	5.31	14.2	9.26	4.63	2.01	6.21	14.19	9.26	4.58	1.95	7.11	14.27	9.31	4.61	1.98
4.43	14.21	9.25	4.61	1.97	5.33	14.18	9.26	4.63	2	6.23	14.14	9.2	4.54	1.92	7.12	14.24	9.26	4.56	1.97
4.45	14.21	9.24	4.61	2	5.35	14.2	9.26	4.63	1.99	6.24	14.16	9.2	4.56	1.94	7.14	14.27	9.31	4.62	2
4.47	14.16	9.2	4.56	1.99	5.36	14.2	9.26	4.63	1.97	6.26	14.22	9.26	4.59	1.94	7.16	14.3	9.31	4.62	1.96

RH=80%, Tair=22°C, Tc=21°C, Q=9.33 L/s

Time (s)	Tray#1 (°C)	Tray#2 (°C)	Tray#3 (°C)	Tray#4 (°C)	Time (s)	Tray#1 (°C)	Tray#2 (°C)	Tray#3 (°C)	Tray#4 (°C)	Time (s)	Tray#1 (°C)	Tray#2 (°C)	Tray#3 (°C)	Tray#4 (°C)	Time (s)	Tray#1 (°C)	Tray#2 (°C)	Tray#3 (°C)	Tray#4 (°C)
0	21.78	21.31	20.43	19.59	0.86	20.42	20.26	20.21	19.57	1.71	20.21	20.10	20.20	19.60	2.56	20.13	20.09	20.28	19.69
0.02	21.58	21.09	20.39	19.59	0.87	20.41	20.25	20.21	19.62	1.73	20.25	20.14	20.25	19.65	2.58	20.11	20.09	20.28	19.69
0.04	21.31	20.90	20.38	19.59	0.89	20.37	20.21	20.21	19.62	1.74	20.24	20.14	20.26	19.69	2.6	20.11	20.08	20.28	19.74
0.05	21.11	20.70	20.38	19.54	0.91	20.37	20.21	20.21	19.62	1.76	20.20	20.10	20.28	19.69	2.61	20.10	20.09	20.28	19.74
0.07	21.10	20.67	20.34	19.53	0.92	20.37	20.21	20.21	19.57	1.78	20.24	20.14	20.24	19.69	2.63	20.10	20.09	20.28	19.69
0.09	21.08	20.67	20.31	19.50	0.94	20.37	20.21	20.21	19.57	1.8	20.24	20.14	20.25	19.64	2.65	20.11	20.09	20.28	19.74
0.11	21.03	20.66	20.35	19.54	0.96	20.37	20.21	20.21	19.57	1.81	20.23	20.14	20.26	19.69	2.67	20.12	20.09	20.28	19.74
0.12	20.95	20.58	20.33	19.54	0.98	20.37	20.21	20.21	19.62	1.83	20.22	20.14	20.25	19.69	2.68	20.12	20.09	20.28	19.74
0.14	20.91	20.58	20.34	19.59	0.99	20.34	20.21	20.24	19.57	1.85	20.23	20.13	20.28	19.69	2.7	20.13	20.09	20.28	19.74
0.16	20.94	20.63	20.33	19.54	1.01	20.33	20.21	20.21	19.65	1.86	20.22	20.14	20.26	19.69	2.72	20.13	20.09	20.28	19.74
0.18	20.90	20.59	20.33	19.54	1.03	20.33	20.20	20.24	19.62	1.88	20.21	20.12	20.27	19.70	2.73	20.12	20.09	20.28	19.69
0.19	20.88	20.58	20.33	19.59	1.05	20.34	20.19	20.24	19.65	1.9	20.20	20.14	20.27	19.65	2.75	20.12	20.09	20.28	19.74
0.21	20.83	20.58	20.33	19.59	1.06	20.34	20.20	20.21	19.57	1.92	20.20	20.12	20.25	19.71	2.77	20.13	20.09	20.28	19.69
0.23	20.83	20.54	20.33	19.59	1.08	20.35	20.22	20.24	19.60	1.93	20.20	20.12	20.26	19.69	2.79	20.11	20.09	20.28	19.74
0.25	20.78	20.53	20.33	19.59	1.1	20.35	20.22	20.24	19.60	1.95	20.20	20.11	20.27	19.69	2.8	20.10	20.08	20.28	19.69
0.26	20.76	20.53	20.30	19.59	1.12	20.32	20.19	20.24	19.60	1.97	20.20	20.12	20.28	19.71	2.82	20.10	20.08	20.28	19.74
0.28	20.74	20.48	20.29	19.59	1.13	20.35	20.20	20.24	19.65	1.99	20.20	20.11	20.28	19.65	2.84	20.11	20.08	20.28	19.75
0.3	20.73	20.48	20.29	19.59	1.15	20.35	20.19	20.24	19.65	2	20.20	20.11	20.27	19.69	2.86	20.11	20.09	20.28	19.73
0.32	20.71	20.48	20.28	19.59	1.17	20.35	20.19	20.24	19.65	2.02	20.20	20.11	20.27	19.69	2.87	20.11	20.08	20.28	19.73
0.33	20.69	20.46	20.28	19.59	1.19	20.33	20.19	20.24	19.60	2.04	20.19	20.10	20.28	19.65	2.89	20.11	20.09	20.28	19.71
0.35	20.67	20.45	20.28	19.59	1.2	20.31	20.19	20.24	19.65	2.06	20.18	20.10	20.27	19.67	2.91	20.10	20.08	20.28	19.75
0.37	20.66	20.43	20.28	19.54	1.22	20.30	20.19	20.24	19.65	2.07	20.20	20.10	20.28	19.69	2.93	20.11	20.09	20.28	19.75
0.39	20.65	20.43	20.31	19.62	1.24	20.30	20.19	20.24	19.65	2.09	20.18	20.10	20.28	19.68	2.94	20.10	20.08	20.28	19.70
0.4	20.62	20.40	20.31	19.62	1.26	20.30	20.18	20.24	19.65	2.11	20.18	20.09	20.27	19.71	2.96	20.10	20.08	20.28	19.75
0.42	20.62	20.40	20.31	19.62	1.27	20.30	20.18	20.24	19.60	2.13	20.18	20.09	20.27	19.73	2.98	20.10	20.08	20.28	19.75
0.44	20.65	20.41	20.30	19.57	1.29	20.30	20.17	20.24	19.65	2.14	20.18	20.10	20.28	19.71	3	20.10	20.08	20.28	19.75
0.45	20.62	20.41	20.26	19.62	1.31	20.30	20.17	20.24	19.60	2.16	20.17	20.10	20.27	19.71	3.01	20.10	20.08	20.28	19.74
0.47	20.60	20.40	20.26	19.62	1.33	20.30	20.17	20.24	19.60	2.18	20.17	20.09	20.28	19.69	3.03	20.10	20.08	20.28	19.74
0.49	20.60	20.38	20.26	19.62	1.34	20.29	20.17	20.23	19.65	2.2	20.19	20.09	20.28	19.70	3.05	20.10	20.08	20.28	19.74
0.51	20.59	20.38	20.26	19.62	1.36	20.26	20.17	20.23	19.60	2.21	20.18	20.09	20.27	19.65	3.07	20.10	20.08	20.28	19.74
0.52	20.58	20.37	20.26	19.62	1.38	20.25	20.16	20.22	19.65	2.23	20.17	20.09	20.28	19.70	3.08	20.11	20.09	20.28	19.74
0.54	20.55	20.36	20.26	19.62	1.39	20.25	20.15	20.21	19.60	2.25	20.15	20.09	20.28	19.66	3.1	20.11	20.08	20.28	19.79
0.56	20.55	20.36	20.26	19.59	1.41	20.25	20.13	20.21	19.66	2.27	20.15	20.09	20.27	19.70	3.12	20.12	20.07	20.28	19.79
0.58	20.54	20.36	20.26	19.57	1.43	20.25	20.14	20.20	19.65	2.28	20.15	20.09	20.27	19.70	3.14	20.11	20.08	20.28	19.74
0.59	20.53	20.33	20.26	19.57	1.45	20.25	20.12	20.20	19.65	2.3	20.15	20.09	20.28	19.73	3.15	20.11	20.08	20.28	19.79
0.61	20.52	20.33	20.26	19.57	1.46	20.25	20.12	20.24	19.66	2.32	20.15	20.09	20.25	19.70	3.17	20.10	20.08	20.28	19.79
0.63	20.52	20.33	20.26	19.57	1.48	20.25	20.12	20.22	19.65	2.33	20.15	20.09	20.25	19.66	3.19	20.10	20.07	20.28	19.79
0.65	20.52	20.32	20.26	19.57	1.5	20.24	20.12	20.24	19.60	2.35	20.15	20.09	20.25	19.67	3.2	20.10	20.07	20.28	19.79
0.66	20.52	20.31	20.26	19.62	1.52	20.25	20.12	20.21	19.65	2.37	20.15	20.09	20.25	19.69	3.22	20.10	20.07	20.28	19.74
0.68	20.48	20.31	20.26	19.62	1.53	20.23	20.12	20.19	19.61	2.39	20.15	20.09	20.27	19.73	3.24	20.09	20.08	20.29	19.79
0.7	20.47	20.30	20.25	19.62	1.55	20.24	20.12	20.21	19.61	2.4	20.15	20.09	20.26	19.70	3.26	20.09	20.07	20.29	19.79
0.72	20.47	20.29	20.25	19.62	1.57	20.21	20.12	20.21	19.61	2.42	20.15	20.09	20.26	19.70	3.27	20.09	20.07	20.28	19.79
0.73	20.47	20.27	20.26	19.62	1.59	20.21	20.12	20.20	19.61	2.44	20.15	20.09	20.28	19.71	3.29	20.08	20.07	20.29	19.79
0.75	20.47	20.26	20.26	19.62	1.6	20.21	20.12	20.22	19.61	2.46	20.13	20.09	20.28	19.67	3.31	20.08	20.07	20.30	19.74
0.77	20.43	20.26	20.23	19.62	1.62	20.21	20.12	20.21	19.65	2.47	20.13	20.09	20.28	19.69	3.33	20.07	20.07	20.28	19.79
0.79	20.43	20.26	20.23	19.62	1.64	20.21	20.12	20.20	19.65	2.49	20.12	20.09	20.28	19.69	3.34	20.09	20.08	20.30	19.79
0.8	20.42	20.26	20.26	19.62	1.66	20.21	20.10	20.20	19.65	2.51	20.13	20.09	20.28	19.74	3.36	20.09	20.07	20.28	19.81
0.82	20.42	20.26	20.23	19.57	1.67	20.21	20.11	20.25	19.69	2.53	20.12	20.09	20.28	19.69	3.38	20.09	20.08	20.29	19.79
0.84	20.42	20.26	20.23	19.57	1.69	20.21	20.11	20.26	19.69	2.54	20.13	20.09	20.27	19.69	3.4	20.09	20.07	20.29	19.79

RH=80%, Tair=22°C, Tc=21°C, Q=9.33 L/s

Time (s)	Tray#1 (°C)	Tray#2 (°C)	Tray#3 (°C)	Tray#4 (°C)	Time (s)	Tray#1 (°C)	Tray#2 (°C)	Tray#3 (°C)	Tray#4 (°C)	Time (s)	Tray#1 (°C)	Tray#2 (°C)	Tray#3 (°C)	Tray#4 (°C)	Time (s)	Tray#1 (°C)	Tray#2 (°C)	Tray#3 (°C)	Tray#4 (°C)
3.41	20.09	20.08	20.31	19.80	4.27	20.05	20.07	20.33	19.84	5.12	20.02	20.07	20.33	19.89	5.97	20.02	20.06	20.38	19.84
3.43	20.08	20.07	20.33	19.79	4.28	20.04	20.07	20.33	19.84	5.14	20.02	20.06	20.34	19.89	5.99	20.02	20.05	20.38	19.84
3.45	20.08	20.08	20.33	19.79	4.3	20.05	20.07	20.33	19.84	5.15	20.02	20.07	20.33	19.89	6.01	20.02	20.06	20.38	19.84
3.47	20.09	20.08	20.33	19.75	4.32	20.04	20.07	20.33	19.79	5.17	20.02	20.07	20.34	19.89	6.02	20.01	20.05	20.41	19.84
3.48	20.09	20.08	20.33	19.80	4.34	20.03	20.07	20.33	19.84	5.19	20.02	20.07	20.33	19.89	6.04	20.02	20.06	20.41	19.92
3.5	20.09	20.07	20.33	19.78	4.35	20.04	20.07	20.33	19.79	5.21	20.02	20.06	20.33	19.88	6.06	20.02	20.05	20.41	19.88
3.52	20.09	20.07	20.33	19.78	4.37	20.05	20.07	20.33	19.79	5.22	20.02	20.06	20.33	19.84	6.08	20.04	20.09	20.38	19.84
3.54	20.10	20.08	20.33	19.79	4.39	20.04	20.07	20.33	19.79	5.24	20.03	20.07	20.33	19.84	6.09	20.05	20.09	20.41	19.88
3.55	20.10	20.09	20.33	19.79	4.41	20.03	20.07	20.33	19.79	5.26	20.02	20.07	20.34	19.84	6.11	20.05	20.10	20.38	19.89
3.57	20.10	20.09	20.33	19.78	4.42	20.04	20.07	20.33	19.79	5.28	20.02	20.07	20.33	19.89	6.13	20.02	20.05	20.41	19.92
3.59	20.10	20.08	20.33	19.79	4.44	20.04	20.07	20.33	19.79	5.29	20.02	20.07	20.33	19.89	6.15	20.05	20.08	20.41	19.92
3.61	20.11	20.08	20.33	19.84	4.46	20.05	20.07	20.33	19.79	5.31	20.02	20.06	20.33	19.84	6.16	20.02	20.06	20.41	19.92
3.62	20.09	20.08	20.33	19.83	4.48	20.05	20.07	20.33	19.84	5.33	20.02	20.07	20.33	19.89	6.18	20.05	20.08	20.41	19.92
3.64	20.09	20.07	20.33	19.79	4.49	20.05	20.07	20.33	19.82	5.35	20.02	20.07	20.33	19.84	6.2	20.05	20.08	20.41	19.92
3.66	20.08	20.07	20.32	19.83	4.51	20.04	20.07	20.33	19.80	5.36	20.02	20.07	20.33	19.89	6.22	20.05	20.08	20.41	19.92
3.67	20.08	20.07	20.33	19.83	4.53	20.05	20.07	20.33	19.80	5.38	20.02	20.06	20.33	19.84	6.23	20.04	20.09	20.41	19.87
3.69	20.08	20.07	20.33	19.78	4.54	20.04	20.07	20.33	19.80	5.4	20.02	20.06	20.33	19.89	6.25	20.03	20.09	20.41	19.92
3.71	20.08	20.07	20.33	19.82	4.56	20.05	20.07	20.33	19.85	5.41	20.02	20.06	20.33	19.89	6.27	20.05	20.09	20.41	19.92
3.73	20.07	20.08	20.33	19.84	4.58	20.04	20.07	20.33	19.85	5.43	20.02	20.05	20.33	19.89	6.29	20.04	20.09	20.41	19.92
3.74	20.07	20.07	20.33	19.84	4.6	20.03	20.07	20.33	19.79	5.45	20.02	20.06	20.33	19.84	6.3	20.05	20.09	20.41	19.92
3.76	20.07	20.07	20.33	19.84	4.61	20.02	20.07	20.33	19.84	5.47	19.99	20.06	20.33	19.84	6.32	20.03	20.09	20.41	19.92
3.78	20.07	20.07	20.33	19.79	4.63	20.03	20.07	20.33	19.84	5.48	20.02	20.06	20.33	19.84	6.34	20.03	20.09	20.41	19.92
3.8	20.07	20.07	20.33	19.84	4.65	20.03	20.07	20.33	19.84	5.5	20.02	20.06	20.33	19.84	6.35	20.04	20.08	20.41	19.92
3.81	20.07	20.07	20.33	19.84	4.67	20.04	20.07	20.33	19.84	5.52	20.02	20.06	20.33	19.84	6.37	20.04	20.08	20.39	19.92
3.83	20.07	20.07	20.33	19.84	4.68	20.05	20.07	20.33	19.84	5.54	20.02	20.06	20.33	19.84	6.39	20.03	20.08	20.39	19.92
3.85	20.07	20.07	20.33	19.84	4.7	20.04	20.07	20.33	19.84	5.55	20.02	20.05	20.34	19.84	6.41	20.03	20.08	20.41	19.92
3.87	20.07	20.07	20.33	19.79	4.72	20.04	20.07	20.34	19.79	5.57	20.02	20.05	20.37	19.84	6.42	20.03	20.08	20.41	19.92
3.88	20.07	20.07	20.33	19.79	4.74	20.04	20.07	20.33	19.84	5.59	20.02	20.05	20.39	19.89	6.44	20.03	20.08	20.41	19.92
3.9	20.06	20.07	20.33	19.84	4.75	20.04	20.07	20.33	19.84	5.61	20.02	20.05	20.36	19.92	6.46	20.04	20.08	20.41	19.87
3.92	20.07	20.07	20.33	19.84	4.77	20.02	20.07	20.33	19.84	5.62	20.02	20.05	20.38	19.89	6.48	20.02	20.08	20.41	19.87
3.94	20.07	20.07	20.33	19.79	4.79	20.02	20.07	20.33	19.79	5.64	20.04	20.07	20.38	19.84	6.49	20.03	20.08	20.41	19.87
3.95	20.07	20.07	20.33	19.79	4.81	20.02	20.07	20.33	19.81	5.66	20.03	20.06	20.35	19.84	6.51	20.04	20.08	20.41	19.87
3.97	20.07	20.07	20.33	19.79	4.82	20.02	20.07	20.33	19.82	5.68	20.05	20.09	20.35	19.84	6.53	20.04	20.08	20.41	19.87
3.99	20.07	20.07	20.33	19.79	4.84	20.03	20.07	20.33	19.82	5.69	20.02	20.05	20.33	19.89	6.55	20.03	20.09	20.41	19.87
4.01	20.07	20.07	20.33	19.79	4.86	20.02	20.07	20.33	19.85	5.71	20.02	20.07	20.33	19.84	6.56	20.03	20.08	20.41	19.92
4.02	20.07	20.07	20.33	19.79	4.88	20.02	20.07	20.33	19.81	5.73	20.02	20.06	20.38	19.89	6.58	20.03	20.08	20.41	19.92
4.04	20.07	20.07	20.33	19.79	4.89	20.02	20.07	20.33	19.86	5.75	20.02	20.06	20.35	19.89	6.6	20.03	20.08	20.41	19.87
4.06	20.06	20.07	20.33	19.79	4.91	20.02	20.07	20.33	19.85	5.76	20.01	20.05	20.35	19.84	6.62	20.05	20.08	20.41	19.92
4.07	20.07	20.07	20.33	19.84	4.93	20.03	20.07	20.33	19.81	5.78	20.02	20.05	20.34	19.89	6.63	20.04	20.08	20.41	19.92
4.09	20.07	20.07	20.33	19.84	4.95	20.03	20.07	20.33	19.85	5.8	20.00	20.06	20.34	19.89	6.65	20.03	20.08	20.41	19.92
4.11	20.07	20.07	20.33	19.84	4.96	20.03	20.07	20.33	19.87	5.82	20.00	20.06	20.37	19.87	6.67	20.03	20.08	20.41	19.92
4.13	20.07	20.07	20.33	19.84	4.98	20.02	20.07	20.33	19.83	5.83	20.00	20.06	20.34	19.89	6.69	20.04	20.08	20.41	19.93
4.14	20.07	20.07	20.33	19.79	5	20.02	20.07	20.33	19.82	5.85	20.02	20.06	20.35	19.84					
4.16	20.06	20.07	20.33	19.84	5.01	20.02	20.07	20.33	19.80	5.87	20.05	20.08	20.35	19.89					
4.18	20.07	20.07	20.33	19.84	5.03	20.02	20.07	20.33	19.83	5.88	20.02	20.05	20.37	19.89					
4.2	20.07	20.07	20.33	19.84	5.05	20.02	20.07	20.33	19.83	5.9	20.02	20.06	20.36	19.89					
4.21	20.07	20.07	20.33	19.84	5.07	20.02	20.07	20.33	19.87	5.92	20.02	20.06	20.36	19.89					
4.23	20.05	20.07	20.33	19.84	5.08	20.02	20.07	20.33	19.89	5.94	20.02	20.06	20.38	19.89					
4.25	20.05	20.07	20.33	19.79	5.1	20.02	20.07	20.33	19.84	5.95	20.02	20.05	20.38	19.89					

RH=65%, Tair=22°C, Tc=21°C, Q=9.33 L/s

Time (s)	Tray#1 (°C)	Tray#2 (°C)	Tray#3 (°C)	Tray#4 (°C)	Time (s)	Tray#1 (°C)	Tray#2 (°C)	Tray#3 (°C)	Tray#4 (°C)	Time (s)	Tray#1 (°C)	Tray#2 (°C)	Tray#3 (°C)	Tray#4 (°C)	Time (s)	Tray#1 (°C)	Tray#2 (°C)	Tray#3 (°C)	Tray#4 (°C)
0.00	20.48	20.29	19.84	19.45	0.90	20.01	19.91	19.76	19.46	1.79	20.04	19.94	19.88	19.50	2.69	20.07	19.99	19.96	19.61
0.02	20.42	20.27	19.85	19.40	0.91	20.00	19.87	19.76	19.40	1.81	20.04	19.94	19.88	19.53	2.71	20.07	20.01	19.96	19.61
0.03	20.37	20.22	19.81	19.37	0.93	19.96	19.87	19.76	19.40	1.83	20.04	19.94	19.88	19.53	2.73	20.07	20.01	19.96	19.57
0.05	20.36	20.21	19.82	19.37	0.95	19.99	19.90	19.76	19.48	1.85	20.02	19.94	19.86	19.48	2.75	20.07	19.99	19.96	19.61
0.07	20.34	20.19	19.83	19.40	0.97	19.99	19.90	19.74	19.47	1.87	20.02	19.97	19.86	19.51	2.77	20.07	20.00	19.96	19.61
0.09	20.29	20.14	19.78	19.37	0.99	19.99	19.86	19.74	19.43	1.89	20.02	19.95	19.86	19.51	2.78	20.07	20.00	19.96	19.56
0.11	20.27	20.17	19.80	19.38	1.01	19.96	19.85	19.74	19.40	1.90	20.02	19.96	19.86	19.56	2.80	20.07	20.02	19.96	19.63
0.13	20.22	20.12	19.76	19.40	1.02	19.98	19.88	19.77	19.41	1.92	20.02	19.92	19.86	19.51	2.82	20.06	20.02	19.96	19.61
0.14	20.20	20.10	19.78	19.36	1.04	19.97	19.88	19.77	19.41	1.94	20.02	19.92	19.86	19.52	2.84	20.07	20.02	19.96	19.57
0.16	20.18	20.08	19.77	19.44	1.06	19.97	19.88	19.76	19.41	1.96	20.05	19.95	19.89	19.54	2.86	20.02	19.97	19.96	19.56
0.18	20.17	20.05	19.72	19.39	1.08	20.00	19.91	19.75	19.41	1.98	20.05	19.95	19.89	19.52	2.88	20.03	19.97	19.96	19.56
0.20	20.16	20.06	19.76	19.38	1.10	19.95	19.86	19.75	19.39	2.00	20.05	19.95	19.89	19.54	2.89	20.03	19.99	19.96	19.62
0.22	20.14	20.04	19.78	19.39	1.12	19.95	19.86	19.75	19.44	2.01	20.05	19.95	19.89	19.54	2.91	20.06	20.00	19.96	19.57
0.24	20.13	20.02	19.74	19.40	1.13	19.95	19.86	19.75	19.44	2.03	20.01	19.95	19.89	19.55	2.93	20.06	19.98	19.96	19.56
0.25	20.12	20.02	19.77	19.39	1.15	20.00	19.90	19.79	19.43	2.05	20.03	19.98	19.92	19.53	2.95	20.06	19.98	19.96	19.61
0.27	20.07	19.97	19.72	19.42	1.17	19.97	19.87	19.79	19.43	2.07	20.03	19.98	19.88	19.52	2.97	20.04	19.98	19.96	19.61
0.29	20.10	20.00	19.75	19.42	1.19	19.97	19.88	19.77	19.41	2.09	20.03	19.96	19.87	19.52	2.99	20.09	20.00	19.99	19.59
0.31	20.05	19.95	19.70	19.37	1.21	19.98	19.88	19.77	19.45	2.11	20.03	19.94	19.87	19.57	3.00	20.07	20.01	19.99	19.64
0.33	20.08	19.96	19.73	19.39	1.23	19.98	19.88	19.77	19.43	2.12	20.03	19.93	19.88	19.52	3.02	20.10	20.02	19.99	19.59
0.35	20.03	19.93	19.71	19.40	1.24	19.98	19.88	19.77	19.44	2.14	20.03	19.93	19.87	19.49	3.04	20.05	19.99	19.99	19.54
0.36	20.07	19.95	19.72	19.44	1.26	19.98	19.88	19.77	19.41	2.16	20.07	19.97	19.91	19.56	3.06	20.05	20.00	19.98	19.59
0.38	20.02	19.92	19.72	19.44	1.28	20.00	19.91	19.80	19.44	2.18	20.06	19.97	19.91	19.61	3.08	20.05	20.00	19.99	19.59
0.40	20.05	19.94	19.71	19.37	1.30	19.96	19.89	19.80	19.43	2.20	20.05	19.97	19.91	19.57	3.10	20.05	20.00	19.99	19.59
0.42	20.02	19.94	19.73	19.37	1.32	19.96	19.86	19.78	19.42	2.22	20.03	19.97	19.91	19.56	3.11	20.06	20.00	19.99	19.59
0.44	20.03	19.94	19.73	19.40	1.34	19.96	19.86	19.76	19.45	2.23	20.02	19.97	19.91	19.56	3.13	20.05	20.00	19.99	19.65
0.46	20.05	19.93	19.72	19.43	1.35	19.99	19.89	19.78	19.42	2.25	20.02	19.97	19.91	19.51	3.15	20.05	20.00	19.99	19.61
0.47	20.04	19.92	19.71	19.38	1.37	19.99	19.89	19.78	19.47	2.27	20.02	19.94	19.90	19.51	3.17	20.05	20.00	19.97	19.61
0.49	20.04	19.91	19.71	19.43	1.39	19.99	19.89	19.78	19.42	2.29	20.05	19.97	19.91	19.54	3.19	20.05	20.00	19.99	19.64
0.51	20.02	19.92	19.74	19.41	1.41	20.02	19.92	19.81	19.46	2.31	20.03	19.96	19.92	19.54	3.21	20.06	20.01	19.99	19.64
0.53	20.02	19.92	19.71	19.37	1.43	20.01	19.92	19.81	19.46	2.33	20.01	19.95	19.92	19.54	3.22	20.00	19.95	19.93	19.54
0.55	20.02	19.90	19.74	19.44	1.45	19.98	19.90	19.81	19.46	2.34	20.01	19.96	19.93	19.54	3.24	20.05	20.00	19.95	19.64
0.57	20.00	19.90	19.74	19.44	1.46	19.97	19.88	19.81	19.46	2.36	20.05	19.95	19.93	19.54	3.26	20.05	20.00	19.95	19.59
0.58	20.03	19.92	19.73	19.47	1.48	20.01	19.91	19.85	19.47	2.38	20.05	19.95	19.92	19.59	3.28	20.05	20.00	19.98	19.59
0.60	19.99	19.88	19.76	19.42	1.50	20.01	19.91	19.81	19.50	2.40	20.08	19.98	19.94	19.57	3.30	20.05	20.00	19.97	19.59
0.62	20.02	19.92	19.76	19.46	1.52	20.01	19.91	19.81	19.46	2.42	20.08	19.98	19.95	19.57	3.32	20.05	20.00	19.98	19.64
0.64	20.02	19.92	19.76	19.41	1.54	20.04	19.94	19.83	19.53	2.44	20.08	19.98	19.92	19.62	3.33	20.05	20.00	19.99	19.65
0.66	20.05	19.90	19.75	19.43	1.56	20.01	19.92	19.83	19.48	2.45	20.03	19.98	19.92	19.55	3.35	20.05	20.00	19.97	19.59
0.68	20.00	19.90	19.75	19.45	1.57	20.04	19.94	19.83	19.53	2.47	20.03	19.98	19.92	19.52	3.37	20.05	20.00	19.99	19.60
0.69	20.03	19.93	19.78	19.42	1.59	20.02	19.96	19.86	19.51	2.49	20.03	19.98	19.92	19.52	3.39	20.05	20.00	19.99	19.59
0.71	20.03	19.88	19.74	19.42	1.61	20.02	19.94	19.86	19.54	2.51	20.04	19.98	19.93	19.52	3.41	20.05	20.00	19.97	19.59
0.73	19.98	19.88	19.73	19.41	1.63	20.02	19.92	19.86	19.55	2.53	20.04	19.98	19.92	19.58	3.43	20.05	20.00	19.99	19.65
0.75	20.01	19.91	19.76	19.45	1.65	20.02	19.92	19.86	19.46	2.55	20.03	19.98	19.92	19.53	3.44	20.05	20.00	19.99	19.65
0.77	20.01	19.89	19.76	19.40	1.67	20.02	19.92	19.81	19.47	2.56	20.03	19.98	19.92	19.57	3.46	20.05	20.00	19.99	19.59
0.79	19.96	19.86	19.72	19.44	1.68	20.06	19.96	19.86	19.55	2.58	20.03	19.98	19.92	19.52	3.48	20.05	20.00	19.99	19.59
0.80	19.99	19.89	19.74	19.45	1.70	20.02	19.96	19.85	19.51	2.60	19.98	19.93	19.87	19.48	3.50	20.05	20.00	19.99	19.60
0.82	19.99	19.89	19.74	19.39	1.72	20.01	19.96	19.85	19.50	2.62	20.03	19.98	19.92	19.58	3.52	20.05	20.00	19.99	19.64
0.84	20.00	19.88	19.77	19.41	1.74	20.01	19.92	19.85	19.54	2.64	20.03	19.98	19.92	19.58	3.54	20.05	20.00	19.99	19.67
0.86	19.97	19.87	19.77	19.41	1.76	20.03	19.94	19.88	19.53	2.66	20.03	19.98	19.92	19.53	3.55	20.05	20.00	19.99	19.65
0.88	19.97	19.87	19.73	19.46	1.78	20.04	19.94	19.88	19.49	2.67	20.07	20.00	19.96	19.57	3.57	20.05	20.00	19.99	19.67

RH=65%, Tair=22°C, Tc=21°C, Q=9.33 L/s

Time (s)	Tray#1 (°C)	Tray#2 (°C)	Tray#3 (°C)	Tray#4 (°C)	Time (s)	Tray#1 (°C)	Tray#2 (°C)	Tray#3 (°C)	Tray#4 (°C)	Time (s)	Tray#1 (°C)	Tray#2 (°C)	Tray#3 (°C)	Tray#4 (°C)	Time (s)	Tray#1 (°C)	Tray#2 (°C)	Tray#3 (°C)	Tray#4 (°C)
3.59	20.05	20.00	19.99	19.66	4.49	20.06	20.05	20.04	19.69	5.39	20.08	20.08	20.12	19.73	6.29	20.08	20.13	20.17	19.82
3.61	20.05	20.00	19.99	19.62	4.51	20.08	20.05	20.04	19.69	5.41	20.08	20.08	20.11	19.76	6.30	20.08	20.13	20.17	19.82
3.63	20.05	20.00	19.99	19.67	4.53	20.05	20.05	20.04	19.74	5.42	20.08	20.08	20.12	19.81	6.32	20.08	20.13	20.17	19.87
3.65	20.05	20.00	19.99	19.60	4.54	20.08	20.05	20.04	19.74	5.44	20.08	20.10	20.09	19.81	6.34	20.08	20.13	20.17	19.82
3.66	20.05	20.00	19.99	19.63	4.56	20.06	20.05	20.04	19.74	5.46	20.05	20.13	20.12	19.72	6.36	20.13	20.13	20.17	19.87
3.68	20.05	20.00	19.99	19.62	4.58	20.06	20.05	20.04	19.74	5.48	20.11	20.13	20.12	19.77	6.38	20.06	20.08	20.12	19.82
3.70	20.05	20.00	19.99	19.64	4.60	20.10	20.07	20.06	19.74	5.50	20.11	20.13	20.12	19.77	6.40	20.09	20.13	20.17	19.82
3.72	20.05	20.00	19.99	19.65	4.62	20.10	20.09	20.07	19.74	5.52	20.06	20.08	20.07	19.77	6.41	20.09	20.13	20.17	19.82
3.74	20.05	20.00	19.99	19.65	4.64	20.05	20.05	20.05	19.69	5.53	20.06	20.08	20.07	19.72	6.43	20.08	20.13	20.17	19.87
3.76	20.05	20.00	19.99	19.68	4.65	20.06	20.05	20.08	19.69	5.55	20.03	20.08	20.07	19.77	6.45	20.08	20.13	20.17	19.82
3.77	20.05	20.00	19.99	19.68	4.67	20.07	20.05	20.06	19.70	5.57	20.08	20.13	20.12	19.82	6.47	20.08	20.13	20.17	19.87
3.79	20.05	20.00	19.99	19.64	4.69	20.09	20.05	20.05	19.69	5.59	20.08	20.13	20.12	19.77	6.49	20.11	20.14	20.17	19.85
3.81	20.00	19.95	19.94	19.59	4.71	20.07	20.05	20.05	19.74	5.61	20.03	20.08	20.07	19.72	6.51	20.08	20.13	20.17	19.82
3.83	20.05	20.00	19.99	19.60	4.73	20.05	20.05	20.04	19.69	5.63	20.08	20.13	20.12	19.77	6.52	20.08	20.14	20.17	19.87
3.85	20.05	20.00	19.99	19.62	4.75	20.05	20.05	20.04	19.69	5.64	20.09	20.13	20.12	19.77	6.54	20.10	20.14	20.17	19.87
3.87	20.05	20.00	19.99	19.64	4.76	20.08	20.08	20.08	19.77	5.66	20.09	20.13	20.12	19.78	6.56	20.08	20.13	20.17	19.82
3.88	20.05	20.00	19.99	19.63	4.78	20.09	20.08	20.07	19.72	5.68	20.09	20.13	20.12	19.78	6.58	20.10	20.14	20.17	19.82
3.90	20.05	20.00	19.99	19.68	4.80	20.09	20.08	20.07	19.78	5.70	20.08	20.08	20.08	19.77	6.60	20.08	20.09	20.12	19.77
3.92	20.05	20.00	19.99	19.69	4.82	20.09	20.08	20.08	19.77	5.72	20.06	20.08	20.07	19.77	6.62	20.11	20.15	20.17	19.90
3.94	20.05	20.01	19.99	19.64	4.84	20.08	20.08	20.10	19.79	5.74	20.10	20.13	20.14	19.82	6.63	20.07	20.12	20.12	19.82
3.96	20.05	20.01	19.99	19.64	4.86	20.09	20.09	20.10	19.77	5.75	20.12	20.13	20.14	19.85	6.65	20.09	20.14	20.17	19.83
3.98	20.05	20.00	19.99	19.64	4.87	20.08	20.08	20.07	19.72	5.77	20.10	20.13	20.12	19.79	6.67	20.08	20.13	20.17	19.87
3.99	20.05	20.00	19.99	19.69	4.89	20.09	20.08	20.08	19.72	5.79	20.08	20.13	20.12	19.77	6.69	20.08	20.13	20.17	19.83
4.01	20.05	20.00	19.99	19.69	4.91	20.08	20.08	20.07	19.77	5.81	20.08	20.13	20.13	19.82	6.71	20.08	20.13	20.17	19.83
4.03	20.05	20.00	19.99	19.69	4.93	20.08	20.08	20.07	19.77	5.83	20.12	20.13	20.17	19.77	6.73	20.08	20.13	20.17	19.90
4.05	20.05	20.00	19.99	19.69	4.95	20.08	20.08	20.07	19.72	5.85	20.13	20.13	20.17	19.82	6.74	20.10	20.15	20.18	19.87
4.07	20.05	20.00	19.99	19.64	4.97	20.08	20.08	20.07	19.72	5.86	20.13	20.13	20.17	19.79	6.76	20.11	20.18	20.17	19.91
4.09	20.05	20.03	19.99	19.64	4.98	20.08	20.08	20.07	19.72	5.88	20.11	20.13	20.15	19.78	6.78	20.11	20.17	20.18	19.86
4.10	20.05	20.01	19.99	19.64	5.00	20.08	20.08	20.07	19.72	5.90	20.12	20.13	20.17	19.79	6.80	20.10	20.17	20.18	19.86
4.12	20.05	20.01	19.99	19.64	5.02	20.08	20.08	20.07	19.72	5.92	20.12	20.13	20.17	19.82	6.82	20.07	20.14	20.16	19.83
4.14	20.05	20.00	19.99	19.69	5.04	20.08	20.08	20.07	19.72	5.94	20.09	20.13	20.15	19.79	6.84	20.08	20.14	20.15	19.87
4.16	20.05	20.00	19.99	19.64	5.06	20.08	20.08	20.08	19.77	5.96	20.08	20.13	20.13	19.78	6.85	20.08	20.11	20.14	19.84
4.18	20.05	20.00	19.99	19.69	5.08	20.08	20.08	20.11	19.73	5.97	20.08	20.13	20.16	19.82	6.87	20.06	20.15	20.15	19.81
4.20	20.05	20.00	19.99	19.69	5.09	20.09	20.10	20.11	19.76	5.99	20.09	20.13	20.17	19.83	6.89	20.08	20.14	20.17	19.82
4.21	20.03	20.00	19.99	19.64	5.11	20.09	20.09	20.12	19.79	6.01	20.11	20.13	20.17	19.87	6.91	20.08	20.15	20.18	19.84
4.23	20.05	20.00	19.99	19.69	5.13	20.08	20.10	20.12	19.75	6.03	20.13	20.13	20.17	19.82	6.93	20.09	20.15	20.18	19.89
4.25	20.05	20.02	20.00	19.64	5.15	20.09	20.09	20.08	19.81	6.05	20.09	20.13	20.17	19.82	6.95	20.09	20.14	20.19	19.84
4.27	20.05	20.02	20.03	19.65	5.17	20.08	20.08	20.07	19.72	6.07	20.09	20.14	20.17	19.87	6.96	20.10	20.15	20.19	19.87
4.29	20.05	20.05	20.03	19.64	5.19	20.08	20.08	20.07	19.72	6.08	20.08	20.13	20.17	19.82	6.98	20.10	20.15	20.19	19.84
4.31	20.05	20.05	20.04	19.64	5.20	20.08	20.08	20.07	19.77	6.10	20.09	20.13	20.17	19.84	7.00	20.10	20.15	20.19	19.89
4.32	20.05	20.05	20.04	19.64	5.22	20.08	20.08	20.07	19.72	6.12	20.08	20.13	20.16	19.85	7.02	20.10	20.15	20.19	19.89
4.34	20.05	20.05	20.04	19.69	5.24	20.08	20.08	20.12	19.72	6.14	20.13	20.14	20.17	19.82	7.04	20.10	20.15	20.19	19.89
4.36	20.07	20.05	20.04	19.72	5.26	20.08	20.08	20.11	19.79	6.16	20.08	20.13	20.17	19.82	7.06	20.10	20.15	20.14	19.84
4.38	20.07	20.05	20.04	19.69	5.28	20.08	20.08	20.10	19.73	6.18	20.08	20.13	20.17	19.87	7.07	20.10	20.15	20.19	19.85
4.40	20.09	20.05	20.04	19.74	5.30	20.08	20.08	20.09	19.72	6.19	20.08	20.13	20.17	19.86	7.09	20.10	20.15	20.19	19.85
4.42	20.10	20.05	20.04	19.69	5.31	20.08	20.08	20.10	19.76	6.21	20.10	20.13	20.17	19.82	7.11	20.10	20.15	20.19	19.89
4.43	20.05	20.05	20.04	19.66	5.33	20.08	20.08	20.10	19.78	6.23	20.10	20.13	20.17	19.82	7.13	20.10	20.15	20.19	19.92
4.45	20.05	20.05	20.04	19.69	5.35	20.08	20.08	20.09	19.72	6.25	20.09	20.13	20.17	19.87	7.15	20.10	20.15	20.19	19.84
4.47	20.05	20.05	20.04	19.68	5.37	20.08	20.08	20.10	19.81	6.27	20.08	20.13	20.17	19.87	7.17	20.10	20.15	20.19	19.84

RH=45%, Tair=22°C, Tc=21°C, Q=9.33 L/s

Time (s)	Tray#1 (°C)	Tray#2 (°C)	Tray#3 (°C)	Tray#4 (°C)	Time (s)	Tray#1 (°C)	Tray#2 (°C)	Tray#3 (°C)	Tray#4 (°C)	Time (s)	Tray#1 (°C)	Tray#2 (°C)	Tray#3 (°C)	Tray#4 (°C)	Time (s)	Tray#1 (°C)	Tray#2 (°C)	Tray#3 (°C)	Tray#4 (°C)
0	21.36	21.26	20.63	19.79	0.9	20.53	20.38	20.24	19.77	1.79	20.54	20.39	20.33	19.86	2.69	20.51	20.4	20.33	19.85
0.02	21.3	21.24	20.58	19.81	0.91	20.53	20.38	20.22	19.81	1.81	20.53	20.39	20.33	19.8	2.71	20.5	20.39	20.33	19.89
0.04	21.23	21.19	20.58	19.76	0.93	20.53	20.38	20.22	19.77	1.83	20.52	20.39	20.33	19.84	2.73	20.5	20.39	20.33	19.89
0.05	21.14	21.12	20.51	19.78	0.95	20.56	20.4	20.26	19.81	1.85	20.52	20.39	20.33	19.83	2.75	20.5	20.39	20.33	19.84
0.07	21.15	21.1	20.54	19.82	0.97	20.53	20.37	20.26	19.81	1.87	20.51	20.39	20.33	19.78	2.76	20.49	20.39	20.33	19.88
0.09	21.01	21	20.44	19.77	0.99	20.52	20.37	20.21	19.81	1.89	20.5	20.39	20.33	19.78	2.78	20.49	20.39	20.33	19.84
0.11	20.98	20.94	20.42	19.76	1.01	20.55	20.4	20.24	19.84	1.9	20.49	20.39	20.33	19.78	2.8	20.49	20.39	20.33	19.9
0.13	20.96	20.91	20.4	19.78	1.02	20.55	20.4	20.24	19.76	1.92	20.49	20.39	20.33	19.79	2.82	20.53	20.43	20.38	19.89
0.14	20.91	20.86	20.36	19.73	1.04	20.53	20.4	20.24	19.76	1.94	20.49	20.39	20.33	19.78	2.84	20.53	20.43	20.38	19.89
0.16	20.89	20.84	20.39	19.77	1.06	20.54	20.39	20.27	19.77	1.96	20.49	20.39	20.32	19.78	2.86	20.53	20.43	20.39	19.88
0.18	20.93	20.85	20.43	19.85	1.08	20.53	20.38	20.27	19.82	1.98	20.49	20.39	20.29	19.83	2.87	20.54	20.44	20.38	19.95
0.2	20.83	20.75	20.36	19.78	1.1	20.53	20.38	20.27	19.77	2	20.49	20.39	20.32	19.83	2.89	20.53	20.44	20.38	19.9
0.22	20.81	20.72	20.34	19.78	1.12	20.53	20.38	20.26	19.82	2.01	20.49	20.39	20.31	19.78	2.91	20.53	20.44	20.39	19.97
0.24	20.79	20.7	20.34	19.76	1.13	20.56	20.41	20.25	19.79	2.03	20.49	20.39	20.3	19.78	2.93	20.53	20.43	20.39	19.94
0.26	20.78	20.71	20.32	19.76	1.15	20.52	20.41	20.25	19.81	2.05	20.49	20.39	20.33	19.83	2.95	20.53	20.43	20.38	19.94
0.27	20.82	20.71	20.33	19.84	1.17	20.51	20.36	20.25	19.75	2.07	20.49	20.39	20.33	19.81	2.97	20.53	20.43	20.38	19.88
0.29	20.76	20.67	20.31	19.78	1.19	20.51	20.36	20.25	19.75	2.09	20.49	20.39	20.33	19.81	2.98	20.53	20.43	20.38	19.9
0.31	20.76	20.67	20.31	19.83	1.21	20.55	20.4	20.29	19.84	2.1	20.49	20.39	20.31	19.79	3	20.53	20.43	20.38	19.94
0.33	20.73	20.6	20.29	19.75	1.23	20.54	20.4	20.29	19.84	2.12	20.49	20.39	20.32	19.8	3.02	20.53	20.43	20.38	19.92
0.35	20.69	20.55	20.24	19.78	1.24	20.55	20.4	20.28	19.79	2.14	20.49	20.39	20.33	19.85	3.04	20.53	20.43	20.38	19.87
0.36	20.67	20.58	20.27	19.79	1.26	20.54	20.43	20.28	19.82	2.16	20.49	20.39	20.32	19.87	3.06	20.53	20.43	20.38	19.92
0.38	20.7	20.56	20.25	19.81	1.28	20.53	20.4	20.28	19.78	2.18	20.49	20.39	20.33	19.87	3.08	20.53	20.43	20.38	19.92
0.4	20.7	20.56	20.28	19.83	1.3	20.53	20.38	20.27	19.77	2.2	20.49	20.39	20.33	19.84	3.09	20.53	20.43	20.38	19.87
0.42	20.67	20.54	20.26	19.8	1.32	20.53	20.38	20.27	19.77	2.21	20.49	20.39	20.31	19.81	3.11	20.53	20.43	20.38	19.92
0.44	20.64	20.49	20.26	19.72	1.34	20.53	20.38	20.27	19.82	2.23	20.49	20.39	20.33	19.87	3.13	20.53	20.43	20.38	19.92
0.46	20.65	20.52	20.27	19.74	1.35	20.52	20.41	20.3	19.8	2.25	20.49	20.39	20.33	19.88	3.15	20.53	20.43	20.38	19.87
0.47	20.65	20.5	20.25	19.79	1.37	20.51	20.41	20.3	19.85	2.27	20.49	20.39	20.33	19.83	3.17	20.53	20.43	20.38	19.92
0.49	20.63	20.49	20.27	19.78	1.39	20.51	20.4	20.29	19.8	2.29	20.49	20.39	20.33	19.83	3.19	20.53	20.43	20.38	19.87
0.51	20.63	20.48	20.23	19.77	1.41	20.51	20.39	20.27	19.83	2.31	20.49	20.39	20.33	19.88	3.2	20.53	20.43	20.38	19.87
0.53	20.62	20.46	20.26	19.79	1.43	20.51	20.36	20.32	19.75	2.32	20.49	20.39	20.33	19.88	3.22	20.53	20.43	20.38	19.87
0.55	20.61	20.46	20.21	19.75	1.45	20.55	20.4	20.3	19.84	2.34	20.49	20.39	20.33	19.88	3.24	20.53	20.43	20.38	19.92
0.57	20.6	20.47	20.25	19.8	1.46	20.55	20.4	20.29	19.79	2.36	20.49	20.39	20.33	19.83	3.26	20.53	20.43	20.38	19.92
0.59	20.6	20.46	20.25	19.75	1.48	20.55	20.4	20.29	19.79	2.38	20.49	20.39	20.33	19.88	3.28	20.53	20.43	20.38	19.87
0.6	20.59	20.45	20.22	19.73	1.5	20.53	20.4	20.29	19.79	2.4	20.49	20.39	20.33	19.88	3.3	20.53	20.43	20.38	19.88
0.62	20.58	20.44	20.23	19.73	1.52	20.51	20.4	20.29	19.84	2.42	20.49	20.39	20.33	19.88	3.31	20.52	20.43	20.38	19.92
0.64	20.61	20.47	20.26	19.76	1.54	20.53	20.43	20.32	19.87	2.43	20.49	20.39	20.33	19.83	3.33	20.53	20.43	20.38	19.89
0.66	20.59	20.43	20.26	19.76	1.56	20.53	20.39	20.32	19.87	2.45	20.49	20.39	20.33	19.88	3.35	20.53	20.43	20.38	19.93
0.68	20.56	20.42	20.21	19.81	1.57	20.53	20.39	20.32	19.86	2.47	20.5	20.39	20.33	19.83	3.37	20.52	20.43	20.38	19.94
0.69	20.59	20.45	20.24	19.74	1.59	20.53	20.38	20.3	19.82	2.49	20.49	20.39	20.33	19.83	3.39	20.51	20.43	20.38	19.93
0.71	20.56	20.4	20.24	19.79	1.61	20.53	20.38	20.27	19.84	2.51	20.49	20.39	20.33	19.88	3.41	20.52	20.43	20.38	19.92
0.73	20.55	20.4	20.22	19.74	1.63	20.51	20.38	20.34	19.82	2.53	20.49	20.39	20.33	19.83	3.42	20.49	20.43	20.38	19.87
0.75	20.58	20.43	20.22	19.81	1.65	20.57	20.42	20.32	19.86	2.54	20.49	20.39	20.33	19.88	3.44	20.52	20.43	20.38	19.94
0.77	20.54	20.39	20.22	19.72	1.67	20.52	20.42	20.31	19.81	2.56	20.49	20.39	20.33	19.83	3.46	20.52	20.46	20.38	19.96
0.79	20.57	20.42	20.26	19.76	1.68	20.52	20.42	20.31	19.81	2.58	20.49	20.39	20.33	19.88	3.48	20.56	20.46	20.41	19.97
0.8	20.57	20.42	20.22	19.76	1.7	20.52	20.42	20.31	19.86	2.6	20.49	20.39	20.33	19.88	3.5	20.53	20.43	20.38	19.91
0.82	20.52	20.38	20.25	19.78	1.72	20.52	20.42	20.31	19.86	2.62	20.49	20.39	20.33	19.83	3.52	20.53	20.43	20.38	19.92
0.84	20.55	20.4	20.24	19.77	1.74	20.52	20.41	20.31	19.81	2.64	20.49	20.39	20.33	19.88	3.53	20.56	20.46	20.41	20
0.86	20.55	20.4	20.24	19.75	1.76	20.52	20.38	20.31	19.86	2.65	20.51	20.39	20.34	19.83	3.55	20.55	20.46	20.41	19.99
0.88	20.58	20.43	20.27	19.82	1.78	20.54	20.4	20.33	19.87	2.67	20.51	20.4	20.33	19.88	3.57	20.55	20.46	20.41	19.95

RH=45%, Tair=22°C, Tc=21°C, Q=9.33 L/s

Time (s)	Tray#1 (°C)	Tray#2 (°C)	Tray#3 (°C)	Tray#4 (°C)	Time (s)	Tray#1 (°C)	Tray#2 (°C)	Tray#3 (°C)	Tray#4 (°C)	Time (s)	Tray#1 (°C)	Tray#2 (°C)	Tray#3 (°C)	Tray#4 (°C)	Time (s)	Tray#1 (°C)	Tray#2 (°C)	Tray#3 (°C)	Tray#4 (°C)
3.59	20.52	20.46	20.41	19.95	4.49	20.55	20.49	20.48	20.03	5.38	20.55	20.53	20.55	20.11	6.28	20.55	20.55	20.59	20.14
3.61	20.52	20.46	20.41	19.9	4.5	20.57	20.51	20.48	20.03	5.4	20.57	20.53	20.54	20.11	6.3	20.55	20.55	20.59	20.1
3.63	20.51	20.46	20.41	19.95	4.52	20.54	20.49	20.48	19.98	5.42	20.57	20.53	20.56	20.06	6.32	20.55	20.55	20.59	20.16
3.64	20.51	20.46	20.41	19.96	4.54	20.53	20.49	20.48	20.02	5.44	20.57	20.53	20.56	20.11	6.34	20.55	20.55	20.59	20.15
3.66	20.52	20.46	20.41	19.95	4.56	20.53	20.49	20.48	20.03	5.46	20.57	20.53	20.53	20.1	6.35	20.52	20.51	20.55	20.06
3.68	20.52	20.46	20.41	19.9	4.58	20.54	20.49	20.48	19.97	5.47	20.56	20.53	20.53	20.11	6.37	20.54	20.55	20.55	20.09
3.7	20.51	20.46	20.41	19.9	4.6	20.53	20.49	20.48	20.02	5.49	20.57	20.53	20.53	20.11	6.39	20.53	20.55	20.55	20.1
3.72	20.52	20.46	20.41	19.91	4.61	20.53	20.49	20.48	20.02	5.51	20.54	20.53	20.53	20.06	6.41	20.54	20.55	20.55	20.1
3.74	20.52	20.46	20.41	19.96	4.63	20.53	20.49	20.48	19.97	5.53	20.54	20.53	20.54	20.06	6.43	20.55	20.54	20.55	20.1
3.75	20.51	20.46	20.41	19.9	4.65	20.53	20.49	20.48	19.97	5.55	20.56	20.53	20.57	20.06	6.45	20.56	20.56	20.57	20.1
3.77	20.52	20.46	20.43	19.98	4.67	20.53	20.49	20.48	20.02	5.57	20.56	20.53	20.57	20.11	6.46	20.56	20.56	20.57	20.15
3.79	20.51	20.46	20.42	19.97	4.69	20.53	20.49	20.48	19.98	5.58	20.57	20.53	20.57	20.11	6.48	20.56	20.56	20.59	20.15
3.81	20.51	20.46	20.41	19.9	4.71	20.53	20.49	20.48	19.97	5.6	20.57	20.54	20.57	20.07	6.5	20.56	20.56	20.59	20.1
3.83	20.51	20.46	20.45	20	4.72	20.53	20.49	20.48	19.97	5.62	20.57	20.54	20.57	20.06	6.52	20.56	20.56	20.57	20.15
3.85	20.52	20.46	20.45	19.95	4.74	20.53	20.49	20.48	19.97	5.64	20.57	20.55	20.57	20.06	6.54	20.56	20.56	20.6	20.15
3.86	20.54	20.46	20.45	20	4.76	20.53	20.49	20.48	19.97	5.66	20.57	20.58	20.57	20.11	6.56	20.56	20.56	20.6	20.1
3.88	20.53	20.46	20.45	19.95	4.78	20.53	20.49	20.48	20.02	5.68	20.57	20.58	20.57	20.11	6.57	20.56	20.56	20.6	20.1
3.9	20.52	20.46	20.45	19.95	4.8	20.57	20.53	20.52	20.06	5.69	20.57	20.57	20.57	20.06	6.59	20.56	20.56	20.6	20.11
3.92	20.56	20.51	20.5	19.99	4.82	20.57	20.53	20.52	20.01	5.71	20.57	20.55	20.57	20.06	6.61	20.56	20.56	20.6	20.15
3.94	20.56	20.51	20.5	19.98	4.83	20.57	20.53	20.52	20.01	5.73	20.57	20.54	20.57	20.11	6.63	20.56	20.56	20.6	20.1
3.95	20.55	20.51	20.5	20.04	4.85	20.57	20.53	20.52	20.01	5.75	20.57	20.53	20.57	20.06	6.65	20.56	20.56	20.6	20.11
3.97	20.55	20.51	20.5	20.04	4.87	20.57	20.53	20.52	20.06	5.77	20.57	20.54	20.57	20.11	6.67	20.56	20.56	20.6	20.17
3.99	20.55	20.51	20.5	19.98	4.89	20.57	20.53	20.52	20.06	5.79	20.53	20.54	20.53	20.11	6.68	20.56	20.56	20.6	20.16
4.01	20.55	20.51	20.5	20.03	4.91	20.56	20.53	20.52	20.06	5.8	20.53	20.54	20.53	20.03	6.7	20.56	20.56	20.6	20.15
4.03	20.55	20.51	20.5	19.97	4.93	20.57	20.53	20.52	20.01	5.82	20.53	20.53	20.53	20.08	6.72	20.56	20.56	20.6	20.16
4.05	20.55	20.51	20.5	19.97	4.94	20.56	20.53	20.52	20.01	5.84	20.53	20.52	20.53	20.08	6.74	20.56	20.56	20.6	20.11
4.06	20.55	20.51	20.5	20	4.96	20.56	20.53	20.52	20.06	5.86	20.53	20.54	20.53	20.12	6.76	20.56	20.56	20.6	20.13
4.08	20.55	20.51	20.5	19.99	4.98	20.54	20.53	20.52	20.06	5.88	20.53	20.54	20.53	20.12	6.78	20.56	20.56	20.6	20.14
4.1	20.55	20.51	20.48	20.01	5	20.54	20.53	20.52	20.06	5.9	20.53	20.54	20.53	20.12	6.79	20.56	20.56	20.6	20.15
4.12	20.55	20.51	20.47	19.97	5.02	20.57	20.53	20.52	20.06	5.91	20.53	20.54	20.53	20.07	6.81	20.56	20.56	20.6	20.15
4.14	20.55	20.51	20.46	20.01	5.04	20.57	20.53	20.52	20.01	5.93	20.53	20.54	20.53	20.12	6.83	20.56	20.56	20.6	20.2
4.16	20.55	20.51	20.45	20.03	5.05	20.56	20.53	20.52	20.06	5.95	20.5	20.51	20.5	20.04	6.85	20.56	20.56	20.6	20.2
4.17	20.55	20.51	20.45	19.94	5.07	20.57	20.53	20.52	20.06	5.97	20.5	20.51	20.53	20.09	6.87	20.56	20.56	20.6	20.15
4.19	20.55	20.5	20.46	19.95	5.09	20.56	20.53	20.52	20.01	5.99	20.5	20.51	20.54	20.04	6.88	20.56	20.56	20.6	20.15
4.21	20.55	20.51	20.47	20.01	5.11	20.56	20.53	20.52	20.03	6.01	20.5	20.51	20.54	20.04	6.9	20.56	20.56	20.6	20.15
4.23	20.55	20.51	20.49	20.02	5.13	20.55	20.53	20.52	20.01	6.02	20.5	20.51	20.54	20.04	6.92	20.56	20.56	20.6	20.2
4.25	20.55	20.51	20.45	19.99	5.15	20.52	20.53	20.52	20.01	6.04	20.5	20.51	20.54	20.09	6.94	20.56	20.56	20.6	20.2
4.27	20.55	20.51	20.45	19.96	5.16	20.56	20.53	20.52	20.06	6.06	20.51	20.51	20.54	20.09	6.96	20.56	20.56	20.6	20.18
4.28	20.55	20.51	20.46	19.96	5.18	20.53	20.53	20.52	20.06	6.08	20.54	20.52	20.54	20.04	6.98	20.56	20.56	20.6	20.15
4.3	20.55	20.51	20.45	19.98	5.2	20.55	20.53	20.52	20.02	6.1	20.52	20.53	20.55	20.13	7	20.56	20.57	20.6	20.15
4.32	20.55	20.51	20.46	19.97	5.22	20.55	20.53	20.52	20.05	6.12	20.55	20.55	20.56	20.09	7.01	20.56	20.57	20.6	20.2
4.34	20.55	20.51	20.45	19.97	5.24	20.57	20.53	20.52	20.02	6.13	20.55	20.55	20.58	20.14	7.03	20.56	20.57	20.6	20.15
4.36	20.55	20.5	20.45	20.02	5.26	20.55	20.53	20.52	20.05	6.15	20.55	20.55	20.59	20.09	7.05	20.56	20.57	20.6	20.15
4.38	20.51	20.47	20.45	19.95	5.27	20.56	20.53	20.52	20.05	6.17	20.55	20.55	20.59	20.09	7.07	20.56	20.56	20.6	20.2
4.39	20.52	20.46	20.45	19.94	5.29	20.52	20.53	20.52	20.02	6.19	20.55	20.55	20.59	20.09	7.09	20.56	20.56	20.6	20.2
4.41	20.55	20.49	20.45	19.94	5.31	20.53	20.53	20.52	20.07	6.21	20.55	20.55	20.59	20.09	7.1	20.56	20.57	20.6	20.15
4.43	20.52	20.46	20.48	20	5.33	20.52	20.53	20.52	20.06	6.23	20.55	20.55	20.59	20.09	7.12	20.56	20.56	20.6	20.15
4.45	20.58	20.53	20.48	20	5.35	20.56	20.53	20.52	20.04	6.24	20.55	20.55	20.59	20.14	7.14	20.56	20.56	20.6	20.15
4.47	20.56	20.52	20.48	19.98	5.36	20.54	20.53	20.52	20.11	6.26	20.55	20.55	20.59	20.1	7.16	20.56	20.56	20.6	20.15

APPENDIX I

COMPARISONS BETWEEN SIMULATION RESULTS AND EXPERIMENTAL DATA FOR LANIGAN GRANULAR POTASH

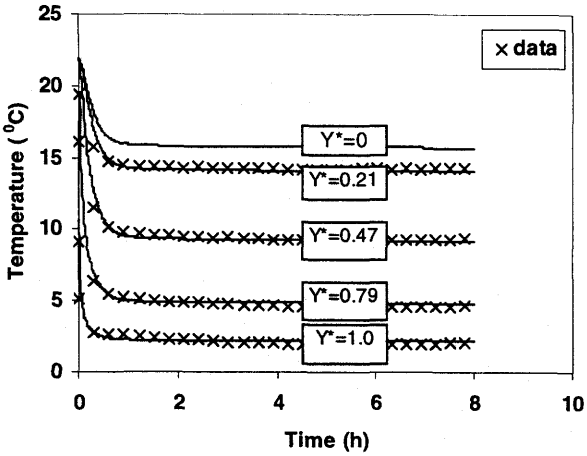

(a) Temperature

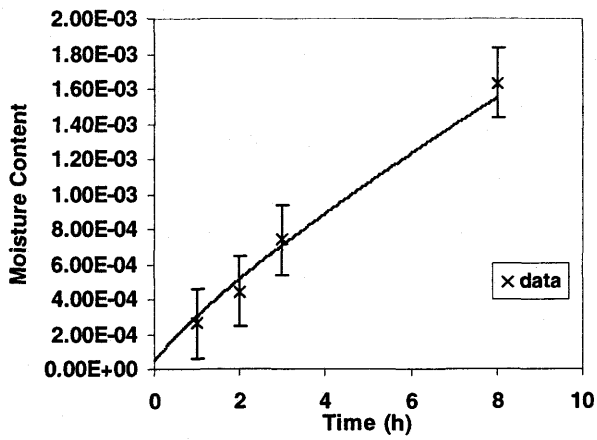

(b) Moisture Content

Figure I.1 Measured and Simulated Temperature and Averaged Moisture Content for Q=9.33 L/s, RH=45%, T_∞=22°C, T_c=2°C

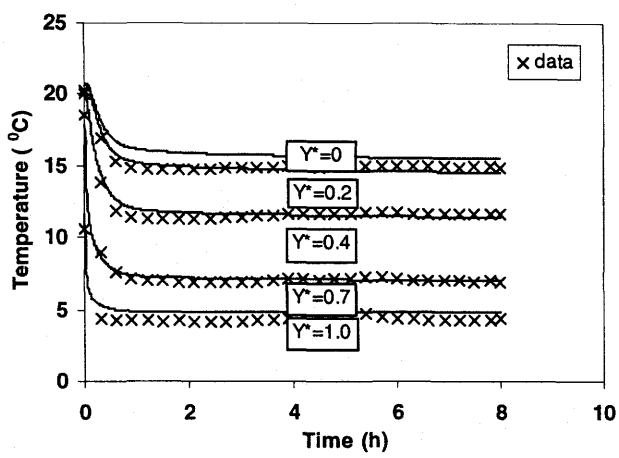

(a) Temperature

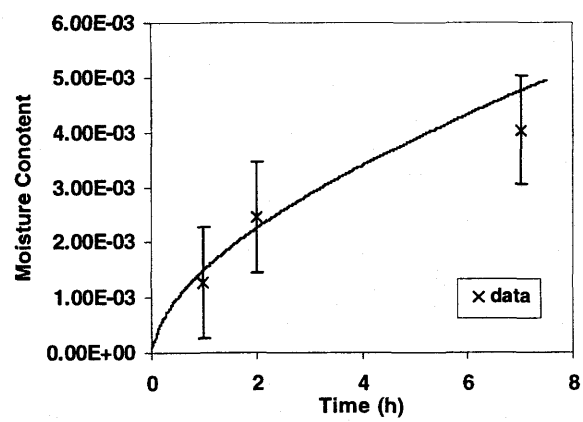

(b) Moisture Content

Figure I.2 Measured and Simulated Temperature and Averaged Moisture Content for Q=9.33 L/s, RH=65%, T_∞=22°C, T_c=2°C

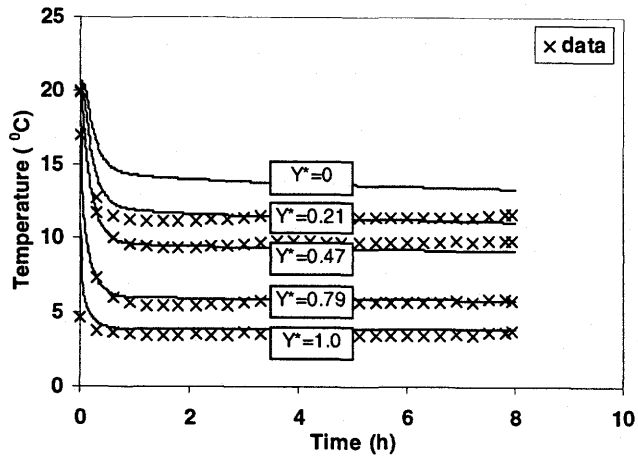

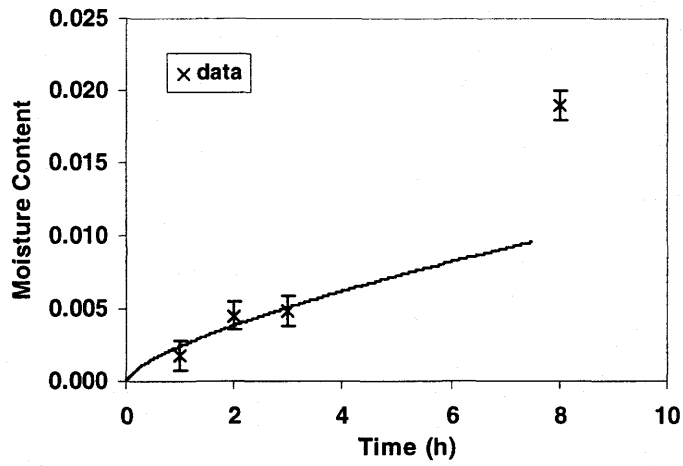

(a) Temperature

(b) Moisture Content

Figure I.3 Measured and Simulated Temperature and Averaged Moisture Content for

Q=9.33 L/s, RH=85%, T_∞=22°C, T_c=2°C

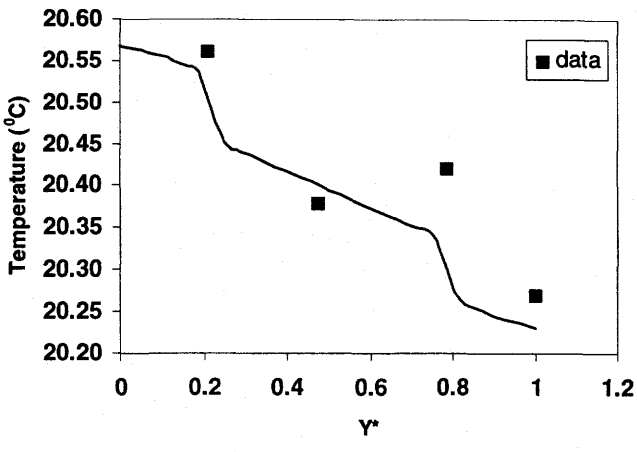

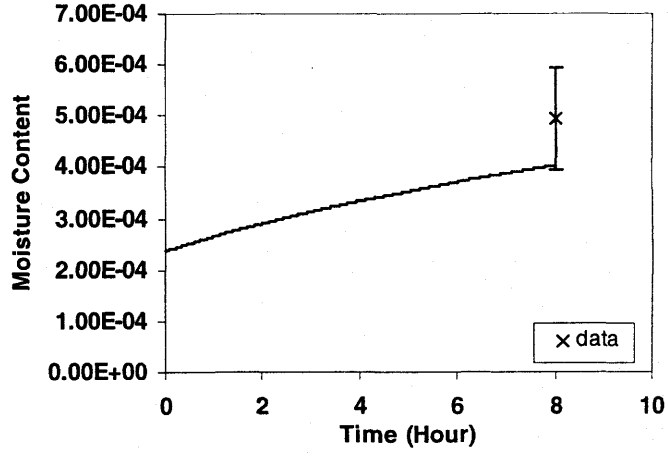

(a) Spatial Temperature at 8 h

(b) Moisture Content

Figure I.4 Measured and Simulated Temperature and Averaged Moisture Content for

Q=9.33 L/s, RH=45%, T_∞=20.8°C, T_c=19.9°C

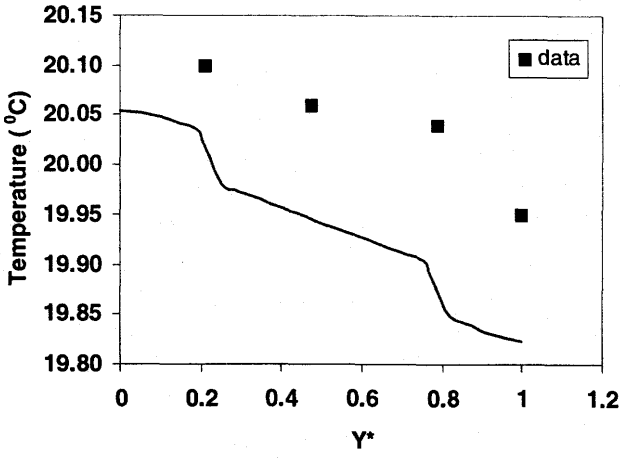

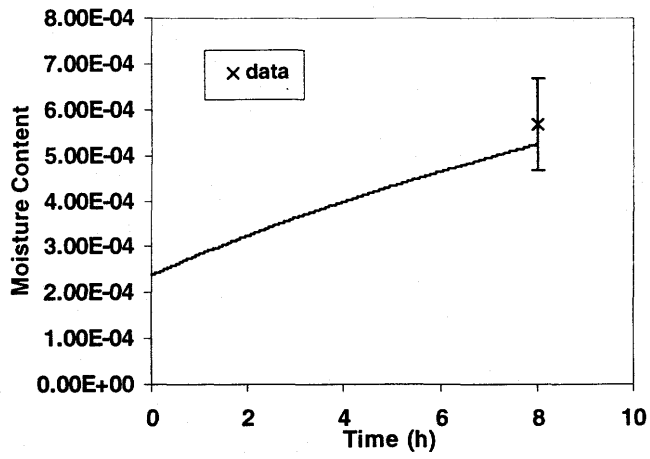

(a) Spatial Temperature at 8 h (b) Moisture Content

Figure I.5 Measured and Simulated Temperature and Averaged Moisture Content for Q=9.33 L/s, RH=65%, T_∞=20°C, T_c=19.5°C

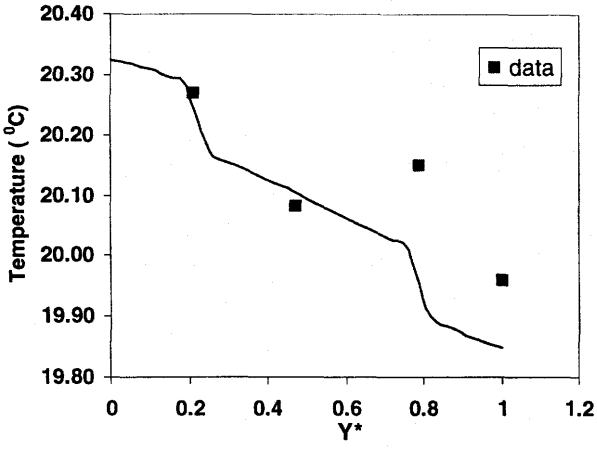

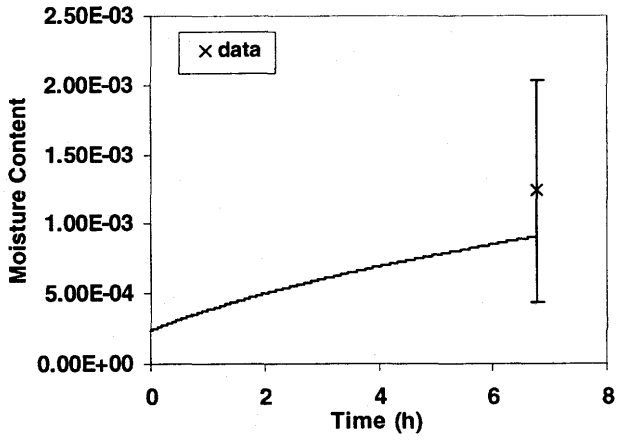

(a) Spatial Temperature at 8 h (b) Moisture Content

Figure I.6 Measured and Simulated Temperature and Averaged Moisture Content for Q=9.33 L/s, RH=85%, T_∞=20.3°C, T_c=19.5°C

APPENDIX J

FORTRAN PROGRAM FOR HEAT AND MOISTURE DIFFUSION IN POTASH BED

```
************************************************************************
*   PROGRAM TO MODEL 1-D HEAT AND MASS TRANSFER IN THE DRY GRANULAR    *
*   POTASH BED SUBJECT TO A CONVECTIVE BOUNDARY CONDITION ON THE TOP.  *
*   THE BOTTOM BOUNDARY CONDITION IS A TEMPERATURE WITH STEP CHANGE    *
*   AND IMPERMEABLE BOUNDARY TO WATER VAPOR TRANSFER. THE MODEL        *
*   INCLUDES ADSORPTION, CONDENSATION AND DISSOLUTION.                 *
*                                                                      *
*   BY:     QIANG ZHOU                                                 *
*   DATE:   JANUARY/06/2000                                            *
************************************************************************


      IMPLICIT REAL*8 (A-H,O-Z)
C DECLARE THE SPACE GRID NUMBER
      PARAMETER(N=22)
C DECLARE THE FORWARD TIME STEPS
      PARAMETER(KTIME=576)
C DECLARE THE ESSENTIAL VARIABLES IN THE PROGRAM
      INTEGER JTIME,ITERA,MP,NN,LT1,LT2,LT3,LT4,LT5,LT6,LT7,KKK
      REAL*8 XM,XC,TAO,DT,HEIGHT,DDX,DELTA,DELTAS
      REAL*8 K_AIR,K_POTASH_0,K_VAPOR,K_LIQUID
      REAL*8 PATM,RAIR,RVAPOR,HFG
      REAL*8 RHO_B,RHO_POTASH,RHO_HAL,RHO_CARN,RHO_VAPOR_INF,EPSS
      REAL*8 CP_POTASH, CP_LIQUID,CP_AIR,CP_VAPOR
      REAL*8 H_AIR,H_MASS,D_AIR,RHO_AIR_INF
      REAL*8 TEMP_INF,PHI_INF,PV_SAT_INF,TEMP_PLATE,XAIR_INF
      REAL*8 AW,AK,ANA,AMG,ACL,SI
      REAL*8 H2O,MK,MNA,MMG,MCL,KCL,NACL,KMG
      REAL*8 WKMG,WNACL,WKCL,DP,SV
      REAL*8 RP,RQ,RE,RW,R_PART,JT,RELAX1,RELAX2,RELAX3
      REAL*8 RATIOP,RATIOE,RATIOW,RATIOQ
      REAL*8 MAXT,MAXRHOV,MAXMDOT,MAXEPG,MAXEPB,MAXW,MAXH
      REAL*8 THICK1,THICK2,THICK3
      REAL*8 LOW,UP
C  DECLARE THE VARIABLES' ARRAYS

      INTEGER FLAG(N)
      REAL*8 EPB1(N),EPB2(N),EPB3(N)
      REAL*8 EPG1(N),EPG2(N),EPG3(N)
      REAL*8 EPSS1(N),EPSS2(N),EPSS3(N)
      REAL*8 TEMP1(N),TEMP2(N),TEMP3(N)
      REAL*8 RHOV1(N),RHOV2(N),RHOV3(N)
      REAL*8 PHI1(N),PHI2(N),PHI3(N)
      REAL*8 RHOVS1(N),RHOVS2(N),RHOVS3(N)
      REAL*8 DEFF1(N),DEFF2(N),DEFF3(N)
      REAL*8 KEFF1(N),KEFF2(N),KEFF3(N)
      REAL*8 CPT1(N),CPT2(N),CPT3(N)
      REAL*8 RHOT1(N),RHOT2(N),RHOT3(N)
      REAL*8 SPEC1(N),SPEC2(N),SPEC3(N)
      REAL*8 PVSAT1(N),PVSAT2(N),PVSAT3(N)
      REAL*8 MDOT1(N),MDOT2(N),MDOT3(N)
      REAL*8 XP1(N),XP2(N),XP3(N)
      REAL*8 XXP1(N),XXP2(N),XXP3(N)
      REAL*8 RHOA1(N),RHOA2(N),RHOA3(N)
      REAL*8 PV1(N),PV2(N),PV3(N)
      REAL*8 DMDT(N),DPHIDT(N),DX(N),DXE(N),DXW(N)
      REAL*8 PA1(N),PA2(N),PA3(N)
      REAL*8 ATE(N),ATW(N),ATP(N),ATS(N)
      REAL*8 KEFFE(N),KEFFW(N),DEFFE(N),DEFFW(N)
      REAL*8 ALPHA(N),BETA(N),ALPHA1(N),BETA1(N)
      REAL*8 ARHOE(N),ARHOW(N),ARHOP(N),ARHOS(N)
      REAL*8 S_C(N),S_P(N)
```

```
      REAL*8 HAD1(N),HAD2(N),HAD3(N)
      REAL*8 OMEG_S(N),OMEG_L(N)
      REAL*8 W1(N),W2(N),W3(N)
      REAL*8 SUM_MC(N),XP_INITIAL(N),RESIDUE(N)
      REAL*8 WEIGHT1(N),WEIGHT2(N),WEIGHT3(N),WEIGHT4(N)

C  DECLARE SOME COMMON VARIABLES WITH SPECIFIC FIELD NAMES

      COMMON/ACTIV/AW,AK,ANA,AMG,ACL,SI
      COMMON/NEWRAP/H2O,MK,MNA,MMG,MCL,KCL,NACL,KMG
      COMMON/POTASH/WKMG,WNACL,WKCL,DP,SV

C  THE POTASH COMPONENT IS COMPOSED OF THREE DIFFERENT SOURCES: CARNOLITE,
C  HALITE AND POTASSSIUM. THE COMPONETS MASS PERCENTAGE IS GIVEN AS BELOW
C  AND COULD BE ADJUSTED BY SIMULATION PROCESS.

      DATA WKMG/0.81/
      DATA WNACL/0.51/
      DATA WKCL/98.68/
      DATA DP/8.0D-04/
      DATA SV/4.10D+03/

C OPEN UNIT TO SAVE THE THE OUTPUTS AT THE END OF PROGRAM

      OPEN(UNIT=1,FILE='TOP.DAT',STATUS='UNKNOWN')
      OPEN(UNIT=2,FILE='TRAY1_TM.DAT',STATUS='UNKNOWN')
      OPEN(UNIT=3,FILE='TRAY2_TM.DAT',STATUS='UNKNOWN')
      OPEN(UNIT=4,FILE='TRAY3_TM.DAT',STATUS='UNKNOWN')
      OPEN(UNIT=5,FILE='TRAY4_TM.DAT',STATUS='UNKNOWN')
      OPEN(UNIT=6,FILE='RHOV_12.DAT',STATUS='UNKNOWN')
      OPEN(UNIT=7,FILE='RHOV_34.DAT',STATUS='UNKNOWN')
      OPEN(UNIT=8,FILE='PHI_12.DAT',STATUS='UNKNOWN')
      OPEN(UNIT=9,FILE='PHI_34.DAT',STATUS='UNKNOWN')
      OPEN(UNIT=10,FILE='FLUX.DAT',STATUS='UNKNOWN')
      OPEN(UNIT=11,FILE='MC.DAT',STATUS='UNKNOWN')
      OPEN(UNIT=12,FILE='LAST.DAT',STATUS='UNKNOWN')
      OPEN(UNIT=13,FILE='VOLUME.DAT',STATUS='UNKNOWN')
      OPEN(UNIT=14,FILE='VF1.DAT',STATUS='UNKNOWN')
      OPEN(UNIT=15,FILE='VF2.DAT',STATUS='UNKNOWN')
      OPEN(UNIT=16,FILE='VF3.DAT',STATUS='UNKNOWN')
      OPEN(UNIT=17,FILE='VF4.DAT',STATUS='UNKNOWN')
      OPEN(UNIT=18,FILE='INTER.DAT',STATUS='UNKNOWN')
      OPEN(UNIT=19,FILE='WET1.DAT',STATUS='UNKNOWN')
      OPEN(UNIT=20,FILE='WET2.DAT',STATUS='UNKNOWN')
      OPEN(UNIT=21,FILE='COND.DAT',STATUS='UNKNOWN')
      OPEN(UNIT=22,FILE='KEFF1.DAT',STATUS='UNKNOWN')
      OPEN(UNIT=23,FILE='KEFF2.DAT',STATUS='UNKNOWN')

      KKK=10000   ! ALLOWED MAXIMUM ITERATION NUMBER

C1----> INITIALIZE THE DOMAIN SYSTEM

      NN=N        ! THE NUMBER OF GRID TO CREATE THE UNIFORM GRIDS
      HEIGHT=3.8D-02
      DELTAS=2*DP    ! FOR ROCONVILLE STD
C
C HERE THE GRID IS CREATED BY NN GRIDS WITH NN-1 GRIDS OF R_PART AND ANOTHER
C TWO AT THE TOP AND BOTTOM OF HALF OF R_PART SPACE
C
      R_PART=(HEIGHT-DELTAS)/FLOAT(NN-1)
      DDX=R_PART/2.0

C1-1----> THE DEPTH OF THE FOUR TRAYS IN THE EXPERIMENTS FROM THE
C         TOP ONE TO BOTTOM ONE ARE : 8MM,10MM,12MM,10MM IN TURN.

       THICK1=8.0D-03-DELTAS-DDX
       THICK2=18.0D-03-DELTAS-DDX
       THICK3=30.0D-03-DELTAS-DDX
C
C LT1-THE POTASH SPACE WITH SPACE OF R_PART/2 IN TRAY#1;(#4)
C LT2-THE LOWER CONDUCTION LAYER WITH SPACE OF R_PART;(#5)
```

```
C
        LT1=NINT((THICK1*1000)/(R_PART*1000))+1
        LT2=LT1+1
C
C LT3-THE POTASH SPACE WITH SPACE OF R_PART/2 IN TRAY#2;(#10)
C LT4-THE LOWER CONDUCTION LAYER WITH SPACE OF R_PART;(#11)
C
        LT3=NINT((THICK2*1000)/(R_PART*1000))+2
        LT4=LT3+1
C
C LT5-THE POTASH SPACE WITH SPACE OF R_PART/2 IN TRAY#3;(#17)
C LT6-THE LOWER CONDUCTION LAYER WITH SPACE OF R_PART;(#18)
C
        LT5=NINT((THICK3*1000)/(R_PART*1000))+3
        LT6=LT5+1
        LT7=N

C2----> CREATE THE SPACE GRIDS

C TRAY#1 SPACE ALIGNMENT

       DX(1)=DDX+R_PART/2.0
       DO I=2,LT1-1
          DX(I)=R_PART
       ENDDO
       DX(LT1)=R_PART/2.0
       DX(LT2)=DX(LT1)

C TRAY#2 SPACE ALIGNMENT

       DO I=LT2+1,LT3-1
          DX(I)=R_PART
       ENDDO
       DX(LT3)=R_PART/2.0
       DX(LT4)=DX(LT3)

C TRAY#3 SPACE ALIGNMENT

       DO I=LT4+1,LT5-1
          DX(I)=R_PART
       ENDDO
       DX(LT5)=R_PART/2.0
       DX(LT6)=DX(LT5)

C TRAY#4 SPACE ALIGNMENT

       DO I=LT6+1,N-1
          DX(I)=R_PART
       ENDDO
       DX(N)=DX(1)

C SPACE DRID OF DXE
C TRAY#1 EAST GRID SPACE

       DXE(1)=DX(1)
       DO I=2,LT1-2
          DXE(I)=R_PART
       ENDDO
       DXE(LT1-1)=(DX(LT1-1)+DX(LT1))/2.0
       DXE(LT1)=(DX(LT1)+DX(LT2))/2.0
       DXE(LT2)=(DX(LT2)+DX(LT2+1))/2.0

C TRAY#2 EAST GRID SPACE

       DO I=LT2+1,LT3-2
          DXE(I)=R_PART
       ENDDO
       DXE(LT3-1)=(DX(LT3-1)+DX(LT3))/2.0
       DXE(LT3)=(DX(LT3)+DX(LT4))/2.0
       DXE(LT4)=(DX(LT4)+DX(LT4+1))/2.0
```

```
C TRAY#3 EAST GRID SPACE

        DO I=LT4+1,LT5-2
           DXE(I)=R_PART
        ENDDO
        DXE(LT5-1)=(DX(LT5-1)+DX(LT5))/2.0
        DXE(LT5)=(DX(LT5)+DX(LT6))/2.0
        DXE(LT6)=(DX(LT6)+DX(LT6+1))/2.0

C TRAY#4 EAST GRID SPACE

        DO I=LT6+1,N-2
           DXE(I)=R_PART
        ENDDO
        DXE(N-1)=DX(N)
        DXE(N)=0

C SPACE GRID OF DXW

        DXW(1)=0
        DO I=2,N
           DXW(I)=DXE(I-1)
        ENDDO

C WEIGHTING COEFFICIENTS FOR THE CUMULATED MOISTURE CONTENT INSIDE THE EACH
C TRAY OF THE FOUR
C----> THE FIRST TRAY

        WEIGHT1(1)=(DELTAS+DDX)/8.0D-03
        DO I=2,LT2
           WEIGHT1(I)=DX(I)/8.0D-03
        ENDDO

C----> THE SECOND TRAY

        DO I=LT2+1,LT4
           WEIGHT2(I)=DX(I)/10D-03
        ENDDO

C----> THE THIRD TRAY

        DO I=LT4+1,LT6
           WEIGHT3(I)=DX(I)/12D-03
        ENDDO

C----> THE LAST TRAY

        DO I=LT6+1,N-1
           WEIGHT4(I)=DX(I)/8.0D-03
        ENDDO
           WEIGHT4(N)=DDX/8.0D-03

        SUM1=0
        SUM2=0
        SUM3=0
        SUM4=0

        DO I=1,LT2
          SUM1=SUM1+WEIGHT1(I)
        ENDDO
        DO I=LT2+1,LT4
          SUM2=SUM2+WEIGHT2(I)
        ENDDO
        DO I=LT4+1,LT6
           SUM3=SUM3+WEIGHT3(I)
        ENDDO
        DO I=LT6+1,N
           SUM4=SUM4+WEIGHT4(I)
        ENDDO

C SET UP THE INITIAL VALUE FOR EACH GRID TO CONTINUE THE LOOP
```

```
        DO I=1,N
           FLAG(I)=0
        ENDDO

C3----> INPUT THE SOLID STATE POTASH/HALITE/CARNOLITE PROPERTIES

        D_AIR=2.6D-05     ! MOLECULAR DIFFUSION COEFFICIENT
        EPSS=0.65         ! VOLUME FRACTION OF SOLID
        XM=9.8D-04        ! ENTHALPY CONST
        XC=1.54          ! ENTHALPY CNST
        TAO=1.10          ! TOTRUSITY
        RHO_POTASH=1987
        RHO_HAL=2163
        RHO_CARN=1610
        K_POTASH_0=0.597
        CP_POTASH=750

C4----> INPUT THE AMBIENT AIR PROPERTIES

        K_AIR=0.0263
        CP_AIR=1007
        RAIR=287
        H_AIR=23.4253
        H_MASS=5.0D-05
        PATM=101325
        TEMP_INF=294              !B.C OF AMBIENT AIR TEMPERATURE
        PHI_INF=0.45              !B.C OF AMBIENT AIR TEMPERATURE
        DELTA=5D-03
        TEMP_PLATE=275.5          !B.C OF THE BOTTOM PLATE

C5----> INPUT THE LIQUID/GASEOUS STATE WATER VAPOR PROPERTIES

        HFG=2500000
        RVAPOR=462
        CP_VAPOR=1872
        K_VAPOR=0.0196
        RHO_B=997
        CP_LIQUID=4179
        K_LIQUID=0.613

C6----> CALCULATE THE SPACE AVERAGE RATIO OF EAST AND WEST

        RP=DDX
        RE=R_PART/2.0
        RQ=RP
        RW=RE
        RATIOP=RP/(RP+RE)
        RATIOE=RE/(RP+RE)
        RATIOQ=RQ/(RQ+RW)
        RATIOW=RW/(RQ+RW)

C7----> INPUT THE FORWARD TIME STEP LEMGTH

        DT=50

C8----> CALCULATE THE AMBIENT AIR PROPERTIES: PRESSURE, DENSITY AND MOISTURE
C       CONTENT

        CALL SATURATION_PRESSURE(TEMP_INF,PV_SAT_INF)
        RHO_VAPOR_INF=PV_SAT_INF/(RVAPOR*TEMP_INF)*PHI_INF
        RHO_AIR_INF=(PATM-PV_SAT_INF*PHI_INF)/(RAIR*TEMP_INF)
        XAIR_INF=0.62198*(PV_SAT_INF*PHI_INF)/(PATM-PV_SAT_INF*
     $           PHI_INF)

C9----> INITIALIZE THE INTERNAL GRIDS' PROPERTIES AT THE BEGINING TIME BASED
C       ON TEMPERATURE AND HUMIDITY

        DO I=1,N
           TEMP1(I)=TEMP_INF
           PHI1(I)=0.20
```

```
            CALL SATURATION_PRESSURE(TEMP1(I),PVSAT1(I))
            RHOVS1(I)=PVSAT1(I)/(RVAPOR*TEMP1(I))
            RHOV1(I)=RHOVS1(I)*PHI1(I)
             PA1(I)=PATM-PVSAT1(I)*PHI1(I)
            RHOA1(I)=(PATM-PVSAT1(I)*PHI1(I))/(RAIR*TEMP1(I))
            PV1(I)=PVSAT1(I)*PHI1(I)
            CALL MOISTURE_XP(PHI1(I),XM,XC,XP1(I))
            EPB1(I)=XP1(I)*RHO_POTASH/RHO_B
            EPSS1(I)=EPSS
            EPG1(I)=1-EPB1(I)-EPSS1(I)
            MDOT1(I)=-0.5D-18
            W1(I)=XP1(I)
            XP_INITIAL(I)=XP1(I)
            XXP1(I)=XP1(I)
            CALL CAL_ENTHALPY(W1(I),HFG,HAD1(I))
         ENDDO

C10----> WITH THE INITIAL CONDITIONS AND PROPERTIES, CALCULATE THE
C         COMPREHENSIVE KEFF,DEFF,RHO AND CP,ETC.

         DO I=1,N
            CALL PROPERTY(EPSS1(I),EPG1(I),EPB1(I),RHO_POTASH,RHO_B,
     $                    RHOV1(I),RHOA1(I),RHOT1(I),XP1(I),K_POTASH_0,
     $                    KEFF1(I),D_AIR,TAO,DEFF1(I),CP_POTASH,
     $                    CP_LIQUID,CP_AIR,CP_VAPOR,CPT1(I))
             CALL COEFF_SPEC(RHO_POTASH,EPSS1(I),CP_POTASH,RHO_B,EPB1(I),
     $                       CP_LIQUID,RHOV1(I),RHOA1(I),EPG1(I),
     $                       CP_AIR,CP_VAPOR,SPEC1(I))
         ENDDO

C----> INPUT THE LOW CONDUCTIVITY

            KEFF1(LT2)=0.50
            KEFF1(LT4)=0.12
            KEFF1(LT6)=0.20

C11----> INPUT THE RELAXATION COEFFICIENT

         RELAX1=0.006
         RELAX2=0.006
         RELAX3=0.006

C12----> START THE TIME RECORDER

         JT=0.0    ! TIME RECORDER
         DO JTIME=1,KTIME    !TIME COUNTER FOR ITERATIONS

          JT=JT+DT

C13----> EXCHANGE THE VALUE BETWEEN LAST TIME T AND CURRENT T+DT

         DO I=1,N
            RHOT3(I)=RHOT1(I)
            CPT3(I)=CPT1(I)
            SPEC3(I)=SPEC1(I)
            MDOT3(I)=MDOT1(I)
            XP3(I)=XP1(I)
            XXP3(I)=XXP1(I)
            W3(I)=W1(I)
            KEFF3(I)=KEFF1(I)
            DEFF3(I)=DEFF1(I)
            PHI3(I)=PHI1(I)
            PV3(I)=PV1(I)
            RHOA3(I)=RHOA1(I)
            EPG3(I)=EPG1(I)
            EPB3(I)=EPB1(I)
            EPSS3(I)=EPSS1(I)
            TEMP3(I)=TEMP1(I)
            RHOV3(I)=RHOV1(I)
            RHOVS3(I)=RHOVS1(I)
            PVSAT3(I)=PVSAT1(I)
```

```
          HAD3(I)=HAD1(I)
          PA3(I)=PA1(I)
        ENDDO

C14----> START THE ITERATION TOWARD CONVERGENCY

          ITERA=0

C14-1---->EXCHANGE THE NEW/OLD ITERATION VALUES

 100       DO I=1,N
             TEMP2(I)=TEMP3(I)
             RHOV2(I)=RHOV3(I)
             EPG2(I)=EPG3(I)
             EPB2(I)=EPB3(I)
             EPSS2(I)=EPSS3(I)
             KEFF2(I)=KEFF3(I)
             DEFF2(I)=DEFF3(I)
             PHI2(I)=PHI3(I)
             MDOT2(I)=MDOT3(I)
             XP2(I)=XP3(I)
             XXP2(I)=XXP3(I)
             W2(I)=W3(I)
             CPT2(I)=CPT3(I)
             PV2(I)=PV3(I)
             RHOVS2(I)=RHOVS3(I)
             PVSAT2(I)=PVSAT3(I)
             HAD2(I)=HAD3(I)
             RHOT2(I)=RHOT3(I)
             RHOA2(I)=RHOA3(I)
             SPEC2(I)=SPEC3(I)
             PA2(I)=PA3(I)
           ENDDO

C14-2----> CALCULATE THE COEFFICIENT IN TDMA
C14-2-1----> TEMPERATURE COEFFICIENTS

       CALL COEFF_KEFFE(LT1,LT2,LT3,LT4,LT5,LT6,
     $                  KEFF2,RATIOP,RATIOE,RATIOW,RATIOQ,N,KEFFE)
       CALL COEFF_ATE(KEFFE,DXE,N,ATE)
       CALL COEFF_KEFFW(KEFFE,KEFF2,RATIOP,RATIOE,RATIOW,RATIOQ,N,
     $                  KEFFW)
       CALL COEFF_ATW(KEFFW,DXW,N,ATW)
       CALL COEFF_ATP(ATE,ATW,RHOT2,CPT2,SPEC2,DX,DT,N,H_AIR,DELTAS,
     $                DELTA,
     $                K_AIR,K_POTASH_0,DDX,ATP)
       CALL COEFF_ATS(RHOT1,CPT1,SPEC1,TEMP1,DX,DT,MDOT2,HAD2,DELTAS,
     $                K_AIR,K_POTASH_0,
     $                N,H_AIR,TEMP_INF,DDX,TEMP_PLATE,DELTA,ATS)
C14-2-2----> CALL TDMA TO SOLVE THE NEW TEMPERATURE PROFILE

       CALL TDMA_TEMP(ATW,ATE,ATP,ATS,N,ALPHA,BETA,TEMP3)

C14-2-3----> WATER VAPOR DENSITY COEFFICIENTS

       CALL COEFF_SOURCE(N,PHI1,PHI2,XM,XC,RHOVS2,DT,RHO_POTASH,
     $                   H_MASS,RHOA2,SV,RVAPOR,TEMP2,PA2,
     $                   XAIR_INF,S_C,S_P,FLAG)
       CALL COEFF_DEFFE(LT1,LT2,LT3,LT4,LT5,LT6,
     $                  DEFF2,RATIOP,RATIOE,RATIOQ,RATIOW,N,DEFFE)
       CALL COEFF_ARHOE(FLAG,DEFFE,DXE,N,ARHOE)
       CALL COEFF_DEFFW(DEFFE,DEFF2,RATIOP,RATIOE,RATIOW,RATIOQ,N,
     $                  DEFFW)
       CALL COEFF_ARHOW(FLAG,DEFFW,DXW,N,ARHOW)
       CALL COEFF_ARHOP(FLAG,N,ARHOW,ARHOE,S_P,EPG2,DX,DT,DELTAS,DDX,
     $                  ARHOP)
       CALL COEFF_ARHOS(FLAG,RHOVS2,EPG1,RHOV1,DX,DT,MDOT2,DELTAS,EPB1,
     $                 RHO_B,EPSS1,RHO_POTASH,W1,RHOA1,EPB2,EPSS2,W2,
     $                  EPG2,RHOA2,S_C,DDX,N,ARHOS)
C14-2-4----> CALL TDMA TO SOLVE THE WATER VAPOR DENSITY PROFILE
```

```
        CALL TDMA_RHO(ARHOW,ARHOE,ARHOP,ARHOS,N,ALPHA1,BETA1,RHOV3)
        CALL COEFF_RES(N,ARHOW,ARHOE,ARHOP,ARHOS,RHOV3,RESIDUE,R_MAX,
     $                 R_SUM,MP)

C15-----> CALCULATE THE NEW SATURATION WATER VAPOR PRESSURE, THEN CALCULATE THE
C          SATURATION VAPOR DENSITY AND RELATIVE HUMIDITY.
C16----> FIRST NODE AT THE TOP

        CALL SATURATION_PRESSURE(TEMP3(1),PVSAT3(1))
        RHOVS3(1)=PVSAT3(1)/(RVAPOR*TEMP3(1))
        PHI3(1)=RHOV3(1)/RHOVS3(1)

          IF (FLAG(1).EQ.0) THEN
           CALL MOISTURE_XP(PHI3(1),XM,XC,XP3(1))
           PV3(1)=RHOV3(1)*RVAPOR*TEMP3(1)
           PA3(1)=PATM-PV3(1)
           RHOA3(1)=(PATM-PV3(1))/(RAIR*TEMP3(1))

C RATE OF PHASE CHANGE IS NOT ALLOWED TO DESORPTION IN THIS LAYER.
C THE LOOP WILL GOES TO CONDENSATION WHEN THE SIGN CHANGED TO POSITIVE
C
           MDOT3(1)=SV*RHOA3(1)*H_MASS*(XP3(1)-XAIR_INF)
           XXP3(1)=XXP1(1)-MDOT3(1)*DT/(1-EPSS)/RHO_POTASH
           CALL MOIST(TEMP3(1),XP3(1))
           CALL CAL_COMPONENT(RHO_POTASH,RHO_HAL,RHO_CARN,RHO_B,KCL,
     $                      NACL,KMG,MK,MNA,MMG,OMEG_S(1),OMEG_L(1))
           CALL VOL_SOLID(EPSS1(1),MDOT3(1),OMEG_S(1),DT,EPSS3(1))
           CALL VOL_LIQUID(EPB1(1),MDOT3(1),OMEG_L(1),DT,EPB3(1))
           EPG3(1)=1-EPSS3(1)-EPB3(1)
           W3(1)=EPB3(1)*RHO_B/RHO_POTASH
           CALL CAL_ENTHALPY(W3(1),HFG,HAD3(1))
           CALL PROPERTY(EPSS3(1),EPG3(1),EPB3(1),RHO_POTASH,RHO_B,
     $                   RHOV3(1),RHOA3(1),RHOT3(1),W3(1),K_POTASH_0,
     $                   KEFF3(1),D_AIR,TAO,DEFF3(1),CP_POTASH,
     $                   CP_LIQUID,CP_AIR,CP_VAPOR,CPT3(1))
           CALL COEFF_SPEC(RHO_POTASH,EPSS3(1),CP_POTASH,RHO_B,EPB3(1),
     $                     CP_LIQUID,RHOV3(1),RHOA3(1),EPG3(1),CP_AIR,
     $                     CP_VAPOR,SPEC3(1))

        ELSE

           PHI3(1)=1
           PV3(1)=PV1(1)
           PA3(1)=PATM-PV3(1)
           RHOA3(1)=PA3(1)/(RAIR*TEMP3(1))
           RHOV3(1)=RHOV1(1)
           EPB3(1)=EPB2(1)
           EPG3(1)=EPG2(1)
           XP3(1)=XP2(1)
           XXP3(1)=XXP2(1)
           EPSS3(1)=EPSS2(1)
           W3(1)=W2(1)
           CALL PROPERTY(EPSS1(1),EPG1(1),EPB1(1),RHO_POTASH,RHO_B,
     $                   RHOV1(1),RHOA1(1),RHOT3(1),W3(1),K_POTASH_0,
     $                   KEFF3(1),D_AIR,TAO,DEFF3(1),CP_POTASH,
     $                   CP_LIQUID,CP_AIR,CP_VAPOR,CPT3(1))
           CALL COEFF_SPEC(RHO_POTASH,EPSS1(1),CP_POTASH,RHO_B,EPB1(1),
     $                     CP_LIQUID,RHOV1(1),RHOA1(1),EPG1(1),CP_AIR,
     $                     CP_VAPOR,SPEC3(1))
           DEFFE(1)=DEFF3(1)*DEFF2(2)/(RATIOP*DEFF2(2)+RATIOE*
     $                DEFF3(1))
           MDOT3(1)=DEFFE(1)*(RHOV3(2)-RHOV3(1))/DXE(1)-DELTAS*
     $                (EPB3(1)*RHO_B+EPSS3(1)*RHO_POTASH*XP3(1)+
     $                EPG3(1)*RHOV3(1)-(EPB1(1)*RHO_B+
     $                EPSS1(1)*RHO_POTASH*XP1(1)
     $                +EPG1(1)*RHOV1(1)))/DT
           MDOT3(1)=MDOT3(1)/(DELTAS+DDX)
           XP3(1)=XP1(1)-MDOT3(1)*DT/(1-EPSS)/RHO_POTASH
           XXP3(1)=XXP1(1)-MDOT3(1)*DT/(1-EPSS)/RHO_POTASH
           CALL MOIST(TEMP3(1),XP3(1))
           CALL CAL_COMPONENT(RHO_POTASH,RHO_HAL,RHO_CARN,RHO_B,KCL,
```

```
     $                    NACL,KMG,MK,MNA,MMG,OMEG_S(1),OMEG_L(1))
           CALL VOL_SOLID(EPSS1(1),MDOT3(1),OMEG_S(1),DT,EPSS3(1))
           CALL VOL_LIQUID(EPB1(1),MDOT3(1),OMEG_L(1),DT,EPB3(1))
           EPG3(1)=1-EPSS3(1)-EPB3(1)
           W3(1)=EPB3(1)*RHO_B/RHO_POTASH
           CALL CAL_ENTHALPY(W3(1),HFG,HAD3(1))

         ENDIF

C17----> MIDDLE NODES

          DO I=2,N-1
             CALL SATURATION_PRESSURE(TEMP3(I),PVSAT3(I))
             RHOVS3(I)=PVSAT3(I)/(RVAPOR*TEMP3(I))
             PHI3(I)=RHOV3(I)/RHOVS3(I)

             IF (FLAG(I).EQ.0) THEN
                CALL MOISTURE_XP(PHI3(I),XM,XC,XP3(I))
                DPHIDT(I)=(PHI3(I)-PHI1(I))/DT
                CALL MASS_PROD(SV,PHI3(I),XM,XC,RHO_POTASH,DPHIDT(I),
     $                         DMDT(I),MDOT3(I))
                XXP3(I)=XXP1(I)-MDOT3(I)*DT/(1-EPSS)/RHO_POTASH
                CALL MOIST(TEMP3(I),XP3(I))
                CALL CAL_COMPONENT(RHO_POTASH,RHO_HAL,RHO_CARN,RHO_B,
     $                             KCL,NACL,KMG,MK,MNA,MMG,OMEG_S(I),
     $                             OMEG_L(I))
                CALL VOL_SOLID(EPSS1(I),MDOT3(I),OMEG_S(I),DT,EPSS3(I))
                CALL VOL_LIQUID(EPB1(I),MDOT3(I),OMEG_L(I),DT,EPB3(I))
                EPG3(I)=1-EPSS3(I)-EPB3(I)
                W3(I)=EPB3(I)*RHO_B/RHO_POTASH
                CALL CAL_ENTHALPY(W3(I),HFG,HAD3(I))
                PV3(I)=RHOV3(I)*RVAPOR*TEMP3(I)
                PA3(I)=PATM-PV3(I)
                RHOA3(I)=(PATM-PV3(I))/(RAIR*TEMP3(I))
                CALL PROPERTY(EPSS3(I),EPG3(I),EPB3(I),RHO_POTASH,RHO_B,
     $                        RHOV3(I),RHOA3(I),RHOT3(I),W3(I),K_POTASH_0,
     $                        KEFF3(I),D_AIR,TAO,DEFF3(I),CP_POTASH,
     $                        CP_LIQUID,CP_AIR,CP_VAPOR,CPT3(I))
              CALL COEFF_SPEC(RHO_POTASH,EPSS3(I),CP_POTASH,RHO_B,
     $                        EPB3(I),CP_LIQUID,RHOV3(I),RHOA3(I),
     $                        EPG3(I),CP_AIR,CP_VAPOR,SPEC3(I))
             ELSE

                PHI3(I)=1
                PV3(I)=PVSAT3(I)*0.80
                PA3(I)=PATM-PV3(I)
                RHOA3(I)=PA3(I)/(RAIR*TEMP3(I))
                RHOV3(I)=RHOVS3(I)*0.80
                EPB3(I)=EPB2(I)
                EPSS3(I)=EPSS2(I)
                EPG3(I)=EPG2(I)
                XP3(I)=XP2(I)
                W3(I)=W2(I)
              CALL PROPERTY(EPSS1(I),EPG1(I),EPB1(I),RHO_POTASH,RHO_B,
     $                      RHOV1(I),RHOA1(I),RHOT3(I),W3(I),K_POTASH_0,
     $                      KEFF3(I),D_AIR,TAO,DEFF3(I),CP_POTASH,
     $                      CP_LIQUID,CP_AIR,CP_VAPOR,CPT3(I))
               CALL COEFF_SPEC(RHO_POTASH,EPSS1(I),CP_POTASH,RHO_B,
     $                         EPB1(I),CP_LIQUID,RHOV1(I),RHOA1(I),
     $                         EPG1(I),CP_AIR,CP_VAPOR,SPEC3(I))

                DEFFW(I)=2*DEFF3(I-1)*DEFF3(I)/(DEFF3(I)+DEFF3(I-1))
                DEFFE(I)=2*DEFF2(I+1)*DEFF3(I)/(DEFF2(I+1)+DEFF3(I))
                CALL MASS_MIDDLE(DEFFE(I),DEFFW(I),RHOV3(I-1),RHOV3(I),
     $                           RHOV3(I+1),EPG3(I),EPG1(I),RHOV1(I),
     $                           DT, DX(I),DXW(I),DXE(I),MDOT3(I))
               XP3(I)=XP1(I)-MDOT3(I)*DT/(1-EPSS)/RHO_POTASH
               XXP3(I)=XXP1(I)-MDOT3(I)*DT/(1-EPSS)/RHO_POTASH
               CALL MOIST(TEMP3(I),XP3(I))
               CALL CAL_COMPONENT(RHO_POTASH,RHO_HAL,RHO_CARN,RHO_B,
     $                            KCL,NACL,KMG,MK,MNA,MMG,OMEG_S(I),
```

```
     $                              OMEG_L(I))
               CALL VOL_SOLID(EPSS1(I),MDOT3(I),OMEG_S(I),DT,EPSS3(I))
               CALL VOL_LIQUID(EPB1(I),MDOT3(I),OMEG_L(I),DT,EPB3(I))
               EPG3(I)=1-EPSS3(I)-EPB3(I)
                W3(I)=EPB3(I)*RHO_B/RHO_POTASH
               CALL CAL_ENTHALPY(W3(I),HFG,HAD3(I))
             ENDIF
          ENDDO

C18----> LAST NODE AT THE BOTTOM

          CALL SATURATION_PRESSURE(TEMP3(N),PVSAT3(N))
          RHOVS3(N)=PVSAT3(N)/(RVAPOR*TEMP3(N))
          PHI3(N)=RHOV3(N)/RHOVS3(N)

           IF (FLAG(N).EQ.0) THEN
             CALL MOISTURE_XP(PHI3(N),XM,XC,XP3(N))
             DPHIDT(N)=(PHI3(N)-PHI1(N))/DT

             CALL MASS_PROD(SV,PHI3(N),XM,XC,RHO_POTASH,DPHIDT(N),
     $                      DMDT(N),MDOT3(N))
              XXP3(N)=XXP1(N)-MDOT3(N)*DT/(1-EPSS)/RHO_POTASH
             CALL MOIST(TEMP3(N),XP3(N))
             CALL CAL_COMPONENT(RHO_POTASH,RHO_HAL,RHO_CARN,RHO_B,KCL,
     $                          NACL,KMG,MK,MNA,MMG,OMEG_S(N),OMEG_L(N))
             CALL VOL_SOLID(EPSS1(N),MDOT3(N),OMEG_S(N),DT,EPSS3(N))
             CALL VOL_LIQUID(EPB1(N),MDOT3(N),OMEG_L(N),DT,EPB3(N))
             EPG3(N)=1-EPSS3(N)-EPB3(N)
             W3(N)=EPB3(N)*RHO_B/RHO_POTASH
             CALL CAL_ENTHALPY(W3(N),HFG,HAD3(N))
             PV3(N)=RHOV3(N)*RVAPOR*TEMP3(N)
             PA3(N)=PATM-PV3(N)
             RHOA3(N)=(PATM-PV3(N))/(RAIR*TEMP3(N))
             CALL PROPERTY(EPSS3(N),EPG3(N),EPB3(N),RHO_POTASH,RHO_B,
     $                     RHOV3(N),RHOA3(N),RHOT3(N),W3(N),K_POTASH_0,
     $                     KEFF3(N),D_AIR,TAO,DEFF3(N),CP_POTASH,
     $                     CP_LIQUID,CP_AIR,CP_VAPOR,CPT3(N))
             CALL COEFF_SPEC(RHO_POTASH,EPSS3(N),CP_POTASH,RHO_B,EPB3(N),
     $                       CP_LIQUID,RHOV3(N),RHOA3(N),EPG3(N),CP_AIR,
     $                       CP_VAPOR,SPEC3(N))

          ELSE

             PHI3(N)=1
             PV3(N)=PVSAT3(N)*0.80
             PA3(N)=PATM-PV3(N)
             RHOA3(N)=PA3(N)/(RAIR*TEMP3(N))
             RHOV3(N)=RHOVS3(N)*0.80
             XP3(N)=XP2(N)
             EPB3(N)=EPB1(N)
             EPSS3(N)=EPSS1(N)
             EPG3(N)=EPG1(N)
             W3(N)=W2(N)
             CALL PROPERTY(EPSS1(N),EPG1(N),EPB1(N),RHO_POTASH,RHO_B,
     $                     RHOV1(N),RHOA1(N),RHOT3(N),W3(N),K_POTASH_0,
     $                     KEFF3(N),D_AIR,TAO,DEFF3(N),CP_POTASH,
     $                     CP_LIQUID,CP_AIR,CP_VAPOR,CPT3(N))
             CALL COEFF_SPEC(RHO_POTASH,EPSS1(N),CP_POTASH,RHO_B,EPB1(N),
     $                       CP_LIQUID,RHOV1(N),RHOA1(N),EPG1(N),CP_AIR,
     $                       CP_VAPOR,SPEC3(N))
             DEFFW(N)=DEFF3(N)*DEFF3(N-1)/(DEFF3(N)*RATIOW+DEFF3(N-1)
     $                *RATIOQ)
             MDOT3(N)=DEFFW(N)*(4*RHOV3(N-1)-RHOV3(N-2)-3*RHOV3(N))/
     $                (DX(N-1)+DX(N))
             XP3(N)=XP1(N)-MDOT3(N)*DT/(1-EPSS)/RHO_POTASH
              XXP3(N)=XXP1(N)-MDOT3(N)*DT/(1-EPSS)/RHO_POTASH
             CALL MOIST(TEMP3(N),XP3(N))
             CALL CAL_COMPONENT(RHO_POTASH,RHO_HAL,RHO_CARN,RHO_B,KCL,
     $                          NACL,KMG,MK,MNA,MMG,OMEG_S(N),OMEG_L(N))
             CALL VOL_SOLID(EPSS1(N),MDOT3(N),OMEG_S(N),DT,EPSS3(N))
             CALL VOL_LIQUID(EPB1(N),MDOT3(N),OMEG_L(N),DT,EPB3(N))
```

```
          EPG3(N)=1-EPSS3(N)-EPB3(N)
          W3(N)=EPB3(N)*RHO_B/RHO_POTASH
          CALL CAL_ENTHALPY(W3(N),HFG,HAD3(N))
        ENDIF

C19----> CONVERGENCY CHECK UP

          MAXT=ABS((TEMP3(1)-TEMP2(1))/TEMP2(1))
          DO I=2,N
             IF(ABS((TEMP3(I)-TEMP2(I))/TEMP2(I)).GT.MAXT) THEN
                 MAXT=ABS((TEMP3(I)-TEMP2(I))/TEMP2(I))
             ENDIF
          ENDDO

          MAXRHOV=ABS((RHOV3(1)-RHOV2(1))/RHOV2(1))
           I_RHO=1
          DO I=2,N
             IF(ABS((RHOV3(I)-RHOV2(I))/RHOV2(I)).GT.MAXRHOV) THEN
                MAXRHOV=ABS((RHOV3(I)-RHOV2(I))/RHOV2(I))
                I_RHO=I
             ENDIF
          ENDDO

          MAXEPG=ABS((EPG3(1)-EPG2(1))/EPG2(1))
          DO I=2,N
             IF(ABS((EPG3(I)-EPG2(I))/EPG2(I)).GT.MAXEPG) THEN
               MAXEPG=ABS((EPG3(I)-EPG2(I))/EPG2(I))
             ENDIF
          ENDDO

          MAXEPB=ABS((EPB3(1)-EPB2(1))/EPB2(1))
          DO I=2,N
             IF(ABS((EPB3(I)-EPB2(I))/EPB2(I)).GT.MAXEPB) THEN
                MAXEPB=ABS((EPB3(I)-EPB2(I))/EPB2(I))
             ENDIF
          ENDDO

          MAXMDOT=DABS(MDOT3(1)-MDOT2(1))/DABS(MDOT3(1))
          I_POSITION=1
          DO I=2,N
             IF(DABS(MDOT3(I)-MDOT2(I))/DABS(MDOT3(I)).GT.MAXMDOT) THEN
                MAXMDOT=DABS(MDOT3(I)-MDOT2(I))/DABS(MDOT3(I))
                I_POSITION=I
             ENDIF
          ENDDO

          MAXW=ABS((PHI3(1)-PHI2(1))/PHI2(1))
          DO I=2,N
             IF(ABS((PHI3(I)-PHI2(I))/PHI2(I)).GT.MAXW) THEN
                MAXW=ABS((PHI3(I)-PHI2(I))/PHI2(I))
             ENDIF
          ENDDO

          MAXH=ABS((HAD3(1)-HAD2(1))/HAD2(1))
          DO I=2,N
             IF(ABS((HAD3(I)-HAD2(I))/HAD2(I)).GT.MAXH) THEN
                MAXH=ABS((HAD3(I)-HAD2(I))/HAD2(I))
             ENDIF
          ENDDO

C20----> RELAXATION OF EACH ITERATION RESULTS

        KEFF3(LT2)=0.50
        KEFF3(LT4)=0.12
        KEFF3(LT6)=0.20

         DO I=1,N

            TEMP3(I)=TEMP2(I)+(TEMP3(I)-TEMP2(I))*RELAX1
            RHOV3(I)=RHOV2(I)+(RHOV3(I)-RHOV2(I))*RELAX2
            EPG3(I)=EPG2(I)+(EPG3(I)-EPG2(I))*RELAX3
```

```
            EPB3(I)=EPB2(I)+(EPB3(I)-EPB2(I))*RELAX3
            EPSS3(I)=EPSS2(I)+(EPSS3(I)-EPSS2(I))*RELAX3
            KEFF3(I)=KEFF2(I)+(KEFF3(I)-KEFF2(I))*RELAX3
            DEFF3(I)=DEFF2(I)+(DEFF3(I)-DEFF2(I))*RELAX3
            PHI3(I)=PHI2(I)+(PHI3(I)-PHI2(I))*RELAX3
            MDOT3(I)=MDOT2(I)+(MDOT3(I)-MDOT2(I))*RELAX3
            W3(I)=W2(I)+(W3(I)-W2(I))*RELAX3
             XP3(I)=XP2(I)+(XP3(I)-XP2(I))*RELAX3
             XXP3(I)=XXP2(I)+(XXP3(I)-XXP2(I))*RELAX3
            CPT3(I)=CPT2(I)+(CPT3(I)-CPT2(I))*RELAX2
            RHOT3(I)=RHOT2(I)+(RHOT3(I)-RHOT2(I))*RELAX2
            RHOA3(I)=RHOA2(I)+(RHOA3(I)-RHOA2(I))*RELAX2
            PV3(I)=PV2(I)+(PV3(I)-PV2(I))*RELAX2
            RHOVS3(I)=RHOVS2(I)+(RHOVS3(I)-RHOVS2(I))*RELAX2
            PVSAT3(I)=PVSAT2(I)+(PVSAT3(I)-PVSAT2(I))*RELAX2
            HAD3(I)=HAD2(I)+(HAD3(I)-HAD2(I))*RELAX2
             PA3(I)=PA2(I)+(PA3(I)-PA2(I))*RELAX2
            SPEC3(I)=SPEC2(I)+(SPEC3(I)-SPEC2(I))*RELAX2

         ENDDO

          IF(ITERA.GT.KKK) THEN
             WRITE(*,*) 'NO CONVERGE SOLUTION AT THIS TIME STEP'
             STOP
             GOTO  200
          ENDIF

          IF(MAXT.GT.1D-04) THEN
            ITERA=ITERA+1
            GOTO 100
          ELSE IF(MAXRHOV.GT.1D-04) THEN
            ITERA=ITERA+1
            GOTO 100
          ELSE IF(MAXMDOT.GT.1D-03) THEN
            ITERA=ITERA+1
            GOTO 100
          ENDIF

 200       WRITE(*,*) 'ITERA=',ITERA

C21-1----> CALCULATE THE HEAT FLUX THROUGH THE BOTTOM

           Q_FLUX=ABS(KEFFW(N)*(TEMP3(N)-TEMP3(N-1))/DX(N))

C21-2----> CALCULATE THE TIME-SUMMED MOISTURE IN THE POTASH

           DO I=1,N
            CALL MC_AVERAGE(RHO_POTASH,MDOT3(I),EPSS,DT,XXP1(I),
     $              SUM_MC(I))
           ENDDO

C21-3----> CALCULATE THE AVERAGED MOISTURE CONTENT IN THE POTASH BED

C21-3-1----> TOP TRAY#1

          TRAY1=0
          DO I=1,LT2
             TRAY1=TRAY1+SUM_MC(I)*WEIGHT1(I)
          ENDDO

          TRAY2=0
          DO I=LT2+1,LT4
             TRAY2=TRAY2+SUM_MC(I)*WEIGHT2(I)
          ENDDO

          TRAY3=0
          DO I=LT4+1,LT6
             TRAY3=TRAY3+SUM_MC(I)*WEIGHT3(I)
          ENDDO

          TRAY4=0
```

```
          DO I=LT6+1,N
             TRAY4=TRAY4+SUM_MC(I)*WEIGHT4(i)
          ENDDO

        IF (FLAG(1).EQ.1) THEN
            FLAG(1)=1
        ELSE IF (PHI3(1).GE.0.65) THEN
            FLAG(1)=1
        END IF
        DO I=2,N
           IF (FLAG(I).EQ.1) THEN
              FLAG(I)=1
           ELSE IF (PHI3(I).GE.0.80) THEN
              FLAG(I)=1
           ENDIF
        ENDDO

C22----> PUT THE CONVERGED DATA INTO GROUPS OF INITIAL FOR THE NEXT TIME STEP

         DO I=1,N
            TEMP1(I)=TEMP3(I)
            RHOV1(I)=RHOV3(I)
            MDOT1(I)=MDOT3(I)
            EPG1(I)=EPG3(I)
            EPB1(I)=EPB3(I)
            EPSS1(I)=EPSS3(I)
            KEFF1(I)=KEFF3(I)
            DEFF1(I)=DEFF3(I)
            PHI1(I)=PHI3(I)
            W1(I)=W3(I)
            XP1(I)=XP3(I)
            XXP1(I)=XXP3(I)
            CPT1(I)=CPT3(I)
            RHOT1(I)=RHOT3(I)
            PV1(I)=PV3(I)
            RHOVS1(I)=RHOVS3(I)
            PVSAT1(I)=PVSAT3(I)
            HAD1(I)=HAD3(I)
            RHOA1(I)=RHOA3(I)
             PA1(I)=PA3(I)
            SPEC1(I)=SPEC3(I)
         ENDDO

C23----> WRITE THE DATA INTO FILES

        WRITE(1,10) JT,TEMP3(1),PHI3(1),MDOT3(1)
        WRITE(2,20) TEMP3(LT2),TEMP3(LT2+1),MDOT3(LT2),MDOT3(LT2+1)
        WRITE(3,20) TEMP3(LT4),TEMP3(LT4+1),MDOT3(LT4),MDOT3(LT4+1)
        WRITE(4,20) TEMP3(LT6),TEMP3(LT6+1),MDOT3(LT6),MDOT3(LT6+1)
        WRITE(5,10) JT,TEMP3(N),PHI3(N),MDOT3(N)
        WRITE(6,21) RHOV3(1),RHOV3(LT2),RHOV3(LT2+1),RHOV3(LT3)
        WRITE(7,21) RHOV3(LT4),RHOV3(LT4+1),RHOV3(LT6),RHOV3(N)
        WRITE(8,21) PHI3(LT2),PHI3(LT2+1),PHI3(LT4),PHI3(LT4+1)
        WRITE(9,21) PHI3(LT5),PHI3(LT6),PHI3(2),PHI3(3)
        WRITE(10,11) JT,Q_FLUX,TRAY4,MDOT3(2)
        WRITE(11,11) JT,TRAY1,TRAY2,TRAY3
        WRITE(14,11) JT,EPSS3(2),EPB3(2),EPG3(2)
        WRITE(15,11) JT,EPSS3(LT2+1),EPB3(LT2+1),EPG3(LT2+1)
        WRITE(16,11) JT,EPSS3(LT4+1),EPB3(LT4+1),EPG3(LT4+1)
        WRITE(17,11) JT,EPSS3(LT6),EPB3(LT6),EPG3(LT6)
        WRITE(18,21) TEMP3(2),RHOV3(2),TEMP3(3),RHOV3(3)
        WRITE(19,21) XXP3(1),XXP3(2),XXP3(LT2+1),XXP3(LT2)
        WRITE(20,21) XXP3(LT4),XXP3(LT4+1),XXP3(LT6),XXP3(LT6+1)
        WRITE(22,21) KEFF3(1),KEFF3(LT1),KEFF3(LT2),KEFF3(LT3)
        WRITE(23,21) KEFF3(LT4),KEFF3(LT5),KEFF3(LT6),KEFF3(N)

  10     FORMAT(F8.2,1X,F14.6,1X,E14.6,1X,E14.6)
  11     FORMAT(F8.2,1X,E14.6,1X,E14.6,1X,E14.6)
  20    FORMAT(F14.6,1X,F14.6,1X,E14.6,1X,E14.6)
  21     FORMAT(E14.6,1X,E14.6,1X,E14.6,1X,E14.6)
  30     FORMAT(E14.6,1X,E14.6)
```

```
  40    FORMAT(E8.2,1X,E14.6,1X,E14.6)

C24----> SAVE THE VALUES OF THE LAST MINUTE

         IF((KTIME-JTIME).LT.1) THEN
           DO I=1,N
              WRITE(12,12) TEMP3(I),RHOV3(I),MDOT3(I),XP3(I)
              WRITE(13,15) EPSS3(I),EPB3(I),EPG3(I)
              WRITE(21,*) FLAG(I),KEFF3(I)
  15          FORMAT(E14.6,1X,E14.6,1X,E14.6)
  12          FORMAT(F14.6,1X,E14.6,1X,E14.6,1X,E14.6)
           ENDDO
         ENDIF
        ENDDO

C25----> OUTPUT A MESSAGE TO END USER ON THE COMPLETEMENT OF THE CALCULATION

        WRITE(*,*) 'THE CALCULATION HAS BEEN SUCCESSFUL COMPLETED'

        CLOSE(UNIT=1)
        CLOSE(UNIT=2)
        CLOSE(UNIT=3)
        CLOSE(UNIT=4)
        CLOSE(UNIT=5)
        CLOSE(UNIT=6)
        CLOSE(UNIT=7)
        CLOSE(UNIT=8)
        CLOSE(UNIT=9)
        CLOSE(UNIT=10)
        CLOSE(UNIT=11)
        CLOSE(UNIT=12)
        CLOSE(UNIT=13)
        CLOSE(UNIT=14)
        CLOSE(UNIT=15)
        CLOSE(UNIT=16)
        CLOSE(UNIT=17)
        CLOSE(UNIT=18)
        CLOSE(UNIT=19)
        CLOSE(UNIT=20)
        CLOSE(UNIT=21)
        CLOSE(UNIT=22)
        CLOSE(UNIT=23)

        END

        INCLUDE 'MOIST.FOR'
        INCLUDE 'APHI.FOR'
        INCLUDE 'BETA.FOR'
        INCLUDE 'CHEMP0.FOR'
        INCLUDE 'KCAL.FOR'
        INCLUDE 'NEWTON.FOR'
        INCLUDE 'FUNC1.FOR'
        INCLUDE 'FUNC2.FOR'
        INCLUDE 'FUNC3.FOR'
        INCLUDE 'THETA.FOR'
        INCLUDE 'ACTCOF.FOR'
        INCLUDE 'GAUSS.FOR'
        INCLUDE 'JX.FOR'
        INCLUDE 'VIRCOF.FOR'

*************************
*   RESIDUE CHECK UP    *
*************************

        SUBROUTINE COEFF_RES(N,ARHOW,ARHOE,ARHOP,ARHOS,RHOV3,
     $                       RESIDUE,R_MAX,R_SUM,MP)
         IMPLICIT REAL*8(A-H,O-Z)
        INTEGER N,MP
        REAL*8 ARHOW(N),ARHOE(N),ARHOP(N),ARHOS(N),RHOV3(N),RESIDUE(N)
        REAL*8 R_MAX,R_SUM
```

```
      RESIDUE(1)=ABS(ARHOP(1)*RHOV3(1)-ARHOE(1)*RHOV3(2)-
     $            ARHOS(1))
      DO I=2,N-1
      RESIDUE(I)=ABS(ARHOP(I)*RHOV3(I)-ARHOW(I)*RHOV3(I-1)-
     $            ARHOE(I)*RHOV3(I+1)-ARHOS(N))
      ENDDO
      RESIDUE(N)=ABS(ARHOP(N)*RHOV3(N)-ARHOW(N)*RHOV3(N-1)-
     $             ARHOS(N))
      R_MAX=RESIDUE(N)
       MP=N

      DO I=1,N-1
          IF(RESIDUE(I).GT.R_MAX) THEN
           R_MAX=RESIDUE(I)
            M_P=I
        ENDIF
      ENDDO

      R_SUM=0
      DO I=1,N
       R_SUM=R_SUM+RESIDUE(I)
      ENDDO
      R_SUM=R_SUM/FLOAT(N)

      RETURN
      END

*********************************************************
*   CALCULATION OF SATURATION WATER VAPOR PRESSURE      *
*********************************************************

      SUBROUTINE SATURATION_PRESSURE(TO,PVSAT)
      IMPLICIT REAL*8 (A-H,O-Z)
      REAL*8 C1,C2,C3,C4,C5,C6,C7
      REAL*8 C8,C9,C10,C11,C12,C13
      REAL*8 TO,PVSAT

      C1=-5.6745359D+03
      C2=6.3925247
      C3=-9.677843D-03
      C4=6.22115701D-07
      C5=2.0747825D-09
      C6=-9.484024D-13
      C7=4.1635019

      C8=-5.8002206D+03
      C9=1.3914993
      C10=-4.8640239D-02
      C11=4.1764768D-05
      C12=-1.4452093D-08
      C13=6.5459673

      IF(TO.GT.273.15) THEN

         PVSAT=EXP(C8/TO+C9+C10*TO+C11*TO**2+C12*TO**3+C13*
     $              LOG(TO))
      ELSE
         PVSAT=EXP(C1/TO+C2+C3*TO+C4*TO**2+C5*TO**3+C6*TO**4+
     $             C7*LOG(TO))
      ENDIF

      RETURN
      END

*************************************************************
*   CALCULATION OF THE MOISTURE CONTENT IN THE POTASH BED    *
*   IT'S ASSUMED THE GASEOUS,LIQUID AND SOLID PHASES ARE     *
*   IN THE THERMODYNAMIC EQUILIBRIUM STATE.                  *
*************************************************************

      SUBROUTINE MOISTURE_XP(PHIV,XM,XC,XP)
```

```
      IMPLICIT REAL*8(A-H,O-Z)
      REAL*8 XM,XC
      REAL*8 X1,X2,X3
      REAL*8 X4,X5,X6,X7
      REAL*8 LOW,UP,PHIV,XP

      LOW=5D-05    ! 295K
      UP=8.1468    ! 295K
      XP=LOW*EXP(UP*PHIV)
      RETURN
      END

*****************************************************************
*   CALCULATE THE COMPREHENSIVE THREE PHASES TOTAL PROPERTIES    *
*****************************************************************

      SUBROUTINE PROPERTY(EPSS,EPG,EPB,RHO_POTASH, RHO_B,RHO_VAPOR,
     $                    RHO_AIR,RHO_TOTAL,XP,K_POTASH,KEFF,D_AIR,
     $                    TAO,DEFF,CP_POTASH,CP_LIQUID,CP_AIR,
     $                    CP_VAPOR,CP_TOTAL)

      IMPLICIT REAL*8 (A-H,O-Z)
      REAL*8 EPSS,EPG,PEB
      REAL*8 RHO_POTASH,RHO_B,RHO_VAPOR,RHO_AIR,RHO_TOTAL
      REAL*8 K_POTASH,XP,KEFF
      REAL*8 D_AIR,TAO,DEFF
      REAL*8 CP_POTASH,CP_LIQUID,CP_AIR,CP_VAPOR,CP_TOTAL

      RHO_TOTAL=RHO_POTASH*EPSS+RHO_B*EPB+(RHO_VAPOR+RHO_AIR)*EPG
      CP_TOTAL=(EPSS*CP_POTASH*RHO_POTASH+EPB*CP_LIQUID*RHO_B+EPG*(
     $          RHO_VAPOR*CP_VAPOR+RHO_AIR*CP_AIR))/RHO_TOTAL
      DEFF=D_AIR*EPG/TAO
      KEFF=K_POTASH+0.45*(XP*100)

      RETURN
      END
*********************************************
*   CALCULATION OF THE SPEC PRODUCT TERM     *
*********************************************

      SUBROUTINE COEFF_SPEC(RHO_POTASH,EPSS,CP_POTASH,RHO_B,EPB,
     $                      CP_LIQUID,RHOV,RHOA,EPG,CP_AIR,CP_VAPOR,
     $                      SPEC)
      IMPLICIT REAL*8(A-H,O-Z)
      REAL*8 RHO_POTASH,RHO_B,RHOV,RHOA
       REAL*8 CP_POTASH,CP_LIQUID,CP_AIR,CP_VAPOR
       REAL*8 EPSS,EPB,EPG
      REAL*8 SPEC

      SPEC=RHO_POTASH*EPSS*CP_POTASH+RHO_B*EPB*CP_LIQUID+(RHOV+RHOA)
     $     *EPG*(RHOA*CP_AIR+RHOV*CP_VAPOR)/(RHOV+RHOA)

      RETURN
      END
*********************************************
*  CALCULATION OF THE KEFFE COEFFICIENT     *
*********************************************
      SUBROUTINE COEFF_KEFFE(LT1,LT2,LT3,LT4,LT5,LT6,
     $                       KEFF2,RATIOP,RATIOE,RATIOW,RATIOQ,N,
     $                       KEFFE)
      IMPLICIT REAL*8 (A-H,O-Z)
      INTEGER N,LT1,LT2,LT3,LT4,LT5,LT6
      REAL*8 KEFF2(N),KEFFE(N)
      REAL*8 RATIOP,RATIOQ,RATIOE,RATIOW

      KEFF2(LT2)=0.50
      KEFF2(LT4)=0.12
      KEFF2(LT6)=0.20

C TRAY#1 SPACE AVERAGE CONDUCTIVITY
        KEFFE(1)=KEFF2(1)*KEFF2(2)/(RATIOP*KEFF2(2)+RATIOE*
```

```
     $              KEFF2(1))
        DO I=2,LT1-2
           KEFFE(I)=2*KEFF2(I)*KEFF2(I+1)/(KEFF2(I)+KEFF2(I+1))
        ENDDO
           KEFFE(LT1-1)=KEFF2(LT1-1)*KEFF2(LT1)/(RATIOP*KEFF2(LT1)+
     $                  RATIOE*KEFF2(LT1-1))
           KEFFE(LT1)=2*KEFF2(LT1)*KEFF2(LT2)/(KEFF2(LT1)+KEFF2(LT2))
           KEFFE(LT2)=KEFF2(LT2)*KEFF2(LT2+1)/(RATIOP*KEFF2(LT2+1)+
     $                RATIOE*KEFF2(LT2))

C TRAY#2 SPACE AVERAGE CONDUCTIVITY

        DO I=LT2+1,LT3-2
           KEFFE(I)=2*KEFF2(I)*KEFF2(I+1)/(KEFF2(I)+KEFF2(I+1))
        ENDDO
           KEFFE(LT3-1)=KEFF2(LT3-1)*KEFF2(LT3)/(RATIOP*KEFF2(LT3)+
     $                  RATIOE*KEFF2(LT3-1))
           KEFFE(LT3)=2*KEFF2(LT3)*KEFF2(LT4)/(KEFF2(LT3)+KEFF2(LT4))
           KEFFE(LT4)=KEFF2(LT4)*KEFF2(LT4+1)/(RATIOP*KEFF2(LT4+1)+
     $                RATIOE*KEFF2(LT4))

C TRAY#3 SPACE AVERAGE CONDUCTIVITY

        DO I=LT4+1,LT5-2
           KEFFE(I)=2*KEFF2(I)*KEFF2(I+1)/(KEFF2(I)+KEFF2(I+1))
        ENDDO
           KEFFE(LT5-1)=KEFF2(LT5-1)*KEFF2(LT5)/(RATIOP*KEFF2(LT5)+
     $                  RATIOE*KEFF2(LT5-1))
           KEFFE(LT5)=2*KEFF2(LT5)*KEFF2(LT6)/(KEFF2(LT5)+KEFF2(LT6))
           KEFFE(LT6)=KEFF2(LT6)*KEFF2(LT6+1)/(RATIOP*KEFF2(LT6+1)+
     $                RATIOE*KEFF2(LT6))

C TRAY#4 SPACE AVERAGE CONDUCTIVITY

        DO I=LT6+1,N-2
           KEFFE(I)=2*KEFF2(I)*KEFF2(I+1)/(KEFF2(I)+KEFF2(I+1))
        ENDDO
           KEFFE(N-1)=KEFF2(N-1)*KEFF2(N)/(RATIOQ*KEFF2(N-1)+
     $                RATIOW*KEFF2(N))
           KEFFE(N)=0
        RETURN
        END

*********************************************
*    CALCULATION OF THE COEFFICIENT ATE       *
*********************************************
        SUBROUTINE COEFF_ATE(KEFFE,DXE,N,ATE)
        IMPLICIT REAL*8 (A-H,O-Z)
        INTEGER N
        REAL*8 KEFFE(N),DXE(N), ATE(N)

        DO I=2,N-2
           ATE(I)=KEFFE(I)/DXE(I)
        ENDDO
           ATE(1)=KEFFE(1)/DXE(1)
           ATE(N-1)=KEFFE(N-1)/DXE(N-1)
           ATE(N)=0
        RETURN
        END

************************************
*  CALCULATION OF COEFFICIENT KEFFW  *
************************************

        SUBROUTINE COEFF_KEFFW(KEFFE,KEFF2,RATIOP,RATIOE,RATIOW,RATIOQ,
     $                         N,KEFFW)
        IMPLICIT REAL*8(A-H,O-Z)
        INTEGER N
        REAL*8 KEFFE(N),KEFF2(N),KEFFW(N)
        REAL*8 RATIOP,RATIOQ,RATIOW,RATIOE
```

```
      KEFFW(1)=0
      DO I=2,N
         KEFFW(I)=KEFFE(I-1)
      ENDDO
      RETURN
      END

*********************************************
*    CALCULATION OF THE COEFFICIENT ATW     *
*********************************************

      SUBROUTINE COEFF_ATW(KEFFW,DXW,N,ATW)
      IMPLICIT REAL*8 (A-H,O-Z)
      INTEGER N
      REAL*8 KEFFW(N),DXW(N),ATW(N)
      DO I=3,N-1
         ATW(I)=KEFFW(I)/DXW(I)
      ENDDO
      ATW(1)=0
      ATW(2)=KEFFW(2)/DXW(2)
      ATW(N)=KEFFW(N)/DXW(N)
      RETURN
      END

*********************************************
*    CALCULATIN OF THE COEFFICIENT ATP      *
*********************************************

      SUBROUTINE COEFF_ATP(ATE,ATW,RHOT2,CPT2,SPEC2,DX,DT,N,H_AIR,
     $                     DELTAS,DELTA,K_AIR,K_POTASH_0,DDX,ATP)
      IMPLICIT REAL*8 (A-H,O-Z)
      INTEGER N
      REAL*8 ATE(N),ATW(N),ATP(N)
      REAL*8 RHOT2(N),CPT2(N),DX(N),SPEC2(N)
      REAL*8 DT,H_AIR,DELTAS,DELTA,K_AIR,DDX,K_POTASH_0

         ATP(1)=ATE(1)+H_AIR+(DELTAS+DDX)*SPEC2(1)/DT
      DO I=2,N-1
         ATP(I)=ATE(I)+ATW(I)+RHOT2(I)*CPT2(I)*DX(I)/DT
      ENDDO
         ATP(N)=ATW(N)+RHOT2(N)*CPT2(N)*DDX/DT+K_POTASH_0/DELTA
      RETURN
      END

*********************************************
*    CALCULATION OF THE COEFFICIENT ATS     *
*********************************************

      SUBROUTINE COEFF_ATS(RHOT1,CPT1,SPEC1,TEMP1,DX,DT,MDOT2,HAD2,
     $                     DELTAS,K_AIR,K_POTASH_0,N,H_AIR,TEMP_INF,DDX,
     $                     TEMP_PLATE,DELTA,ATS)
      IMPLICIT REAL*8 (A-H,O-Z)
      INTEGER N
      REAL*8 RHOT1(N),CPT1(N),TEMP1(N),DX(N),SPEC1(N)
      REAL*8 MDOT2(N),HAD2(N),ATS(N)
      REAL*8 DT,H_AIR,TEMP_INF,DDX,TEMP_PLATE,DELTA,K_AIR,K_POTASH_0

         ATS(1)=(DELTAS+DDX)*SPEC1(1)*TEMP1(1)/DT+H_AIR*TEMP_INF-
     $          MDOT2(1)*HAD2(1)*(DDX+DELTAS)
      DO I=2,N-1
         ATS(I)=RHOT1(I)*CPT1(I)*TEMP1(I)*DX(I)/DT-MDOT2(I)*HAD2(I)
     $          *DX(I)
      ENDDO
         ATS(N)=RHOT1(N)*CPT1(N)*TEMP1(N)*DDX/DT+K_POTASH_0/DELTA*
     $          TEMP_PLATE-2*MDOT2(N)*DDX*HAD2(N)
      RETURN
      END

*************************************************
*          TDMA FOR TEMPERATURE PROFILE         *
*************************************************
```

```
      SUBROUTINE TDMA_TEMP(ATW,ATE,ATP,ATS,N,ALPHA,BETA,TEMP3)
      IMPLICIT REAL*8 (A-H,O-Z)
      INTEGER N
      REAL*8 ATW(N),ATE(N),ATP(N),ATS(N)
      REAL*8 ALPHA(N),BETA(N),TEMP3(N)

         ALPHA(1)=ATE(1)/ATP(1)
         BETA(1)=ATS(1)/ATP(1)
      DO I=2,N-1
         ALPHA(I)=ATE(I)/(ATP(I)-ATW(I)*ALPHA(I-1))
         BETA(I)=(ATS(I)+ATW(I)*BETA(I-1))/(ATP(I)-ATW(I)*
     $              ALPHA(I-1))
      ENDDO
         ALPHA(N)=0
         BETA(N)=(ATS(N)+ATW(N)*BETA(N-1))/(ATP(N)-ATW(N)*
     $              ALPHA(N-1))
         TEMP3(N)=BETA(N)
      DO I=N-1,1,-1
          TEMP3(I)=ALPHA(I)*TEMP3(I+1)+BETA(I)
      ENDDO
      RETURN
      END

*******************************************************
*  CALCULATION OF THE SOURCE TERM IN VAPOR DENSITY    *
*******************************************************

      SUBROUTINE COEFF_SOURCE(N,PHI1,PHI2,XM,XC,RHOVS2,DT,
     $                        RHO_POTASH,H_MASS,RHOA2,
     $                        SV,RVAPOR,TEMP2,PA2,
     $                        XAIR_INF,S_C,S_P,FLAG)
      IMPLICIT REAL*8(A-H,O-Z)
      INTEGER N
      REAL*8 XM,XC,DT,RHO_POTASH,H_MASS,SV,RVAPOR,XAIR_INF
      REAL*8 X1,X2,X3
      REAL*8 X4,X5,X6,X7
      REAL*8 LOW,UP,STD
      REAL*8 PHI1(N),PHI2(N),RHOVS2(N),RHOA2(N),TEMP2(N),PA2(N)
       REAL*8 S_C(N),S_P(N)
      INTEGER FLAG(N)

      LOW=5D-05  ! 295K
      UP=8.1468  ! 295K
      STD=4.10D+03
      S_C(1)=H_MASS*RHOA2(1)*SV*XAIR_INF
      S_P(1)=H_MASS*RHOA2(1)*SV*RVAPOR*TEMP2(1)/PA2(1)*0.62918

      DO I=2,N
        S_C(I)=LOW*UP*EXP(UP*PHI2(I))*PHI1(I)/DT*RHO_POTASH*SV/STD
        S_P(I)=-1*LOW*UP*EXP(UP*PHI2(I))/DT/RHOVS2(I)*RHO_POTASH
     $          *SV/STD
      ENDDO
      RETURN
      END

*****************************************
*  CALCULATION OF THE DEFFE COEFFICIENT  *
*****************************************

      SUBROUTINE COEFF_DEFFE(LT1,LT2,LT3,LT4,LT5,LT6,
     $                       DEFF2,RATIOP,RATIOE,RATIOQ,RATIOW,
     $                       N,DEFFE)
      IMPLICIT REAL*8 (A-H,O-Z)
      INTEGER N,LT1,LT2,LT3,LT4,LT5,LT6
      REAL*8 DEFF2(N),DEFFE(N)
      REAL*8 RATIOP,RATIOQ,RATIOW,RATIOE

C TRAY#1 MOISTURE DIFFUSION COEFFICIENT

         DEFFE(1)=DEFF2(1)*DEFF2(2)/(RATIOP*DEFF2(2)+RATIOE*
```

```
     $              DEFF2(1))
        DO I=2,LT1-2
           DEFFE(I)=2*DEFF2(I)*DEFF2(I+1)/(DEFF2(I)+DEFF2(I+1))
        ENDDO
           DEFFE(LT1-1)=DEFF2(LT1-1)*DEFF2(LT1)/(RATIOP*DEFF2(LT1)+
     $                  RATIOE*DEFF2(LT1-1))
           DEFFE(LT1)=2*DEFF2(LT1)*DEFF2(LT2)/(DEFF2(LT1)+DEFF2(LT2))
           DEFFE(LT2)=DEFF2(LT2)*DEFF2(LT2+1)/(RATIOP*DEFF2(LT2+1)+
     $                RATIOE*DEFF2(LT2))

C TRAY#2 MOISTURE DIFFUSION COEFFICIENT

        DO I=LT2+1,LT3-2
           DEFFE(I)=2*DEFF2(I)*DEFF2(I+1)/(DEFF2(I)+DEFF2(I+1))
        ENDDO
           DEFFE(LT3-1)=DEFF2(LT3-1)*DEFF2(LT3)/(RATIOP*DEFF2(LT3)+
     $                  RATIOE*DEFF2(LT3-1))
           DEFFE(LT3)=2*DEFF2(LT3)*DEFF2(LT4)/(DEFF2(LT3)+DEFF2(LT4))
           DEFFE(LT4)=DEFF2(LT4)*DEFF2(LT4+1)/(RATIOP*DEFF2(LT4+1)+
     $                RATIOE*DEFF2(LT4))

C TRAY#3 MOISTURE DIFFUSION COEFFICIENT

        DO I=LT4+1,LT5-2
           DEFFE(I)=2*DEFF2(I)*DEFF2(I+1)/(DEFF2(I)+DEFF2(I+1))
        ENDDO
           DEFFE(LT5-1)=DEFF2(LT5-1)*DEFF2(LT5)/(RATIOP*DEFF2(LT5)+
     $                  RATIOE*DEFF2(LT5-1))
           DEFFE(LT5)=2*DEFF2(LT5)*DEFF2(LT6)/(DEFF2(LT5)+DEFF2(LT6))
           DEFFE(LT6)=DEFF2(LT6)*DEFF2(LT6+1)/(RATIOP*DEFF2(LT6+1)+
     $                RATIOE*DEFF2(LT6))

C TRAY#4 MOISTURE DIFFUSION COEFFICIENT

        DO I=LT6+1,N-2
           DEFFE(I)=2*DEFF2(I)*DEFF2(I+1)/(DEFF2(I)+DEFF2(I+1))\
        ENDDO
           DEFFE(N-1)=DEFF2(N)*DEFF2(N-1)/(RATIOW*DEFF2(N)+RATIOQ*
     $                DEFF2(N-1))
           DEFFE(N)=0
        RETURN
        END

*********************************************
*    CALCULATION OF THE ARHOE COEFFICIENT    *
*********************************************

        SUBROUTINE COEFF_ARHOE(FLAG,DEFFE,DXE,N,ARHOE)
        IMPLICIT REAL*8(A-H,O-Z)
        INTEGER N
        INTEGER FLAG(N)
        REAL*8 DEFFE(N),DXE(N),ARHOE(N)

        DO I=2,N-2
            IF(FLAG(I).EQ.0) THEN
              ARHOE(I)=DEFFE(I)/DXE(I)
           ELSE
              ARHOE(I)=0
           END IF
        ENDDO

         IF(FLAG(1).EQ.0) THEN
           ARHOE(1)=DEFFE(1)/DXE(1)
         ELSE
           ARHOE(1)=0
         ENDIF

          IF(FLAG(N-1).EQ.0) THEN
             ARHOE(N-1)=DEFFE(N-1)/DXE(N-1)
          ELSE
             ARHOE(N-1)=0
```

```
          END IF
          ARHOE(N)=0
        RETURN
        END

*****************************************
*  CALCULATION OF THE DEFFW COEFFICIENT  *
*****************************************

        SUBROUTINE COEFF_DEFFW(DEFFE,DEFF2,RATIOP,RATIOE,RATIOW,RATIOQ,
     $                          N,DEFFW)
        IMPLICIT REAL*8 (A-H,O-Z)
        INTEGER N
        REAL*8 DEFFE(N),DEFF2(N),DEFFW(N)
        REAL*8 RATIOP,RATIOQ,RATIOE,RATIOW

        DEFFW(1)=0
        DO I=2,N
        DEFFW(I)=DEFFE(I-1)
        ENDDO
        RETURN
        END

*******************************************
*   CALCULATION OF THE ARHOW COEFFICIENT   *
*******************************************

        SUBROUTINE COEFF_ARHOW(FLAG,DEFFW,DXW,N,ARHOW)
        IMPLICIT REAL*8 (A-H,O-Z)
        INTEGER N
        INTEGER FLAG(N)
        REAL*8 DEFFW(N),DXW(N),ARHOW(N)

        DO I=3,N-1
           IF(FLAG(I).EQ.0) THEN
              ARHOW(I)=DEFFW(I)/DXW(I)
           ELSE
              ARHOW(I)=0
           ENDIF
        ENDDO
           ARHOW(1)=0

            IF (FLAG(2).EQ.0) THEN
              ARHOW(2)=DEFFW(2)/DXW(2)
           ELSE
              ARHOW(2)=0
           END IF

          IF (FLAG(N).EQ.0) THEN
              ARHOW(N)=DEFFW(N)/DXW(N)
          ELSE
              ARHOW(N)=0
          ENDIF

        RETURN
        END

*****************************************
*   CALCULATION OF THE ARHOP COEFFICIENT  *
*****************************************

        SUBROUTINE COEFF_ARHOP(FLAG,N,ARHOW,ARHOE,S_P,EPG2,DX,DT,
     $                          DELTAS,DDX,ARHOP)
        IMPLICIT REAL*8 (A-H,O-Z)
        INTEGER N
        INTEGER FLAG(N)
        REAL*8 ARHOW(N),ARHOE(N),ARHOP(N),S_P(N)
        REAL*8 EPG2(N),DX(N)
        REAL*8 DDX,DT,DELTAS

        IF (FLAG(1).EQ.0) THEN
```

```
          ARHOP(1)=ARHOE(1)+S_P(1)+(DELTAS+DDX)*EPG2(1)/DT
         ELSE
          ARHOP(1)=1
         ENDIF

        DO I=2,N-1
          IF(FLAG(I).EQ.0) THEN
           ARHOP(I)=ARHOE(I)+ARHOW(I)+EPG2(I)*DX(I)/DT-S_P(I)*DX(I)
          ELSE
           ARHOP(I)=1
          ENDIF
        ENDDO

          IF (FLAG(N).EQ.0) THEN
             ARHOP(N)=ARHOW(N)+EPG2(N)*DDX/DT-S_P(N)*DDX
          ELSE
             ARHOP(N)=1
           END IF
        RETURN
        END

*****************************************
*  CALCULATION OF THE ARHOS COEFFICIENT   *
*****************************************

        SUBROUTINE COEFF_ARHOS(FLAG,RHOVS2,EPG1,RHOV1,DX,DT,MDOT2,
     $               DELTAS,EPB1,RHO_B,EPSS1,RHO_POTASH,W1,RHOA1,EPB2,
     $                     EPSS2,W2,EPG2,RHOA2,S_C,DDX,N,ARHOS)

        IMPLICIT REAL*8 (A-H,O-Z)
        INTEGER N
        INTEGER FLAG(N)
        REAL*8 EPG1(N),EPG2(N),EPSS1(N),EPSS2(N),EPB1(N),EPB2(N)
        REAL*8 RHOA1(N),RHOA2(N),S_C(N),W1(N),W2(N)
         REAL*8 RHOVS2(N),RHOV1(N)
        REAL*8 MDOT2(N),ARHOS(N),DX(N)
        REAL*8 DT,DELTAS,RHO_POTASH,RHO_B,DDX

        IF (FLAG(1).EQ.0) THEN

        ARHOS(1)=S_C(1)+(DELTAS+DDX)/DT*((EPB1(1)*RHO_B+EPSS1(1)
     $           *RHO_POTASH
     $           *W1(1)+EPG1(1)*RHOV1(1))-(EPB2(1)*RHO_B
     $           +EPSS2(1)*RHO_POTASH*W2(1)))
        ELSE
        ARHOS(1)=RHOV1(1)
        ENDIF

        DO I=2,N-1
          IF (FLAG(I).EQ.0) THEN
            ARHOS(I)=EPG1(I)*RHOV1(I)*DX(I)/DT+S_C(I)*DX(I)
          ELSE
            ARHOS(I)=RHOVS2(I)*0.80
          END IF
        ENDDO

          IF (FLAG(N).EQ.0) THEN
            ARHOS(N)=EPG1(N)*RHOV1(N)*DDX/DT+S_C(N)*DDX
           ELSE
            ARHOS(N)=RHOVS2(N)*0.80
           END IF
        RETURN
        END

*********************************************
*   TDMA TO SOLVE THE VAPOR DENSITY PROFILE   *
*********************************************

        SUBROUTINE TDMA_RHO(ARHOW,ARHOE,ARHOP,ARHOS,
     $                      N,ALPHA1,BETA1,RHOV3)
        IMPLICIT REAL*8 (A-H,O-Z)
```

```
      INTEGER N
      REAL*8 ARHOW(N),ARHOE(N),ARHOP(N),ARHOS(N)
      REAL*8 ALPHA1(N),BETA1(N),RHOV3(N)
         ALPHA1(1)=ARHOE(1)/ARHOP(1)
         BETA1(1)=ARHOS(1)/ARHOP(1)
      DO I=2,N-1
         ALPHA1(I)=ARHOE(I)/(ARHOP(I)-ARHOW(I)*ALPHA1(I-1))
         BETA1(I)=(ARHOS(I)+ARHOW(I)*BETA1(I-1))/(ARHOP(I)-
     $               ARHOW(I)*ALPHA1(I-1))
      ENDDO
         ALPHA1(N)=0
         BETA1(N)=(ARHOS(N)+ARHOW(N)*BETA1(N-1))/(ARHOP(N)-
     $               ARHOW(N)*ALPHA1(N-1))
         RHOV3(N)=BETA1(N)
      DO I=N-1,1,-1
         RHOV3(I)=ALPHA1(I)*RHOV3(I+1)+BETA1(I)
      ENDDO
      RETURN
      END

*************************************************************************
*  CALCULATION OF SOLID,LIQUID PHASE VOLUME CHANGE WITH CHEMICAL COMPONENT  *
*************************************************************************

      SUBROUTINE CAL_COMPONENT(RHO_POTASH,RHO_HAL,RHO_CARN,RHO_B,
     $                         KCL,NACL,KMG,MK,MNA,MMG,OMEG_S,
     $                          OMEG_L)
      IMPLICIT REAL*8 (A-H,O-Z)
      REAL*8 RHO_POTASH,RHO_HAL,RHO_CARN
      REAL*8 KCL,NACL,KMG,MK,MNA,MMG
      REAL*8 OMEG_S,OMEG_L

      IF(KMG.GT.1D-12) THEN
         OMEG_S=MK*74.5513/(1000.0*RHO_POTASH)+MNA*58.4428/
     $          (1000.0*RHO_HAL)+MMG*277.85398/(1000.0*RHO_CARN)
         OMEG_L=1.0/RHO_B+MK*74.5513/(1000.0*RHO_POTASH)+
     $          MNA*58.4428/(1000.0*RHO_HAL)+MMG*277.85398/
     $          (1000.0*RHO_CARN)
      ELSE IF (KMG.LE.1D-12.AND.NACL.GT.1D-12) THEN
         OMEG_S=MK*74.5513/(1000.0*RHO_POTASH)+MNA*55.4428/
     $          (1000.0*RHO_HAL)
         OMEG_L=1.0/RHO_B+MK*74.5513/(1000.0*RHO_POTASH)+
     $          MNA*55.4428/(1000.0*RHO_HAL)
      ELSE
         OMEG_S=MK*74.5513/(1000.0*RHO_POTASH)
         OMEG_L=1.0/RHO_B+MK*74.5513/(1000.0*RHO_POTASH)
      ENDIF
      RETURN
      END

***********************************************
*  CALCULATION OF THE SOLID VOLUME FRACTION    *
***********************************************

      SUBROUTINE VOL_SOLID(EPSS_1,MDOT,OMEG_S,DT,EPSS_3)
      IMPLICIT REAL*8 (A-H,O-Z)
      REAL*8 EPSS_1,EPSS_3,MDOT,OMEG_S,DT

      EPSS_3=EPSS_1+MDOT*OMEG_S*DT

      RETURN
      END

*****************************************************
*  CALCULATION OF THE LIQUID PHASE VOLUME FRACTION   *
*****************************************************

      SUBROUTINE VOL_LIQUID(EPB_1,MDOT,OMEG_L,DT,EPB_3)
      IMPLICIT REAL*8 (A-H,O-Z)
      REAL*8 EPB_1,EPB_3,MDOT,OMEG_L,DT
```

```
      EPB_3=EPB_1-MDOT*OMEG_L*DT
      RETURN
      END

************************************************
*   CALCULATION OF THE ENTHALPY CHANGE IN HAD    *
************************************************

      SUBROUTINE CAL_ENTHALPY(XP,HFG,HAD)
      IMPLICIT REAL*8 (A-H,O-Z)
      REAL*8 XP,HFG,HAD

      IF(XP.LE.1D-02) THEN
        HAD=(-0.48*(XP*100)**3+1.77*(XP*100)**2-2.11*(XP*100)+
     $            1.71)*HFG
      ELSE
        HAD=0.89*HFG
      ENDIF
      RETURN
      END

*********************************************************************
*  CALCULATION OF THE MASS OF WATER VAPOR PHASE CHANGE (KG/M3.S)  *
*********************************************************************

      SUBROUTINE MASS_PROD(SV,PHIV,XM,XC,RHO_POTASH,DPHIDT,DMDT,MDOT)
      IMPLICIT REAL*8 (A-H,O-Z)
      REAL*8 PHIV,XM,XC,RHO_POTASH
      REAL*8 X1,X2,X3
      REAL*8 X4,X5,X6,X7
      REAL*8 LOW,UP,SV,STD
      REAL*8 DPHIDT,DMDT,MDOT

      LOW=5D-05     ! 295K
      UP=8.1468     ! 295K
      STD=4.10D+03
      DMDT=LOW*UP*EXP(UP*PHIV)*DPHIDT*RHO_POTASH*SV/STD
      MDOT=-1*DMDT

      RETURN
      END

************************************************************
*   CALCULATION OF THE MASS OF VAPOR PHASE CHANGE IN THE    *
*   MIDDLE NODES. (KG/M3.S)                                 *
************************************************************

      SUBROUTINE MASS_MIDDLE(DEFFE,DEFFW,RHOV3_I,RHOV3_J,RHOV3_K,
     $                       EPG3,EPG1,RHOV1,DT,DX,DXW,DXE,MDOT3)

      IMPLICIT REAL*8 (A-H,O-Z)
      REAL*8 DEFFE,DEFFW,RHOV3_I,RHOV3_J,RHOV3_K
      REAL*8 EPG3,EPG1,RHOV1,MDOT3
      REAL*8 DT,DX,DXW,DXE

      MDOT3=(EPG3*DX/DT+DEFFE/DXE+DEFFW/DXW)*(RHOV3_J/DX)-(DEFFE/DXE)
     $       *(RHOV3_K/DX)-(DEFFW/DXW)*(RHOV3_I/DX)-EPG1*RHOV1/DT

      RETURN
      END
************************************************************
*  CALCULATE THE MOISTURE CONTENT IN EACH GRID WITH TIME   *
************************************************************

       SUBROUTINE MC_AVERAGE(RHO_POTASH,MDOT3,EPSS,DT,XXP1,SUM)
      IMPLICIT REAL*8 (A-H,O-Z)
      REAL*8 MDOT3

       SUM=XXP1-MDOT3*DT/(1-EPSS)/RHO_POTASH
      RETURN
      END
```